Catalytic Intramolecular Carbene Transfer Reactions into σ and π Bonds

（σ 及び π 結合への触媒的分子内カルベン移動反応）

March, 2020

Doctor of Philosophy (Engineering)

PHAN THI THANH NGA

ファン ティ タン ガ

Toyohashi University of Technology

ACKNOWLEDGEMENTS

First and foremost, I would like to express my deep thanks to my supervisor, Professor Dr. Seiji Iwasa, for everything he did for me during my study within four years. Actually, there is no words can express my deep sense of gratitude towards him. I would like to thanks him for his endless support, encouragement, advices and patience throughout my PhD work.

I would like to express Prof. Dr. Kazutaka Shibatomi for his investing time and providing interesting and valuable feedback throughout my research period.

And I would like to thank to my doctoral committee members, Prof. Dr. Shinichi Itsuno for his valuable suggestions.

I am thankful for Dr. Ikuhide Fujisawa for his hospitality and for assisting me with the X-ray measurements. I am very grateful to Mr. Masaya Tone, Mr. Hayato Inoue, Ms. Huong for their cooperation, suggestion, and valuable discussion throughout my research period.

I also would like to acknowledge all the labmates whom I had the pleasure of working with: Dr. Soda, Dr. Hamada, Dr. Kotozaki, Dr. Nakagawa, Dr. Chi, Ms. Doan, Mr. Augus, Mr. Liang, Mr. Fujii, Mr. Fukuda, Ms. Nansalmaa, Ms. Matozaki, Mr. Ogura, Mr. Yamaguchi, Ms. Linhda, Ms. Zolzaya and all other research scholars of the department who have been very friendly and helped me in various ways.

I acknowledge all the staff members of the international and educational affairs division at Toyohashi University of Technology for their support during the progress of my graduation steps.

I would like to thank all the friends that I have met in Toyohashi: Mona, Hằng, Huế, Bảo, Trinh, Hường, Khôn, Hoài. I really cherish the great time we spent together: the dinner parties, summer barbecues, autumn red leaves, skiing and Tết.

With my appreciation and respect, this work would not have been possible without the financial support of the Hitachi Global Foundation, they gave me the chance to study in Japan under their financial support to my work.

I want to thank all the staffs of Faculty of Chemical Engineering, HCMC University of Technology for their supports in the fulfilment of my PhD program. I also acknowledge Prof. Le Thi Kim Phung – director external relations office of HCMC University of Technology for her support and encouragement.

My deepest gratitude is reserved for my family, for having filled my life with every joy, helping me to get through so many gloomy days and lighting up every last corner. For my parents, my brother Ấn who have always been there for me. Needless to say, they have helped immeasurably to get me to this point in my life.

Thank you very much!

PHAN THI THANH NGA

Department of Applied Chemistry and Life Science

Toyohashi University of Technology, 1-1 Tempaku-cho,

Toyohashi, Aichi 441-8580 (Japan)

E-mail: phanthanhnga@hcmut.edu.vn

ABSTRACT

Keywords: asymmetric synthesis, cyclopropanation, Buchner reaction, Ru(II)-Pheox catalyst.

A carbene known as a most active intermediate is complexed with a transition metal, which affords the corresponding metal-carbene complex and catalytically inserts into σ and π bonds of the organic compound. Even though there are many reports on the carbene transfer process to develop a new approach for the synthesis of medicine and other bioactive compounds, the regio-, stereo- and chemoselective approaches are still limited and remained as the main subject in the field of synthetic organic chemistry. For this background, I developed an efficient catalytic intramolecular carbene transfer reactions by using originally developed ruthenium catalyst into σ and π bonds and successfully applied for the synthesis of γ-lactam ring fused aromatics (oxindoles), γ-lactone ring fused cyclopropanes, and γ-lactam ring fused seven-membered rings via Buchner reaction.

Although the ruthenium complex is a newcomer in the field of catalytic carbene transfer reaction, it has emerged as a useful transition metal for the carbenoid chemistry of diazo compounds, besides copper and rhodium. And recently, we have developed a Ru(II)-Pheox complex, which is efficient for carbene transfer reactions, in particular, asymmetric cyclopropanation, N-H insertion, C-H insertion and Si-H insertion reactions.

Therefore, driven by my interests in the catalytic asymmetric carbene transfer reaction and the efficiency displayed by the Ru(II)-Pheox catalyst, I started to explore the asymmetric cyclopropanation, C-H insertion, Buchner reactions of various diazo compounds, which are potentially building blocks and expectant to be applied in pharmaceutical and medicinal fields.

In my thesis, **Chapter 1** describes the importance of carbene transfer reactions. And a short review of the metal carbene intermediates in C-H insertion, asymmetric cyclopropanations, and Buchner reaction have been also illustrated in this chapter. In addition, the application of metal carbene complexes in the synthesis of biologically-active or natural product-like compounds is also mentioned.

Chapter 2 is for the synthesis of oxindoles. The oxindole ring is prevalent as an important scaffold found in numerous natural products and pharmaceutically active compounds. Over the past few decades, the emerging therapeutic potential of the structural motif of oxindole has encouraged the medicinal chemists to synthesize novel oxindole derivatives. I report Ru(II)-Pheox

was found to be a highly efficient catalyst for the synthesis of oxindole derivatives in excellent yields. We developed the efficient synthesis of oxindole derivatives via intramolecular ArC_{sp2}-H insertion reaction of diazo acetamides derived from the corresponding anilines by using Ru(II)-Pheox catalyst. The reaction proceeds smoothly under mild conditions, providing the corresponding oxindole derivatives in excellent yield (up to 99%). No other side reactions related to metal-carbene reactivity such as dimerization, aromatic ring expansion and C_{sp3}-H on amide nitrogen insertion reaction were observed.

On the other hand, the cyclopropane subunit is also present in many biologically important compounds and it shows a large spectrum of biological properties. Transition metal-catalyzed cyclopropanation involving carbene intermediate is powerful and useful methods for constructing important substructures of targeted molecules, and therefore they have been extensively studied for the past couple of decades. Thus, **Chapter 3** presents the development of asymmetric catalysts based on Ru(II)-Pheox complexes, I developed a new series of Ru-$C_{olefin}(sp^2)$ bond-containing organometallic complexes and successfully applied them to the catalytic asymmetric inter- and intramolecular cyclopropanations, which are carbene transfer reaction. It is noteworthy that high yields and stereoselectivity were achieved for *trans*-cyclopropane carboxylates even with a low catalyst loading. Catalytic asymmetric cyclopropanations of diazoesters with olefins in the presence of the Ru-$C_{olefin}(sp^2)$-phenyloxazoline complexes proceeded smoothly to give the corresponding optically active cyclopropanes in high yields, with a *trans*/*cis* ratio 97/3 to >99/1 and 97% to >99% ee (*trans*). The enantioselectivities were affected by the geminal substituent on the Ru-C_{olefin} (sp^2) bond; the highest enantioselectivities were obtained when using Ru(II)-Prox catalyst with no substituent at the germinal position of the metal.

Furthermore, medium ring-containing organic molecules, such as seven-membered rings, are also the cornerstone of many bioactive natural compounds such as guaiane sesquiterpenes, guaianolide sesquiterpene lactones. However, there are few reports on their synthesis. Thus, the development of an efficient method to prepare these scaffolds has attracted a significant amount of research attention. This unique strategy toward seven-membered carbocycles has been utilized in natural product synthesis. In **Chapter 4**, I report the development of an intramolecular Buchner reaction of a variety of *N*-benzyl diazoamide derivatives in the presence of a chiral Ru(II)–Pheox catalyst. The aromatic rings are converted into the corresponding γ-lactam ring fused seven-membered ring system with high regio- and stereoselectivity. A variety of γ-lactam fused 5,7-

bicyclic-heptatriene derivatives have been prepared from diazoacetamides in up to 99% yield with high enantioselectively (up to 99% ee) using a chiral Ru(II)-Pheox catalyst under mild reaction conditions.

In conclusion, **Chapter 5**, the Ru(II)−Pheox catalyzed C-H insertion reaction and asymmetric Buchner reaction proved to be the efficient and straightforward methods for the preparation of oxindole and seven-membered ring which are important intermediates in the synthesis of many biologically active compounds. Moreover, we have successfully designed and synthesized a novel Ru-Prox type catalyst. This catalyst showed excellent reactivities and selectivities in asymmetric cyclopropanation reactions. And it is expected to provide many further opportunities in asymmetric catalysis.

And in **Chapter 6,** all the experimental and analytical data as the evidence for Chapter 2 to 4 are described.

LIST OF SCHEMES

LIST OF FIGURES

LIST OF TABLES

LIST OF ABBREVIATIONS

Ar	aryl
atm	atmosphere
Bn	benzoyl
Bu	butyl
Calcd	calculated
Conc.	concentrated
d	doublet
dd	doublet of doublet
DFT	density functional theory
dr	diastereomeric ratio
dt	doublet of triplet
EDA	ethyl diazo acetate
ee	enantiomeric excess
EDG	electron-donating group
EPR	electron paramagnetic resonance technique
equiv.	equivalent
ESI-MS	electrospray ionization – mass spectrometry technique
Et	ethyl
Et_3N	triethyl amine
EtOAc	ethyl acetate
EWG	electron-withdrawing group
g	gram
h	hour
HPLC	high performance liquid chromatography
Hz	hertz
*i*Pr	isopropyl
IR	infrared
m	multilplet
M	molar
Me	methyl

mg	milligram
MHz	megahertz
min	minute
mL	milliter
mmol	millimole
Mp	melting point
NMR	nuclear magnetic resonance
Ph	phenyl
ppm	parts per million
q	quartet
R_f	retention factor (in chromatography)
rt	room temperature
s	singlet
t	triplet
*t*Bu	tertiary butyl
td	triplet of douplet
temp.	temperature
tert	tertiary
THF	tetrahydrofuran
TLC	thin layer chromatography
TMS	tetramethylsilane
tR	retention time
U.V	ultra violet

NOTATIONS

α	alpha
$[\alpha]_D$	specific rotation
^{1}H NMR	proton nuclear magnetic resonance spectroscopy
^{13}C NMR	carbon nuclear magnetic resonance spectroscopy
^{19}F NMR	flourine nuclear magnetic resonance spectroscopy

^{31}P NMR	phosphorus nuclear magnetic resonance spectroscopy
Å	Angstrom (10^{-10} m)
β	beta
%	percentage
J	coupling constant
$[M + H]^+$	protonated molecular ion (mass spectrometry)
δ	chemical shift
^oC	degree Celsius

CHAPTER 1

Introduction

1.1 Carbenes

Carbene is a neutral and divalent carbon active species. The general formula is R-(C:)-R' or R=C:. The term "carbene" may also refer to the specific compound H_2C:, also called methylene, the parent hydride from which all other carbene compounds are formally derived. Carbenes are classified as either singlets or triplets, depending upon their electronic structure. If the non-bonding electrons have parallel spins, it is the singlet carbene while the non-bonding electrons have parallel spins in different orbitals, it is the triplet carbene.

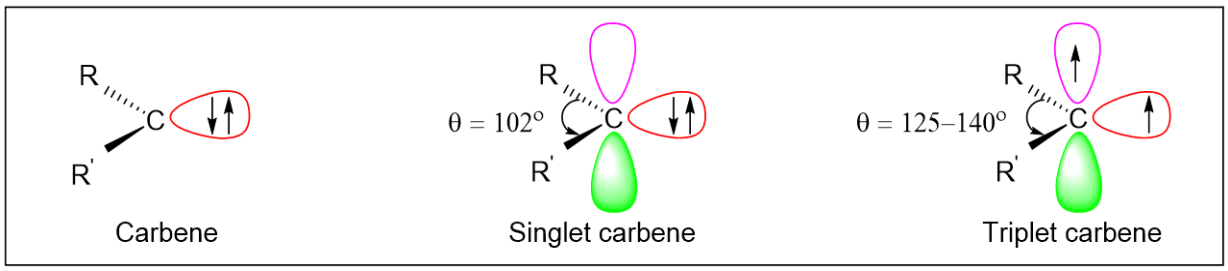

Figure 1. The electronic structure of carbenes.

Triplet carbenes are paramagnetic and may be observed by electron spin resonance spectroscopy if they persist long enough. Bond angles are 125-140° for triplet methylene and 102° for singlet methylene. Triplet carbenes are generally stable in the gaseous state, while singlet carbenes occur more often in aqueous media (Figure 1). For simple hydrocarbons, triplet carbenes usually have energies 8 kcal/mol (33 kJ/mol) lower than singlet carbenes (see also Hund's rule of maximum multiplicity), thus, in general, the triplet is the more stable state (the ground state) and singlet is the excited state species. Substituents that can donate electron pairs may stabilize the singlet state by delocalizing the pair into an empty p-orbital. If the energy of the singlet state is sufficiently reduced it will actually become the ground state.

1.1.1. The history of carbenes

In 1885, the first assumption of a carbene species was reported by Geuther and Hermann.[1] They suggested that the alkaline hydrolysis of chloroform proceeds though the formation of a reaction intermediate with a divalent carbon called dichlorocarbene. In 1897, Nef proposed the same reaction intermediate for the Reimer–Tiemann reaction and the transformation of pyrrol to -

chloropyridine in chloroform[2]. They both showed a lot of intuition and courage for their postulations considering that most chemists did not even believe in the existence of free radicals at that time.

Indeed, it was only 3 years later that Gomberg characterized the first example of a free radical, triphenylchloromethylene **2** (Scheme 1), through elemental analysis and chemical reactivity[3]. Its discovery was freshly welcomed by the scientific community[4]. Prior to the Great War, Staudinger and Kupfer contributed to the recognition of carbenic reaction intermediates by studying the formation of methylene derivatives[5] and diazomethane[6].

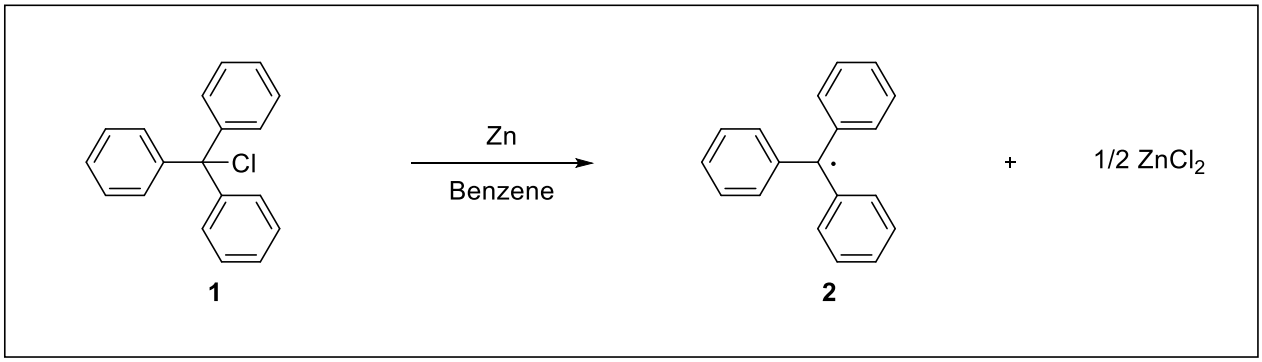

Scheme 1. Generation of the first stable radical.

Throughout the 1920s and 1930s, the existence of free radicals was finally well recognized, and their use in organic chemistry as reaction intermediates was growing extremely rapidly[4]. In this context, carbene moieties were regarded as diradicals[7]. The methylene carbene was seen as a linear species, with two degenerate p-orbitals inevitably leading to a triplet state[8]. At the beginning of the 1950s, there was a resurgence of interest in the organic chemical reactions of carbenes[9]. In 1953, Doering and Knox disclosed an elegant synthesis of tropolones **3** via an addition of methylene to substituted benzene (Scheme 2)[10].

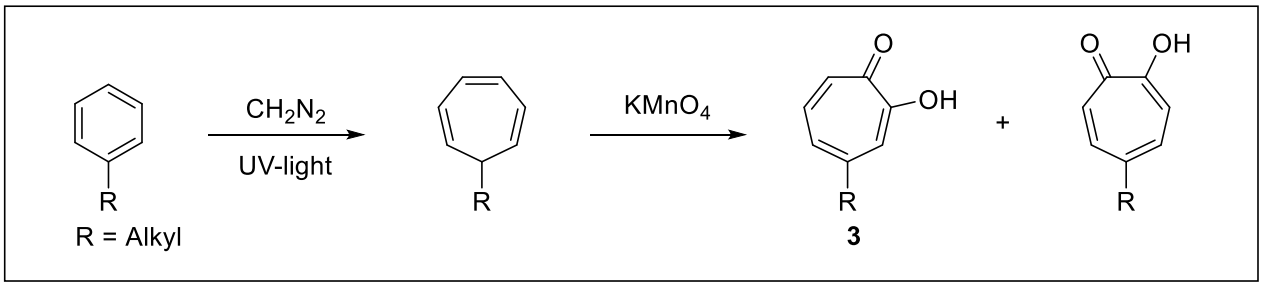

Scheme 2. Synthesis of tropolone-derivatives via the insertion of a methylene intermediate.

The most important contribution of Doering and his collaborators came a year later when they proved the existence of a dibromomethylene intermediate **5**, in the first cyclopropanation product **6** operating via the addition of bromoform to an alkene **4** (Scheme 3)[11].

Then more organic synthesis involving the use of methylene were reported[12], prompting chemists and physicists to have a closer look at this carbenic intermediate.

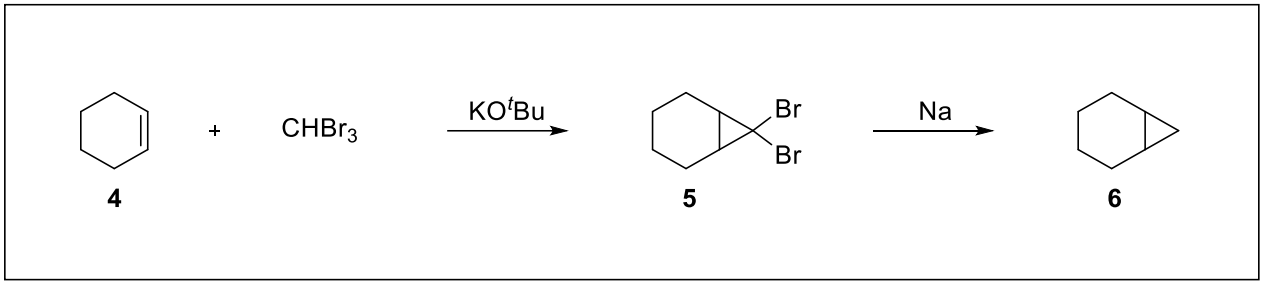

Scheme 3. Alkene cyclopropanation via methylene intermediate.

1.1.2. Carbene–metal bond formation

The formation of the C–M bond of a carbene–metal complex by orbitals overlapping requires a narrowing of the valence angle (XCY) at the carbene center [13]. Carbenes stabilized by the donation from both -groups (+M/+M), such as diaminocarbenes or dialkoxycarbenes, adopt a bent geometry with a small valence angle at the central carbon [14]. They have the required geometry to strongly and easily bind a metal fragment. In contrast push–pull carbenes, alkylidenes, and triplet carbenes adopt a widened valence angle and tend to be linear [14]. They do not have adequate geometry to bind the metal fragment and any changes of conformation to narrow their valence angle are energetically unfavorable [13]. Consequently, they are very reluctant to form a metal complex and give a weaker metal–carbon bond.

1.1.3. Fischer carbene complexes

Well-stabilized heteroatomcontaining singlet carbenes, such aminocarbenes, and alkoxycarbenes have a significant gap between their singlet and triplet ground states [15]. They form a metal–carbon bond constituted by mutual donor–acceptor interaction of two closed-shell (singlet) fragments. The dominant bonding arises from carbene–metal π-donation and simultaneously from metal–carbene π-back donation (Scheme 4) [16].

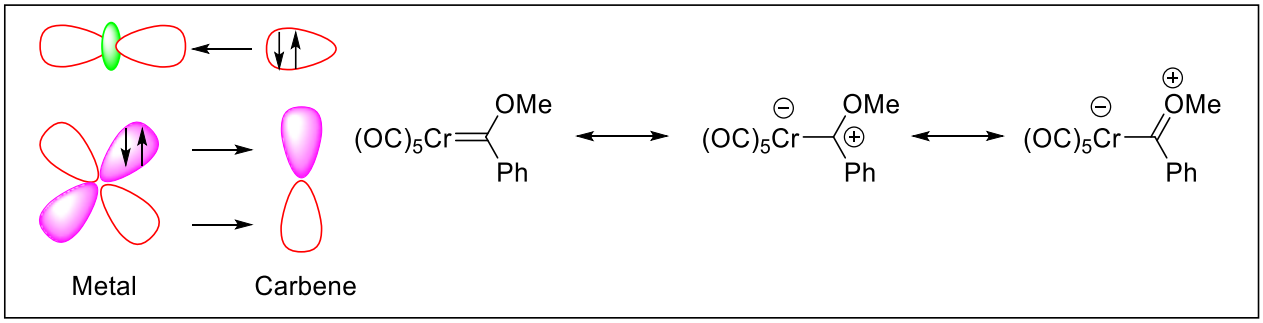

Scheme 4. Metal–carbon bonding in Fischer carbene complexes.

The π-electrons are usually polarized toward the metal and the carbon–metal bond has a partial double bond character, which diminishes with the stabilization of the carbene by its -groups [16, 17]. For instance, in diaminocarbenes, including NHCs, the metal–carbon bond is seen as a simple bond; the π-back donation is usually weak because the carbenic carbon is already well stabilized by π-donation from its amino-groups [18, 19]. Fischer carbene complexes are electrophilic at the carbon–metal bond and are prone to nucleophilic attack at the carbene center (OMe/NMe_2 exchange for instance) [13, 16, 18]. They are associated with low oxidation state metals [16, 18, 19].

1.1.4. Schrock carbene complexes

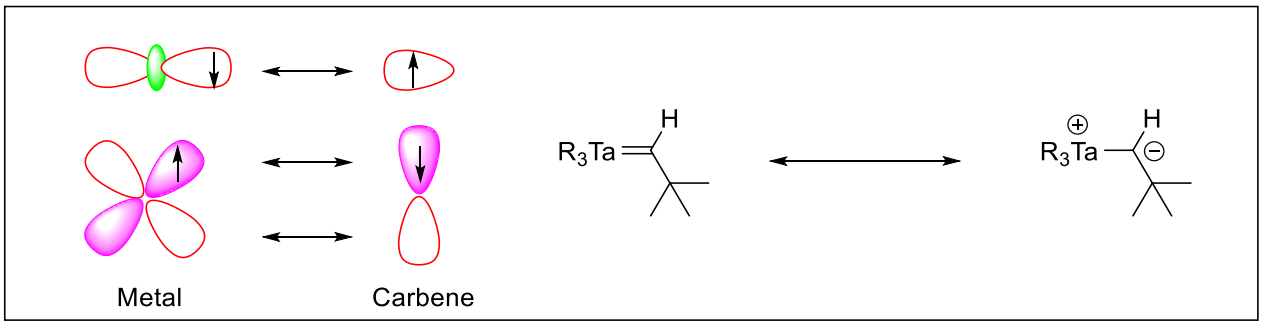

Scheme 5. Metal–carbon bonding in Schrock carbene complexes.

Poorly stabilized carbenes such as dialkylcarbenes or alkylidenes have a small gap between their singlet and triplet ground state. They form a covalent metal–carbon bond in nature created by the coupling of two triplet fragments (Scheme 5) [13b, 20]. The *π*-electrons are nearly equally dis tributed between the carbon and the metal, and the metal–carbon bond is seen as a true double bond.[16, 20] Schrock carbene complexes are nucleophilic at the carbon–metal bond and are susceptible to react at the carbene center with electrophiles as in a Wittig reaction involving a ylide

instead of a carbene.[18] They are found exclusively among early transition metals with the highest oxidation state.[16]

1.1.5. Generation of carbene

A method that is broadly applicable to organic synthesis is induced elimination of halides from gem-dihalides employing organolithium reagents. It remains uncertain if under these conditions free carbenes are formed or metal-carbene complex. Nevertheless, these metallocarbenes (or carbenoids) give the expected organic products.

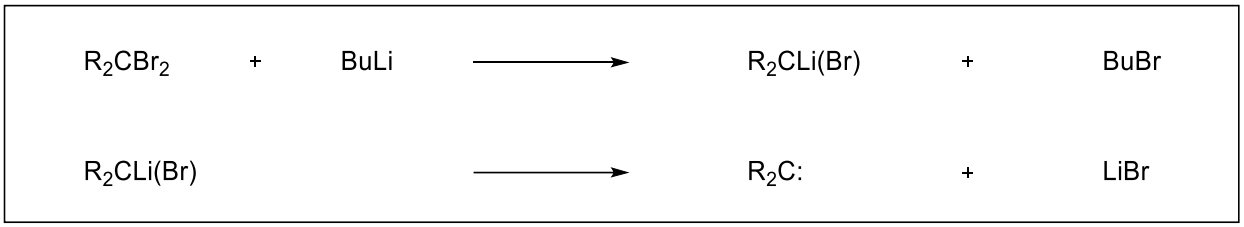

Scheme 6. Generation of carbene.

For cyclopropanations, zinc is employed in the Simmons–Smith reaction. In a specialized but instructive case, alpha-halomercury compounds can be isolated and separately thermolyzed. Most commonly, carbenes are generated from diazoalkanes, via photolytic, thermal, or transition metal-catalyzed routes. Catalysts typically feature rhodium and copper.

1.2. Diazocarbonyl compounds

The chemistry of diazocarbonyl compounds has a long history.[22] It has attracted the researchers owing to their diverse applications in organic synthesis. Curtius reported the first synthesis of α-diazo carbonyl compound in 1883. It involved the diazotization of the natural α-amino acid Glycine to give ethyl diazoacetate. In 1912, Wolff discovered the well-known rearrangement that bears his name, 'Wolff Rearrangement'. But, the availability of a wide range of diazo compounds came about as a result of the works of Arndt and Eistert and Bradley and Robinson. Since then, the diazo moiety has become very popular.

1.2.1. Properties of α-diazo carbonyl compounds

In 1935, Boetsch did an electron diffraction experiment, and in 1957, Clusius proceeded a subsequent labeling experiment. They proved that the correct structure for aliphatic diazo

compounds is the linear structure.[22] The bonding structure of α-diazo carbonyls is described by the resonance structures shown in Scheme 7.

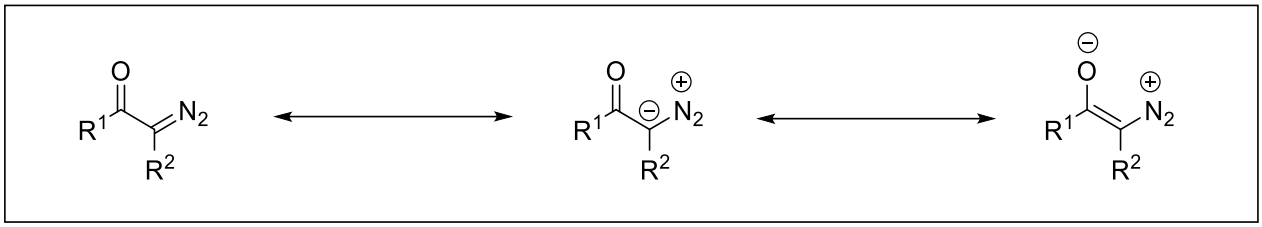

Scheme 7. The resonance structures of α-diazo carbonyls.

Most aliphatic diazo compounds have yellow to red color and absorb strongly in the IR region from 1950 to 2300 cm^{-1} which is assigned to the N-N stretching mode. In ^{13}C NMR spectra, the signal for the diazo carbon of diazomethane appears at $\delta = 23.1$ ppm relative to TMS, whereas for α-diazo carbonyl compounds the diazo carbon signal is shifted downfield.[23]

In general, the thermal stability of diazo compounds varies very much with substituents attached to the diazo group. Substituents with electron acceptor ability make α-diazo carbonyl compounds less thermally stable via stabilizing the resonance contributing structure (Scheme 7) through delocalization of the charge and hence favoring the nitrogen elimination.

1.2.2. Reactivity of α-diazo carbonyl compounds

Reactions of diazo carbonyl compounds proceed via thermal, photochemical or catalytic expulsion of nitrogen ($-N_2$), which will lead to give different types of reactive intermediates. For example, free carbenes, metal carbenoids, carbonyl ylides, and diazonium ions (Figure 2).

Figure 2. Intermediates of α-diazo carbonyls.

These reactive intermediates lead to a wide variety of reactions, which can be organized into the following categories: 1,3-dipolar cycloaddition reactions of the diazo group, [3+2] cycloaddition reactions of carbonyl ylides from carbene intermediates, cyclopropanations,

aromatic cycloadditions, insertion into X-H (X = C, O, S, N) bonds, Wolff rearrangements, ylide formation and its subsequent reactions, α,α-substitution reactions and oxidation of the α-diazo group (Scheme 8).[22c]

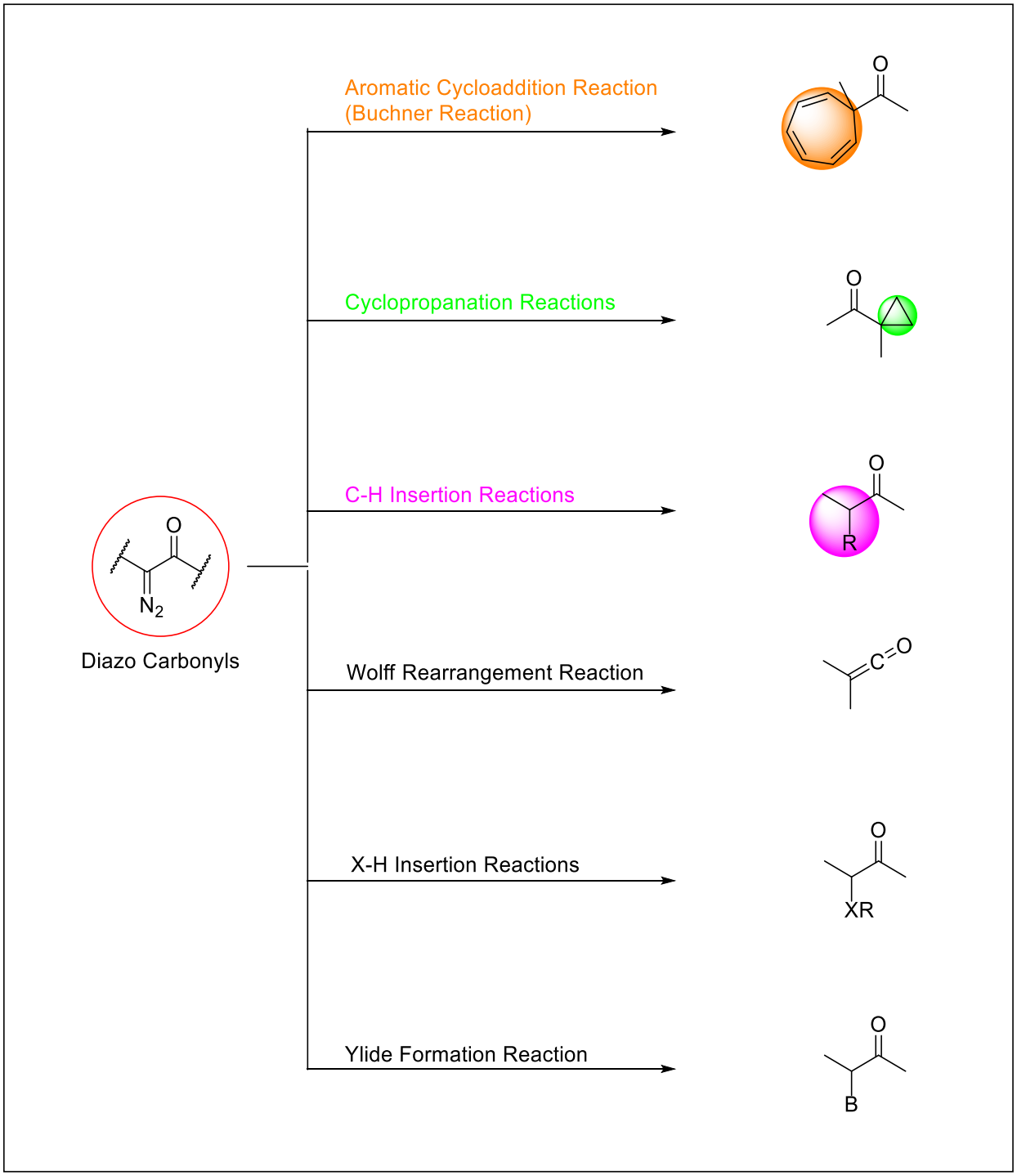

Scheme 8. Reactivity of α-diazo carbonyls.

Catalytic aromatic cycloaddition and cyclopropanation reactions of α-diazo carbonyl compounds will be explained in detail since they relate to the chemistry to be discussed in this dissertation.

1.3. Transition–metal–catalyzed aromatic C−H insertion reactions

Reactions of α-diazo carbonyl compounds with aromatic substrates leading to aromatic substitution products is a significant pathway which, depending on the substrate structure, can compete effectively with the aromatic cycloaddition process. In some cases, exclusive aromatic substitution is observed, while in other mixtures of products are formed. Although incorrectly termed C−H insertion, the process differs mechanistically from aliphatic C−H insertion in that aromatic C−H insertion is believed to involve the formation of a zwitterionic intermediate from electrophilic addition of a metal carbene to the aromatic ring and a subsequent rapid proton transfer.[46, 47]

These types of reactions, which can proceed both in an intermolecular and in an intramolecular fashion, are a powerful synthetic tool by which C−C bonds can be formed between two sp^2-hybridized carbons under relatively mild conditions. These reactions have been traditionally carried out in the presence of a transition metal catalyst, usually, rhodium or copper.

1.3.1. Intermolecular aromatic C−H insertion reactions

The area of intermolecular aromatic substitution has received increased attention in recent years. In there, gold, copper, and rhodium complexes have emerged as potentially useful catalysts for intermolecular aromatic substitution reactions.[49−52]

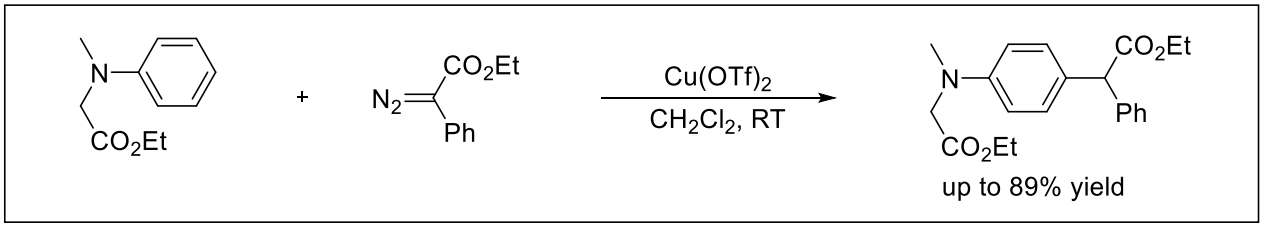

Scheme 9. Copper-Catalyzed Intermolecular Aromatic Substitution Reaction.

Tayama and coworkers reported high yields in the intermolecular reactions of α-diazoesters with N,N-disubstituted anilines (Scheme 9).[48] Reactions were carried out in the presence a range

of Lewis acid catalysts, and were found to proceed efficiently and with high yields in the presence of $Cu(OTf)_2$.

Diaz-Requejo and Perez found that that the complex IPrAuCl in the presence of Na(BARF) as a halide scavenger promoted the conversion of toluene and ethyl diazoacetate into a 4:1 mixture of aromatic C−H functionalization product and cycloheptatriene product (Scheme 10). [49,50]

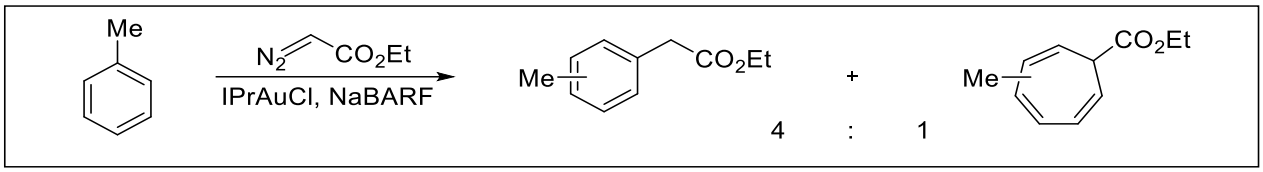

Scheme 10. Gold-catalyzed reaction of EDA with toluene.

On another hand, Li *et* al reported that rhodium(III)-catalyzed intermolecular aromatic C−H functionalization reactions of diazocarbonyl compounds with aromatics bearing azacycle directing groups. The range of azacycle directing groups included pyrazoles, pyrimidines, and oxazoles (Scheme 11).[53]

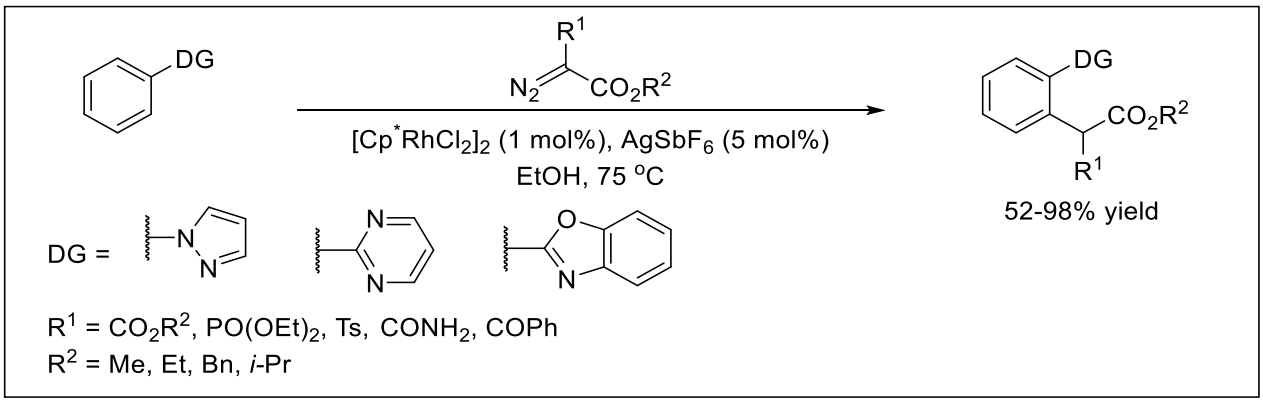

Scheme 11. Catalyzed azacycle-directed intermolecular aromatic C−H functionalization.

1.3.2. Intramolecular aromatic C−H insertion reactions

The intramolecular aromatic substitution reaction has been more extensively investigated than its intermolecular counterpart. It represents a versatile method of annulation of a benzene nucleus and has much appeal in medicinal heterocyclic chemistry. A number of successful reactions involving the formation of [6,5]-bicyclic systems have been reported, allowing the formation of both carbocyclic and heterocyclic systems such as indanones,[54] oxindoles,[55−60]

benzofuranones,[61] and sultans.[62] Formation of other bicyclic systems, such as [6,6]-bicycles, is possible; however, competition between reaction pathways may occur in such cases.[63–65]

The reactions of α-diazo-β-ketoesters leading to 4-carbonylchromane derivatives were investigated and were found to be more selective than their nitrogen-based counterparts, achieving yields up to 97%. (Scheme 12).[65]

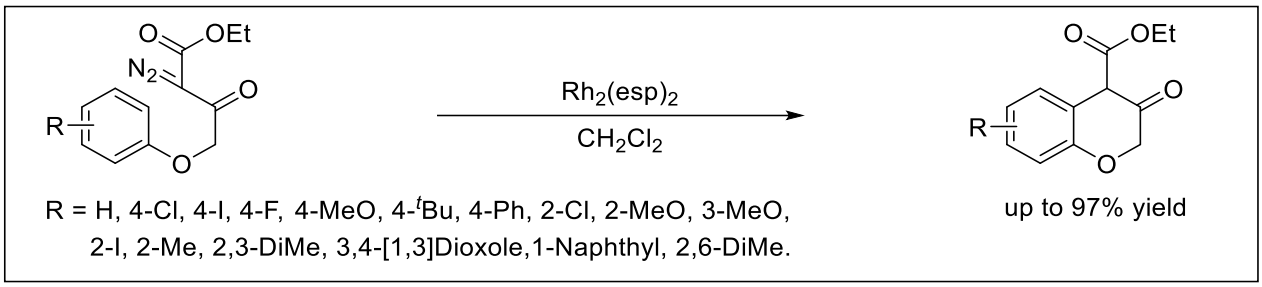

Scheme 12. Rhodium(II)-catalyzed aromatic substitution reactions of α-diazo-β-ketoesters.

Traditionally, intramolecular aromatic substitution reactions have been carried out in the presence of rhodium(II) or copper catalysts. However, in recent times other metals have emerged as potentially useful catalysts for this type of transformation, although, in most instances, these catalysts have seen themselves restricted to certain diazocarbonyl substrates. Rhodium,[48,55,66] copper,[59] ruthenium,[58] and silver[57] catalysts have all found applicability in reactions involving α-diazo-β-ketoanilides forming [6,5]-bicyclic products.

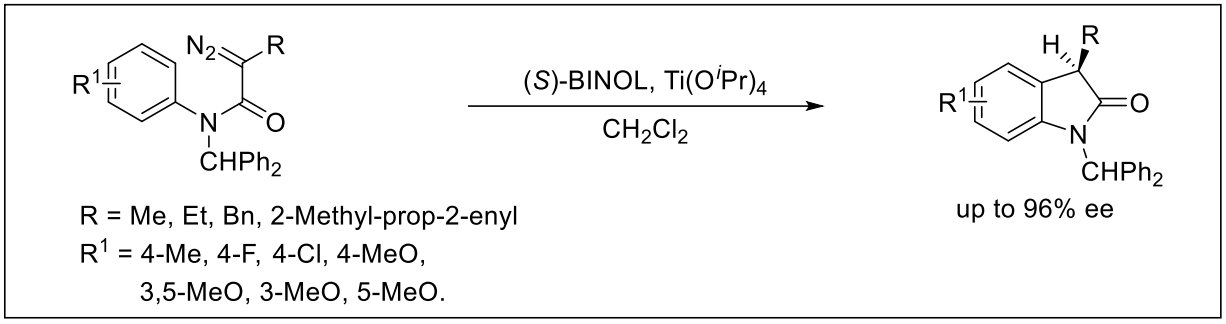

Scheme 13. Titanium BINOLate-catalyzed enantioselective intramolecular aromatic C–H functionalization.

A titanium complex has also recently been reported as a successful catalyst for these types of substrates.[60] The reactions were found to proceed efficiently, resulting in oxindoles in both high yields and high enantioselectivities (Scheme 13).

1.4. Cyclopropanations

The cyclopropane subunit is present in many biologically important compounds including terpenes, pheromones, fatty acid metabolites, and unusual amino acids [67], and it shows a large spectrum of biological properties, including enzyme inhibition and insecticidal, antifungal, herbicidal, antimicrobial, antibiotic, antibacterial, antitumor, and antiviral activities. This fact has inspired chemists to find novel and diverse approaches to their synthesis, and thousands of cyclopropane compounds have been prepared. In particular, naturally occurring cyclopropanes bearing simple or complex functionalities are chiral compounds; thus, the cyclopropane motif has long been established as a valuable platform for the development of new asymmetric technologies. The enantioselective synthesis of cyclopropanes has remained a challenge, since it was demonstrated that members of the pyrethroid class of compounds were effective insecticides.[68]

1.4.1. Simmons–Smith cyclopropanation

In the late 1950s, Simmons and Smith discovered that the reaction of alkenes with diiodomethane in the presence of activated zinc afforded cyclopropanes in high yields. The reactive intermediate is an organozinc species, and the preparation of such species, including $RZnCH_2I$ or $IZnCH_2I$ compounds and samarium derivatives, was developed in the following years. The popularity of the Simmons–Smith reaction arose from the broad substrate generality, the tolerance of a variety of functional groups, the stereospecificity with respect to the alkene geometry, and the *syn*-directing and rate-enhancing effect observed with proximal oxygen atoms.[69]

In spite of the practical importance of the asymmetric Simmons-Smith cyclopropanation, the reaction pathway is not completely clear yet.[70] Theoretically, the Simmons–Smith cyclopropanation can proceed via a concerted [2+1] methylene transfer (Scheme 14, path A), in which the pseudo-trigonal methylene group of a halomethylzinc halide adds to an alkene π-bond and forms two new carbon-carbon bonds simultaneously, accompanying a 1,2-migration of the halide anion from the carbon to the zinc atom. Alternatively, a [2+2] carbometallation mechanism, in which the halomethyl group and the zinc halide add to both termini of the alkene π-bond followed by intramolecular nucleophilic substitution of the pseudo-carbanion, can be supposed (Scheme 14, path B). Experimental studies show that, using a zinc carbenoid, the cyclopropanation very likely proceeds by the [2+1] pathway, primarily because the carbon-zinc bond is covalent and

unpolarized. In 2003, Nakamura et al. studied the reaction pathways of cyclopropanation using the Simmons–Smith reagent by means of the B3LYP hybrid density functional method, confirming that the methylene-transfer pathway was the favored reaction course.[70]

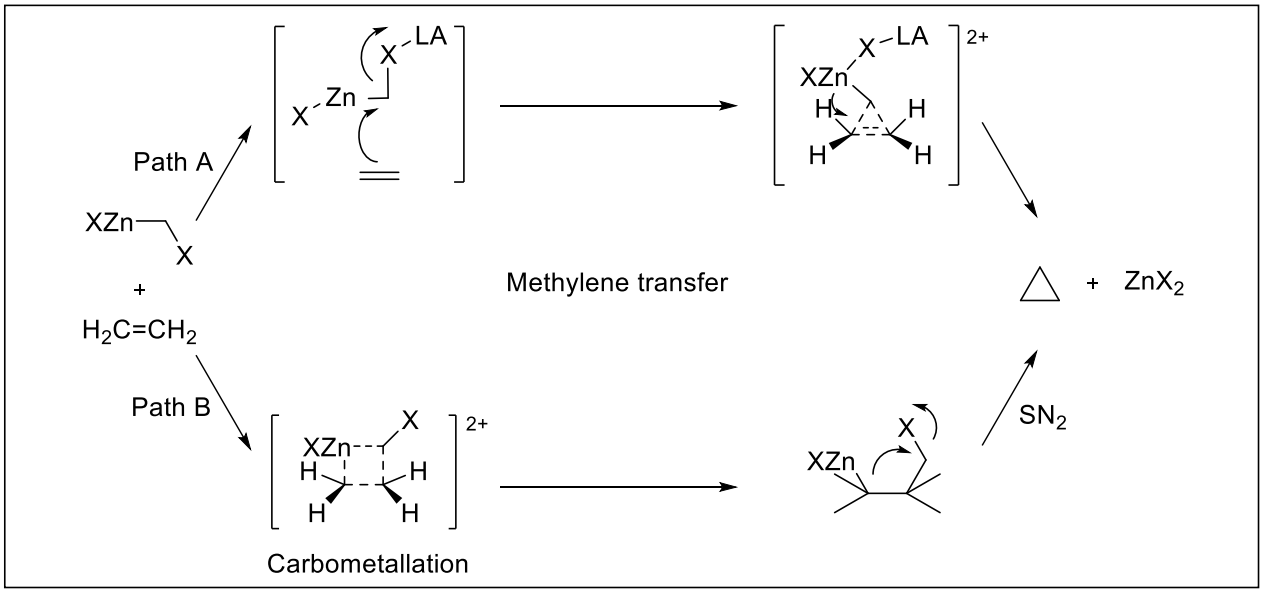

Scheme 14. Possible mechanisms for the Simmons–Smith reaction

It took place through two stages, an SN_2-like displacement of the leaving group by the olefin, followed by cleavage of the C-Zn bond to give the cyclopropane ring. However, the alternative carbometallation and cyclization pathway was found to be preferred when the carbon-metal bond is more polarized, such as in lithium carbenoids, and this hypothesis has received experimental support.[71]

Kinetic studies on the cyclopropanation of dihydropyrroles show an induction period that is consistent with a change in the structure of the carbenoid reagent during the course of the reaction. This mechanistic transition is associated with an underlying Schlenk equilibrium that favors the formation of monoalkylzinc carbenoid $IZnCH_2I$ relative to dialkylzinc carbenoid $Zn(CH_2I)_2$, which is responsible for the initiation of the cyclopropanation. Density functional theory (DFT) computational studies were also conducted to study the factors influencing reaction rates and diastereoselectivities.[72]

1.4.2. Transition-metal-catalyzed decomposition of diazoalkanes

Since the pioneering work of Nozaki et al. in 1966,[73] the transition-metal catalyzed cyclopropanation of alkenes with diazo compounds has emerged as one of the most highly effective and stereocontrolled routes to functionalized cyclopropanes.

The diasterocontrol in the cyclopropanation is often governed by the particular substituents on both the alkene and the diazo compounds, and thus, the catalyst must be cleverly designed in order to enhance selective formation of *cis* versus *trans* or *syn* versus *anti*-cyclopropanes. As already seen in the previous section, the most ancient attempts to achieve enantioenriched cyclopropanes used chiral auxiliaries. Since the 1990s, many chiral ligands surrounding the metal center of the catalyst have been introduced for obtaining the enantiocontrol. The accepted catalytic cycle of the carbenoid cyclopropanation reaction involves interaction of the catalyst with the diazo precursor to afford a metallo-carbene complex followed by transfer of the carbene species to the alkene (Scheme 15).

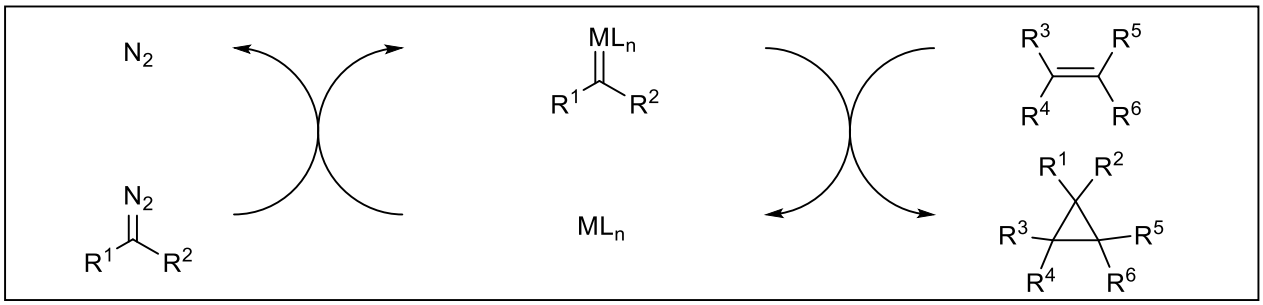

Scheme 15. Accepted catalytic cycle for the carbenoid cyclopropanation reaction

The type of the reaction to be carried out (inter- vs intramolecular) plays a key role in the appropriate selection of the most efficient catalyst for a given transformation. In light of this, this section is divided into inter- and intramolecular cyclopropanation reactions, and in each subsection, chiral auxiliaries are described before and then chiral ligands are listed according to the involved metal ion.

1.4.2.1. Cobalt

Cobalt complexes have been shown to be reactive catalysts for the α-diazoester decomposition, leading to a metal carbene that could convert alkenes to cyclopropanes. The mechanism of this reaction was examined by EPR and electrospray ionization–mass spectrometry

(ESI-MS) techniques, especially when cobalt–porphyrin catalysts were used, and evidence for a two-step mechanism was uncovered (Scheme 16).[74]

The first step is an adduct formation that could exist as two isomers: the "terminal carbene" and the "bridging carbene." In the former, the "carbene" behaves as a redox noninnocent ligand having a d6 cobalt center and the unpaired electron resides on the "carbene" carbon atom. In the latter, the "carbene" is bound to the metal and one of the pyrrolic nitrogen atoms of the porphyrin. DFT calculations suggested that the formation of the carbene is the rate-limiting step and that the cyclopropane ring formation proceeds by way of a stepwise radical process.

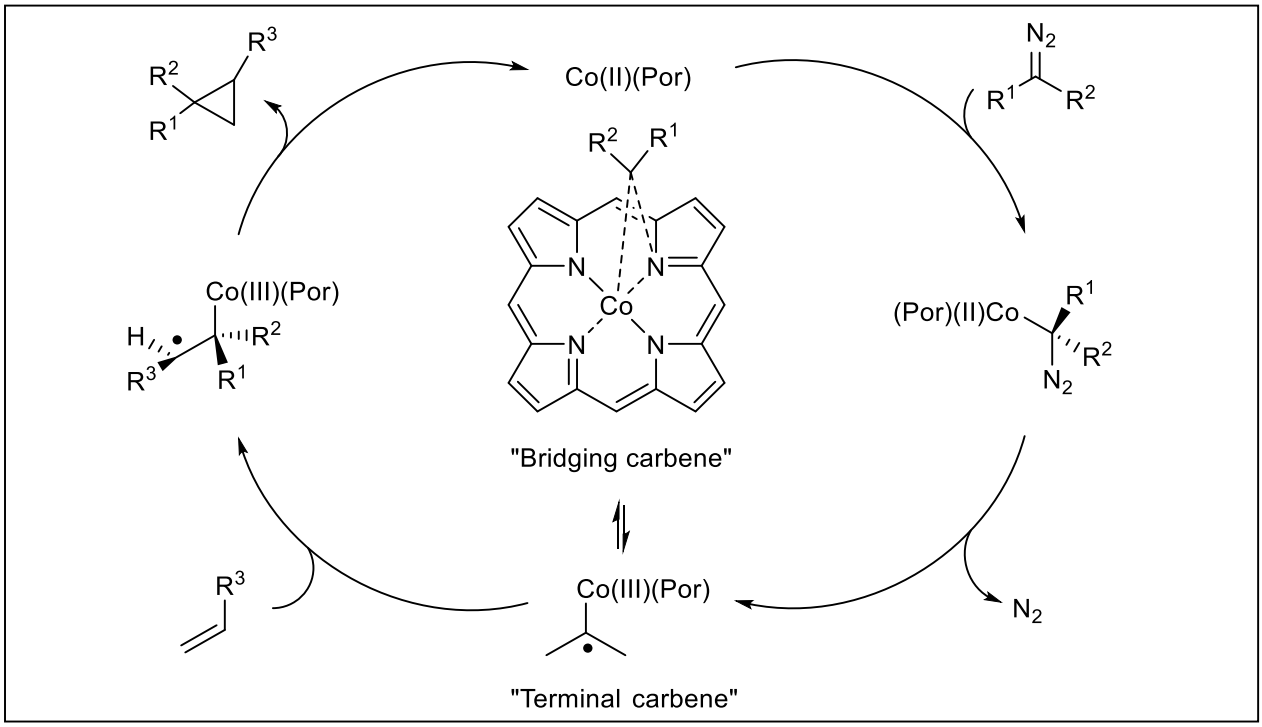

Scheme 16. Mechanism of cobalt–porphyrin catalysis.

1.4.2.2. Copper

Chiral copper-based catalysts are the most effective catalysts for the preparation of the trans-isomer of cyclopropanes with the widest reaction scope. Among them, nonracemic C2-symmetric bidentate bisoxazoline (box) ligands have been used in cyclopropanation reactions with copper for more than 30 years.[75] Many investigations have shown that the ligand structure has a strong influence on the stereoselectivity of the cyclopropanation. Even very small structural changes often have drastic and sometimes unpredictable effects on the enantioselectivity, and the

phenomenon comprehension is complicated by very low enthalpic barrier for the transition states leading to the *R*- and *S*-products.

However, since 2001, using DFT calculations, Salvatella and coworkers rationalized the stereochemical prediction of the cyclopropanation. The calculated relative energies are in good agreement with the experimental enantiomeric excesses as well as with the Z/E ratio. In 2004, Mend et al. studied again this reaction by means of DFT, showing that it was exothermic and that the turnover-limiting step was the formation of metal catalyst–cyclopropyl carboxylate complexes. Then, Maseras and coworkers found a barrier, which arises from the entropic term, in the Gibbs free-energy surface compatible with the experimentally observed enantioselectivity. The enantioselectivity of asymmetric catalysis was predicted based on quantitative quadrant-diagram representations of the catalysts and quantitative structure–selectivity relationship (QSSR) modeling.[76] The data set included 30 chiral ligands belonging to four different oxazoline-based ligand families. In a simpler approach, the derived stereochemical model indicated that an enantioselective catalyst could be obtained by placing very large groups at two diagonal quadrants and leaving free the two other quadrants. A higher-order approach revealed that bulky substituents in diagonal quadrants operate synergistically. Some chiral ligands for the copper-catalyzed cyclopropanation are listed in figure 3.

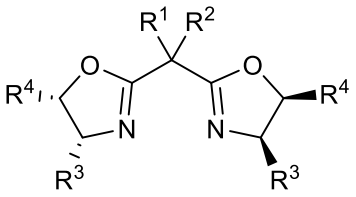

7 $R^1 = R^2 = Me$; $R^3 = {}^{i}Pr$; $R^4 = H$
8 $R^1 = R^2 = Me$; $R^3 = {}^{t}Bu$; $R^4 = H$
9 $R^1 = H$; $R^2 = Me$; $R^3 = {}^{t}Bu$; $R^4 = H$
10 $R^1 = R^2 = Me$; $R^3 = Ph$; $R^4 = H$
11 $R^1 = R^2 = H$; $R^3 = R^4 = Ph$

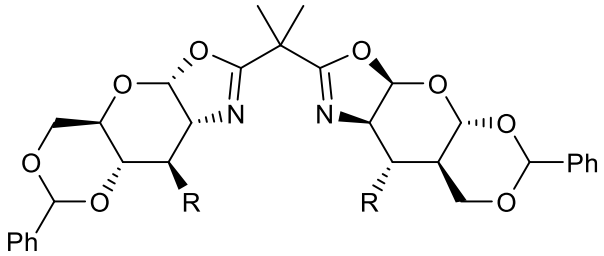

12 R = OCHO
13 R = O_2CMe

Figure 3. Box ligands' structures for asymmetric cyclopropane reactions.

Some of these copper(I)-box catalyzed reaction were then employed in multistep synthesis of natural products. For instance, cyclopropanation of furans was applied to the total syntheses of some key intermediates of natural products and drugs.[77]

For example, the cyclopropanation of *N*-Boc-3-methylindole yielded a key building block for the synthesis of the indole alkaloid (−)-desoxyeseroline in 59% overall yield with 96% ee (Figure 3).[78] Moreover, ligand box **7** (Figure 3) performed the stereoselective preparation of the tetracyclic core, and key intermediate, of cryptotrione (Figure 4) in 93% yield with >91:9 dr.

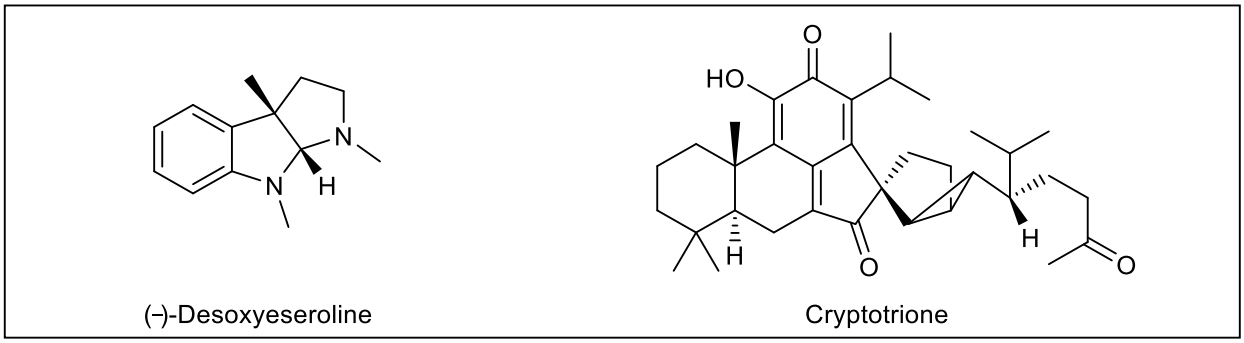

Figure 4. Some natural products prepared by copper-box-catalyzed cyclopropanation.

Diazoalkanes have been employed in copper–bisoxazoline-catalyzed cyclopropanations. For instance, α-diazophosphonate diazomethane was used to obtain cyclopropylphosphonate derivatives under entbox catalysis (Scheme 17a). Another example is the reaction of diazomethane with trans-cinnamate esters (Scheme 17b).[79]

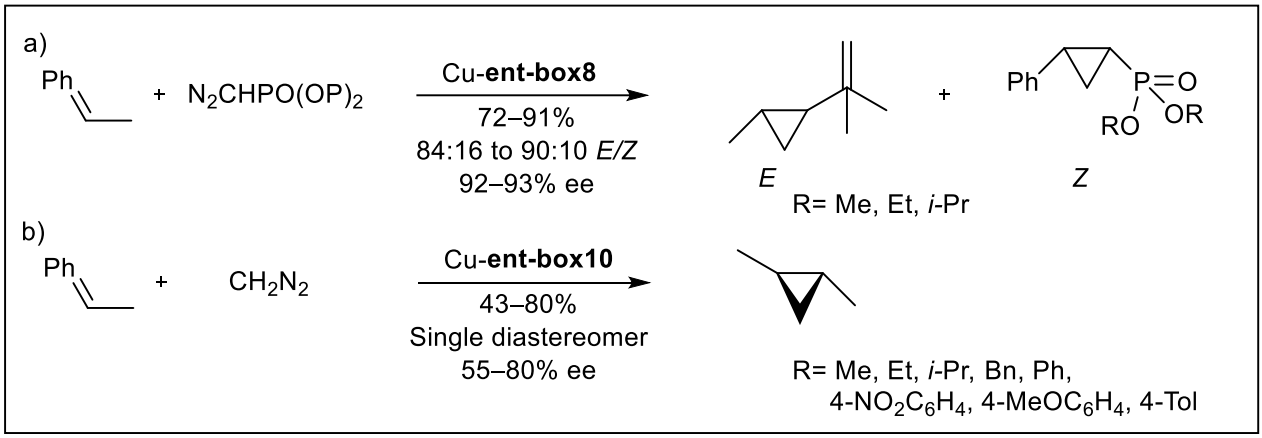

Scheme 17. Copper–bisoxazoline-catalyzed cyclopropanation of some diazoalkanes.

1.4.2.3. Rhodium

Rhodium-based chiral complexes were synthesized and tested in both inter- and intramolecular cyclopropanations. In particular, the development of dirhodium(II) carboxylate and carboxamidate catalysts (Figure 5) has resulted in many highly chemo-, regio-, and stereoselective reactions of α-diazocarbonyl compounds.[80]

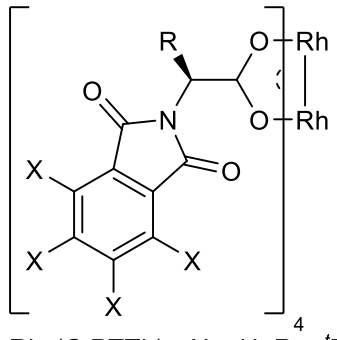

14 Rh_2(*S*-PTTL)$_4$: X = H, R = ^{t}Bu
15 Rh_2(*S*-TCPTTL)$_4$: X = Cl, R = ^{t}Bu
16 Rh_2(*S*-TBPTTL)$_4$: X = Br, R = ^{t}Bu

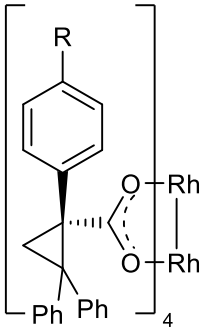

17 Rh_2(*R*-TPCP)$_4$: R = H
18 Rh_2(*R*-BTPCP)$_4$: R = Br
19 Rh_2(*R*-BPCP)$_4$: R = Ph

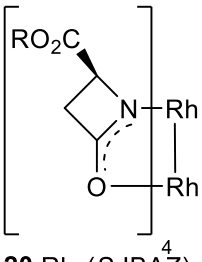

20 Rh_2(*S*-IBAZ)$_4$: R = ^{i}Bu
21 Rh_2(*S*-BNAZ)$_4$: R = Bn
22 Rh_2(*S*-MEAZ)$_4$: R = Me

Figure 5. Chiral dirhodium catalysts for asymmetric cyclopropanations.

Charette's research group found Rh_2(*S*-IBAZ)$_4$ as an efficient catalyst for cyclopropanation of α-cyanodiazophosphonate and α-cyanodiazoacetate.[81] The particular electrophilicity of cyanocarbene intermediates permitted the use of allenes as substrates, affording the first catalytic asymmetric alkylidene cyclopropanation reaction using diazo compounds. In fact, α-cyanocarbenes are forced to stay in-plane, conversely from other electron-withdrawing groups, which adopt an out-of-plane conformation. The in-plane conformation is highly energetic, thus leading to a more electron-deficient reactive carbene, allowing less nucleophilic *π*-systems such as allenes to react.

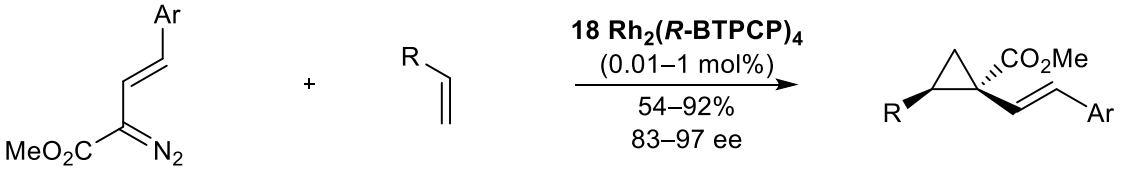

R = Ph, 4–$CF_3C_6H_4$, 4–$NO_2C_6H_4$, 4–ClC_6H_4, 3,4–$Cl_2C_6H_3$, 4–$MeOC_6H_4$, *o*–Tol, 2–$MeO_2CC_6H_4$, Bu
Ar = Ph, 4–$CF_3C_6H_4$, 4–ClC_6H_4, 3,4–$Cl_2C_6H_3$, 3,4–$(MeO)_2C_6H_3$

Scheme 18. Cyclopropanation of styryldiazoacetates.

Dirhodium complex Rh_2(*R*-BTPCP)$_4$ was found to be an effective chiral catalyst for the enantioselective cyclopropanation of styryldiazoacetates (Scheme 18).[82] DFT computational studies at the B3LYP and UFF levels suggested that when the carbenoid binds to the catalyst, two of the 4-bromophenyl groups rotate outward to make room for the carbenoid. Then, the ester group aligns perpendicular to the carbene plane and blocks attack on its side. Thus, the substrate approaches over the donor group, but it finds the Re-face blocked by the aryl ring of the ligand and only the Si-face open for the attack, in agreement with the observed absolute configuration of the product.

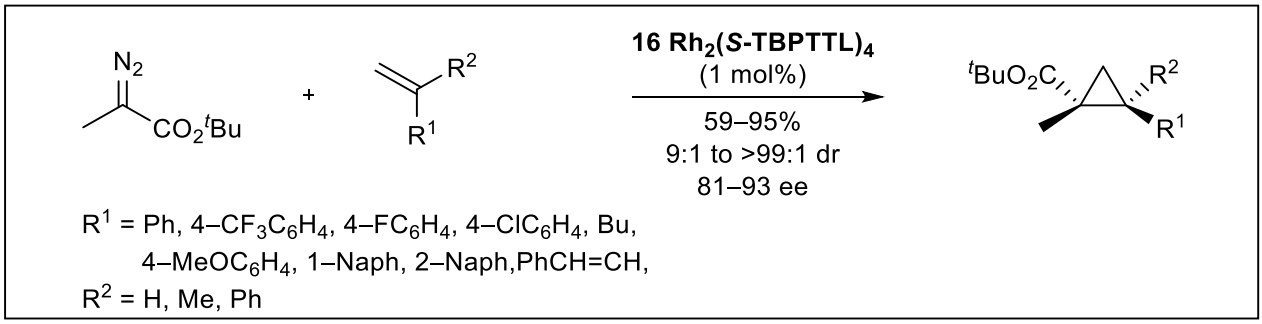

Scheme 19. Enantioselective cyclopropanation with α-diazopropionate.

Hashimoto described that the reaction of 1-aryl-substituted and related conjugated alkenes with tert-butyl α-diazopropionate by catalysis with Rh_2(*S*-TBPTTL)$_4$ led to the corresponding (1*R*,2*S*)-cyclopropanes containing a quaternary stereogenic center (Scheme 19).[83]

Awata and Arai achieved the asymmetric cyclopropanation of diazooxindoles with Rh_2(*S*-PTTL)$_4$ as the catalyst. Spirocyclopropyloxindoles, which constitute biologically important compounds, were obtained in good yield and diastereoselectivity (Scheme 20).[84] Then the mechanism of this reaction was detailed by DFT calculations, which demonstrated that the origin of the *trans*-diastereoselectivity lies in the π–π interactions between the *syn*-indole ring in carbenoid ligand and the phenyl group in styrene. The enantioselectivity could be ascribed both to steric interaction between the phenyl ring in styrene and the phthalimide ligand and to stabilization of π–π and CH–π interactions in the transition states.[85]

Charette's research group prepared various heteroleptic complexes and tested them in the cyclopropanation reaction of styrene with α-nitrodiazoacetophenones.[86] Thus, the replacement of one tetrachlorophthalimide ligand from **15** Rh_2(*S*-TCPTTL)$_4$ with phthalimide, succinimide, or

1,8-naphthalimide ligands did not significantly affect the asymmetric induction, whereas 2-naphthylacetate as the fourth ligand furnished a racemic product.

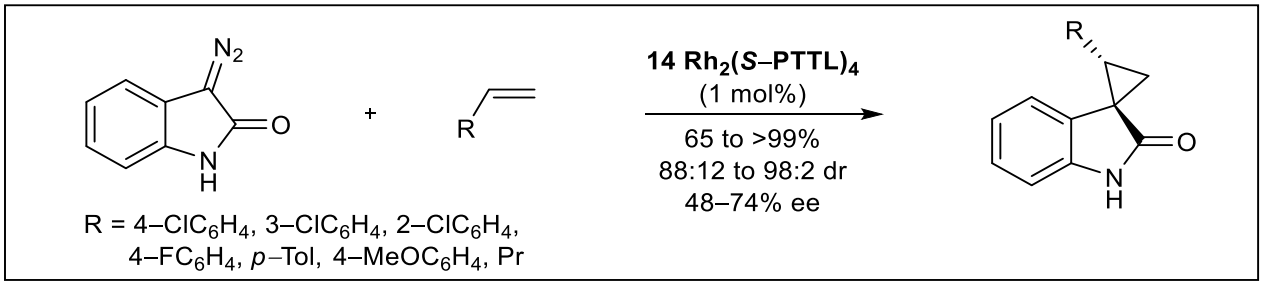

Scheme 20. Enantioselective synthesis of spirocyclopropyl oxindoles.

The absence of enantioinduction was ascribed to a lack of rigidifying halogen bonds in the 2-naphthylacetate complex and to the absence of the *N*-imido moiety evidently necessary in all ligands to achieve a high asymmetric induction, independently of whether or not the fourth carboxylate is chiral. Charette also found that the asymmetric induction increased, replacing one of the four chiral ligands with a ligand that has a gem-dimethyl group instead of the chiral center, because of a conformational change in the catalyst owing to the presence of the two methyl groups in the fourth ligand.

Finally, just one rhodium(I) chiral catalyst was reported for the cyclopropanation of alkenes with dimethyl diazomalonate (Scheme 21).[87] By using the (*R*,*R*)-configured tetrafluorobenzobarrelene complex, the *S*-configured cyclopropanes have been recovered. The reaction of α-methylstyrene gave only 57% ee, and in the reaction of 4-phenylbut-1-ene, as the representative of aliphatic alkenes, the enantioselectivity and yield were both low. Experimental evidence supported a transition state wherein the carbonyl oxygen on the ligand was coordinated to the rhodium(I) center. An active single coordination site on the rhodium cation was essential for the catalytic activity. In fact, the more bonded chloride ion, instead of the tetraborate, was not catalytically active.

1.4.2.4. Ruthenium

Many highly active and selective homogeneous ruthenium catalysts have been introduced for the asymmetric cyclopropanation of alkene.[88] Indeed, ruthenium has emerged as an important catalyst metal for the carbenoid chemistry of diazo compounds, besides copper and rhodium. However, a significant drawback of Ru catalysts is the rather low electrophilic character of the

presumed ruthenium–carbene intermediates, which often restricts the application to terminal activated alkenes and double bonds with a higher degree of alkyl substitution.

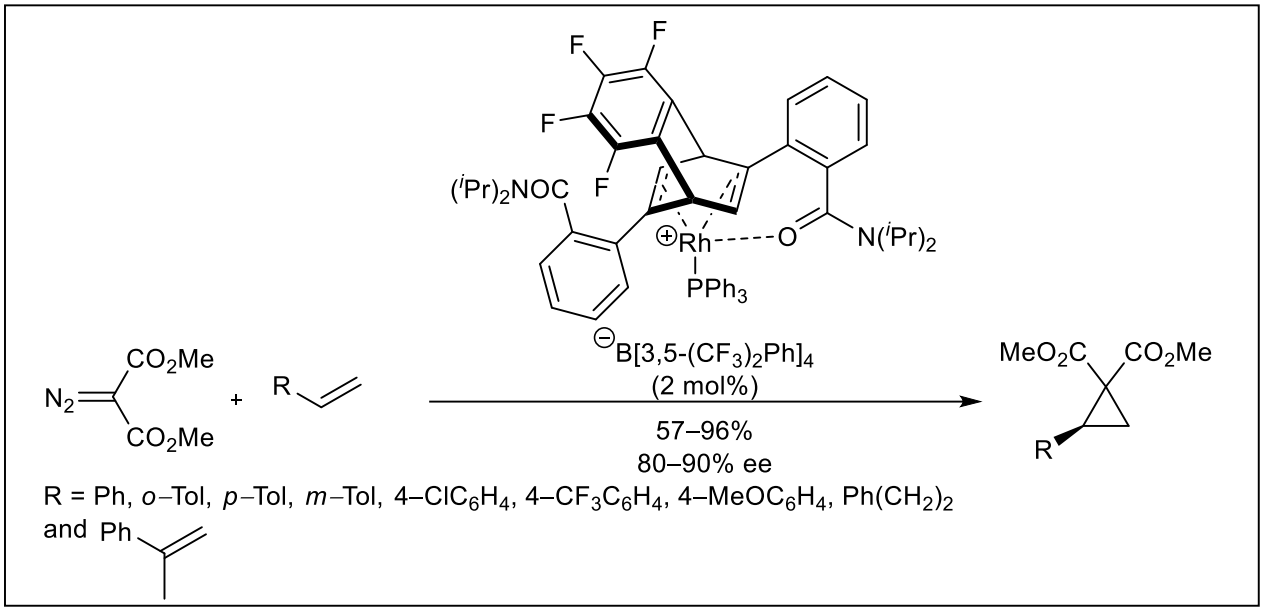

Scheme 21. Asymmetric cyclopropanation catalyzed by a rhodium(I) complex.

Another limitation of some ruthenium complexes is the ability to catalyze other alkene reactions as well as cyclopropanation leading to many by-products. However, if ruthenium catalysts work successfully, they often rival rhodium catalysts in terms of effectiveness and relative, as well as absolute, stereochemistry. Some methods of heterogenization of ruthenium catalysts, for instance, supporting them on polymer or porous silica supports, have been investigated. Their activity, selectivity, and recyclability have all been compared to those of the analogous homogeneous catalysts.

Garcia and coworkers reported an extensive comparison of the two enantioselective catalytic systems Ru-Pybox and Cu-box complexes by *ab initio* calculations in the cyclopropanation of alkenes with methyl diazoacetate. Later, Deshpande et al. used Nishiyama's catalyst to catalyze the cyclopropanation of styrene with EDA, providing the corresponding trans-cyclopropane in 98% yield, with 96:4 dr, and 86% ee (*trans*).[89] Moreover, 1-tosyl-3-vinylindoles were excellently cyclopropanated by Nishiyama's catalyst with ethyl and *t*-butyl diazoacetate (Scheme 22).[90] It should be noted that the E/Z diastereoselectivity was notably improved when using t-butyl diazoacetate. Nishiyama also developed the water-soluble hydroxymethyl derivative. The reaction of styrene with different diazoacetates in aqueous media provided the corresponding

cyclopropanes in 24–75% yields, with 92:8 to 97:3 E/Z ratio, 57–94% ee (1*S*,2*S*), and 26–76% ee (1*R*,2*S*).[91]

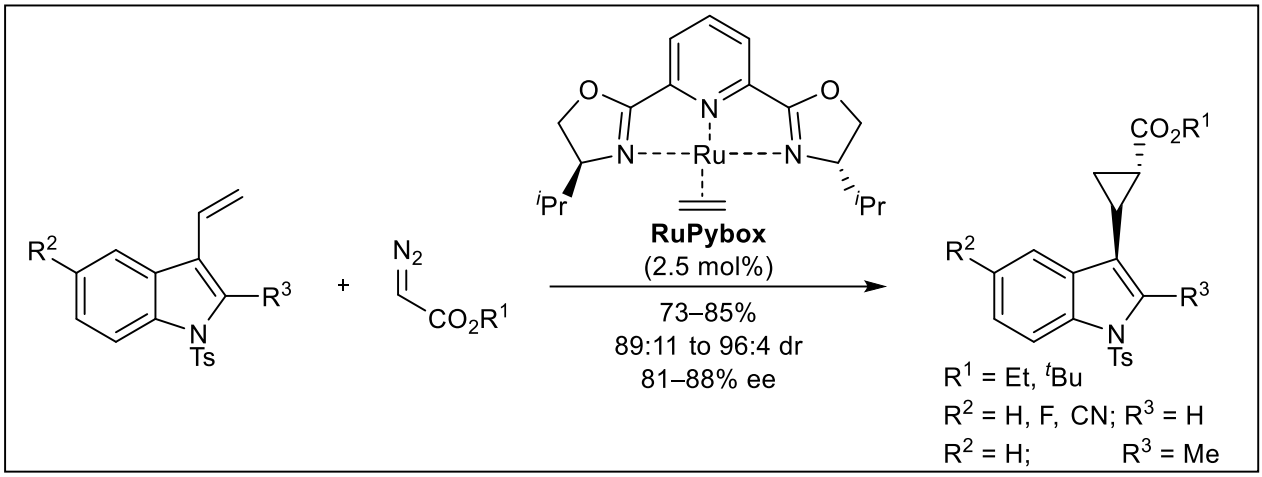

Scheme 22. Asymmetric cyclopropanation of 1-tosyl-3-vinylindoles.

Zingaro and coworkers tested a modified Nishiyama's catalyst (Ru-Thibox) and obtained 70–82% yields with 79:21 to 82:18 E/Z ratio and 87% to >99% ee (1*R*,2*R*), 82% to >99% ee (1*S*,2*R*) for the cyclopropanation of styrenes and 1,1-diphenylethene with EDA.[92]

Bis(oxazolinyl)phenyl ruthenium complex (Ru-Phebox) was efficient for the cyclopropanation reactions of various styrene derivatives with tert-butyl diazoacetate (85–92% yields with 82:8 to 96:4 E/Z ratio and 98–99% ee (1*R*,2*R*).[93] Only α-methylstyrene afforded the cis-isomer (80% overall yield, 67:33 dr, 98% ee (*cis*), and 93% ee (*trans*)). The cyclopropanation of aliphatic alkenes proceeded in lower yield but with good diastereo- and enantioselectivities, whereas cyclopropanation of 1,2-disubstituted alkenes, such as 1-phenylpropene or indene, did not occur. The ruthenium carbene intermediate should be obtained by replacement of the equatorial H_2O ligand with the diazoacetate group, and then the alkene approached the Re-face to minimize the steric repulsion between the tert-butyl group of the diazo compounds and the R group of the alkene.

Ru-salen systems (Figure 6) displayed cis-selectivity in the cyclopropanation reaction (83:17 to 93:7 Z/E ratios, >97% ee).[94] In particular, catalyst Ru-salen also was effective for the cyclopropanation of 2,5-dimethyl-2,4-hexadiene, producing the cis-isomer in 75% ee (94:6 dr) but only in 18% recovered yield.[94] Besides, Ru-salen, with the two free coordinating sites occupied

by pyridine ligands, gave excellent enantiomeric excesses in the cyclopropanation of mono or 1,1-disubstituted alkenes (30–97% yields, 66:34 to >99:1 E/Z ratios, 69–99% ee (trans)).[95]

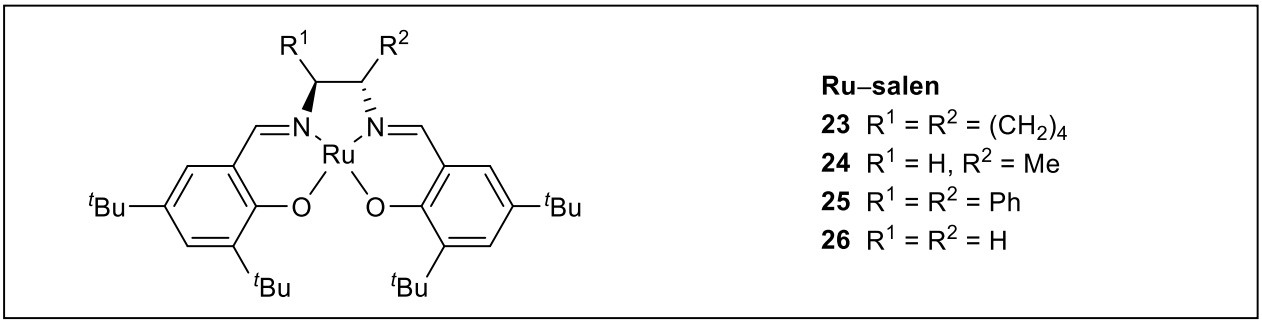

Figure 6. Several ruthenium–salen complexes for asymmetric cyclopropanations.

Recently, our Iwasa's research group reported that ruthenium(II)-phenyloxazolidinyl complex (Ru(II)-pheox **27**) was found to be the crucial catalyst for the cyclopropanation of monosubstituted alkenes with succinimidyldiazoacetate **28** under mild conditions (Scheme 23).[96] The desired cyclopropane products **29** were obtained in high yields (94–98%) with excellent diastereoselectivities (*trans/cis* >99:1). The products then were reduced using $LiAlH_4$. To give the corresponding alcohols **30** without epimerization. The absolute configuration of the products was proved to be (*1R, 2R*). the preferred prochiral face for the attack of the the seven-membered ring formed as a result of coordination between the succinimidyl cyclopropanation of vinylcarbamates with diazo esters was also carried out using Ru(II)-pheox **27**.[97] The corresponding cyclopropylamine derivatives were obtained in high yield (77–99%), excellent d.r (up to 24:1, with *N,N*-disubstituted vinylcarbamates) and enantioselectivity (up to 99% ee). However, the reaction of equimolecular amounts of *cis*- and *trans*-isomers with low enantiomeric excess.

Iwasa's research group also reported an interesting intramolecular cyclopropanation in water as reaction medium.[98] Ru(II)-pheox **31** was completely soluble in water, and completely insoluble in diethyl ether. The easy separation of the ether phase, which contains the cyclopropane product, the catalyst in the water phase was tested for reuse and it was proved to be reused at least five times without significant decrease in reactivity or enantioselectivity. The reaction of *trans*-allylic diazoacetates carried out at room temperature in the presence of 5 mol% of Ru(II)-pheox **31** afforded (1*S*,5*R*,6*R*)-3-oxabicyclo[3.1.0]hexan-2-ones in 89–99% yield with 83–99% ee. Disubstituted allylic diazoacetates gave lower results (76–95% yield, 36–97% ee), while *cis*-allylic diazoacetates were not tested.

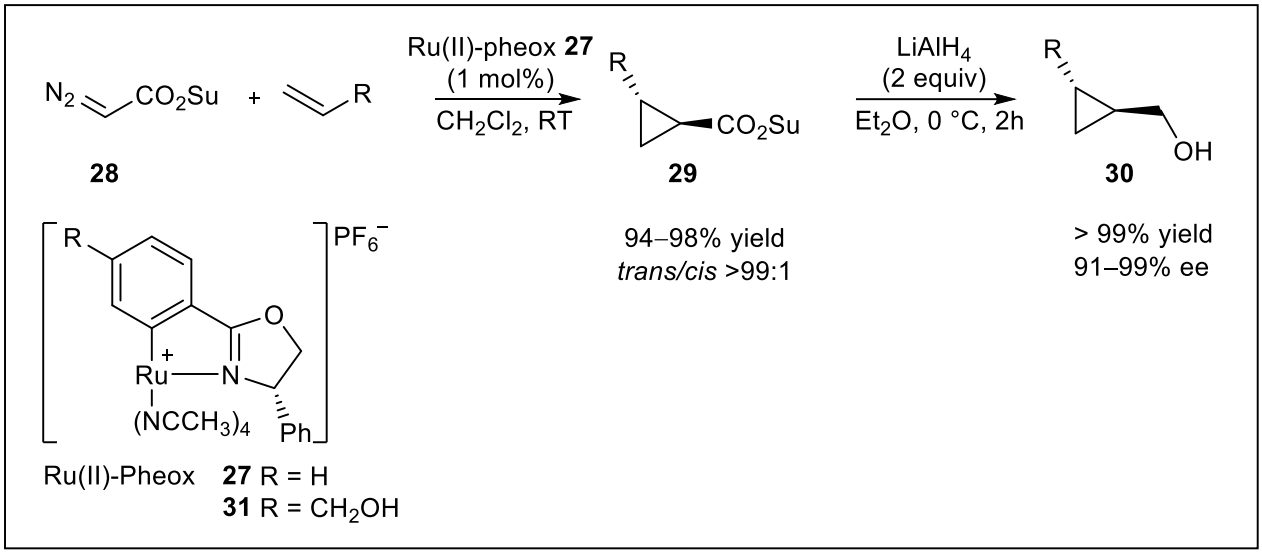

Scheme 23. Ru(II)-pheox catalyzed asymmetric cyclopropanation of terminal alkenes.

The intermolecular cyclopropanation of styrene with diazoacetate catalyzed by the same catalyst Ru(II)-pheox **31** was attempted. Although, the high *trans*-selectivity (97%), the cyclopropanation product was isolated in only 30% yield. Ru(II)-pheox **31** was also supported on the macroporous polymer and gave the best results among the heterogeneous catalyst reported here. Moreover, it was more effective tha the unsupported version at a loading of 6 mol%. In fact, not only did *trans*-allylic diazoacetates react in less than a minute to give (1*S*,5*R*,6*R*)-3-oxabicyclo[3.1.0]hexan-2-ones in 94–99% yield with 83–97% ee, but the supported catalyst also afforded the corresponding (*R,R)*-cyclopropanecarboxylates intermolecularly, by reaction of alkenes and diazoacetate, in 80–99% yield with 91–99% ee.[99] The most relevant feature of this catalyst is its reusability as it can be recycled more than ten times, even after three months of storage of the used catalyst, without any loss in its catalytic activity or selectivity. These valuable results encourage further pursuit in the development of efficient supported ruthenium catalysts.

1.5. Buchner reaction

1.5.1. The history of Buchner reaction

The Buchner ring expansion reaction was first discovered in 1885 by E. Buchner and T. Curtius[24] who prepared a carbene from ethyl diazoacetate for addition to benzene using both thermal and photochemical pathways in the synthesis of cycloheptatriene derivatives. Since this

discovery, the non-catalyzed and metal-mediated variants of this reaction have become important methods for the preparation of seven-membered rings.[22c]

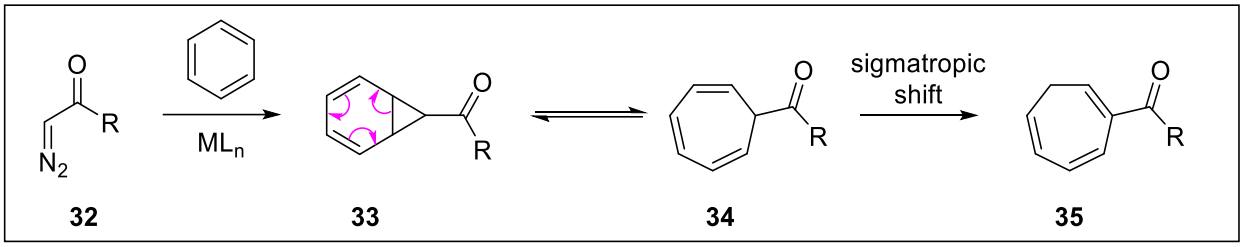

Scheme 24. The Buchner reaction.

The process is believed to involve cyclopropanation of a benzenoid double bond by an α-ketocarbene or a metal carbene. The initial product is an acylnorcaradiene, **33**, which is prone to spontaneous, though reversible, electrocyclic ring opening to form an acylcycloheptatriene, **34** (Scheme 24).[25] This initially formed acylcycloheptatriene **34** may undergo sigmatropic rearrangements to give a thermodynamic mixture of cycloheptatrienes **35**.[26]

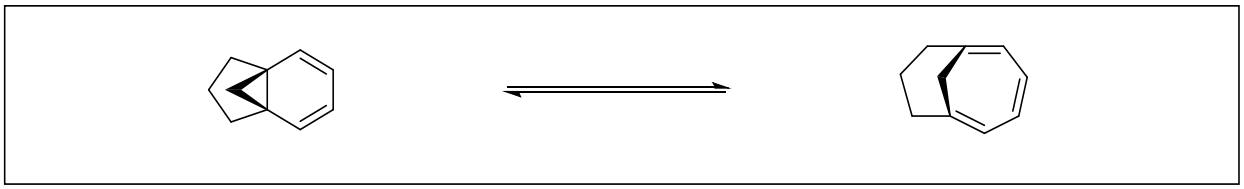

Scheme 25. Predominance of norcaradiene.

There are several cases known where the norcaradiene intermediate is stable and isolable due to prevention of the electrocyclic ring-opening process by geometric (Scheme 25)[27] or electronic (Scheme 26) constraints.[28]

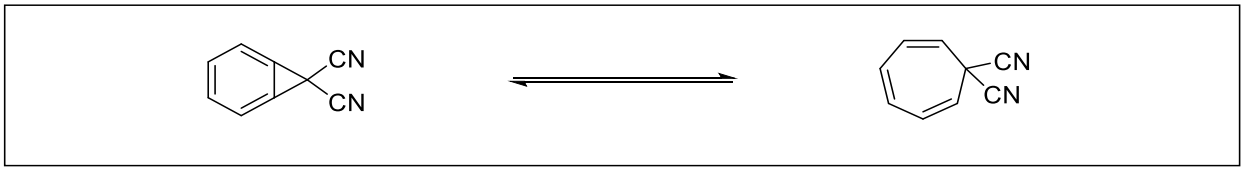

Scheme 26. Stabilization of norcaradiene.

The intermolecular Buchner reaction was discovered with poor yields and the formation of isomeric cycloheptatriene products that were difficult to separate.[29] To improving the synthetic

application, intramolecular Buchner reaction was studied in combination with the use of heterogeneous copper catalysts.

1.5.2. Transition–metal–catalyzed intramolecular Buchner reaction of α-diazo carbonyls

1.5.2.1. Buchner reaction vs C−H insertion

For intramolecular Buchner reactions, the structure of the α-diazocarbonyl can have a dramatic effect on the ensuing reaction, in terms of both chemo- and regioselectivities. Intramolecular aromatic cycloaddition reactions are typically favored in systems having a three-atom spacer between the aromatic ring and the diazo carbon since an alternative C−H insertion would produce a four-membered ring (Scheme 27).

However, the C−H insertion process becomes competitive in substrates containing four-atom spacers since five-membered ring formation is now permitted.[30] The nature of the substituent R on the diazo carbon, and the identity of the catalyst and its attendant ligands, can also affect the outcome.

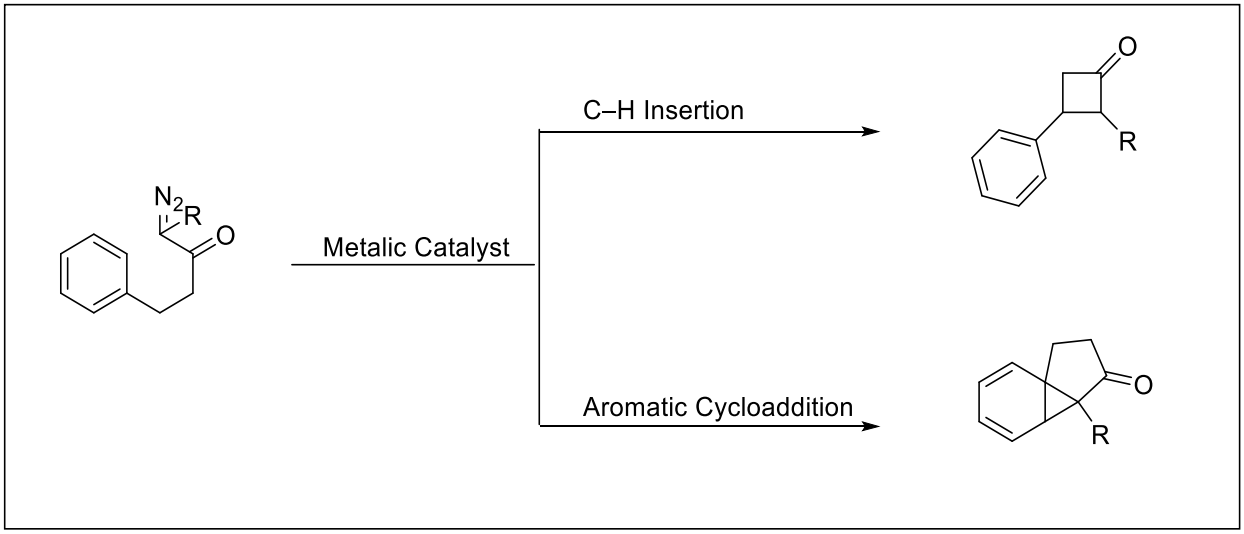

Scheme 27. Buchner reaction vs C−H insertion.

The first intramolecular system studied, in the 1990s, was 1-diazo-4-phenylbutan-2-one **37**, a terminal diazoketone (R = H) possessing a three-atom spacer.[30a] Prior to the advent of rhodium catalysts, the intramolecular Buchner reaction of **37** under copper catalysis had been observed to produce an azulenone, **36**, in low yield.[31] However, the promise implicit in this potentially new direct route to azulenes only became apparent when this reaction was reinvestigated under rhodium

catalysis and was found to yield the isomeric kinetic azulenone **38** in high yield (Scheme 28).[30a, 32]

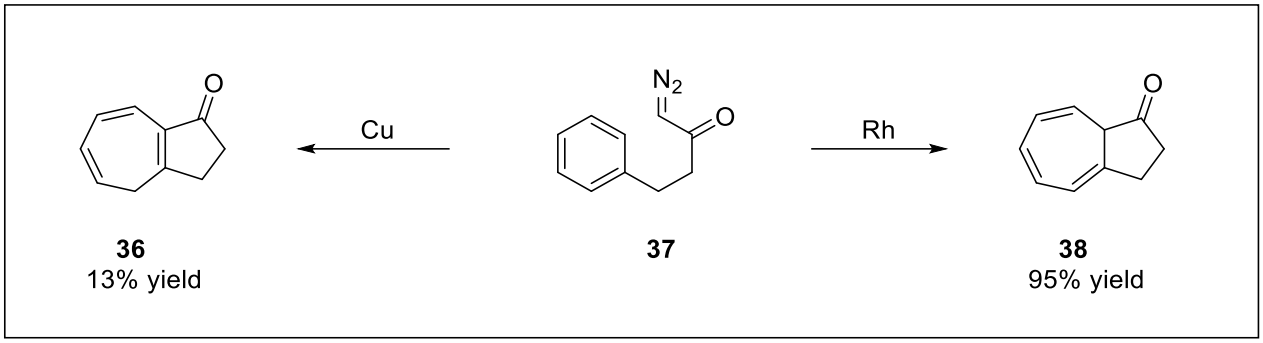

Scheme 28. Copper and rhodium catalyzed intramolecular Buchner reactions.

1.5.2.2. Rhodium catalyzed intramolecular Buchner reaction

Dirhodium(II) catalysts were demonstrated that they improved effectively the intramolecular Buchner reaction. The reports of McKervey, Padwa and others showed the effects of arene substitution, diazo structure and catalyst electronics on the selectivity of the cyclopropanation.

The intramolecular Buchner reaction tolerates a range of substituents on the aromatic ring ranging from nitro to alkyl with a significant degree of regiocontrol: ortho substitution on the aromatic ring generally tends to direct cyclization away from the substituent. There has been some debate in the literature on the directive effect of an *o*-methoxy substituent.[30a, 32, 33, 35]

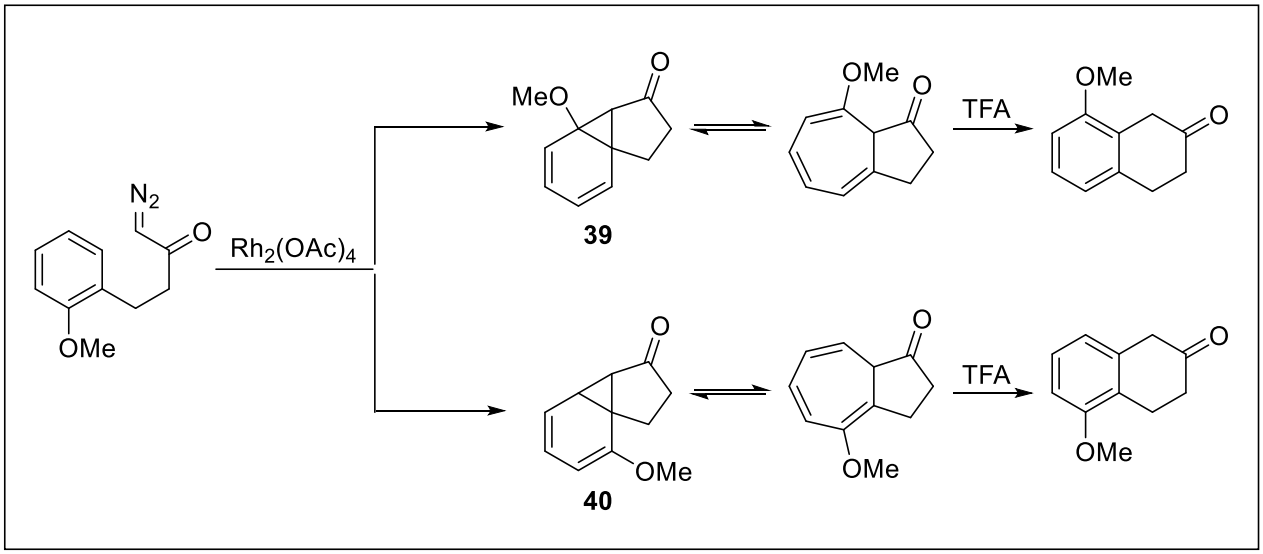

Scheme 29. Rhodium catalyzed intramolecular Buchner reactions.

Since the original report by McKervey[30a, 32] in the early 1990s that an *o*-methoxy substituent favors cyclization toward itself, the issue has been ultimately resolved by independent reports by Manitto[34] and Maguire.[36] The initial product of the reaction is indeed formed by addition away from the methoxy substituent to form the kinetic product **40**, the 5-substituted azulenone, but this kinetic product is thought to rearrange to the thermodynamic product **39**. Subsequent treatment of either azulenone product with trifluoroacetic acid results in the corresponding tetralone product (Scheme 29).

In addition it was found that substitution on the aryl component could affect the product obtained from the reaction.[37] In most cases, substrates bearing electron-donating groups in the ortho or para position reacted efficiently with low catalyst loadings to produce norcaradienes in moderate to high yields in most cases (Scheme 30a).

However, in the case of electron-donating groups in the meta position, the resulting norcaradienes were found to be unstable, rearomatizing easily to benzo-fused cycloheptanones (up to 93% yield) (Scheme 30b).[37]

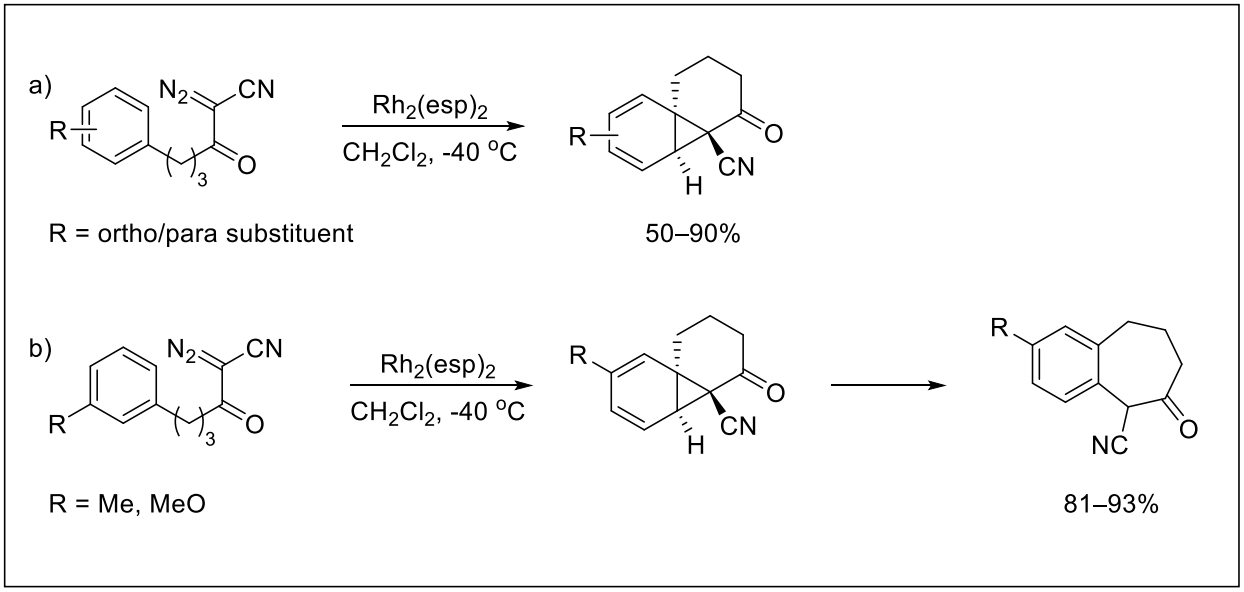

Scheme 30. Buchner reactions of cyano-substituted diazoketones.

Substrates bearing electron withdrawing groups on the aromatic ring also produced stable norcaradienes, though less efficiently and generally in lower yields (Scheme 30a). An analogous series of *α*-diazo-*β*-cyanoamides behaved similarly when subjected to rhodium(II) catalysis,

forming stable norcaradiene products, though yields were typically lower because of increased formation of carbene dimer products.

Reisman's study is the latest demonstration of the power and versatility of the Buchner cycloaddition reaction in fused- and bridged-ring carbocyclic synthesis.

Besides, McKervey and co-workers reported the first example of enantioselectivity in the intramolecular Buchner reaction in the cyclization of 2-diazo-5-phenylpentan-3-one to the azulenone **41**, achieving enantioselectivities up to 33% ee with a rhodium(II) prolinate-based catalyst (Scheme 31).[30a]

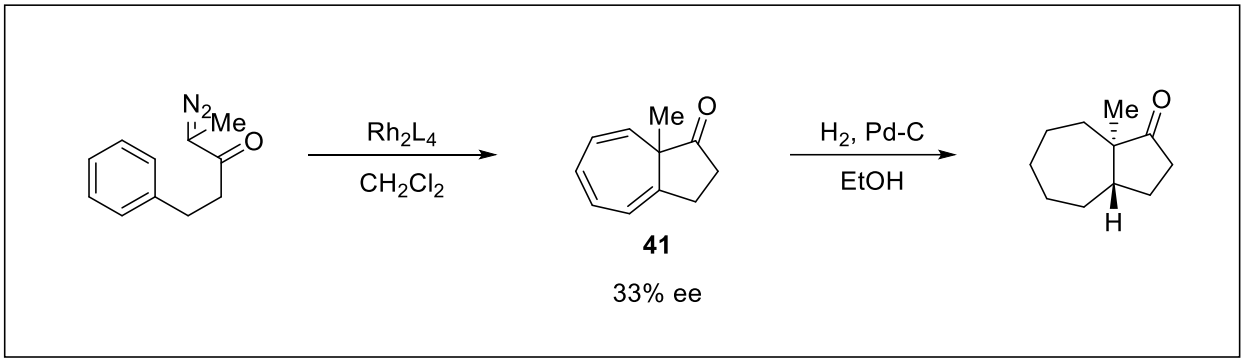

Scheme 31. Enantioselective rhodium-catalyzed intramolecular Buchner reaction.

1.5.2.3. Copper catalyzed intramolecular Buchner reaction

Copper catalysts were also effective for the intramolecular Buchner reaction. Since the early 20th century, using the solubility ligands has enabled further development beyond the heterogeneous catalysts employed. In 1960s, there is a lot of application of homogeneous copper catalysts for alkene cyclopropanation, after the reports of Nozaki and Moser.[38] In 1984, Saba showed that α-diazoketones the reaction rate and efficiency with soluble Cu(II) salts.[39]

In the study of the intramolecular reaction of tetralin 2-diazo ketone **42** (Table 1), Mander summarized the selectivity of both catalyst systems.[40]

The results showed that the yields of arene cyclopropanation are highly dependent on both the catalyst and the arene substitution pattern. While rhodium catalysts provided mixtures of norcaradiene **43** and cyclopentanone **44**, copper catalysts provided lower overall yields, but delivered better selectivity for the norcaradiene. Copper bisoxazoline complexes have recently emerged as successful catalysts for intramolecular Buchner reaction of α-diazoketones, obtaining enantioselectivities up to 95% ee (Scheme 32).[41]

Table 1. Mander's studies of tetralin 2-diazomethyl ketones.

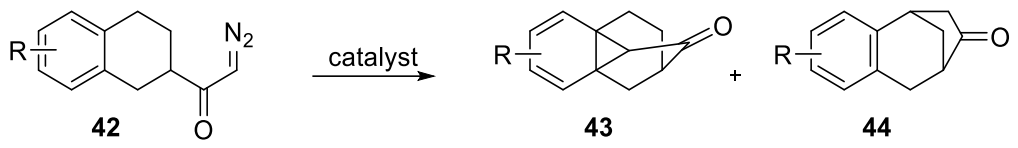

Entry	R	Catalyst	Yield [%] of **43**	Yield [%] of **44**
1	H	$Rh_2(OAc)_4$	39	41
2	H	$Cu(acac)_2$	56	6
3	5-CH_3O	$Rh_2(OAc)_4$	34	41
4	5-CH_3O	$Cu(acac)_2$	56	12
5	6-CH_3O	$Rh_2(OAc)_4$	71	14
6	6-CH_3O	$Cu(acac)_2$	61	17
7	7-CH_3O	$Rh_2(OAc)_4$	46	44
8	7-CH_3O	$Cu(acac)_2$	64	3

This is the highest enantioselectivity to date reported for this transformation. Further work determined that the presence of additives such as Na(BARF) or K(BARF) enhanced the enantiocontrol of the reaction, particularly in the case of α-diazoketones bearing electron-withdrawing groups in the para position of the aryl ring.[42]

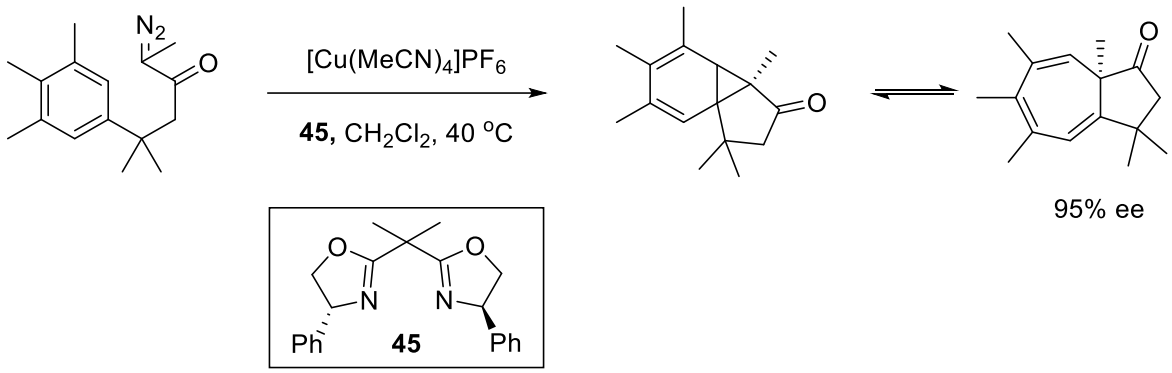

Scheme 32. Enantioselective copper-catalyzed intramolecular Buchner reaction.

1.5.3. Synthesis bioactive compounds by intramolecular Buchner reaction

Selected example of bioactive compounds can be synthesized by intramolecular Buchner reaction

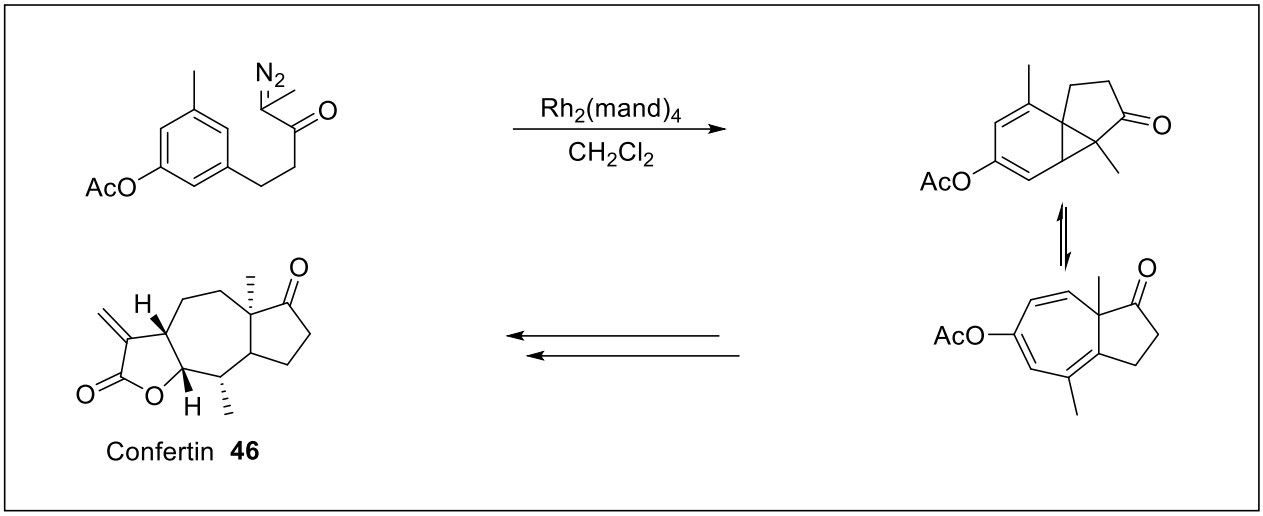

Scheme 33. Formal synthesis of (±)-confertin.

The intramolecular Buchner reaction has also found great applicability in the area of bicyclic synthesis.[43, 44] Here are selected example of bioactive compounds can be synthesized by intramolecular Buchner reaction such as: (±)-confertin **46** (Scheme 33).[43]; diterpenoid harringtonolide **47**, (Scheme 34).[45]; gibberellin derivatives (Scheme 35).[45a]

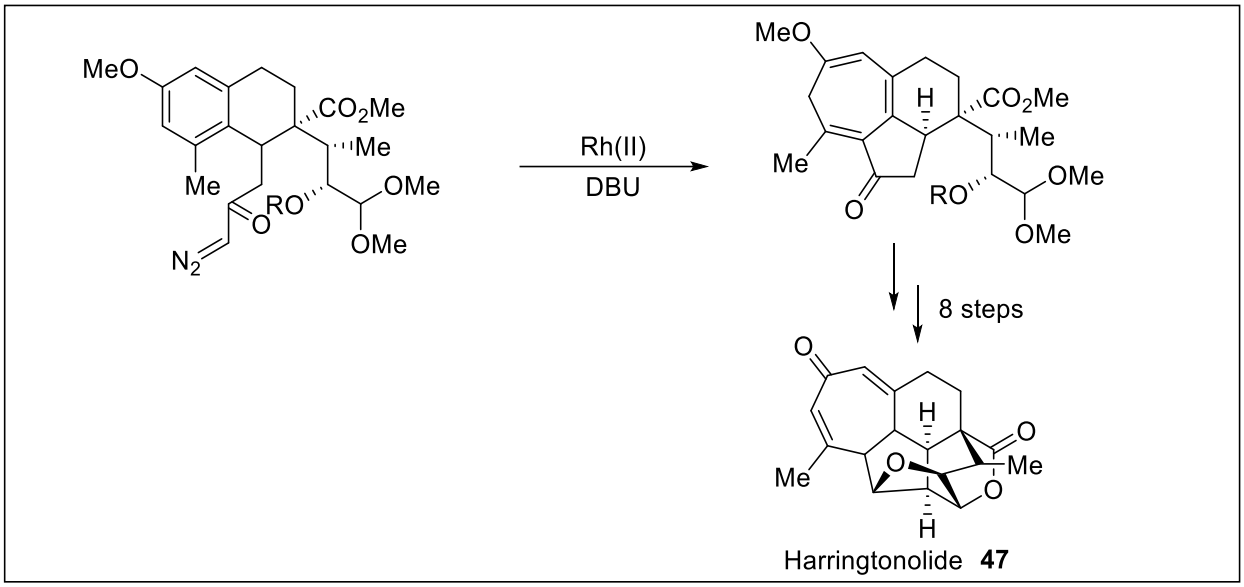

Scheme 34. Synthesis of harringtonolide.

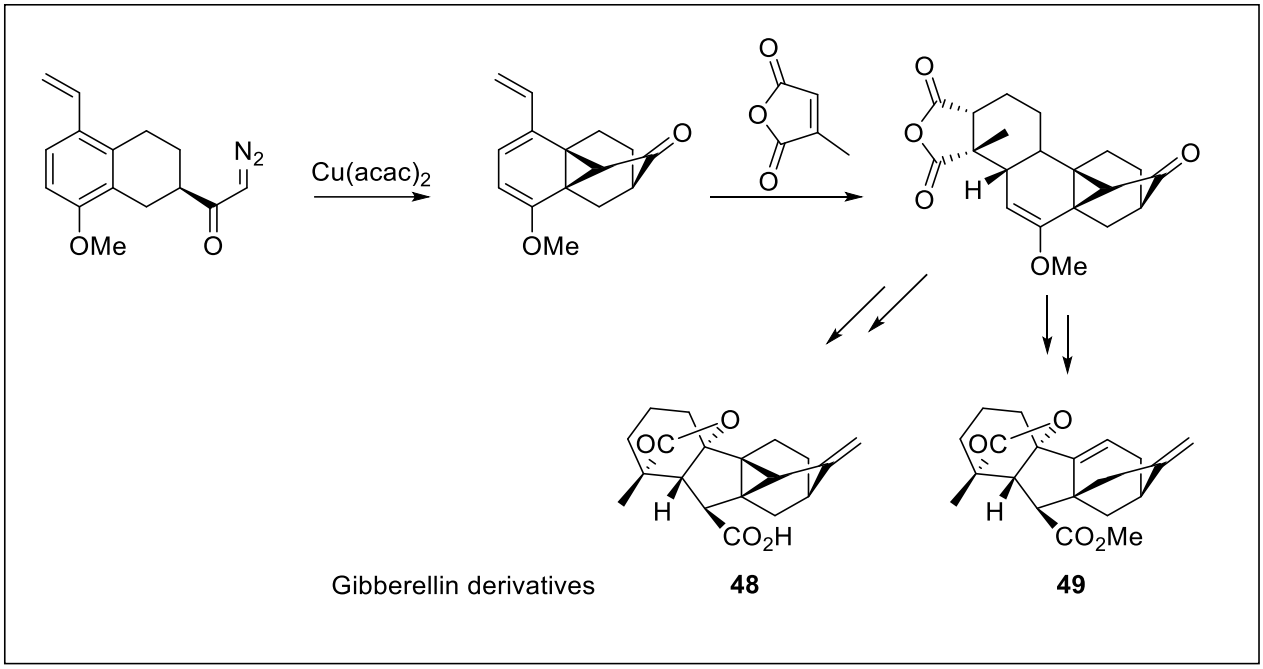

Scheme 35. Synthesis of gibberellin derivatives.

1.6. Research objectives

The typical reactions of free carbene are the addition into π-bond and the insertion into σ-bond. To modulate the reactivity of the free carbene, a complexation with a metal lead to the carbenoid. The metal-carbenoid is a powerful and useful method for constructing targeted molecules. And in our laboratory, we successfully synthesized the Ru(II)-Pheox - an efficient catalyst in the asymmetric carbene transfer reaction.

On another hand, the small and medium ring-containing organic molecules, such as three-, four-, five-, six, and seven-membered rings are presented in many biologically important compounds and they show a large spectrum of biological properties.

It inspired us to find novel and diverse approaches to the new methodology for:

- Synthesis of the oxindole derivatives.
- Synthesis of the cyclopropane ring.
- Synthesis of the 7 membered rings

CHAPTER 2

Highly efficient synthesis of oxindole derivatives via catalytic intramolecular C-H insertion reactions of diazoamides

2.1. Introduction

The oxindole ring is prevalent as an important scaffold found in numerous natural products and pharmaceutically active compounds: antifungal, antibacterial and antiviral activities, antimicrobial activity, antioxidant activity.[108−111] Especially, in our previous report, oxindole derivatives play an important role as a starting material for the synthesis of optically active spiro-cyclopropyl oxindole derivatives.

Over the past few decades, the emerging therapeutic potential of oxindole structural motif has encouraged the medicinal chemists to synthesize novel oxindole derivatives. Therefore, many reports approach toward the oxindole substructure includes: the derivatization of isatin and indoles,[112] application of Heck reactions of aniline derivatives[113] or the Friedel-Crafts procedure using palladium-catalyzed C-H functionalizations.[114]

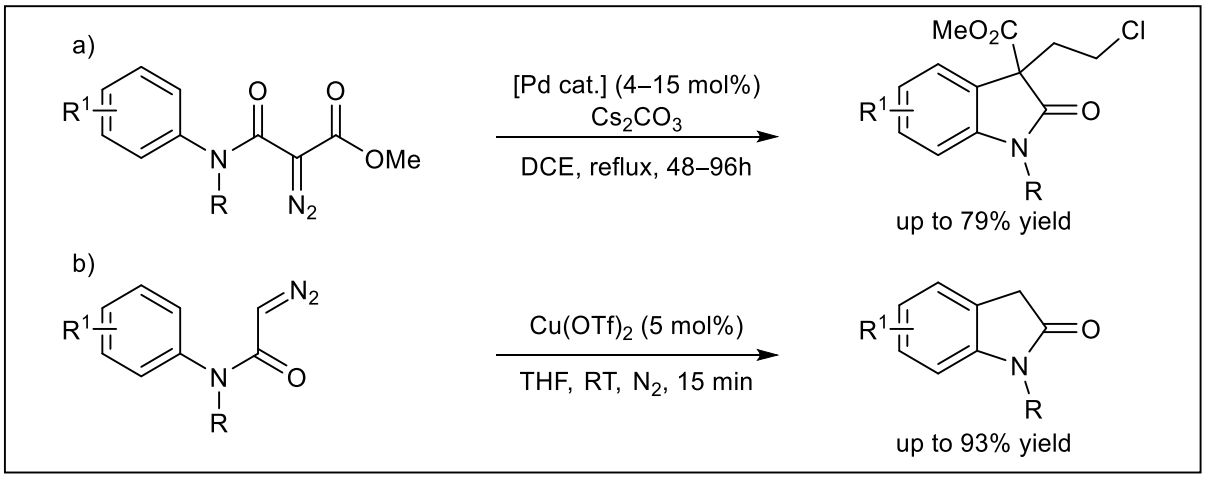

Scheme 36. Transition metal catalyzed C-H insertion reaction of diazoacetamides.

However, those methods usually require harsh reaction conditions (the strongly acidic conditions, high temperatures) and a multi-step synthesis of the corresponding starting materials as a functionalized precursor. So, existing methods are limited in their scope and generality.

On another hand, the oxindole framework can be constructed via intramolecular C−H insertion reactions of α-diazo compouds by using transition metals such as Rh, Ru, Ag, and Pd as catalysts. In this regard, in 2017, a significant contribution was made by Parul Garg et al,

demonstrating that a copper-catalyzed (5 mol%), ligand-free, divergent route toward oxindoles and isatins via intramolecular cyclization of α-diazoanilide with yield up to 93% (Scheme 36b).[121] Recently, the Pd-catalyzed intramolecular carbene C–H insertion of α-diazo-α (methoxycarbonyl)acetamides to prepare oxindoles (yield up to 79%) as well as β-lactams was studied by Solé and coworkers (Scheme 36a). Both these establishments approach to acquire oxindole derivatives still remains challenging such as a large amount of catalyst or special reaction conditions.

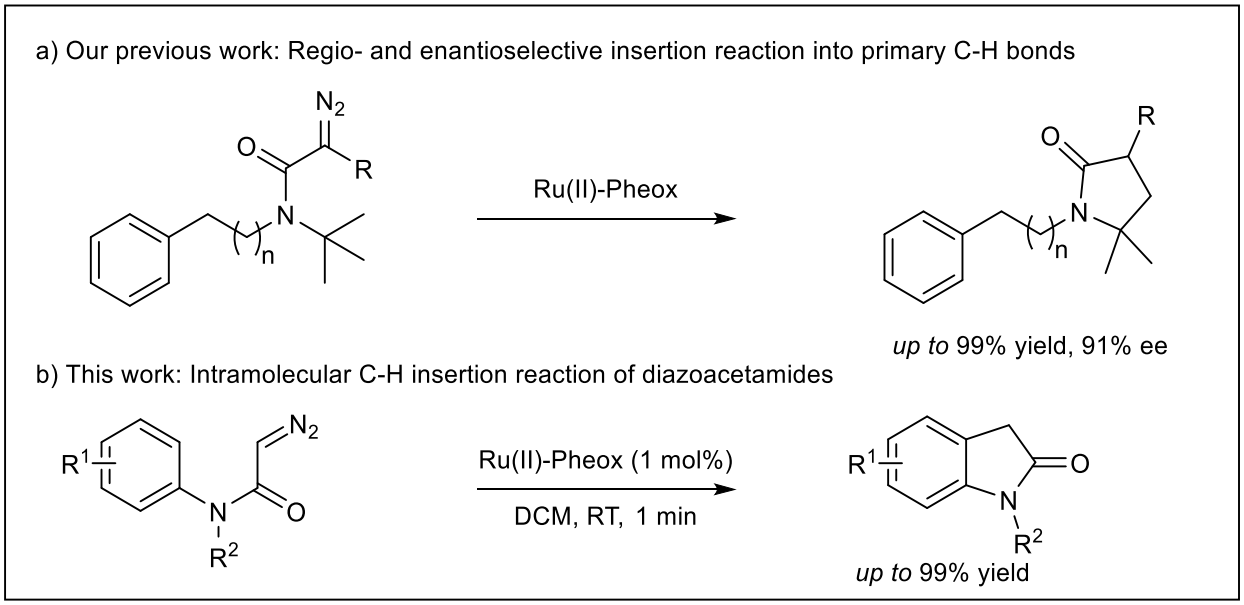

Scheme 37. The efficiency of Ru(II)-Pheox in the synthesis of oxindole derivatives and their spirocyclopropanation.

In the past several years, our group has been engaged in developing a Ru(II)–Pheox complex, which is efficient in carbene transfer reactions, in particular, asymmetric cyclopropanation and Si–H insertion reactions.[106]

Due to the interest in the catalytic C-H insertion reaction of diazoacetamide, as well as the importance of the oxindole scaffold in natural product synthesis, we have recently described the results of experiments designed to probe the efficiency of Ru(II)-Pheox in the synthesis of oxindole. In this paper, we describe the development of an intramolecular C-H reaction of a variety of diazoacetamide derivatives in the presence of Ru(II)–Pheox catalyst for selective synthesis of oxindole derivatives (Scheme 37b).

2.2. Results and discussions

Table 2. Catalyst screening experiments for Ru(II)-Pheox catalyzed intramolecular C-H insertion of 2-diazo-*N*-phenyl-*N*-methylacetamide.

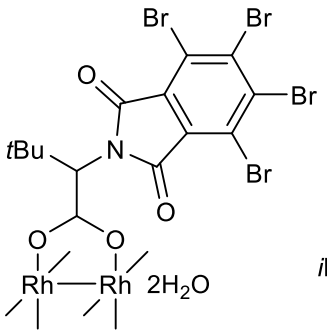

Cat. 1 Rh_2(S-TBPTTL)$_4$

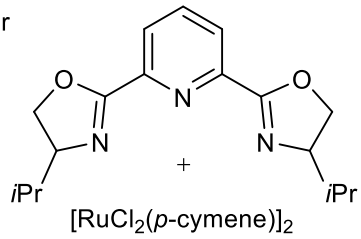

Cat. 2 Ru-Pybox

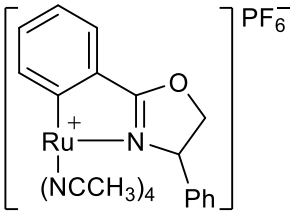

Cat. 3 Ru(II)-Pheox

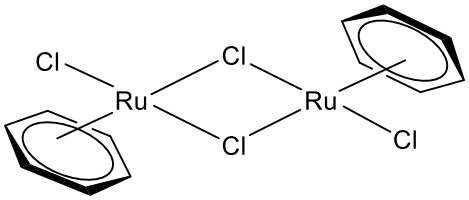

Cat. 4 [Benzene)$RuCl_2$]$_2$

Cat. 5 CuI

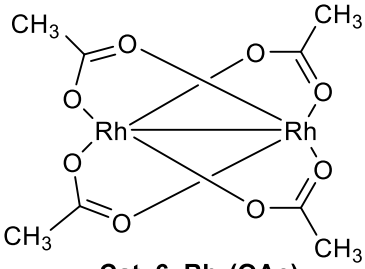

Cat. 6 Rh_2(OAc)$_4$

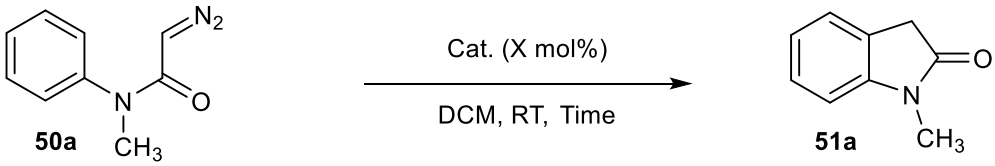

Entry	X [mol%]	Cat.	Time [min]	Yield [%][a]	TON[b]	TOF[[c] [min^{-1}]
1	1	Cat. 1	10	91	91	9.1
2	1	Cat. 2	10	83	83	8.3
3	1	Cat. 3	1	96	96	96
4	1	Cat. 4	30	92	92	3.1
5	1	Cat. 5	72h	30	30	–
6	1	Cat. 6	24h	83	83	0.1
7	0.5	Cat. 3	1	78	156	156
8	0.1	Cat. 3	60	58	580	9.7

[a] Isolated yield. [b] TON = moles of desired product (**51a**)/moles of catalyst.
[c] TOF = TON/reaction time (min).

2.2.1. Catalyst and solvent screening for catalytic intramolecular C-H insertion reactions of diazoamides

Initially, the 2-diazo-*N*-methyl-*N* phenylacetamide **53a** was chosen as the model substrate to screen the reaction conditions. As shown in Table 2, the oxindole **54a** was obtained in 91% yield and under the catalysis of 1 mol% Rh_2(S-TBPTTL)$_4$ at room temperature (entry 1). For another Rh_2(II) complex $Rh_2(OAc)_4$ (Cat.6), the intramolecular C-H insertion reaction dominated as well, giving **51a** in 83% yields after 24h (entry 6).

Subsequently, the CuI[14] catalyst was then tested for this transformation as well. In this case, the reaction proceeded very slowly (72h) and the yield of **51a** decreased dramatically to 30% (Table 2, entry 5). Besides, it is well known that ruthenium complexes are good catalysts for carbene-transfer reactions. Other Ru(II) complexes were also examined to improve reaction performance (Table 2, entries 2–4, 7–8). When Ru-Pybox was used, product **51a** was formed in 83% yield (Table 2, entry 2). In the case of the [Benzene)$RuCl_2]_2$ complexes, the yield of **51a** increased slightly to 92%. However, the reaction time was longer (30 min) (Table 2, entry 4). Screening the Ru(II)–Pheox catalyst with various loadings was also tested for the intramolecular C-H insertion reaction (Table 2, entries 3, 7–8).

Lowering the Ru(II)-Pheox loading from 1 to 0.1 mol% led to higher values TON (up to 580) and TOF (up to 156 min^{-1}), albeit with lower yields 58 and 78%, respectively (Table 2, entry 7–8). In the presence of 1 mol% Ru(II)-Pheox, the reaction of diazoacetamide **50a** proceeded smoothly at room temperature, delivering the corresponding oxindole products **50a** in high yield 96% (Table 2, entry 3).

To get more details of this reaction, the reaction condition was tested for the solvent system. The results are shown in Table 3. Oxindole **51a** was obtained in high yields for most of the common organic solvents (Table 3, entries 1–6). Protic solvent such as methanol also gave high yield without any O-H insertion reaction of the diazo compound (Table 3, entry 4). The reaction proceeded rapidly except coordinatable solvent such as acetone, tetrahydrofuran (THF). In the case of acetonitrile, the rate of reaction becomes slightly slow because of the stabilization of the catalyst (Table 3, entry 6). Dimethyl sulfoxide (DMSO) gave no reaction (Table 3, entry 7). Ligation of DMSO to the ruthenium catalyst may strong and becoming poison to the catalyst. DCM was found as the best solvent for Ru(II)-Pheox catalyzed reactions.

Table 3. The solvent effect for Ru(II)-Pheox catalyzed intramolecular C-H insertion of 2-diazo-*N*-phenyl-*N*-methylacetamide.

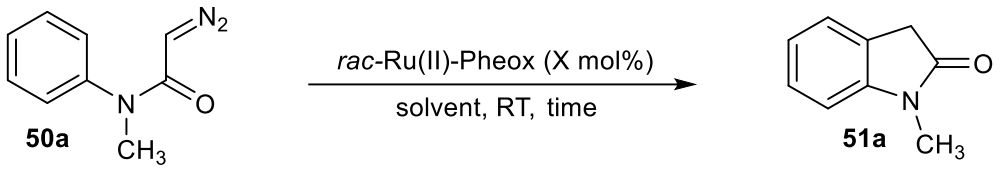

Entry	X [mol%]	Solvent	Time [min]	Yield [%][a]
1	1	DCM	1	96
2	1	THF	1	91
3	1	Acetone	1	79
4	1	Methanol	1	82
5	1	Toluene	1	86
6	1	Acetonitrile	10	78
7	1	DMSO	4 h	–

[a] Isolated yield.

2.2.2. Ru(II)-Pheox catalyzed intramolecular C-H insertion reactions of diazoamides

Based on the optimized reaction conditions for intramolecular C-H insertion of diazoacetamide (Table 3, entry 6), the substrate scope was then examined. As shown in Table 4, all various substituents R^1 at different positions of the phenyl group were also well-tolerated, producing **51a–n** in 91–99% yields.

As substitution R^2=CH_3, R^1 with an electron-donating group (e.g., 4-OCH_3, 2-OCH_3, 3-CH_3) on the *N*-benzyl ring moiety has a strong impact on the reaction (Table 3, entries 2, 7 and 8). The corresponding oxindole products were obtained in excellent yields. Besides, compared to substitution with an electron-donating group, the efficiency of the intramolecular reaction of substitution bearing an electron-withdrawing group (namely H, 4-Cl, 4-Br, 4-NO2, 2-Br and 2-I) slightly decreased with yields (93–99%) (Table 4, entries 1, 3–6 and 9–10). As a plausible explanation, the substituent changes thelectronic properties of the benzene ring. Nucleophilic substituents are regarded as electronic donating groups, which increase the electropositivity of the aryl group and improve the reactivity in the intramolecular ArC_{sp2}-H insertion reaction. In contrast, electrophilic substituents are regarded as electron-withdrawing groups, which decrease the electropositivity of the aryl group.

Table 4 Ru(II)-Pheox catalyzed oxindole synthesis of diazoacetamides via intramolecular C-H insertion of carbene.

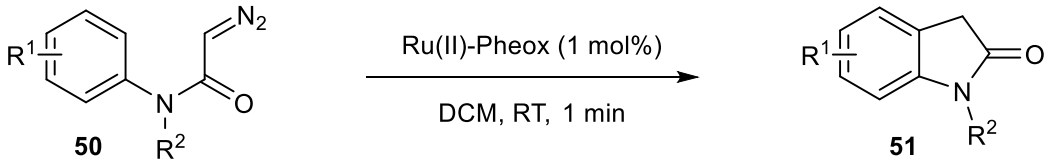

Entry	**50**	R^1	R^2	Yield [%][a]
1	**a**	H	CH_3	96
2	**b**	4-OCH_3	CH_3	99
3	**c**	4-Cl	CH_3	94
4	**d**	4-Br	CH_3	93
5	**e**	4-I	CH_3	99
6	**f**	4-NO_2	CH_3	94
7	**g**	3-CH_3	CH_3	98
8	**h**	2-OCH_3	CH_3	93
9	**i**	2-Br	CH_3	98
10	**j**	2-I	CH_3	97
11	**k**	H	H	–
12	**l**	H	Ph	99
13	**m**	H	CH_2CH_3	94
14	**n**	H	$CH(CH_3)_2$	91
15	**o**	H	$CH_2C_6H_5$	95

[a] Isolated yield.

Switching the substrate to **50g** (R^1 = 3-CH_3) 2-diazo-*N*-methyl-*N*-(*m*-tolyl)acetamide dramatically changed the reaction, affording the corresponding product **51g**. Two regiomers of **51g** were generated in ratio **51ga/51gb** = 2/3 and in high overall yield (98%) (Scheme 38).

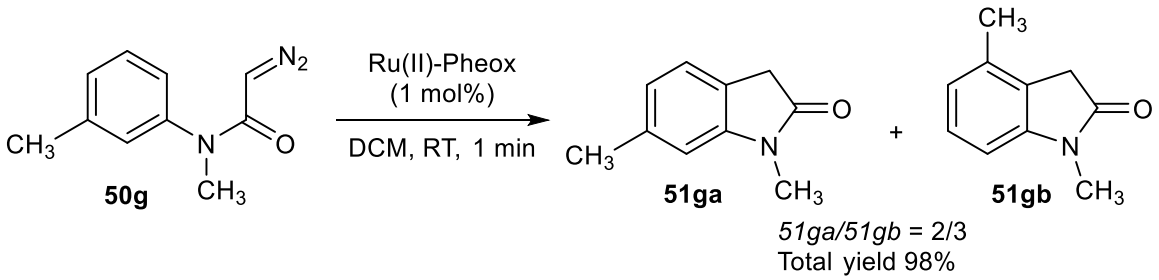

Scheme 38 Intramolecular C-H insertion reaction of diazoacetamide **53g** catalyzed by Ru(II)-Pheox.

Furthermore, the *N*-substituent effect also evaluated, under reaction conditions similar to the intramolecular C-H insertion. *N*-H substituted diazo (**50k**) could not transfer to the desired oxindole because the dimerization reaction prevented (Table 4, entry 11).

However, greater steric demanding substituents R^2 (-C_6H_5, -CH_2CH_3, -$CH(CH_3)_2$, -$CH_2C_6H_5$) were compatible. Entry 12, the efficient synthesis of oxindole still kept on excellent yield 99%. When substitution R^2=-CH_2CH_3, -$CH(CH_3)_2$, in which the newly introduced methyl groups provided additional competitive allylic C-H insertion sites, the reactions selectively took place at the desired ArC_{sp2}-H position and led to the products **51m**, **51n** in decreased yields (94% and 91 %, respectively), probably because of the steric hindrance (Table 4, entries 13–14). And diazoacetamide **50o** (entry 15, Table 4) presented a highly regioselective intramolecular ArC_{sp2}-H insertion reaction. And only oxindole derivative **51o** has been formed in 95% yield.

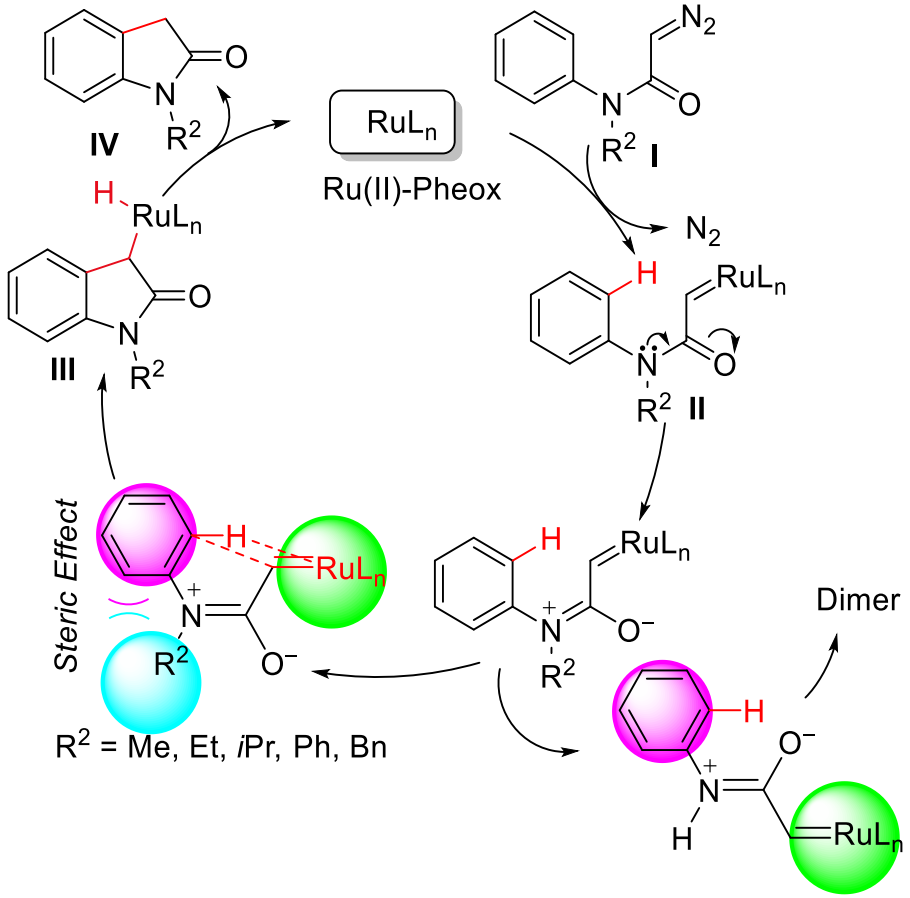

Scheme 39. Plausible mechanism of intramolecular C-H insertion reactions of diazoamides catalyzed by Ru(II)-Pheox.

A mechanistic proposal is outlined in scheme 39. The interaction of diazo amide with the ruthenium catalyst would form the ruthenium-carbene 3. The intermediate **I** would be generated which will undergo a [1,5] hydrogen shift to afford the intermediate **II** which ultimately leads to the oxindole and regenerates the catalyst.

2.3. Conclusion

In conclusion, we developed the efficient synthesis of oxindole derivatives via intramolecular ArC_{sp2}-H insertion reaction of diazo acetamides derived from the corresponding anilines by using Ru(II)-Pheox catalyst. The reaction proceeds smoothly under mild conditions, providing the corresponding oxindole derivatives in excellent yield (up to 99%). No other side reactions related to metal-carbene reactivity such as dimerization, aromatic ring expansion and C_{sp3}-H on amide nitrogen insertion reaction were observed.

CHAPTER 3

Synthesis of a new entries of chiral ruthenium complexes containing Ru-$C_{olefin}(sp^2)$ bond and their application for catalytic asymmetric cyclopropanation reactions

3.1. Introduction

The transition-metal catalyzed carbene transfer reaction of diazo compounds is one of the most useful pathways of synthesis chemistry. The success of the rhodium complexes in catalyzing carbene-transfer reactions is tempered by the high price of this metal. Therefore, ruthenium, a direct neighbor of rhodium in the periodic table, has been more recently introduced in the field of catalytic cyclopropanation, because it costs roughly one-tenth the price of rhodium. Another reason for focusing attention on ruthenium catalysts is the greater diversity of complexes to be evaluated, due to the richer coordination chemistry, as compared to rhodium.

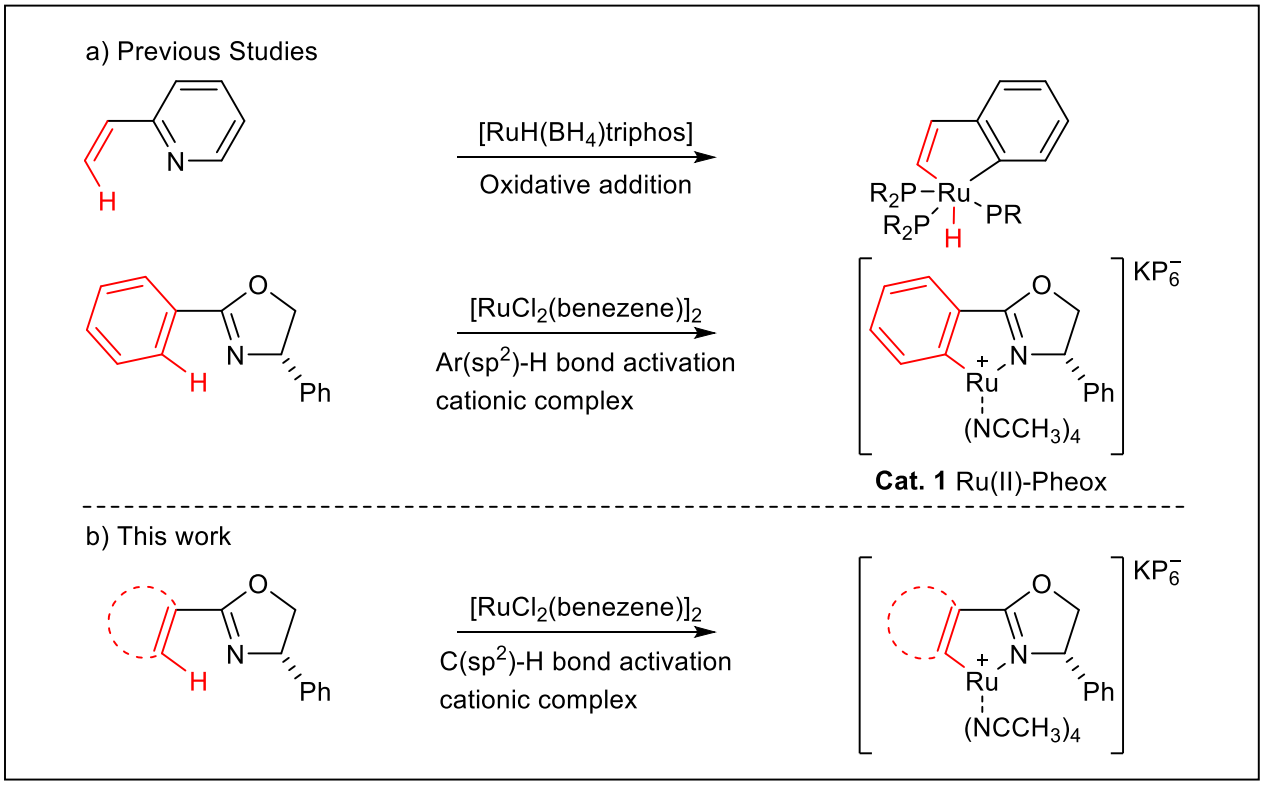

Scheme 40. Procedure for the synthesis of a series of Ru(II) complexes.

In the catalytic asymmetric cyclopropanation reactions, the multidentate chelating ligands of the ruthenium (II) complexes have a strong effect on the stereoselectivity[124]. Kastuki and coworkers reported that the Ru(II) complexes catalyzed the cyclopropanation of styrene and diazoacetate[125] with the high enantioselectivity. Moreover, in 1998, Nishiyama and coworker also

reported highly enantioselective cyclopropanation by C_1-symmetric Ru(II)-Pybox catalyst, explaining that the major carbene intermediate, in which the ester group was anti to the bulky substituent of the ligand, might be selectively attacked by olefins from the third quadrant. Although the enantioselectivities were still lower than those obtained with the corresponding C_2-symmetric analogs, this important report illustrated the potential of C_1-symmetric catalyst[126].

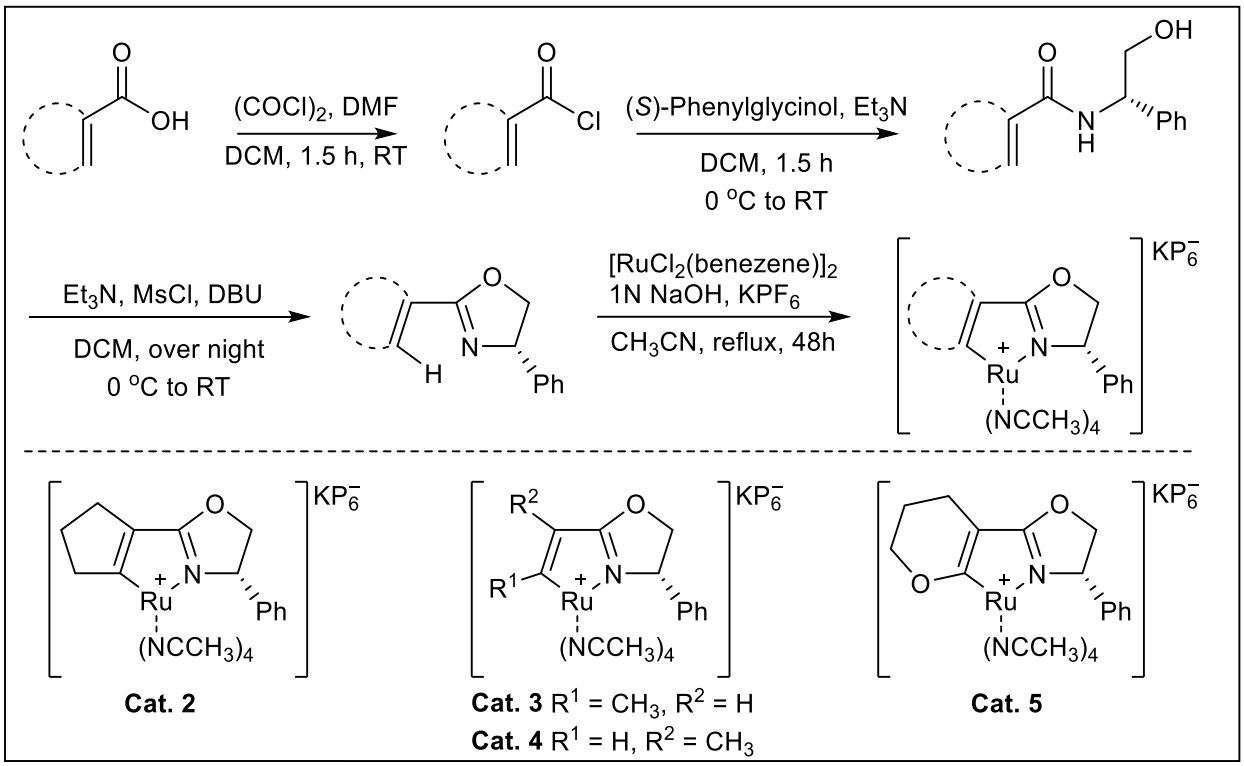

Scheme 41. Synthesis of chiral ruthenium complexes containing Ru-$C_{olefin}(sp^2)$ bond.

Recently, we reported about structure of chiral Ru(II)-phenyloxazoline (Ru(II)-Pheox) complex (Scheme 40), bearing a metal-carbon σ-bond and C_1-symmetric structure. This complex contains the strong electron donating effect of the aromatic $C(sp^2)$ ligand on the ruthenium, which facilitates oxidative addition. We also successfully demonstrated that Ru(II)-Pheox complex can promote catalytic asymmetric intra-molecular cyclopropanation, Si-H and C-H insertion produce the desired products in high yields and high enantioselectivities[106]. On another hand, in 1990, Jia and coworker reported the reaction of ruthenium hydride complexes containing phosphines with olefins (Scheme 40)[127]. The ruthenium complexes formed from these reactions are very dependent on the olefins used. So we supposed that the simple alkenyl oxazoline ligands could react to the ruthenium source. According to these previous research of Ru(II) complexes, we

designed a higher active ruthenium complex, which contains a strong electron-donating effect of the simple alkene C(sp^2)-Ru bond (Scheme 41).

3.2. Results and discussions

3.2.1. Preparing the ruthenium complexes

Initial, the alkenyl oxazoline ligand was readily synthesized in three steps. After chlorination of an unsaturated carboxylic acid, the compound was condensed with (*S*)-phenylglycinol and then oxazoline formation with methanesulfonyl chloride and triethylamine and DBU.

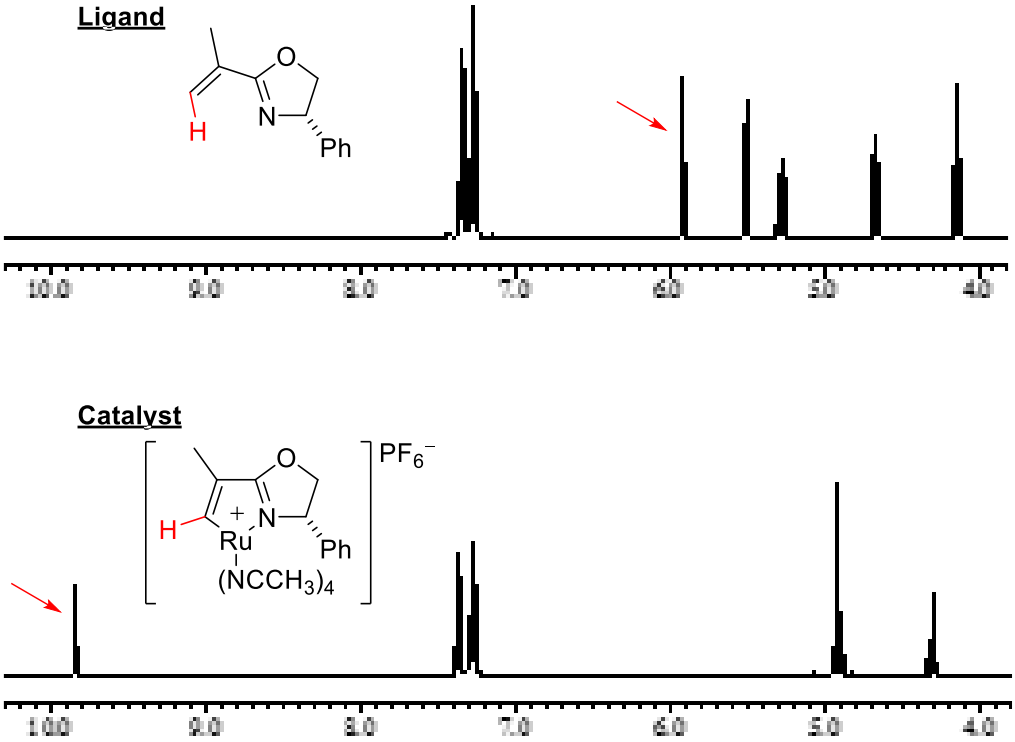

Figure 7. ^{1}H-NMR spectra of ligand and Ru(II) complex.

Follow that, the ruthenium complex was prepared by the C-H bond activation method of alkenyl oxazoline ligand, [$RuCl_2$(benzene)$_2$], 1N NaOH, and KPF_6 in an acetonitrile solution at 85 °C. Finally, the catalysts 2–5 were obtained in high yield up to 91%. And the catalysts were stable under argon atmosphere and could be stored for a long time. Moreover, these complexes' structures also analyzed by ^{1}H NMR and X-ray diffraction (Figure 7, 8).

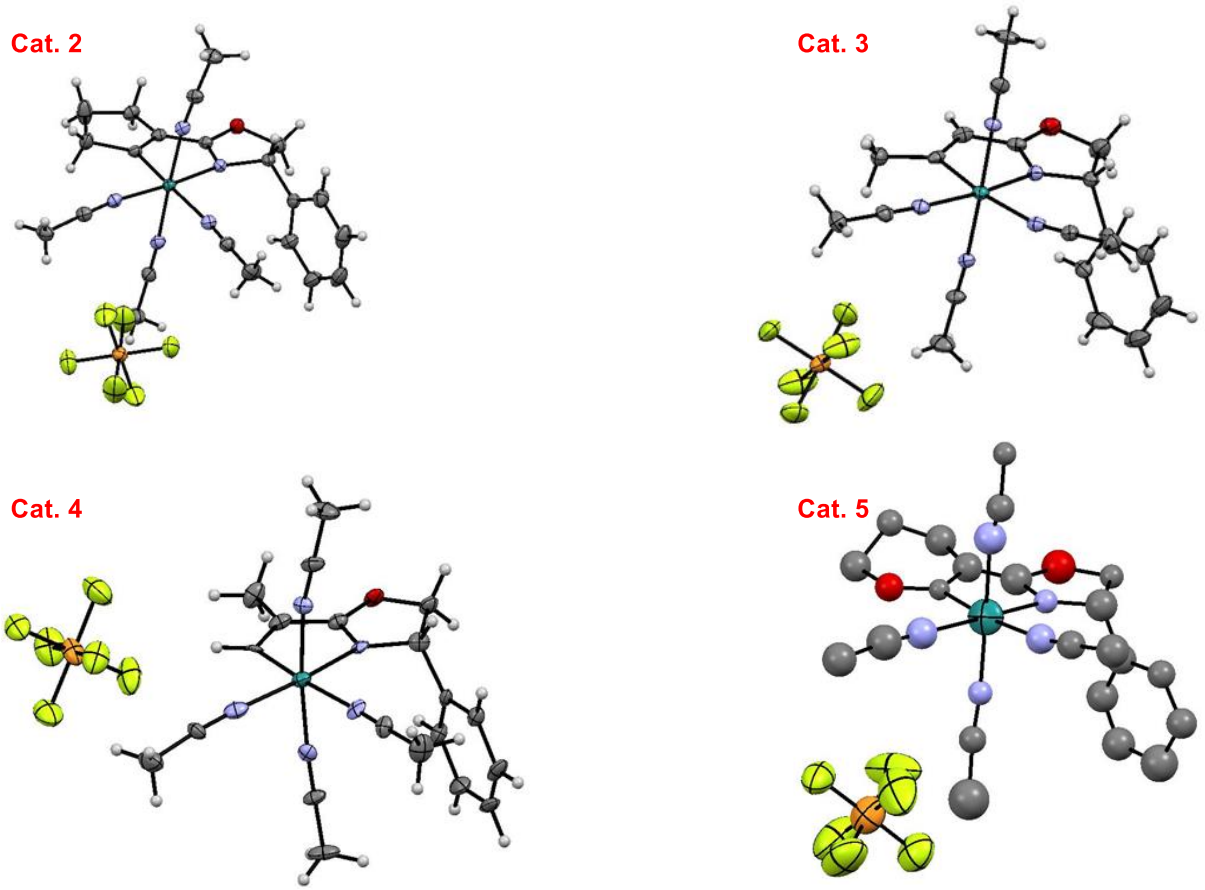

Figure 8. X-ray analysis of a novel Ru(II) complexes.

3.2.2. Ruthenium complexes containing Ru-$C_{olefin}(sp^2)$ bond catalyzed intermolecular cyclopropanation

3.2.2.1 Catalyst screening and optimization conditions for the catalytic intermolecular cyclopropanation reaction

The ruthenium complexes containing Ru-$C_{olefin}(sp^2)$ bond were tested for catalytic cyclopropanation reaction of ethyl diazoacetate **53** and olefins **52b** (Table 5). The reaction proceeded in the presence of 3 mol% of catalyst.

As shown in the Table 5, using cat. 2 and cat. 3, the product **54b** was obtained in the moderate yield (75–79%) and the enantioselectivity up to 90% (Table 5, entries 2, 3). While both cat. 1 and cat. 5 showed their catalytic efficiency in this reaction with not only high yield (up to 91%) but also high enantioselectivity (up to 97%) of the desired product (Table 5, entries 1, 5). However, in comparison, the cat. 4 was demonstrated that it is the most effective catalyst for this

reaction (Table 5, entry 4). The given data showed that compound **54b** was formed in the excellent yield (97%), as well as diastereo- and stereoselectivities (trans/cis = 90/10 and 97% ee).

Table 5. Screening of various catalysts and optimization conditions of intermolecular cyclopropantion reaction.

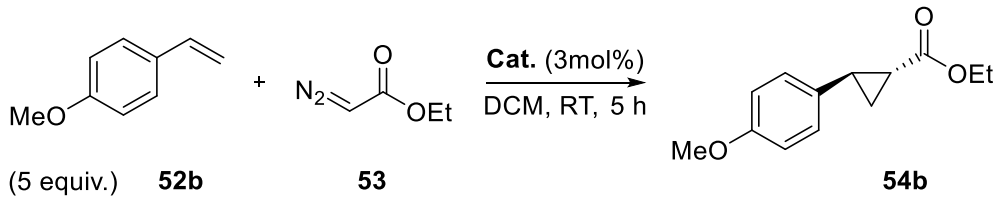

Entry	Cat.	Solvent	Temp.[°C]	Yield [%][a]	*Trans/cis*[b]	ee [%][c]
1	1	DCM	RT	86	88/12	96
2	2	DCM	RT	75	88/12	78
3	3	DCM	RT	79	89/11	90
4	4	DCM	RT	97	90/10	97
5	5	DCM	RT	91	88/12	97
6	4	Toluene	RT	38	92/8	97
7	4	CH_3CN	RT	82	88/12	96
8	4	Et_2O	RT	96	92/8	96
9	4	THF	RT	93	92/8	97
10	4	MTBE	RT	98	93/7	97
11	4	MTBE	0	93	96/4	97
12	4	MTBE	0	92	95/5	97
13	4	MTBE	40	73	93/7	95
14	4	MTBE	–10	96	96/4	98
15	4	MTBE	–30	92	97/3	99

[a] Isolated yield. [b] Determined by ^{1}H NMR. [c] Determined by chiral HPLC analysis.

It can be explained that cat. 4 has planarity of the substituent on β position of Ru-C(sp^2) bond (Scheme 42). This interpretation had already mentioned for the case of Ru(II)-Pheox catalyzed asymmetric cyclopropanation.

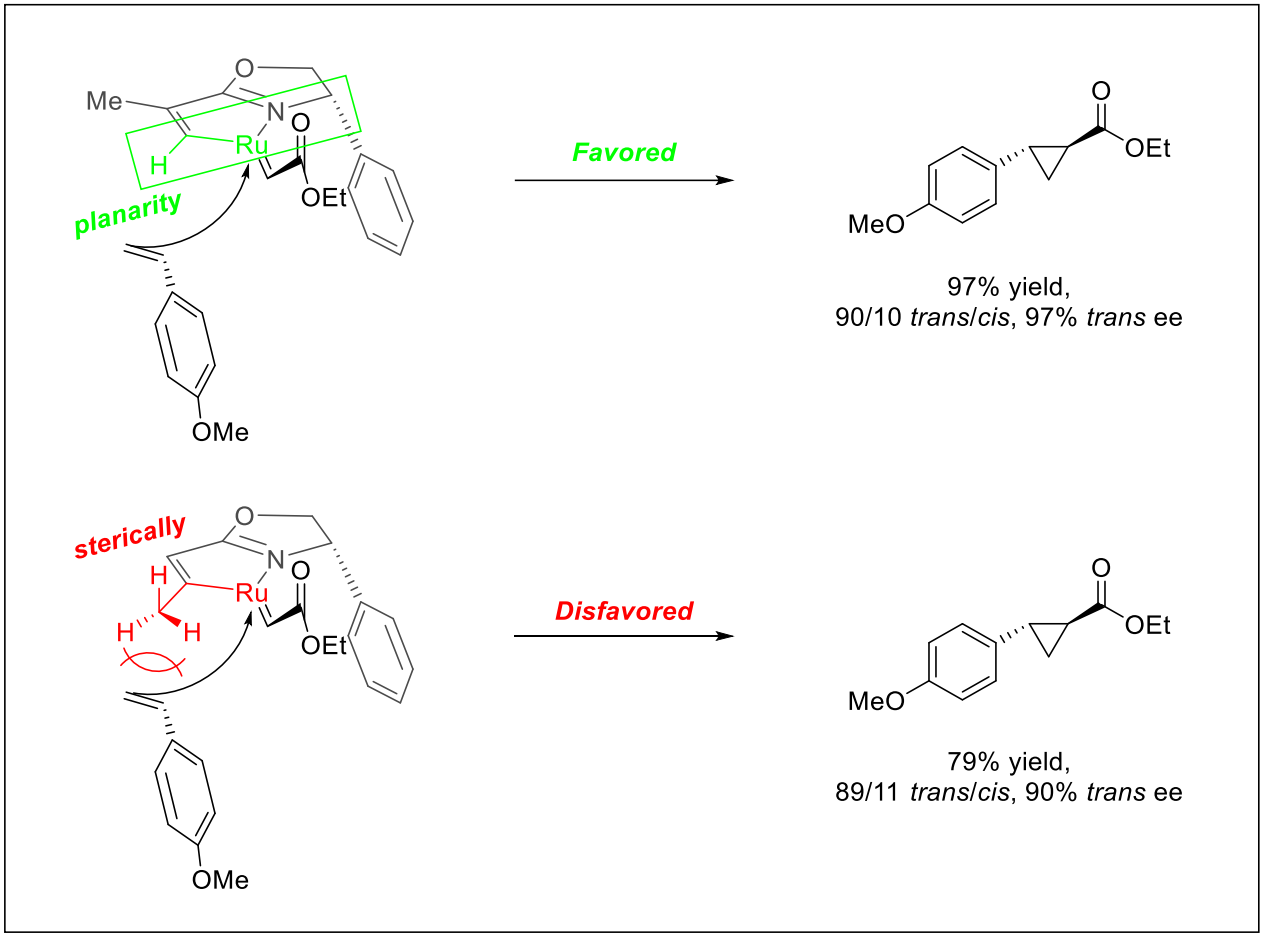

Scheme 42. Planarity of the substituent on β position of Ru-C(sp^2) bond.

Moreover, we're also interested in the influence of various solvents and temperatures on this catalytic cyclopropanation reaction.

The results showed that the product was produced in high yields and enantioselectivitives for most of the common organic solvents (Table 5, entries 4, 7–10). In the case of toluene (Table 5, entry 6), the yield of reaction becomes dramatically decrease. Methyl tert-butyl ether (MTBE) or dichloromethane (DCM) solvents and room temperature were found as best condition for this reaction.

3.2.2.2. The substrate scope for the catalytic intermolecular cyclopropanation reaction

Under the optimized conditions, we decided to explore the substrate scope (Tables 8). Most of the styrene derivatives transformed into cyclopropanes with high yield (up to 99%), excellent diastereoselectivities (up to >99/1) and enantioselectivities (97%–99% ee).

Table 6. Substrate scope of intermolecular cyclopropanation reaction.

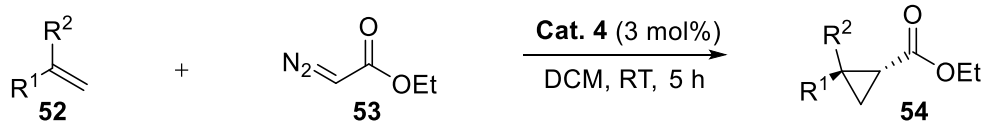

Entry	**55**	R^1	R^2	Yield [%][a]	*Trans/cis*[b]	ee [%][c]
1	**a**	4-Me-Ph	H	90	96/4	98
2	**b**	4-MeO-Ph	H	97	96/4	97
3	**c**	2-MeO-Ph	H	96	99/1	99
4	**d**	4-Cl-Ph	H	92	98/2	98
5	**e**	Ph	Me	87	55/45	97
6	**f**	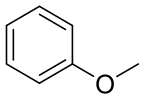	H	87	83/17	97
7	**i**	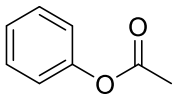	H	55	>99/1	99
8	**j**	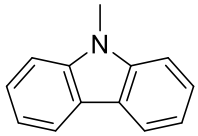	H	97	99/1	99
9	**k**	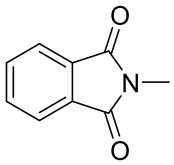	H	83	96/4	99
10	**l**	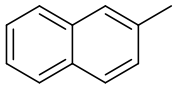	H	99	98/2	98

[a] Isolated yield. [b] Determined by ^{1}H NMR. [c] Determined by chiral HPLC analysis.

On another hand, only the α-methylstyrene provided the desired product in the moderate diastereoselectivity (Table 6, entry 7). It means that the ruthenium complex is very suitable for cyclopropanation of ethyl 2-diazoacetate.

According to the positive result in Table 6, we decided to discover the efficiency of the ruthenium complexes containing Ru-$C_{olefin}(sp^2)$ bond in the intramolecular cyclopropanation of allyl 2-diazoacetate derivatives.

3.2.3. Ruthenium complexes containing Ru-$C_{olefin}(sp^2)$ bond catalyzed intramolecular cyclopropanation

3.2.3.1. Catalyst screening and optimization conditions for the catalytic intramolecular cyclopropanation reaction

Table 7. Screening of various catalysts and optimization conditions of intramolecular cyclopropantion reaction.

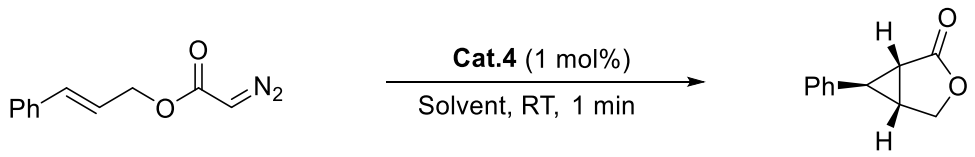

55a **56a**

Entry	Cat.	Solvent	Yield [%][a]	ee [%][b]
1	1	DCM	96	96
2	2	DCM	87	97
3	3	DCM	95	90
4	4	DCM	96	99
5	5	DCM	91	96
6	4	Toluene	69	98
7	4	Et_2O	87	98
8	4	THF	95	97
9	4	MTBE	98	98

[a] Isolated yield. [b] Determined by chiral HPLC analysis.

Table 7 showed that all the catalysts proceeded the reaction to form the product **56** in the high yields (87%–98%) and excellent enantioselectivities (90%–99%). Especially, at room temperature with the presence of 1 mol% of cat. 4, the cinnamyl 2-diazoacetate (**55a**) transformed into the corresponding cyclopropane (**56a**) in excellent both yield and enantioselectivity (Table 7, entry 4).

3.2.3.2. The substrate scope for the catalytic intramolecular cyclopropanation reaction

Base on that, we continued to screen the solvents for this reaction (Table 7, entries 4, 6–9). Many solvents were applied such as dichloromethane, toluene, diethyl ether, tetrahydrofuran, methyl tert-butyl ether. In there, DCM demonstrated to be the best solvent for this intramolecular cyclopropanation reaction.

Table 8. Substrate scope of intramolecular cyclopropanation reaction.

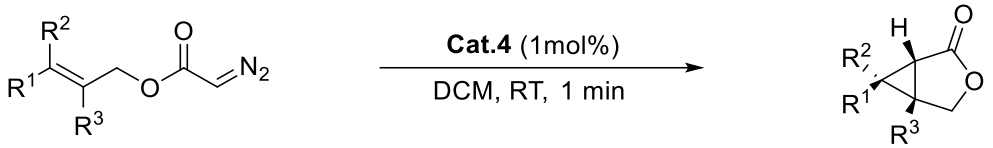

55 **56**

Entry	**55**	R^1	R^2	R^3	Yield [%][a]	ee [%][b]
1	**a**	Ph	H	H	96	99
2	**b**	Ph	H	Me	99	93
3	**c**	4-OMe-Ph	H	H	98	90
4	**d**	4-NO_2-Ph	H	H	96	99
5	**e**	Me	Me	H	99	98
6	**f**	H	H	H	91	99

[a] Isolated yield. [b] Determined by chiral HPLC analysis.

With the optimized conditions in hand, we explored the substrate scope (Table 8). The cycloaddition, of the allyl 2-diazoacetate derivatives **55a**–**55f** were examined as shown in table 8. Similar to our prediction, all the corresponding cyclopropantions **56a**–**56f** were obtained in excellent yields (91%–99%) and enantioselectivities (90%–99%).

3.3. Conclusion

In summarize, we developed successfully a new efficient chiral ruthenium catalyst, which was applied in catalytic asymmetric cyclopropanation of carbene transfer reaction. With an only small amount of catalyst (1–3 mol%), the reaction proceeds smoothly under mild conditions, giving the corresponding cyclopropane carboxylates products in excellent yields (up to 99%) and enantioselectivities (up to 99%).

CHAPTER 4

Highly stereoselective intramolecular Buchner reactions of diazoacetamides catalyzed by Ru(II)-Pheox complex

4.1. Introduction

Medium ring-containing organic molecules, such as seven-membered rings, are the cornerstone of many bioactive natural compounds such as guaiane sesquiterpenes, guaianolide sesquiterpene lactones, and diterpene tiglianes.[100] However, there are few reports on their synthesis. Unlike five- and six-membered rings, the synthesis of seven-membered rings is more challenging and generally limited to multi-step processes rather than direct intramolecular reactions.[101]

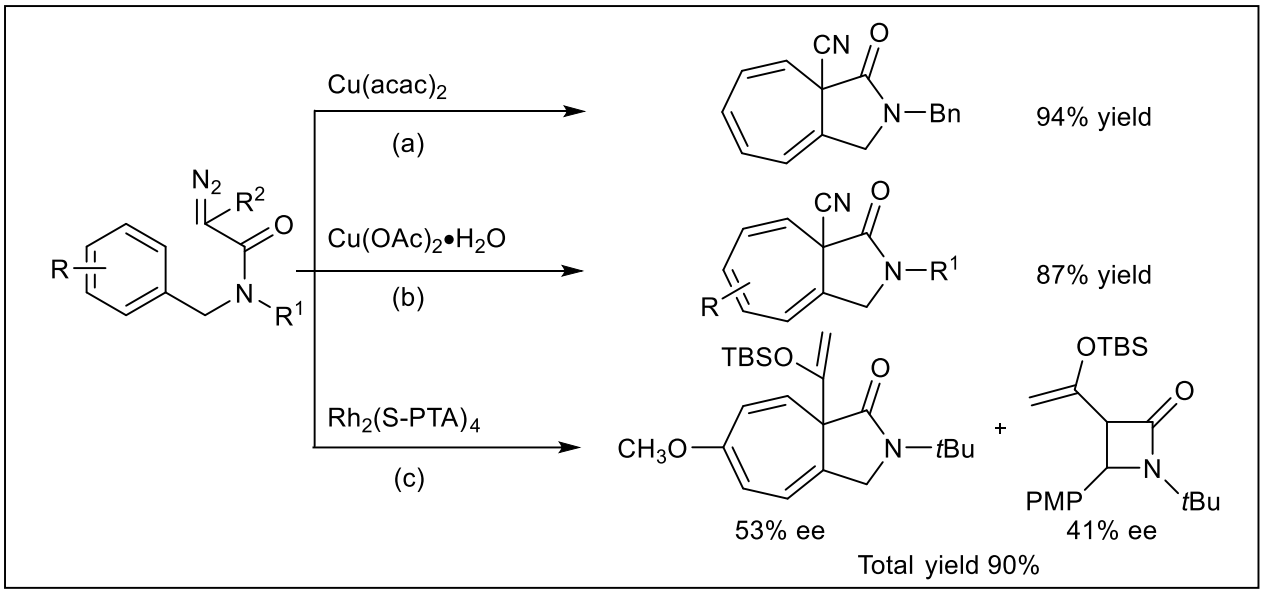

Scheme 43. Transition metal catalytic carbene transfer reaction of diazoacetamides.

Thus, the development of an efficient method to prepare these scaffolds has attracted a significant amount of research attention. Over the past few decades, the transition metal-catalyzed intramolecular Buchner reaction has been reported by several research groups.[102] This unique strategy toward seven-membered carbocycles has been utilized in natural product synthesis.[103]

However, the catalytic intramolecular reaction of diazoacetamides, diazoketones and diazoesters usually leads to competition between the Buchner and C-H insertion reactions.[104]

Therefore, many reports deal with controlling the regioselectivity of the reaction, which not only depends on the type of starting material used, but also the nature of the reaction solvent.

Moreover, when compared to the intramolecular C-H insertion reaction of diazoacetamides, there are fewer reports on the Buchner reaction (Scheme 43a, b).[105] In particular, very few examples have addressed the stereoselectivity of the Buchner product from the corresponding diazoacetamide.[106]

To date, only one research study by Doyle and co-workers (2015) has reported the asymmetric intramolecular Buchner reaction of diazoacetamides, whereby *N*-tert-butyl-N-(p-methoxybenzyl)enoldiazoacetamide resulted in a mixture of the C-H insertion product and Buchner product in a total yield of 90% with moderate enantioselectivities of 41 and 53% ee, respectively (Scheme 36c).[106]

Recently, we have developed a Ru(II)-Pheox complex, which is efficient in carbene transfer reactions, in particular, asymmetric cyclopropanation and Si-H insertion reactions.[107]

Driven by our interests in the catalytic intramolecular Buchner reaction of diazoacetamide and the efficiency displayed by the Ru(II)-Pheox catalyst, we started to study the enantioselective reaction, which is much more challenging (Scheme 44).

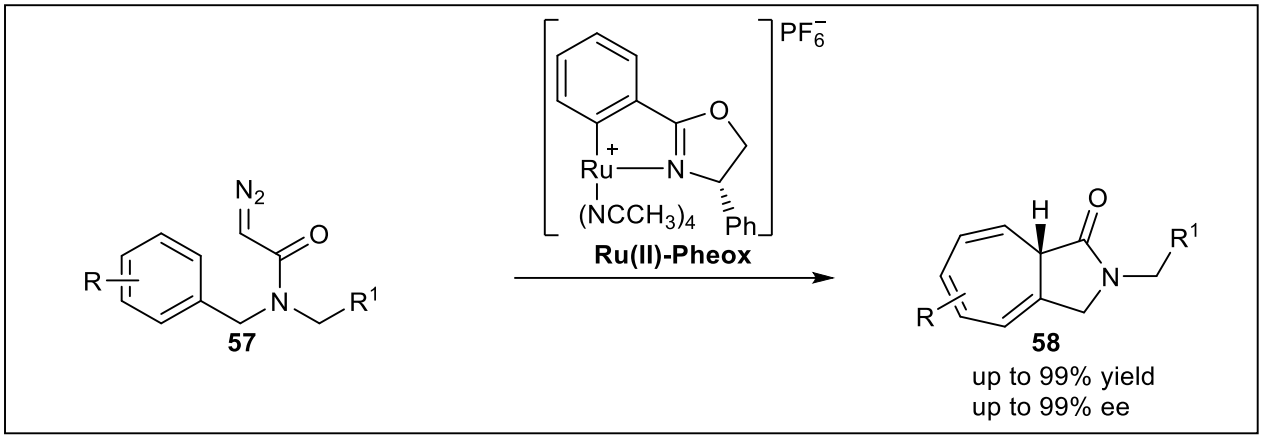

Scheme 44. Asymmetric intramolecular reaction of diazoacetamides catalyzed by the Ru(II)-Pheox complex.

4.2. Results and discussions

4.2.1. Catalyst screening for intramolecular asymmetric Buchner reaction of diazoacetamides

At the outset of this investigation, *N*,*N*-bis(4-methoxybenzyl)-2-diazoacetamide **57b** was chosen as the substrate using 1 mol% of catalyst to optimize the reaction conditions. Initially, well-know carbene transfer catalysts were screened and the results summarized in Table 7.

Table 9. Catalyst screening experiments.

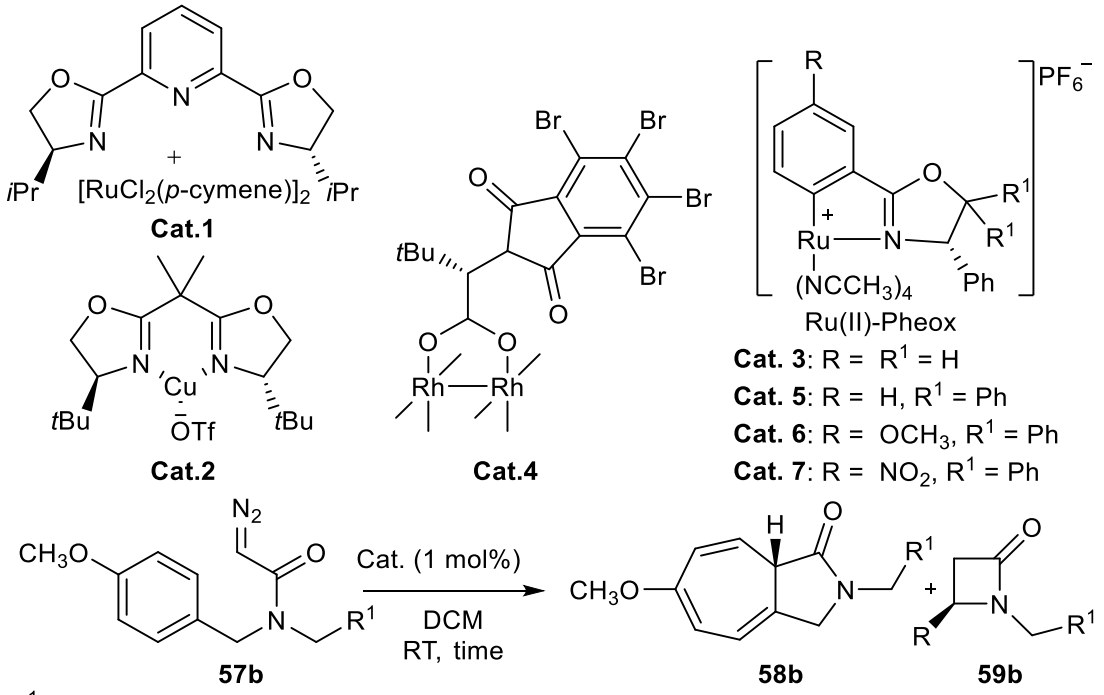

R^1 = -C_6H_4(4-OCH_3)

Entry	Cat.	Time [min.]	Ratio [**58b**:**59b**][a]	Yield[%][b]	ee[%][c] **59b**
1	1	48 h	100:0	52	0
2[d]	2	60	100:0	87	15
3	3	2	100:0	99	99
4	4	2	100:0	95	21
5	5	2	100:0	98	99
6	6	2	100:0	98	99
7	7	2	100:0	93	99

[a] The ratio of **58b:59b** was determined using ^{1}H NMR spectroscopy. [b] Isolated yield. [c] Determined using chiral HPLC analysis. [d] The reaction temperature was 40 ^{o}C.

Extensive studies on the reaction conditions indicated that after 48 h, product **58b** was obtained in 52% yield with no chirality using Ru(II)-Pybox (Table 9, entry 1). When Cu(II)-Box was used, product **58b** was formed in 87% yield and 15% ee (Table 9, entry 2). In the case of the Rh_2(S-TBPTTL)$_4$ complex, the yield of **58b** increased dramatically to 95%. However, the

enantioselectivity was relatively low (21% ee) (Table 9, entry 4). Screening the various Ru(II)-Pheox catalyst derivatives developed by our group showed that the chiral Ru(II)-Pheox complex (cat. 3) was the most effective catalyst (Table 9, entries 3, 5–7).[107] The reaction proceeds rapidly to give **58b** in excellent yield (99%) with almost perfect enantioselectivity (99% ee).

We next focused on the efficiency of the Ru(II)-Pheox catalyst and the results shown in Table 10. We found that decreasing the catalyst loading from 1 to 0.002 mol% showed no change in the enantioselectivity (99% ee) of product **58b**, while the TON and TOF values increased (Table 10). Using a very small amount of the Ru(II)-Pheox catalyst (0.005 mol%) gave product **58b** within 2 min in 99% yield with excellent TOF (9900 min^{-1}) (Table 10, entry 4). When 0.003 mol% of catalyst was used, the TON increased dramatically to 33000 (Table 10, entry 5).

Table 10. Efficiency of the Ru(II)-Pheox catalyst.

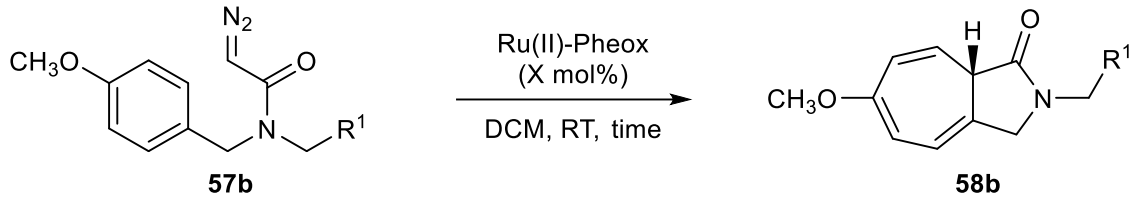

R^1 = $-C_6H_4(4\text{-}OCH_3)$

Entry	X [mol%]	Time [min.]	TON	TOF [min^{-1}]	Yield [%][a]	ee[%][b]
1	1	2	99	44.5	99	99
2	0.1	2	990	445	99	99
3	0.01	2	9990	4450	99	99
4	0.005	2	19800	9900	99	99
5	0.003	30	33000	1100	99	99
6	0.002	60	10000	167	20	99

[a] TON = moles of desired product (**58b**)/moles of catalyst (Ru(II)-Pheox).
[b] TOF = TON/reaction time (min). [c] Isolated yield. [d] Determined using chiral HPLC analysis.

4.2.2. Solvent screening for intramolecular asymmetric Buchner reaction of diazoacetamides

In addition, the influence of various solvents on the decomposition of diazoacetamides was examined and the results shown in Table 11. Bicyclic compound **58b** was obtained in high yield and excellent enantioselectivity in most conventional organic solvents (Table 11, entries 1–6, 8). Protic solvents such as methanol also gave **58b** in high yield without any C-H insertion reaction of the diazo compound (Table 11, entry 8). The reaction proceeded rapidly except in the presence

of a coordinatable solvent, such as acetonitrile and dimethylformamide (DMF). When using toluene, acetonitrile, or dimethylformamide (DMF) (Table 11, entries 2, 5, 6), the rate of the reaction become was reduced. Dimethyl sulfoxide (DMSO) gave no reaction (Table 11, entry 7). Ligation of DMSO to the ruthenium catalyst may be strong and poison the catalyst. DCM was found to be the best solvent for the Ru(II)-Pheox catalyzed reaction.

Table 11. Optimization of the reaction conditions.

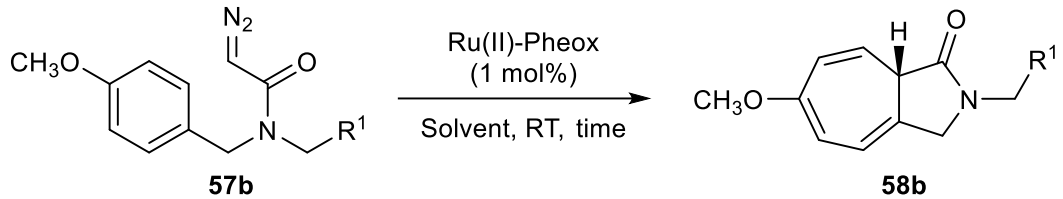

57b **58b**

R^1 = -C_6H_4(4-OCH_3)

Entry	Solvent	Time [min.]	Yield [%][a]	ee[%][b]
1	DCM	2	99	99
2	Toluene	30	98	99
3	Acetone	2	86	99
4	THF	2	99	98
5	Acetonitrile	60	97	98
6	DMF	60	99	96
7	DMSO	5 h	n.r	_
8	Methanol	2	99	94

[a] Isolated yield. [b] Determined by chiral HPLC analysis.

4.2.3. Ru(II)-Pheox catalyzed intramolecular Buchner reactions of diazoacetamides

Using the optimized reaction conditions, we decided to explore the substrate scope of the reaction (Table 10). Various diazoacetamides of *N*,*N*-bis(aryl)-2-diazo-acetamides were examined (Table 10, entries 1–7).

Substrates bearing either electron-withdrawing or electron-donating groups (R = H, F, Cl, Br, CH_3, and OCH_3) on the *N*-benzyl ring were tolerated in the reaction, giving the desired products (**58a–g**) in 69–99% yield and 74–99% ee.

Substitution with an electron-donating group (e.g., 4-OCH_3, 3-OCH_3, and 4-CH_3) on the *N*-benzyl ring moiety has a strong impact on the reaction (Table 10, entries 2, 3, and 7). The corresponding Buchner reaction products were obtained in excellent yield (up to 99%) and enantioselectivity (up to 99% ee).

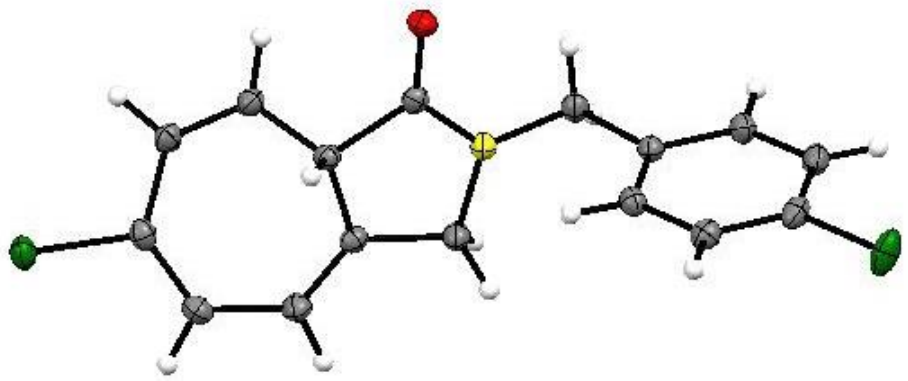

Figure 9. X-Ray analysis of (*S*)-6-chloro-2-(4-chlorobenzyl)-3,8a-dihydrocyclohepta[c]pyrrol-1(2H)-one (**58d**).

In the case of substrates bearing an electron-withdrawing group (namely 4-Cl, 4-Br and 4-F), the rate of the Buchner reaction slightly decreased and formation of the C-H insertion product was observed (Table 10, entries 4–6). Nevertheless, the yield and enantioselectivity of the products (**51d**−**f**) remained excellent (70−91% yield and 90−96% ee). In addition, the bicyclic product **58d** was prepared with the purpose of growing crystals suitable for analysis. The structure of **58d** was confirmed and the absolute configuration was determined to be the *S* configuration using single-crystal X-ray diffraction (Figure 7). In short, entries 1–7 in Table 10 present an overview of the decomposition of a series of *N*,*N*-bis(aryl)-2-diazo-acetamides used to prepare the target seven-membered ring products (**58a**–**g**) with excellent stereo- and regioselectivity. Besides, a diazoamide bearing both electron-withdrawing and electron-donating groups (**57h**) was also investigated as a substrate, affording the desired Buchner reaction product (**58h**) in high yield (84%) and excellent enantioselectivity (99% ee) (Scheme 45).

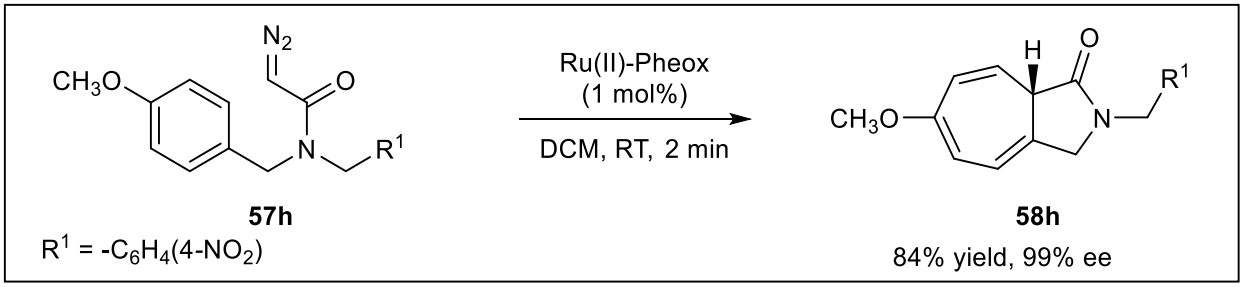

Scheme 45. Asymmetric intramolecular reactions of 2-diazo-*N*-(4-methoxybenzyl)-*N*-(4-nitrobenzyl)acetamide (**50h**) catalyzed by Ru(II)-Pheox.

The reaction afforded the intramolecular Buchner product **58j** (R = 4-OCH_3) in 76% yield with high enantioselectivity (99% ee) (Table 12, entry 9). Switching the substrate to **57k** (R = 4-CH_3) dramatically changed the reaction, affording the corresponding seven-membered ring product (**58k**) in 48% yield in 2 min (Table 12, entry 10). Surprisingly, we found that the reaction could afford product **58k** in 67% yield over a longer reaction time (4 h) (Table 12, entry 11). The dimerization reaction was prevented and the reaction yield was improved upon slow addition of a solution of the diazoacetamide to a stirred mixture of the Ru(II)-Pheox catalyst in DCM over 4 h (Table 12, entries 8, 11–15).

Table 12. Ru(II)-Pheox catalyzed intramolecular Buchner reactions of diazoacetamides.

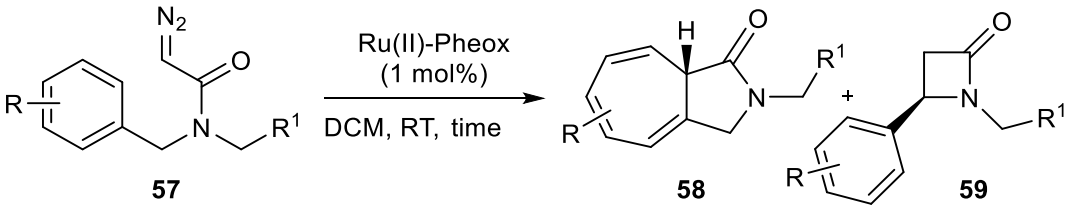

Entry	**57**	R	R^1	Time [min]	[**58**:**59**][a]	Yield [%][b] **58**	**58** ee[%][c]
1	**a**	H	C_6H_5	2	75:25	69	78
2	**b**	4-OCH_3	4-$CH_3OC_6H_4$	2	100:0	99	99
3	**c**	4-CH_3	4-$CH_3C_6H_4$	2	97:3	96	97
4	**d**	4-Cl	4-ClC_6H_4	2	83:17	80	96
5	**e**	4-Br	4-BrC_6H_4	2	80:20	70	95
6	**f**	4-F	4-FC_6H_4	2	92:8	91	90
7	**g**	3-OCH_3	3-$CH_3OC_6H_4$	2	100:0	87	74
8	**i**	H	H	4 h	45:55	47	71
9	**j**	4-OCH_3	H	2	100:0	76	99
10	**k**	4-CH_3	H	2	90:10	48	99
11	**k**	4-CH_3	H	4 h	93:7	67	99
12	**l**	4-Cl	H	4 h	83:17	61	92
13	**m**	4-Br	H	4 h	80:20	43	96
14	**n**	4-F	H	4 h	79:21	55	92
15	**o**	4-NO_2	H	4 h	_	n.o.	_

[a] The ratio was determined using 1H NMR spectroscopy of the reaction mixture.
[b] Isolated yield. [c] Determined using chiral HPLC analysis.

Furthermore, there is intense competition between the reactive sites of the *N*-aryl-2-diazo-*N*-methylacetamide (Table 12, entries 8, 12–14). Therefore, bicyclic products **58i** and **58l**–**58n** could be obtained in moderate yield (43–61%). In the case of diazo compound **57o**, the corresponding product **58o** as not obtained.

As a plausible explanation, the substituent changes the electronic properties of the benzene ring and affects the regioselectivity. Nucleophilic substituents, such as 4-CH_3 and 4-OCH_3, are regarded as electronic donating groups, which increase the electropositivity of the aryl group and improve the reactivity in the aromatic addition reaction. Electrophilic substituents, such as -Cl, -Br, -F, and -H, are regarded as electron-withdrawing groups, which decrease the electropositivity of the aryl group and favor the C-H insertion reaction.

4.3. Conclusion

In summary, we have presented a highly stereoselective intramolecular Buchner reaction of diazoacetamides using a Ru(II)-Pheox catalyst. Specifically, a variety of γ-lactam fused 5,7-bicyclic-heptatriene derivatives have been prepared from diazoacetamides in up to 99% yield with high enantioselectively (up to 99% ee) using a chiral Ru(II)-Pheox catalyst under mild reaction conditions. The product containing diene can be used for further transformation via the Diels-Alder cycloaddition reaction.

CHAPTER 5

Conclusion

The complexation between carbene and a transition metal is a most active intermediate, which affords the catalytically inserts into σ and π bonds of the organic compound. On another hand, recently, we have developed a Ru(II)-Pheox complex, which is efficient for carbene transfer reactions, in particular, asymmetric cyclopropanation, N-H insertion, C-H insertion and Si-H insertion reactions.

They inspired us to develop an efficient catalytic intramolecular carbene transfer reactions by using originally developed ruthenium catalyst into σ and π bonds and successfully applied for the synthesis of γ-lactam ring fused aromatics (oxindoles), γ-lactone ring fused cyclopropanes, and γ-lactam ring fused seven-membered rings via Buchner reaction. Base on the research objectives, we successfully developed the new methodology for the synthesis of the oxindole derivatives, cyclopropane ring, and the 7 membered rings by carbene transfer reaction using catalyst Ru(II)-Pheox:

In Chapter 2, the oxindole ring is prevalent as an important scaffold found in numerous natural products and pharmaceutically active compounds. Over the past few decades, the emerging therapeutic potential of the structural motif of oxindole has encouraged the medicinal chemists to synthesize novel oxindole derivatives. In the presence of Ru(II)-Pheox, the intramolecular C-H insertion reaction proceeds smoothly under mild conditions, providing the corresponding oxindole derivatives in excellent yield (up to 99%). And no other side reactions related to metal-carbene reactivity were observed.

In Chapter 3, cyclopropane subunit is also present in many biologically important compounds and it shows a large spectrum of biological properties. Transition metal-catalyzed cyclopropanation involving carbene intermediate is powerful and useful methods for constructing important substructures of targeted molecules, and therefore they have been extensively studied for the past couple of decades. Continuing our study of the development of asymmetric catalysts based on Ru(II)−Pheox complexes, we focus to tune the reactivity and selectivity of the metal center in the Ru(II)−Pheox complex. And we successfully developed a new series of $Ru{-}C_{olefin}(sp^2)$ bond-containing organometallic complexes and applied them to the catalytic

asymmetric intramolecular cyclopropanations with olefins. The corresponding optically active cyclopropanes were obtained in excellent yield (99%) and excellent enantioselectivity 99% ee.

In Chapter 4, the seven-membered rings are the cornerstone of many bioactive natural compounds such as guaiane sesquiterpenes, guaianolide sesquiterpene lactones. However, there are few reports on their synthesis. Thus, the development of an efficient method to prepare these scaffolds has attracted a significant amount of research attention. This unique strategy toward seven-membered carbocycles has been utilized in natural product synthesis. In this chapter, I demonstrated that the Ru(II)–Pheox was shown to be highly efficient in this first efficient enantioselective intramolecular Buchner reaction of diazoacetamides in terms of both the regio- and enantioselectivity (up to 99% ee) giving the desired products in quantitative yield.

CHAPTER 6

Experimental analytical data

6.1. General:

All reactions were performed under an atmosphere of argon unless otherwise noted. Dichloromethane (DCM) was purchased from Kanto Chemical Co., Inc.. All reactions were monitored by thin layer chromatography (TLC), glass plates pre-coated with silica gel Merck KGaA 60 F_{254}, layer thickness 0.2 mm. The products were visualized by irradiation with UV light or by treatment with a solution of phosphomolybdic acid or by treatment with a solution of *p*-anisaldehyde. Flash column chromatography was performed using silica gel (Merck, Art. No. 7734). ^{1}H NMR (500 MHz, 400 MHz) and ^{13}C NMR (125 MHz, 100 MHz) spectra were recorded on JEOL JNM-ECX500, JEOL JNM-ECS400 spectrometer. Chemical shifts are reported as δ values (ppm) relative to internal tetramethylsilane (0.00 ppm) in $CDCl_3$. Elemental analyses were measured on a Yanaco CHN CORDER MT-6. Optical rotations were performed with a JASCO P-1030 polarimeter at the sodium D line (1.0 mL sample cell). Enantiomeric excesses were determined by high-performance liquid chromatography (HPLC) analyses with a JASCO GULLIVER using Daicel CHIRALPAK or CHIRALCEL columns.

6.2. Experimental analytical data for chapter 2

6.2.1. Procedure for the synthesis of diazoacetamides

To a solution of *N*-methylaniline derivatives (10 mmol) in CH_2Cl_2 (20.0 mL) was added dropwise neat bromoacetyl bromide (0.95 mL, 11 mmol) at 0 °C. The reaction mixture was stirred for 30 min at room temperature. The organic product (bromoacetamide) was then extracted with CH_2Cl_2 (10 mLx3), dried (Na_2SO_4), and filtered. After evaporation of the solvent, the residue was used for the next step without purification. The resulting bromoacetamide and *N*,*N'*-bis(*p*-toluenesulfonyl)hydrazine (5.10 g, 15 mmol) were dissolved in THF (20 mL) and cooled down to 0 °C, then DBU (3 mL, 20 mmol) was added dropwise and stirred at 0 °C for 30 min. After quenched with 10% $NaHCO_3$ aq. and extracted with Et_2O (10 mLx3), the combined organic phase was dried over Na_2SO_4 and evaporated to give the crude product. Purification was performed with flash column chromatography on silica gel eluted with EtOAc/*n*-Hexane (1/5($^v/_v$)) to give the **2-diazo-*N*-phenyl-*N*-methylacetamide (50a)**. 55% yield. Yellow oil. NMR (^{1}H, ^{13}C) and IR data agree with reported[122] values.

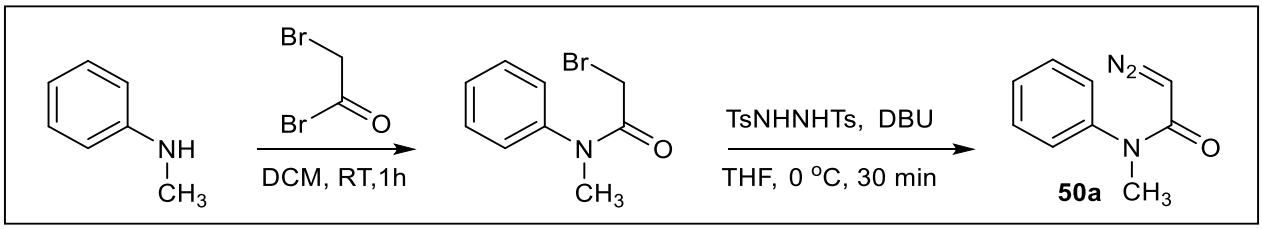

Scheme 46. Procedure for the synthesis of diazo acetamides.

6.2.2. Analytical data for diazoacetamides (50)

2-Diazo-*N*-(4-methoxyphenyl)-*N*-methylacetamide (50b)

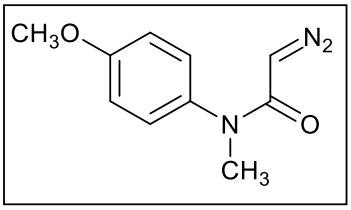

Same procedure as described above for **50a.** 66% yield. Yellow powder. ^{1}H NMR (500MHz, $CDCl_3$) δ 7.12 (ddd, *J* = 8.79, 3.44, 1.91 Hz, 2H), 6.91 (ddd, *J* = 9.56, 3.44, 1.91 Hz, 2H), 4.48 (s, 1H), 3.83 (s, 3H), 3.29 (s, 3H) ppm. ^{13}C NMR (125 MHz, $CDCl_3$) δ 166.19, 159.15, 135.95, 128.68, 115.02, 55.66, 47.22, 37.44 ppm. IR (neat) ν 3116, 2104, 1627, 1415, 1243, 774 cm^{-1}. HRMS (DART) calcd for $C_{10}H_{11}N_3O_2$ [M+H]+: 206.0929 found: 206.0929.

2-Diazo-*N*-(4-chlorophenyl)-*N*-methylacetamide (50c)

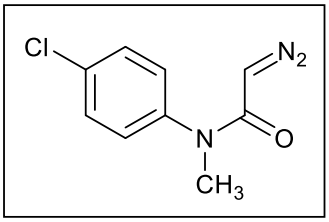

Same procedure as described above for **50a**. 49% yield. Yellow powder. ^{1}H NMR (500MHz, $CDCl_3$) δ 7.39 (ddd, *J* = 8.41, 8.41, 1.91 Hz, 2H), 7.17 (ddd, *J* = 8.41, 8.41, 1.91 Hz, 2H), 4.54 (s, 1H), 3.30 (s, 3H) ppm. ^{13}C NMR (125 MHz, $CDCl_3$) δ 165.75, 141.77, 133.76, 130.11, 128.79, 47.55, 37.26 ppm. IR (neat) ν 3064, 2109, 1623, 1415, 1284, 722 cm^{-1}. HRMS (DART) calcd for $C_9H_8N_3OCl$ [M+H]+: 210.0432 found: 210.0434.

2-Diazo-*N*-(4-bromophenyl)-*N*-methylacetamide (50d)

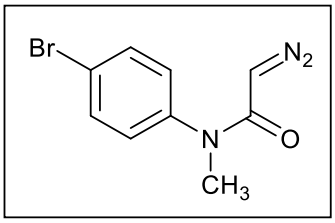

Same procedure as described above for **50a**. 50% yield. Yellow powder. ^{1}H NMR (500MHz, $CDCl_3$) δ 7.54 (ddd, *J* = 8.79, 8.79, 3.06 Hz, 2H), 7.10 (ddd, *J* = 8.79, 8.79, 3.06 Hz, 2H), 4.53 (s, 1H), 3.29 (s, 3H) ppm. ^{13}C NMR (125 MHz, $CDCl_3$) δ 165.81, 142.37, 133.19, 129.18, 121.79, 47.65, 37.30 ppm. IR (neat) ν 3088, 2100, 1623, 1419, 1281, 767 cm^{-1}. HRMS (DART) calcd for $C_9H_8N_3OBr$ [M+H]+: 253.9923 found: 253.9923.

2-Diazo-*N*-(4-iodophenyl)-*N*-methylacetamide (50e)

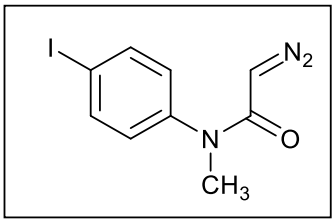

Same procedure as described above for **50a**. 65% yield. Yellow powder. ^{1}H NMR (500MHz, $CDCl_3$) δ 7.74 (ddd, *J* = 8.79, 2.29, 2.29 Hz, 2H), 6.97 (ddd, *J* = 9.94, 2.29, 2.29 Hz, 2H), 4.54 (s, 1H), 3.29 (s, 3H) ppm. ^{13}C NMR (125 MHz, $CDCl_3$) δ 165.61, 142.85, 138.98, 92.64, 47.72, 37.24 ppm. IR (neat) ν 3075, 2105, 1621, 1483, 1281, 787 cm^{-1}. HRMS (DART) calcd for $C_9H_8N_3OBr$ [M+H]+: 301.9795 found: 301.9790.

2-Diazo-*N*-(4-nitrophenyl)-*N*-methylacetamide (50f)

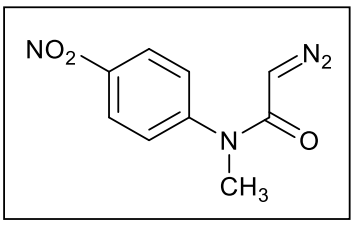

Same procedure as described above for **50a**. 53% yield. Yellow powder. ^{1}H NMR (500MHz, $CDCl_3$) δ 8.28 (ddd, *J* = 8.79, 8.79, 3.06 Hz, 2H), 7.44 (ddd, *J* = 8.79, 8.79, 3.06 Hz, 2H), 4.74 (s, 1H), 3.34 (s, 3H) ppm. ^{13}C NMR (125 MHz, $CDCl_3$) δ 165.60, 149.17, 146.16, 127.22, 125.24, 48.44, 37.19 ppm. IR (neat) ν 3111, 2104, 1627, 1427, 1165, 770 cm^{-1}. HRMS (DART) calcd for $C_9H_8N_4O_3$ [M+H]+: 221.0676 found: 221.0674.

2-Diazo-*N*-(2-methoxyphenyl)-*N*-methylacetamide (50h)

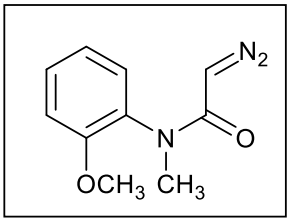

Same procedure as described above for **50a**. 43% yield. Yellow powder. ^{1}H NMR (500MHz, $CDCl_3$) δ 7.26 (ddd, *J* = 7.84, 7.84, 1.91 Hz, 1H), 7.06 (dd, *J* = 7.64, 1.91 Hz, 1H), 6.89 (ddd, *J* = 15.67, 7.64, 1.53 Hz, 2H), 4.54 (s, 1H), 3.76 (s, 3H), 3.13 (s, 3H) ppm. ^{13}C NMR (125 MHz, $CDCl_3$) δ 166.27, 155.46, 131.04, 129.84, 129.48, 121.04, 112.22, 55.62, 46.74, 35.77 ppm. IR (neat) ν 3067, 2103, 1626, 1419, 1242, 751 cm^{-1}. HRMS (DART) calcd for $C_9H_8N_3OBr$ [M+H]+: 206.0923 found: 206.0929.

2-Diazo-*N*-(2-bromophenyl)-*N*-methylacetamide (50i)

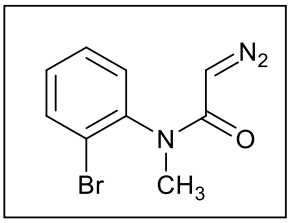

Same procedure as described above for **50a**. 62% yield. Yellow powder. ^{1}H NMR (500MHz, $CDCl_3$) δ 7.69 (dd, *J* = 13.76, 7.26 Hz, 2H), 7.41–7.39 (m, 1H), 7.31–7.26 (m, 2H), 4.31 (s, 1H), 3.25 (s, 3H) ppm. ^{13}C NMR (125 MHz, $CDCl_3$) δ 165.77, 141.58, 134.16, 130.40, 130.28, 129.20, 123.77, 47.38, 35.84 ppm. . IR (neat) ν 3067, 2108, 1627, 1420, 1289, 767 cm^{-1}. HRMS (DART) calcd for $C_9H_8N_3OBr$ [M+H]+: 253.9923 found: 253.9929.

2-Diazo-*N*-(2-iodophenyl)-*N*-methylacetamide (50j)

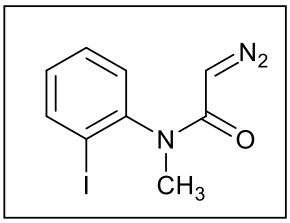

Same procedure as described above for **50a**. 35% yield. Yellow powder. ^{1}H NMR (500MHz, $CDCl_3$) δ 7.93 (dd, *J* = 7.64, 1.53 Hz, 1H), 7.42 (ddd, *J* = 7.64, 7.64, 1.53 Hz, 1H), 7.27 (dd, *J* = 7.64, 1.53 Hz, 1H), 7.09 (ddd, *J* = 7.64, 7.64, 1.53 Hz, 1H), 4.25 (s, 1H), 3.22 (s, 3H) ppm. ^{13}C NMR (125 MHz, $CDCl_3$) δ 165.69, 145.11, 140.50, 130.37, 130.22, 129.67, 99.87, 47.72, 36.07 ppm. IR (neat) ν 3065, 2100, 1634, 1467, 1256, 798 cm^{-1}. HRMS (DART) calcd for $C_9H_8N_3OI$ [M+H]+: 301.97969 found: 301.97903.

2-Diazo-*N*-ethyl-*N*-phenylacetamide (50m)

Same procedure as described above for **50a**. 56% yield. Yellow oil. ^{1}H NMR (500MHz, $CDCl_3$) δ 7.40 (dt, *J* = 7.84, 1.91 Hz, 2H), 7.33 (dt, *J* = 7.64, 1.91 Hz, 1H), 7.16 (dd, *J* = 8.03, 1.15 Hz, 2H), 4.36 (s, 1H), 3.79 (d, *J* = 7.26 Hz 1H), 3.77 (d, *J* = 7.26 Hz, 1H), 1.11(t, *J* = 7.26 Hz, 3H), ppm. ^{13}C NMR (125 MHz, $CDCl_3$) δ 165.43, 141.46, 129.81, 128.64, 128.21, 47.48, 44.12, 13.44 ppm.

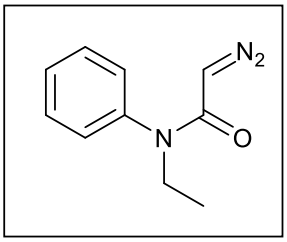

IR (neat) ν 3059, 2106, 1621, 1401, 1257, 700 cm^{-1}. HRMS (DART) calcd for: $C_{10}H_{11}N_3O$ [M+H]+: 190.0980 found: 190.0980.

2-Diazo-*N*-isopropyl-*N*-phenylacetamide (50n)

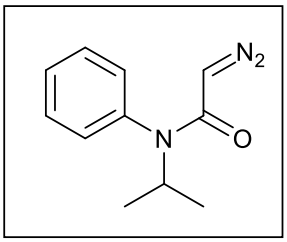

Same procedure as described above for **50a**. 55% yield. Yellow oil. ^1H NMR (500MHz, $CDCl_3$) δ 7.41–736 (m, 3H), 7.11–7.09 (m, 2H), 5.01 (sep., 1H), 4.13 (s, 1H), 1.06 (d, *J* = 6.88 Hz, 6H) ppm. ^{13}C NMR (125 MHz, $CDCl_3$) δ 165.53, 137.85, 130.76, 129.23, 128.82, 47.57, 46.47, 21.26 ppm. IR (neat) ν 3067, 2103, 1624, 1394, 1118, 704 cm^{-1}. HRMS (DART) calcd for: $C_{11}H_{13}N_3O$ [M+H]+: 204.1137 found: 204.1136.

6.2.3. General procedure for the intramolecular C-H insertion reaction of diazo acetamides by using Ru(II)-Pheox catalyst

To a solution of Ru(II)-Pheox catalyst (1.3 mg, 0.002 mmol) in CH_2Cl_2 (1.0 mL) was slowly added a solution of diazoacetamides (0.2 mmol) in CH_2Cl_2 (2.0 mL) at room temperature with stirring under argon atmosphere. After the addition completed, the reaction was monitored by TLC. Most of the case, nitrogen evolution was observed and the reaction rapidly proceeded within 1 min. Upon completion, the solvent was removed and the residue was purified by flash column chromatography on silica gel eluted with EtOAc/*n*-Hexane (1/5($^{v}/_{v}$)) to give the desired product.

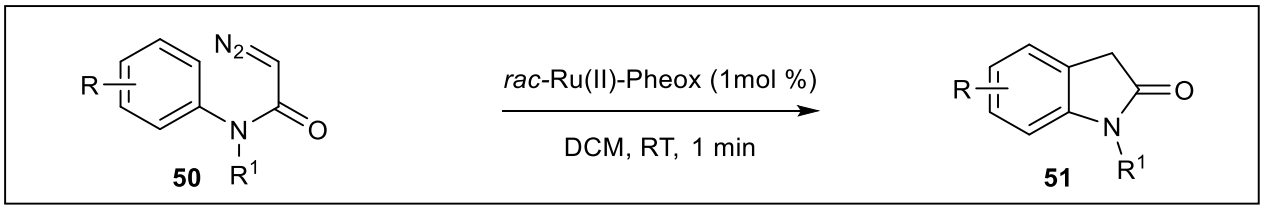

Scheme 47. Decomposition of 2-diazo-*N*-methyl-*N*-phenylacetamide by Ru(II)-Pheox complex.

6.2.4. Analytical data for the intramolecular C-H insertion reaction of diazo acetamides by using Ru(II)-Pheox catalyst

1-Methylindolin-2-one (51a)

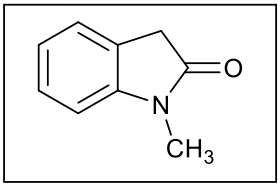

This compound was prepared according to the typical procedure for intramolecular C-H insertion reaction of diazo-*N*-phenyl-*N*-methylacetamide **50a** (29.4 mg, 0.2 mmol). The resulting mixture was purified by silica gel column chromatography with EtOAc/*n*-Hexane as an eluent to give 1-methylindolin-2-one **(51a)** as white powder. 96% yield. NMR(^{1}H, ^{13}C), IR data agree with reported values.[19]

5-Methoxy-1-methylindolin-2-one (51b)

This compound was prepared according to the typical procedure for intramolecular C-H insertion reaction of 2-diazo-*N*-(4-methoxyphenyl)-*N*-methylacetamide **50b** (40.8 mg, 0.2 mmol). The resulting mixture was purified by silica gel column chromatography with EtOAc/*n*-Hexane as an

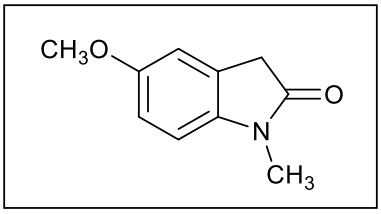

eluent to give 5-methoxy-1-methylindolin-2-one **(51b)** as white powder. NMR(^{1}H, ^{13}C), IR and HRMS data agree with reported values.[10]

5-Chloro-1-methylindolin-2-one (51c)

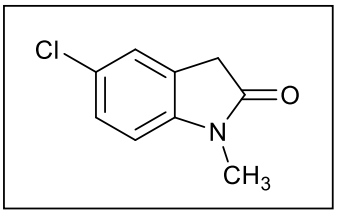

This compound was prepared according to the typical procedure for intramolecular C-H insertion reaction of 2-diazo-*N*-(4-chlorophenyl)-*N*-methylacetamide **50c** (41.7 mg, 0.2 mmol). The resulting mixture was purified by silica gel column chromatography with EtOAc/*n*-Hexane as an eluent to give 5-chloro-1-methylindolin-2-one (**51c**) as white powder. 94% yield. ^{1}H NMR (500MHz, $CDCl_3$) δ 7.26 (dd, *J* = 8.41, 1.91 Hz, 1H), 7.22 (s, 1H), 6.73 (d, *J* = 8.41 Hz, 1H), 3.51 (s, 2H), 3.19 (s, 3H) ppm. ^{13}C NMR (125 MHz, $CDCl_3$) δ 174.63, 143.95, 128.00, 127.84, 126.24, 124.96, 109.07, 35.83, 26.48 ppm. IR (neat) ν 2968, 1702, 1491, 1271, 754 cm^{-1}. HRMS (DART) calcd for C_9H_8NOCl [M+H]+: 182.0376 found: 182.0372.

5-Bromo-1-methylindolin-2-one (51d)

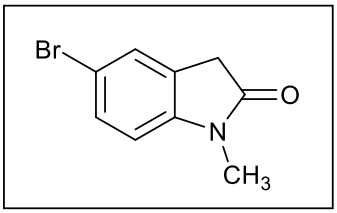

This compound was prepared according to the typical procedure for intramolecular C-H insertion reaction of 2-diazo-*N*-(4-bromophenyl)-*N*-methylacetamide **50d** (41.7 mg, 0.2 mmol). The resulting mixture was purified by silica gel column chromatography with EtOAc/*n*-Hexane as an eluent to give 5-bromo-1-methylindolin-2-one (**51d**) as white powder. 93% yield. NMR(^{1}H, ^{13}C), IR data agree with reported[123] values.

5-Iodo-1-methylindolin-2-one (51e)

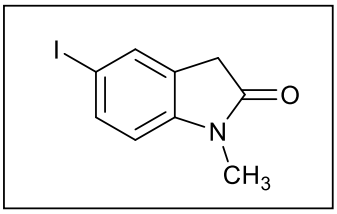

This compound was prepared according to the typical procedure for intramolecular C-H insertion reaction of 2-diazo-*N*-(4-Iodophenyl)-*N*-methylacetamide **50e** (54.6 mg, 0.2 mmol). The resulting mixture was purified by silica gel column chromatography with EtOAc/*n*-Hexane as an eluent to give 5-iodo-1-methylindolin-2-one (**51e**) as

white powder. 99% yield. ^{1}H NMR (500MHz, $CDCl_3$) δ 7.57 (d, *J* = 8.41 Hz, 1H), 7.51 (s, 1H), 6.58 (d, *J* = 8.41 Hz, 1H), 3.48 (s, 2H), 3.16 (s, 3H) ppm. ^{13}C NMR (125 MHz, $CDCl_3$) δ 174.27, 144.76, 136.79, 133.13, 126.91, 110.14, 84.84, 35.42, 26.18 ppm. IR (neat) ν 2935, 1696, 1364, 1100, 810 cm^{-1}. HRMS (DART) calcd for C_9H_8NOI [M+H]+: 273.9722 found: 273.9728.

5-Nitro-1-methylindolin-2-one (51f)

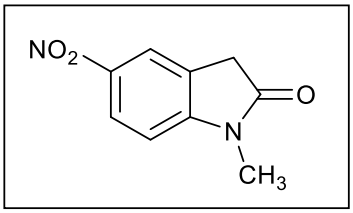

This compound was prepared according to the typical procedure for intramolecular C-H insertion reaction of 2-diazo-*N*-(4-nitrophenyl)-*N*-methylacetamide **50f** (43.8 mg, 0.2 mmol). The resulting mixture was purified by silica gel column chromatography with EtOAc/*n*-Hexane as an eluent to give 5-nitro-1-methylindolin-2-one **(51f)** as white powder. 94% yield. ^{1}H NMR (500MHz, $CDCl_3$) δ 8.28 (dd, *J* = 8.79, 2.29 Hz, 1H), 8.15-8.14 (m, 1H), 6.91 (d, *J* = 8.79 Hz, 1H), 3.64 (s, 2H), 3.29 (s, 3H) ppm. ^{13}C NMR (125 MHz, $CDCl_3$) δ 174.98, 150.99, 143.44, 125.59, 125.22, 120.36, 107.74, 35.45, 26.83 ppm. IR (neat) ν 2913, 1718, 1507, 1288, 746 cm^{-1}. HRMS (DART) calcd for $C_9H_8N_2O_3$ [M+H]+: 193.0613 found: 193.0613.

1,6-Dimethylindolin-2-one (51ga), 1,4-dimethylindolin-2-one (51gb)

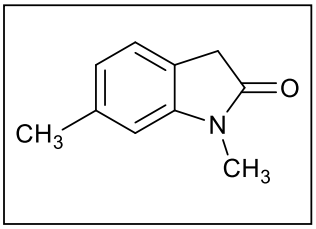

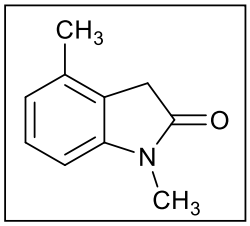

This compound was prepared according to the typical procedure for intramolecular C-H insertion reaction of 2-diazo-*N*-(3-methylphenyl)-*N*-methylacetamide **50g** (37.8 mg, 0.2 mmol). The resulting mixture was purified by silica gel column chromatography with EtOAc/*n*-Hexane as an eluent to give 1,6-dimethylindolin-2-one (**51ga**), 1,4-dimethylindolin-2-one (**51gb**) as yellow powder. 98% yield. NMR(^{1}H, ^{13}C), IR data agree with reported[10] values.

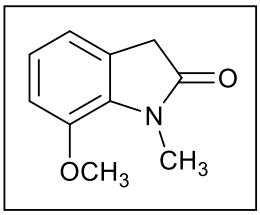

7-Methoxy-1-methylindolin-2-one (51h)

This compound was prepared according to the typical procedure for intramolecular C-H insertion reaction of 2-diazo-*N*-(2-methoxyphenyl)-*N*-methylacetamide **50h** (35.6 mg, 0.2 mmol). The resulting mixture was purified by silica gel column chromatography with EtOAc/*n*-Hexane as an

eluent to give 7-methoxy-1-methylindolin-2-one (**51h**) as yellow powder. 93% yield. ^{1}H NMR (500MHz, $CDCl_3$) δ 6.98–6.95 (m, 1H), 6.86–6.84 (m, 2H), 3.85 (s, 1H), 3.48 (s, 2H), 3.48 (s, 3H) ppm. ^{13}C NMR (125 MHz, $CDCl_3$) δ 175.20, 145.37, 133.11, 125.97, 122.46, 117.07, 111.54, 55.67, 35.62, 28.50 ppm. IR (neat) ν 2978, 1694, 1467, 1253, 754 cm^{-1}. HRMS (DART) calcd for $C_{10}H_{11}NO_2$ [M+H]+: 178.0863 found: 178.0868.

7-Bromo-1-methylindolin-2-one (51i)

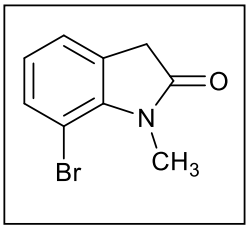

This compound was prepared according to the typical procedure for intramolecular C-H insertion reaction of 2-diazo-*N*-(2-bromophenyl)-*N*-methylacetamide **50i** (45.2 mg, 0.2 mmol). The resulting mixture was purified by silica gel column chromatography with EtOAc/*n*-Hexane as an eluent to give 7-bromo-1-methylindolin-2-one (**51i**) as yellow powder. 98% yield. ^{1}H NMR (500MHz, $CDCl_3$) δ 7.38 (d, *J* = 8.03 Hz, 1H), 7.16 (d, *J* = 8.03 Hz, 1H), 6.89–6.86(m, 1H), 3.59 (s, 3H), 3.53 (s, 2H) ppm. ^{13}C NMR (125 MHz, $CDCl_3$) δ 175.41, 142.25, 133.62, 127.30, 123.44, 102.21, 35.78, 29.75 ppm. IR (neat) ν 2943, 1716, 1462, 1332, 794 cm^{-1}. HRMS (DART) calcd for C_9H_8NOBr [M+H]+: 225.9860 found: 225.9867.

7-Iodo-1-methylindolin-2-one (51j)

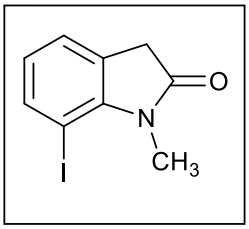

This compound was prepared according to the typical procedure for intramolecular C-H insertion reaction of 2-diazo-*N*-(2-Iodophenyl)-*N*-methylacetamide **50j** (54.6 mg, 0.2 mmol). The resulting mixture was purified by silica gel column chromatography with EtOAc/*n*-Hexane as an eluent to give 7-iodo-1-methylindolin-2-one (**51j**) as yellow powder. 97% yield. ^{1}H NMR (500MHz, $CDCl_3$) δ 7.67 (dd, *J* = 8.03, 1.15 Hz, 1H), 7.18 (dd, *J* = 7.64, 1.15 Hz, 1H), 6.73 (t, *J* = 7.64 Hz, 1H), 3.58 (s, 3H), 3.49 (s, 2H) ppm. ^{13}C NMR (125 MHz, $CDCl_3$) δ 175.14, 145.89, 140.23, 127.48, 124.19, 124. 11, 71.97, 36.12, 29.54 ppm. IR (neat) ν 2942, 1706, 1455, 1333, 766 cm^{-1}. HRMS (DART) calcd for C_9H_8NOI [M+H]+: 273.9721 found: 273.9728.

1-Phenylindolin-2-one (51l)

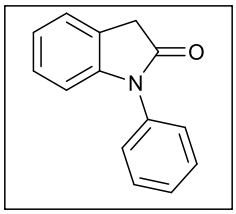

This compound was prepared according to the typical procedure for intramolecular C-H insertion reaction of 2-diazo-*N*,*N*-diphenylacetamide **50l** (47.5 mg, 0.2 mmol). The resulting mixture was purified by silica gel column chromatography with EtOAc/*n*-Hexane as an eluent to give 7-iodo-1-methylindolin-2-one (**51l**) as white powder, yield: 99%. NMR (^{1}H, ^{13}C), IR data agree with reported[10] values.

1-Ethylindolin-2-one (51m)

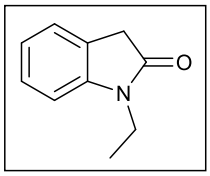

This compound was prepared according to the typical procedure for intramolecular C-H insertion reaction of 2-diazo-*N*-ethyl-*N*-phenylacetamide **50m** (32.4 mg, 0.2 mmol). The resulting mixture was purified by silica gel column chromatography with EtOAc/*n*-Hexane as an eluent to give 1-ethylindolin-2-one (**51m**) as white powder. 94% yield. ^{1}H NMR (500MHz, $CDCl_3$) δ 7.25 (dd, *J* = 16.82, 8.03 Hz, 2H), 7.01 (t, *J* = 7.26 Hz, 1H), 6.83 (d, *J* = 8.03 Hz, 1H), 3.75 (q, *J* = 7.26 Hz, 2H), 3.49 (s, 2H), 1.25 (t, *J* = 7.26 Hz, 3H) ppm. ^{13}C NMR (125 MHz, $CDCl_3$) δ 174.79, 144.05, 127.89, 124.85, 124.58, 122.20, 108.28, 35.94, 34.72, 12.76 ppm. IR (neat) ν 2978, 1699, 1466, 1245, 749 cm^{-1}. HRMS (DART) calcd for C_9H_8NOI [M+H]+: 162.0914 found: 162.0928.

1-Isopropylindolin-2-one (51n)

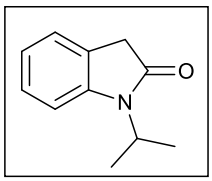

This compound was prepared according to the typical procedure for intramolecular C-H insertion reaction of 2-diazo-*N*-isopropyl-*N*-phenylacetamide **50n** (35.2 mg, 0.2 mmol). The resulting mixture was purified by silica gel column chromatography with EtOAc/*n*-Hexane as an eluent to give 1-isopropylindolin-2-one (**51n**) as white powder. 91% yield. ^{1}H NMR (500MHz, $CDCl_3$) δ 7.25–7.21 (m, 2H), 7.01–6.98 (m, 2H), 4.67 (seq, *J* = 6.88 Hz, 1H), 3.48 (s, 2H), 1.46 (d, *J* = 6.88 Hz, 6H) ppm. ^{13}C NMR (125 MHz, $CDCl_3$) δ 174.79, 143.88, 127.60, 125.09, 124.64, 121.81, 109.92, 43.59, 36.03, 19.40 ppm. IR (neat) ν 2973, 1709, 1485, 1246, 749 cm^{-1}. HRMS (DART) calcd for C_9H_8NOI [M+H]+: 176.1071 found: 176.1074.

6.3. Experimental analytical data for chapter 3

6.3.1. General procedure for catalytic asymmetric intramolecular cyclopropanation reaction (56).

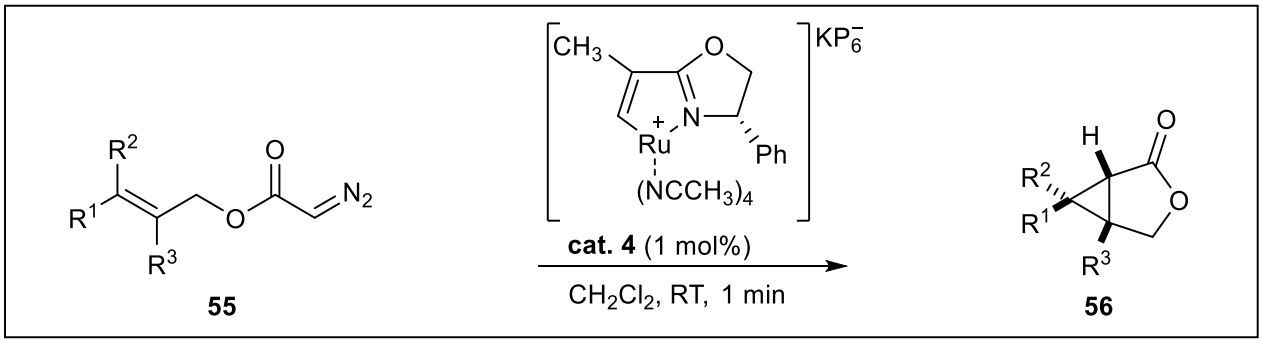

Scheme 48. Procedure for catalytic asymmetric intramolecular cyclopropanation reaction.

To a solution of diazoester (0.2 mmol, 1.0 equiv.) in CH_2Cl_2 (1.0 mL) was added to a mixture of **cat.4** (1.2 mg, 1 mol%) in CH_2Cl_2 (1.0 mL) under argon atmosphere at room temperature. The progress of the reaction was monitored by TLC. Upon completion, the solvent was removed under reduced pressure and the residue was purified by silica gel column chromatography with EtOAc/*n*-Hexane (1/5 (*v/v*)) to give the desired product. The ee value was determined by chiral HPLC analysis.

6.3.2. Analytical data for asymmetric intermolecular cyclopropanation reaction products

(1*S*,5*R*,6*R*)-5-Methyl-6-phenyl-3-oxabicyclo[3.1.0]hexan-2-one (56b)

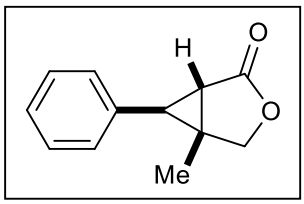

This compound was prepared according to the typical procedure for asymmetric intramolecular cyclopropanation reaction of (*E*)-2-methyl-3-phenylallyl 2-diazoacetate (43.3 mg, 0.2 mmol). The reaction mixture was purified by silica gel column chromatography with EtOAc/*n*-Hexane (1/2 (*v/v*)) as an eluent to give the desired product in 99% yield (37.1 mg, 0.2 mmol) as colorless solid. $[\alpha]^{21.8}_{D} = -120.3$ (c 1.0, $CHCl_3$). 93% *trans* ee. The ee value were determined by HPLC analysis. Column (chiral OJ-H), UV detector 220 nm, eluent: *n*-Hexane/IPA = 4/1, Flow late = 0.5 mL/min, tR = 23.7 min (major product), tR = 26.2 min (minor product). The spectral data were confirmed reported reference.

(1*R*,5*S*)-6,6-Dimethyl-3-oxabicyclo[3.1.0]hexan-2-one (56e)

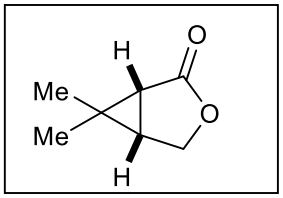

This compound was prepared according to the typical procedure for asymmetric intramolecular cyclopropanation reaction of 3-methylbut-2-en-1-yl 2-diazoacetate (30.8 mg, 0.2 mmol). The reaction mixture was purified by silica gel column chromatography with EtOAc/*n*-Hexane (1/2 (*v/v*)) as an eluent to give the desired product in 96% yield (24.9 mg, 0.2 mmol) as colorless oil. $[\alpha]^{22.3}_{D}$ = –42.7 (c 1.0, $CHCl_3$). 98% *trans* ee. The ee value were determined by HPLC analysis. Column (chiral IC-3), UV detector 220 nm, eluent: Hex/IPA = 7/3, Flow late = 1.0 mL/min, tR = 13.0 min (major product), tR = 16.0 min (minor product). The spectral data were confirmed reported reference.

(1*S*,5*R*)-3-Oxabicyclo[3.1.0]hexan-2-one (56f)

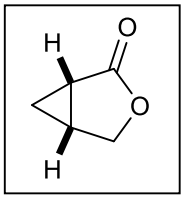

This compound was prepared according to the typical procedure for asymmetric intramolecular cyclopropanation reaction of allyl 2-diazoacetate (25.2 mg, 0.2 mmol). The reaction mixture was purified by silica gel column chromatography with EtOAc/*n*-Hexane (1/2 (*v/v*)) as an eluent to give the desired product in 91% yield (17.8 mg, 0.18 mmol) as colorless oil. $[\alpha]^{22.6}_{D}$ = –51.4 (c 0.65, $CHCl_3$). 99% *trans* ee. The ee value were determined by HPLC analysis. Column (chiral IC-3), UV detector 220 nm, eluent: Hex/IPA = 7/3, Flow late = 1.0 mL/min, tR = 21.9 min (major product), tR = 20.4 min (minor product). The spectral data were confirmed reported reference.

6.4. Experimental analytical data for chapter 4

6.4.1. Preparation of diazoacetamides

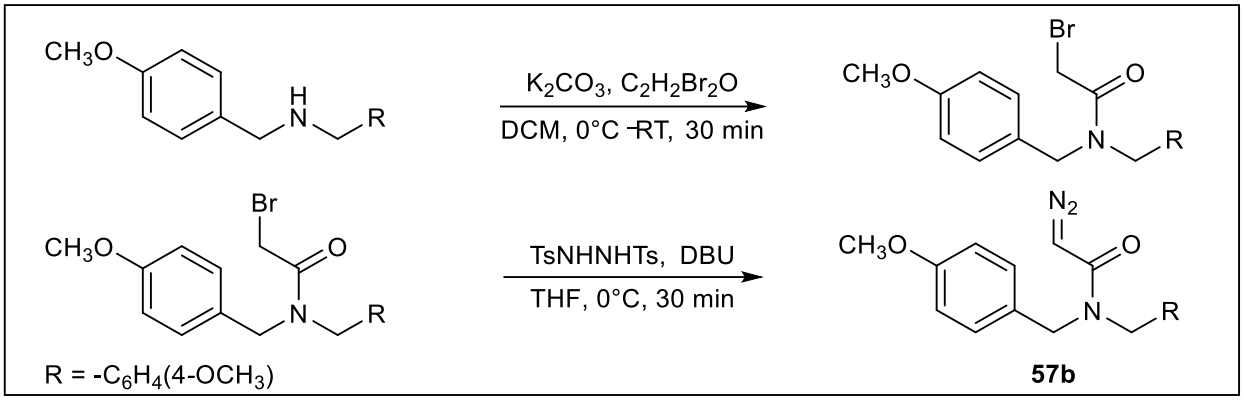

Scheme 49. Synthesis of 2-diazo-*N*,*N*-bis(4-methoxybenzyl)acetamide (**57b**).

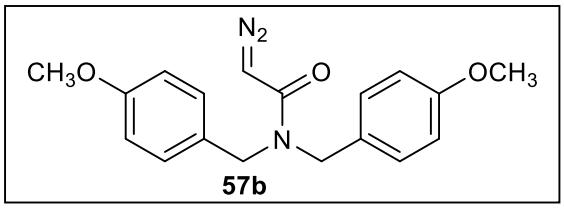

To a suspension of K_2CO_3 (1.66 g, 12 mmol) and bis(4-methoxybenzyl)amine (2.27 g, 10 mmol) in DCM (20.0 mL) was added dropwise bromoacetyl bromide (0.95 mL, 11 mmol) at 0°C. The reaction mixture was stirred for 30 minutes in room temperature. The mixture was then extracted three times with DCM, dried (Na_2SO_4), and filtered. After evaporation of the solvent, the residue was obtained and used in the next step without purification. The resulting bromoacetamide and *N*,*N′*-ditosylhydrazine (5.1 g, 15 mmol) were dissolved in THF (20 mL) and cooled down to 0°C, then DBU (3 mL, 20 mmol) was added dropwise and stirred at 0°C for 30 minutes. After quenched with $NaHCO_3$ aq. and extracted with diethyl ether three times, the organic phase was dried over Na_2SO_4 and evaporated to give the crude product. Purification was performed with flash column chromatography on silica gel eluted with EtOAc/*n*–Hexane (1/5(*v/v*)) to give 2-diazo-*N*,*N*-bis(4-methoxybenzyl)acetamide (1.66 g, 51% yield) as a yellow oil **50b**. ^{1}H NMR (500 MHz, $CDCl_3$) δ 7.13 (br s, 4H), 6.88 (d, *J* = 8.41 Hz, 4H), 4.98 (s, 1H), 4.35 (br s, 4H), 3.77 (s, 6H) ppm. ^{13}C NMR (125 MHz, $CDCl_3$) δ 166.2, 158.9, 129.38, 128.2, 113.8, 55.1, 48.53, 46.64 ppm. IR (neat) ν 3068, 2928, 2837, 2100, 1606, 1440, 814 cm^{-1}. HRMS (DART) calcd for $C_{18}H_{19}N_3O_3$ $[M+H]^+$: 326.1504 found: 326.1504.

6.4.2. Analytical data for diazoacetamides

2-Diazo-*N*,*N*-dibenzylacetamide (57a)

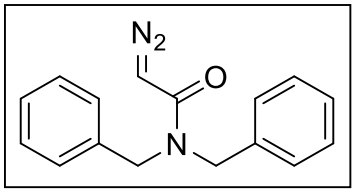

Same procedure as described above for **57b**. (48% yield). Yellow oil. ^{1}H NMR (500 MHz, $CDCl_3$) δ 7.36–7.23 (m, 10H), 4.97 (s, 1H), 4.46 (br s, 4H) ppm. ^{13}C NMR (125 MHz, $CDCl_3$) δ 166.61, 136.62, 128.72, 127.52, 126.56, 49.38, 47.00 ppm. IR (neat) ν 3064, 2921, 2100, 1606, 1427, 727 cm^{-1}. HRMS (DART) calcd for $C_{16}H_{15}N_3O$ $[M+H]^+$: 266.1293 found: 266.1293.

2-Diazo-*N*,*N*-bis(4-methylbenzyl)acetamide (57c)

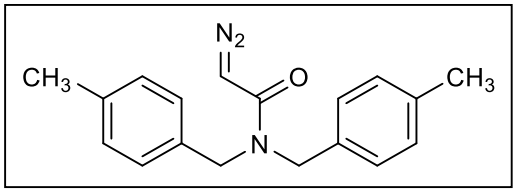

Same procedure as described above for **57b**. (43% yield). Yellow oil. ^{1}H NMR (500 MHz, $CDCl_3$) δ 7.15 (d, *J* = 7.64 Hz, 4H), 7.11 (br s, 4H), 4.96 (s, 1H), 4.39 (br s, 4H), 2.35 (s, 6H) ppm. ^{13}C NMR (125 MHz, $CDCl_3$) δ 166.59, 137.40, 133.88, 129.56, 127.07, 49.10, 47.12, 21.21 ppm. IR (neat) ν 3052, 2921, 2104, 1603, 1432, 798 cm^{-1}. HRMS (DART) calcd for $C_{18}H_{19}N_3O$ $[M+H]^+$: 294.1606 found: 294.1606.

2-Diazo-*N*,*N*-bis(4-chlorobenzyl)acetamide (57d)

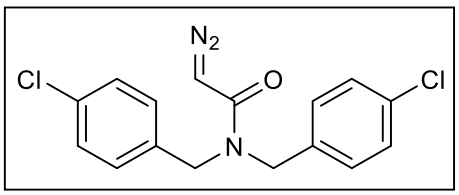

Same procedure as described above for **57b**. (63% yield). Yellow oil. ^{1}H NMR (500 MHz, $CDCl_3$) δ 7.32 (d, *J* = 7.94 Hz, 4H), 7.14 (d, *J* = 7.94 Hz, 4H), 4.94 (s, 1H), 4.39 (br s, 4H) ppm. ^{13}C NMR (125 MHz, $CDCl_3$) δ 166.64, 135.15, 133.66, 129.11, 128.87, 49.06, 47.24 ppm. IR (neat) ν 3072, 2925, 2109, 1606, 1432, 802 cm^{-1}. HRMS (DART) calcd for $C_{16}H_{13}Cl_2N_3O$ $[M+H]^+$: 334.0513 found: 334.0513.

2-Diazo-*N*,*N*-bis(4-bromobenzyl)acetamide (57e)

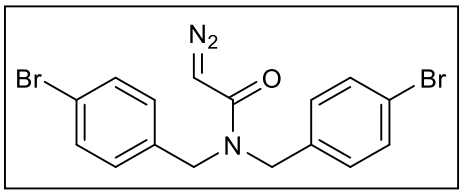

Same procedure as described above for **57b**. (55% yield). Yellow oil. ^{1}H NMR (500 MHz, $CDCl_3$) δ 7.47 (d, *J* = 8.03 Hz, 4H), 7.08 (d, *J* = 8.03 Hz, 4H), 4.94 (s, 1H), 4.40 (br s, 4H) ppm. ^{13}C NMR (125 MHz, $CDCl_3$) δ 166.5, 135.73,

131.82, 128.70, 121.48, 48.93, 47.08 ppm. IR (neat) ν 3069, 2918, 2103, 1623, 1438, 797 cm^{-1}. HRMS (DART) calcd for $C_{16}H_{13}Br_2N_3O$ $[M+H]^+$: 421.9503 found: 421.9503.

2-Diazo-*N*,*N*-bis(4-fluorobenzyl)acetamide (57f)

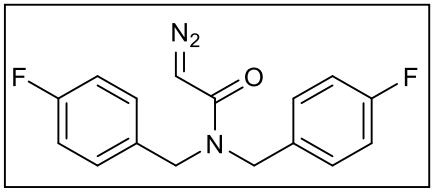

Same procedure as described above for **57b**. (69% yield). Yellow oil. ^{1}H NMR (500 MHz, $CDCl_3$) δ 7.17 (t, *J* = 8.03 Hz, 4H), 7.03 (t, *J* = 8.03 Hz, 4H), 4.96 (s, 1H), 4.40 (br s, 4H) ppm. ^{13}C NMR (125 MHz, $CDCl_3$) δ 166.52, 163.25, 161.29, 132.41, 128.83, 115.80, 48.82, 47.09 ppm. IR (neat) ν 3072, 2921, 2109, 1599, 1440, 818 cm^{-1}. HRMS (DART) calcd for $C_{16}H_{13}F_2N_3O$ $[M+H]^+$: 302.1108 found: 302.1104.

2-Diazo-*N*,*N*-bis(3-methoxybenzyl)acetamide (57g)

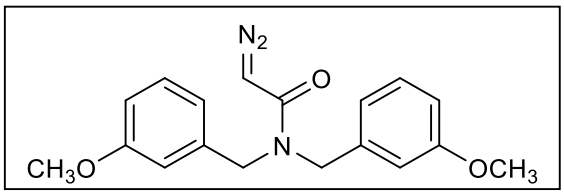

Same procedure as described above for **57b**. (60% yield). Yellow oil. ^{1}H NMR (500 MHz, $CDCl_3$) δ 7.26 (t, *J* = 8.03 Hz, 2H), 6.84–6.75 (m, 6H), 4.96 (s, 1H), 4.76–4.13 (br s, 4H), 3.79 (s, 6H) ppm. ^{13}C NMR (125 MHz, $CDCl_3$) δ 166.55, 160.02, 138.41, 129.84, 119.63, 113.25, 112.90, 55.20, 49.51, 47.00 ppm. IR (neat) ν 3064, 2937, 2104, 1599, 1427, 782 cm^{-1}. HRMS (DART) calcd for $C_{18}H_{19}N_3O_3$ $[M+H]^+$: 326.1509 found: 326.1504.

2-Diazo-*N*-(4-methoxybenzyl)-*N*-(4-nitrobenzyl)acetamide (57h)

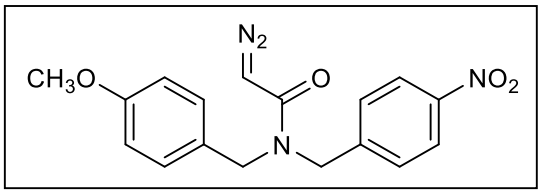

Same procedure as described above for **57b**. (33% yield). Yellow oil. ^{1}H NMR (500 MHz, $CDCl_3$) δ 8.18 (d, *J* = 8.03 Hz, 2H), 7.38 (d, *J* = 8.03 Hz, 2H), 7.11 (d, *J* = 8.03 Hz, 2H), 6.88 (d, *J* = 8.03 Hz, 2H), 5.04 (br s, 1H), 4.6 (br s, 2H), 4.32 (br s, 2H), 3.81 (s, 3H) ppm. ^{13}C NMR (125 MHz, $CDCl_3$) δ 166.73, 159.46, 147.48, 145.05, 128.49, 127.95, 124.06, 114.47, 55.45, 49.85, 48.95, 47.32 ppm. IR (neat) ν 3076, 2933, 2109, 1606, 1440, 822 cm^{-1}. HRMS (DART) calcd for $C_{17}H_{16}N_4O_4$ $[M+H]^+$: 341.1249 found: 341.1249.

2-Diazo-*N*-benzyl-*N*-methylacetamide (57i)

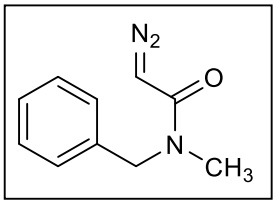

Same procedure as described above for **57b**. (22% yield). Yellow oil. ^{1}H NMR (500 MHz, $CDCl_3$) δ 7.35 (t, *J* = 7.64 Hz, 2H), 7.29 (d, *J* = 7.64 Hz, 1H), 7.23 (d, *J* = 7.64 Hz, 2H), 4.99 (s, 1H), 4.55 (br s, 2H), 2.85 (br s, 3H) ppm. ^{13}C NMR (125 MHz, $CDCl_3$) δ 166.22, 137.05, 128.83, 127.60, 126.64, 51.43, 46.62, 34.59 ppm. IR (neat) ν 3068, 2921, 2104, 1610, 1404, 727 cm^{-1}. HRMS (DART) calcd for $C_{10}H_{11}N_3O$ $[M+H]^+$: 190.0982 found: 190.0980.

2-Diazo-*N*-(4-methoxybenzyl)-*N*-methylacetamide (57j)

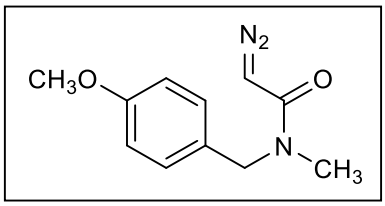

Same procedure as described above for **57b**. (43% yield). Yellow oil. ^{1}H NMR (500 MHz, $CDCl_3$) δ 7.16 (d, *J* = 8.03 Hz, 2H), 6.87 (d, *J* = 8.03 Hz, 2H), 4.98 (s, 1H), 4.45 (br s, 2H), 3.8 (s, 3H), 2.83 (br s, 3H) ppm. ^{13}C NMR (125 MHz, $CDCl_3$) δ 166.11, 159.22, 129.13, 128.82, 114.26, 55.41, 51.24, 46.6, 34.22 ppm. IR (neat) ν 3068, 2933, 2104, 1606, 1455, 814 cm^{-1}. HRMS (DART) calcd for $C_{11}H_{13}N_3O_2$ $[M+H]^+$: 220.1087 found: 220.1086.

2-Diazo-*N*-(4-methylbenzyl)-*N*-methylacetamide (57k)

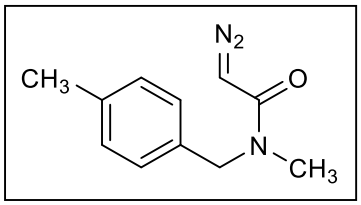

Same procedure as described above for **57b**. (42% yield). Yellow oil. ^{1}H NMR (500 MHz, $CDCl_3$) δ 7.13 (dd, *J* = 17.76, 8.02 Hz, 4H), 4.97 (s, 1H), 4.45 (br s, 2H), 2.86 (br s, 3H), 2.34 (s, 3H) ppm. ^{13}C NMR (125 MHz, $CDCl_3$) δ 166.29, 136.18, 131.98, 129.38, 121.61, 50.89-, 46.7, 34.33, 23.14 ppm. IR (neat) ν 3072, 2921, 2100, 1606, 1399, 798 cm^{-1}. HRMS (DART) calcd for $C_{11}H_{13}N_3O$ $[M+H]^+$: 204.1137 found: 204.1137.

2-Diazo-*N*-(4-chlorobenzyl)-*N*-methylacetamide (57l)

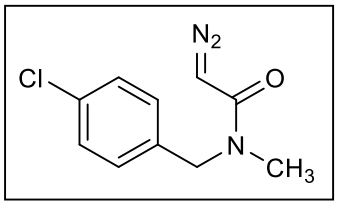

Same procedure as described above for **57b**. (46% yield). Yellow powder. ^{1}H NMR (500 MHz, $CDCl_3$) δ 7.31 (d, *J* = 8.03 Hz, 2H), 7.17 (d, *J* = 8.03 Hz, 2H), 4.97 (s, 1H), 4.49 (br s, 2H), 2.83 (br s, 3H) ppm. ^{13}C NMR (125 MHz, $CDCl_3$) δ 166.24, 135.68, 133.40, 128.97, 128.67, 50.77, 46.64, 34.40 ppm. IR (neat) ν 3072, 2916, 2100, 1606, 1404, 791 cm^{-1}. HRMS (DART) calcd for $C_{10}H_{10}ClN_3O$ $[M+H]^+$: 224.0590 found: 224.0590.

2-Diazo-*N*-(4-bromobenzyl)-*N*-methylacetamide (57m)

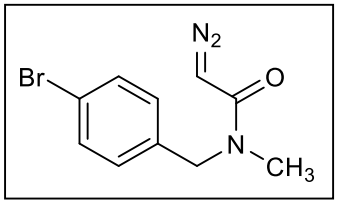

Same procedure as described above for **57b**. (47% yield). Yellow powder. ^{1}H NMR (500 MHz, $CDCl_3$) δ 7.46 (d, *J* = 8.03 Hz, 2H), 7.11 (d, *J* = 8.03 Hz, 2H), 4.97 (s, 1H), 4.47 (br s, 2H), 2.84 (br s, 3H) ppm. ^{13}C NMR (125 MHz, $CDCl_3$) δ 166.23, 136.19, 131.89, 129.37, 121.47, 50.98, 46.63, 34.39 ppm. IR (neat) ν 3072, 2925, 2104, 1610, 1399, 746 cm^{-1}. HRMS (DART) calcd for $C_{10}H_{10}BrN_3O$ $[M+H]^+$: 268.0084 found: 268.0085.

2-Diazo-*N*-(4-flourobenzyl)-*N*-methylacetamide (57n)

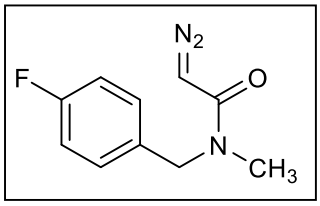

Same procedure as described above for **57b**. (25% yield). Yellow powder. ^{1}H NMR (500 MHz, $CDCl_3$) δ 7.2 (t, *J* = 8.03 Hz, 2H), 7.01 (t, *J* = 8.03 Hz, 2H), 4.98 (s, 1H), 4.49 (br s, 2H), 2.82 (br s, 3H) ppm. ^{13}C NMR (125 MHz, $CDCl_3$) δ 166.29, 163.33, 161.37, 129.35, 115.84, 50.79, 46.69, 34.35 ppm. IR (neat) ν 3072, 2925, 2104, 1606, 1408, 818 cm^{-1}. HRMS (DART) calcd for $C_{10}H_{10}FN_3O$ $[M+H]^+$: 208.0886 found: 208.0886.

2-Diazo-N-(4-nitrobenzyl)-*N*-methylacetamide (57o)

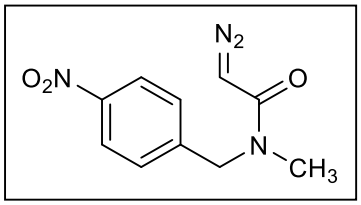

Same procedure as described above for **57b**. (20% yield). Yellow powder. ^{1}H NMR (500 MHz, $CDCl_3$) δ 8.10 (d, *J* = 8.41 Hz, 2H), 7.34 (d, *J* = 8.41 Hz, 2H), 5.04 (s, 1H), 4.59 (br s, 2H), 3.37 (s, 2H), 2.81 (br s, 3H) ppm. ^{13}C NMR (125 MHz, $CDCl_3$) δ 166.49, 147.52, 144.94, 128.37, 124.13, 51.04, 46.77, 34.8 ppm. IR (neat) ν 3072, 2928, 2109, 1606, 1479, 727 cm^{-1}. HRMS (DART) calcd for $C_{10}H_{10}N_4O_3$ $[M+H]^+$: 235.0839 found: 235.0831.

6.4.3. General procedure for catalytic asymmetric intramolecular Buchner reaction of diazoacetamides

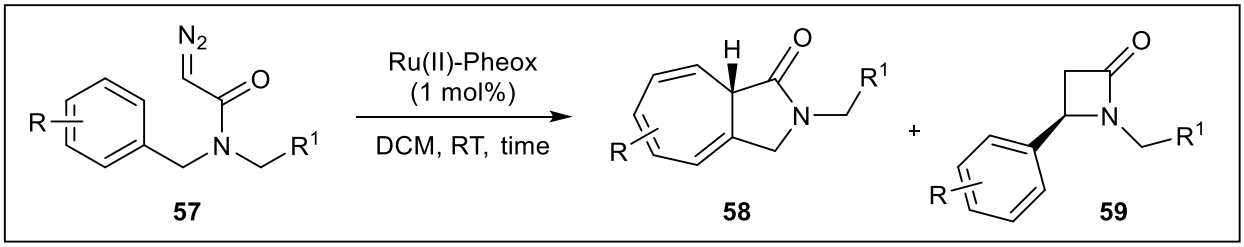

Scheme 50. Catalytic Asymmetric Intramolecular Buchner Reaction of Diazoacetamides.

To a stirred mixture of Ru(II)-Pheox catalyst (1.30 mg, 0.002 mmol) in DCM (1 ml) was slowly added a solution of diazoacetamides (0.2 mmol) in DCM (2.0 ml) (for 2 minutes with *N*,*N*-bisaryl-2-diazo-acetamides or 4 hours with *N*-aryl-2-diazo-*N*-methylacetamides) under argon atmosphere at room temperature. After the addition completed, the progress of the reaction was monitored by TLC. Upon completion, the solvent was removed and the residue was purified by flash column chromatography on silica gel eluted with EtOAc/*n*–Hexane or IPA/*n*–Hexane to give the desired product. The regioselective ratios were determined from the crude ^{1}H NMR spectra, and the ee values were determined by chiral HPLC analysis.

6.4.4. Analytical data for asymmetric intramolecular Buchner reaction products

(*S*)-2-benzyl-3,8a-dihydrocyclohepta[c]pyrrol-1(2H)-one (58a)

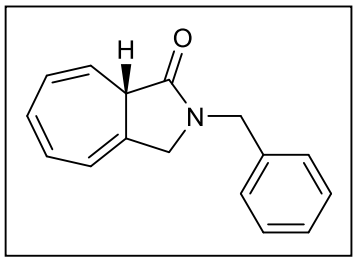

This compound was prepared according to the typical procedure for asymmetric Buchner ring expansion reaction of *N*,*N*-dibenzyl-2-diazoacetamide **57a** (53.1 mg, 0.2 mmol). The resulting mixture was purified by silica gel column chromatography with *n*-Hexane/Et_2O as an eluent to give 2-phenyl-3,8a-dihydro cyclohepta[c]pyrrol-1(2H)-one **58a** as colorless oil (92% yield, 43.7 mg, 0.184 mmol), 78% ee. $[\alpha]^{27.6}_{D}$ = +144.3 (c 0.7, $CHCl_3$). ^{1}H NMR (500MHz, $CDCl_3$) δ 7.38–7.23 (m, 5H), 6.47 (t, *J* = 3.25 Hz, 2H), 6.22–6.17 (m, 1H), 6.08 (ddd, *J* = 4.59, 4.20, 2.29 Hz, 1H), 5.33 (dd, *J* = 9.56, 3.82 Hz, 1H), 4.60 (d, *J* = 14.52 Hz, 1H), 4.54 (d, *J* = 14.52 Hz, 1H), 4.08 (d, *J* = 17.2 Hz, 1H), 4.04 (d, *J* = 17.2 Hz, 1H), 3.15 (s, 1H) ppm. ^{13}C NMR (125 MHz, $CDCl_3$) δ 174.25, 136.10, 130.50, 130.04, 129.30, 128.96, 128.32, 127.93, 127.17, 120.80, 119.70, 50.70, 46.70, 46.47 ppm. IR (neat) ν 3027, 2924, 1683, 1422, 1272, 764 cm^{-1}. The ee value was determined by chiral HPLC analysis. Column (Chiral IA-3), UV

detector 220 nm, eluent: *n*-Hexane/IPA = 10/1, Flow rate = 1.0 ml/min, tR = 14.2 min (major product), tR = 15.9 min (minor product). HRMS (DART) calcd for $C_{16}H_{16}N_1O_1$ [M+H]+: 238.1231 found: 238.1231.

(*S*)-6-Methoxy-2-(4-methoxybenzyl)-3,8a-dihydrocyclohepta[c]pyrrol-1(2H)-one (58b)

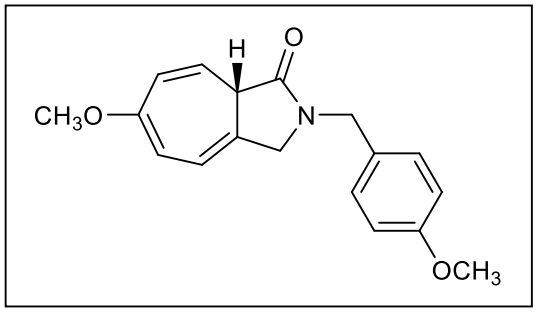

This compound was prepared according to the typical procedure for asymmetric Buchner ring expansion reaction of 2-diazo-*N*,*N*-bis(4-methoxybenzyl)acetamide **57b** (65.1 mg, 0.2mmol). The resulting mixture was purified by silica gel column chromatography with *n*-Hexane/ EtOAc as an eluent to give 6-methoxy-2-(4-methoxybenzyl)-3,8a-dihydrocyclohepta[c]pyrrol-1(2H)-one **(58b)** as white solid (99% yield, 58.9 mg, 0.198 mmol), 99% ee. $[\alpha]^{26.3}{}_{D}$ = –25.34 (c 1.0, $CHCl_3$). ^{1}H NMR (500MHz, $CDCl_3$) δ 7.19 (d, *J* = 8.41 Hz, 2H), 6.86 (d, *J* = 8.41 Hz, 2H), 6.05 (dt, *J* = 10.32, 2.29 Hz, 1H), 5.98 (ddd, *J* = 4.97, 4.20, 2.29 Hz, 1H), 5.67 (d, *J* = 8.41 Hz, 1H), 5.51 (dd, *J* = 10.32, 4.2 Hz, 1H), 5.53 (d, *J* = 14.52 Hz, 1H), 4.46 (d, *J* = 14.52 Hz, 1H), 4.03 (d, *J* = 14.91 Hz, 1H), 3.98 (d, *J* = 14.91 Hz, 1H), 3.79 (s, 3H), 3.62 (s, 3H), 3.20 (s, 1H).^{13}C NMR (125 MHz, $CDCl_3$) δ 173.78, 159.28, 159.24, 129.59, 128.10, 125.15, 123.26, 123.23, 117.71, 114.17, 102.82, 55.34, 54.77, 50.32, 45.98, 45.95 ppm. IR (neat) ν 2992, 2933, 1690, 1511, 1439, 806 cm^{-1}. The ee value was determined by chiral HPLC analysis. Column (Chiral IA-3), UV detector 220 nm, eluent: *n*-Hexane/IPA = 10/1, Flow rate = 1.0 ml/min, tR = 23.1 min (major product), tR = 33.6 min (minor product). HRMS (DART) calcd for $C_{18}H_{19}NO_3$ [M+H]+: 206.0929 found: 206.0929.

(*S*)-6-Methyl-2-(4-methylbenzyl)-3,8a-dihydrocyclohepta[c]pyrrol-1(2H)-one (58c)

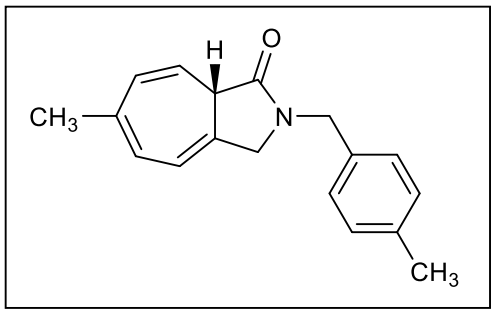

This compound was prepared according to the typical procedure for asymmetric Buchner ring expansion reaction of 2-diazo-*N*,*N*-bis(4-methylbenzyl)acetamide **57c** (58.7 mg, 0.2 mmol). The resulting mixture was purified by silica gel column chromatography with *n*-Hexane/ EtOAc as an eluent to give 6-methyl-2-(4-methylbenzyl)-3,8a-dihydrocyclohepta[c]pyrrol-1(2H)-one **58c** as colorless oil (93% yield, 49.4

mg, 0.186 mmol), 97% ee. $[\alpha]^{23.9}_{D}$ = +40.65 (c 0.5, $CHCl_3$). ^{1}H NMR (500MHz, $CDCl_3$) δ 7.15 (d, *J* = 8.59 Hz, 2H), 7.13 (d, *J* = 8.59 Hz, 2H), 6.26 (d, *J* = 5.73 Hz, 1H), 6.02 (d, *J* = 9.74 Hz, 1H), 5.95 (d, *J* = 5.73 Hz, 1H), 5.31 (dd, *J* = 9.74, 4.01 Hz, 1H), 4.54 (d, *J* = 14.89 Hz, 1H), 4.49 (d, *J* = 14.89 Hz, 1H), 4.04 (d, *J* = 15.75 Hz, 1H), 3.99 (d, *J* = 15.75 Hz, 1H), 3.12 (s, 1H), 2.33 (s, 3H), 2.02 (s, 3H) ppm. ^{13}C NMR (125 MHz, $CDCl_3$) δ 174.25, 139.37, 137.54, 133.08, 130.34, 129.55, 128.30, 127.11, 126.89, 120.00, 119.31, 50.47, 46.37, 46.15, 24.80, 21.21 ppm. IR (neat) ν 3020, 2917, 1686, 1435, 1268, 806 cm^{-1}. The ee value was determined by chiral HPLC analysis. Column (Chiral IA-3), UV detector 220 nm, eluent: *n*-Hexane/IPA = 30/1, Flow rate = 1.0 ml/min, tR = 34.1 min (major product), tR = 38.1 min (minor product). HRMS (DART) calcd for $C_{18}H_{20}N_1O_1$ [M+H]+: 266.1544 found: 266.1544.

(*S*)-6-Chloro-2-(4-chlorobenzyl)-3,8a-dihydrocyclohepta[c]pyrrol-1(2H)-one (58d)

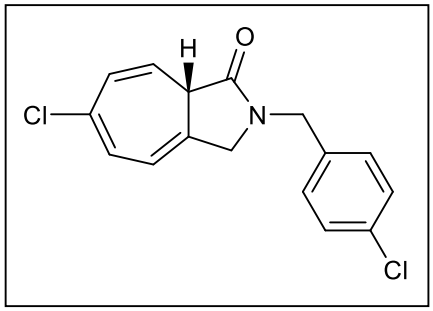

This compound was prepared according to the typical procedure for asymmetric Buchner ring expansion reaction of *N*,*N*-bis(4-chlorobenzyl)-2-diazoacetamide **57d** (66.8 mg, 0.2 mmol). The resulting mixture was purified by silica gel column chromatography with *n*-Hexane/ EtOAc as an eluent to give 6-chloro-2-(4-chlorobenzyl)-3,8a-dihydrocyclohepta[c]pyrrol-1(2H)-one **58d** as white solid (96% yield, 58.8 mg, 0.192 mmol), 96% ee. $[\alpha]^{26.3}_{D}$ = +90.26 (c 1.3, $CHCl_3$). ^{1}H NMR (500MHz, $CDCl_3$) δ 7.31 (d, *J* = 8.41 Hz, 2H), 7.20 (d, *J* = 8.41 Hz, 2H), 6.68 (d, *J* = 6.50 Hz, 1H), 6.20 (d, *J* = 9.94 Hz, 1H), 6.02 (ddd, *J* = 4.59, 4.20, 2.29 Hz, 1H), 5.37 (dd, *J* = 9.94, 4.20 Hz, 1H), 4.56 (d, *J* = 14.91 Hz, 1H), 4.49 (d, *J* = 14.91 Hz, 1H), 4.06 (d, *J* = 15.29 Hz, 1H), 4.01 (d, *J* = 15.29 Hz, 1H), 3.26 (s, 1H) ppm. ^{13}C NMR (125 MHz, $CDCl_3$) δ 173.23, 135.22, 134.34, 133.95, 129.68, 129.23, 129.18, 129.06, 128.64, 122.35, 118.45, 50.48, 46.04, 45.92 ppm. IR (neat) ν 3029, 2909, 1694, 1491, 1268, 811 cm^{-1}. The ee value was determined by chiral HPLC analysis. Column (Chiral IA-3), UV detector 220 nm, eluent: *n*-Hexane/IPA = 10/1, Flow rate = 1.0 ml/min, tR = 17.108 min (major product), tR = 15.908 min (minor product). HRMS (DART) calcd for $C_{16}H_{14}Cl_2N_1O_1$ [M+H]+: 306.0452 found: 306.0452.

(*S*)-6-Bromo-2-(4-bromobenzyl)-3,8a-dihydrocyclohepta[c]pyrrol-1(2H)-one (58e)

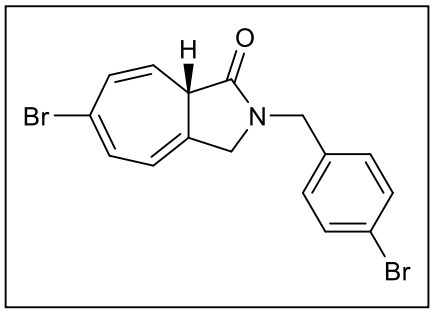

This compound was prepared according to the typical procedure for asymmetric Buchner ring expansion reaction of *N*,*N*-bis(4-bromobenzyl)-2-diazoacetamide **57e** (84.6 mg, 0.2 mmol). The resulting mixture was purified by silica gel column chromatography with *n*-Hexane/ EtOAc as an eluent to give 6-bromo-2-(4-bromobenzyl)-3,8a-dihydrocyclohepta[c]pyrrol-1(2H)-one **58e** as white solid (95% yield, 75.1 mg, 0.190 mmol), 95% ee. $[\alpha]^{27.4}_{D}$ = +107.77 (c 0.6, $CHCl_3$). ^{1}H NMR (500MHz, $CDCl_3$) δ 7.47 (d, *J* = 8.60 Hz, 2H), 7.13 (d, *J* = 8.60 Hz, 2H), 6.90 (d, *J* = 6.50 Hz, 1H), 6.32 (d, *J* = 9.94 Hz, 1H), 5.97 (ddd, *J* = 4.59, 4.20, 2.29 Hz, 1H), 5.27 (dd, *J* = 9.94, 4.59 Hz, 1H), 4.54 (d, *J* = 14.71 Hz, 1H), 4.47 (d, *J* = 14.71 Hz, 1H), 4.03 (d, *J* = 15.29 Hz, 1H), 3.98 (d, *J* = 15.29 Hz, 1H), 3.27 (s, 1H) ppm. ^{13}C NMR (125 MHz, $CDCl_3$) δ 173.19, 134.90, 132.38, 132.16, 131.07, 130.03, 129.97, 124.71, 122.33, 122.07, 119.31, 50.50, 46.16, 45.98 ppm. IR (neat) ν 3032, 2909, 1690, 1483, 1264, 798 cm^{-1}. The ee value was determined by chiral HPLC analysis. Column (Chiral IA-3), UV detector 220 nm, eluent: *n*-Hexane/IPA = 10/1, Flow rate = 1.0 ml/min, tR = 19.9 min (minor product), tR = 27.5 min (major product). HRMS (DART) calcd for $C_{16}H_{14}Br_2N_1O_1$ [M+H]+: 393.9442 found: 393.9442.

(*S*)-6-fluoro-2-(4-fluorobenzyl)-3,8a-dihydrocyclohepta[c]pyrrol-1(2H)-one (58f)

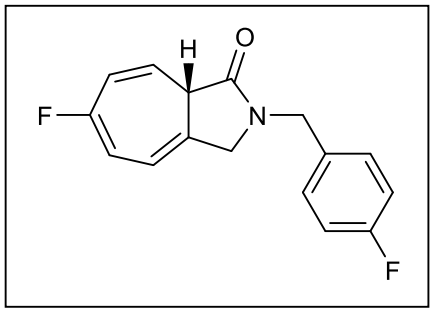

This compound was prepared according to the typical procedure for asymmetric Buchner ring expansion reaction of 2-diazo-*N*,*N*-bis(4-fluorobenzyl)acetamide **57f** (60.3 mg, 0.2 mmol). The resulting mixture was purified by silica gel column chromatography with *n*-Hexane/ EtOAc as an eluent to give 6-fluoro-2-(4-fluorobenzyl)-3,8a-dihydrocyclohepta[c]pyrrol-1(2H)-one **58f** as yellow oil (90% yield, 49.2 mg, 0.180 mmol), 90% ee. $[\alpha]^{24.0}_{D}$ = +63.71 (c 1.0, $CHCl_3$). ^{1}H NMR (500MHz, $CDCl_3$) δ 7.24 (dd, *J* = 8.59, 5.15 Hz, 2H), 7.03 (d, *J* = 8.59 Hz, 2H), 6.28–6.15 (m, 2H), 6.04–5.99 (m, 1H), 5.49 (m, 1H), 4.57 (d, *J* = 14.60 Hz, 1H), 4.49 (d, *J* = 14.60 Hz, 1H), 4.08 (d, *J* = 15.75 Hz, 1H), 4.00 (d, *J* = 15.75 Hz, 1H), 3.26 (s, 1H) ppm. ^{13}C NMR (125 MHz, $CDCl_3$) δ 173.34, 162.81, 160.93, 130.08, 123.67, 122.34, 116.61, 115.99, 115.82, 110.85, 110.63, 50.57, 46.23, 46.03 ppm. IR (neat) ν 3044, 2919, 1689, 1415, 1224, 754 cm^{-1}. The ee value was determined by chiral HPLC analysis. Column (Chiral IA-

3), UV detector 220 nm, eluent: *n*-Hexane/IPA = 10/1, Flow rate = 1.0 ml/min, tR = 13.9 min (major product), tR = 14.7 min (minor product). HRMS (DART) calcd for $C_{16}H_{14}F_2N_1O_1$ [M+H]+: 274.1043 found: 274.1043.

(*S*)-5-Methoxy-2-(3-methoxybenzyl)-3,8a-dihydrocyclohepta[c]pyrrol-1(2H)-one (58g)

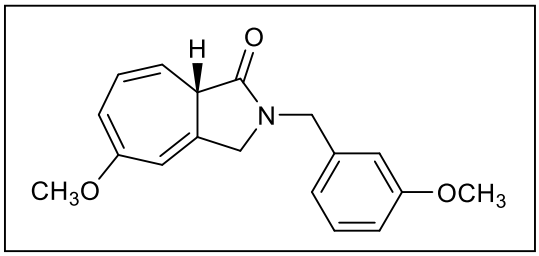

This compound was prepared according to the typical procedure for asymmetric Buchner ring expansion reaction of 2-diazo-*N*,*N*-bis(3-methoxybenzyl)acetamide **57g** (65.1 mg, 0.2 mmol). The resulting mixture was purified by silica gel column chromatography with *n*-Hexane/ EtOAc as an eluent to give 5-methoxy-2-(3-methoxybenzyl)-3,8a-dihydrocyclohepta[c]pyrrol-1(2H)-one **58g** as colorless oil (87% yield, 51.8 mg, 0.174 mmol), 74% ee. $[\alpha]^{26.7}_{D}$ = –196.62 (c 1.0, $CHCl_3$). ^{1}H NMR (500MHz, $CDCl_3$) δ 7.25 (t, *J* = 8.03 Hz, 1H), 6.87–6.77 (m, 3H), 6.12 (ddd, *J* = 7.07, 4.87, 2.29 Hz, 1H), 5.94 (ddd, *J* = 4.59, 2.29, 1.91, Hz, 1H), 5.65 (dd, *J* = 6.88, 1.91 Hz, 1H), 5.17 (dd, *J* = 9.56, 3.44 Hz, 1H), 4.55 (d, *J* = 14.91 Hz, 1H), 4.52 (d, *J* = 14.91 Hz, 1H), 4.07 (d, *J* = 15.86 Hz, 1H), 4.04 (d, *J* = 15.86 Hz, 1H), 3.79 (s, 3H), 3.63 (s, 3H), 3.22 (s, 1H) ppm. ^{13}C NMR (125 MHz, $CDCl_3$) δ 174.18, 160.14, 158.96, 137.55, 131.68, 129.94, 125.65, 120.50, 117.97, 115.75, 113.80, 113.37, 102.80, 55.36, 54.76, 50.45, 46.59, 46.02 ppm. IR (neat) ν 3005, 2928, 1690, 1427, 1260, 703 cm^{-1}. The ee value was determined by chiral HPLC analysis. Column (Chiral IA-3), UV detector 220 nm, eluent: *n*-Hexane/IPA = 10/1, Flow rate = 1.0 ml/min, tR = 20.7 min (major product), tR = 25.8 min (minor product). HRMS (DART) calcd for $C_{16}H_{14}F_2N_1O_1$ [M+H]+: 298.1443 found: 298.1443.

(*S*)-6-Methoxy-2-(4-nitrobenzyl)-3,8a-dihydrocyclohepta[c]pyrrol-1(2H)-one (58h)

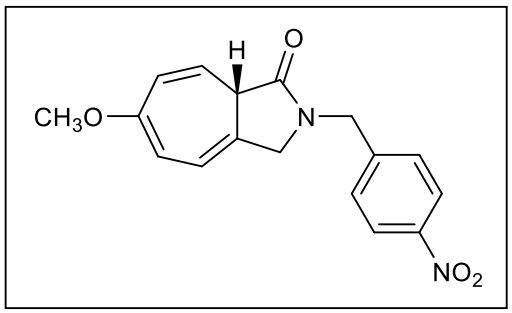

This compound was prepared according to the typical procedure for asymmetric Buchner ring expansion reaction of 2-diazo-*N*-(4-methoxybenzyl)-*N*-(4-nitrobenzyl)acetamide **57h** (65.1 mg, 0.2mmol). The resulting mixture was purified by silica gel column chromatography with *n*-Hexane/ EtOAc as an eluent to give 6-methoxy-2-(4-nitrobenzyl)-3,8a-dihydrocyclohepta[c]pyrrol-1(2H)-one (**58h**) as yellow oil

(84% yield, 52.5 mg, 0.168 mmol), 99% ee. $[\alpha]^{22.7}_{D}$ = –40.09 (c 1.0, $CHCl_3$). ^{1}HNMR (500MHz, $CDCl_3$) δ 8.20 (d, *J* = 8.87 Hz, 2H), 7.43 (d, *J* = 8.87 Hz, 2H), 6.05 (dt., *J* = 10.31, 2.29 Hz, 1H), 6.04 (ddd., *J* = 4.58, 4.58, 2.29 Hz, 1H), 5.69 (d, *J* = 6.87 Hz, 1H), 5.50 (dd, *J* = 10.31, 4.01 Hz, 1H), 4.70 (d, *J* = 15.46 Hz, 1H), 4.63 (d, *J* = 15.46 Hz, 1H), 4.11 (d, *J* = 14.03 Hz, 1H), 4.04 (d, *J* = 14.03 Hz, 1H), 3.64 (s, 3H) , 3.24 (s, 1H) ppm. ^{13}C NMR (125 MHz, $CDCl_3$) δ 174.43, 159.58, 147.71, 143.67, 128.85, 125.55, 124.18, 122.87, 122.30, 118.34, 102.81, 54.87, 50.70, 46.09, 45.54 ppm. IR (neat) ν 3002, 2921, 1696, 1413, 1217, 702 cm^{-1}.The ee value was determined by chiral HPLC analysis. Column (Chiral IA-3), UV detector 220 nm, eluent: *n*-Hexane/IPA = 10/1, Flow rate = 1.0 ml/min, tR = 45.2 min (major product), tR = 59.3 min (minor product). HRMS (DART) calcd for $C_{17}H_{17}N_2O_4$ [M+H]+: 313.1188 found: 313.1188.

(*S*)-2-Methyl-3,8a-dihydrocyclohepta[c]pyrrol-1(2H)-one (58i)

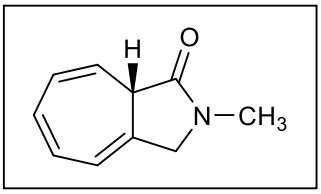

This compound was prepared according to the typical procedure for asymmetric Buchner ring expansion reaction of *N*,*N*-dibenzyl-2-diazoacetamide **57i** (37.8 mg, 0.2 mmol). The resulting mixture was purified by silica gel column chromatography with *n*-Hexane/IPA as an eluent to give 2-methyl-3,8a-dihydrocyclohepta[c]pyrrol-1(2H)-one (**58i**) as white powder (22 % yield, 7.1 mg, 0.044 mmol), 71% ee. $[\alpha]^{22.8}_{D}$ = + 91.67 (c 0.3, $CHCl_3$). ^{1}H NMR (500MHz, CDCl3) δ 6.49 (ddd, *J* = 12.23, 10.32, 5.35 Hz, 2H), 6.20–6.15(m, 2H), 5.28 (*J* = 10.32, 4.2 Hz, 1H), 4.23 (d, *J* = 15.29, 1H), 4.19 (d, *J* = 15.29, 1H), 3.08 (s, 1H), 2.97 (s, 3H) ppm. ^{13}C NMR (125 MHz, $CDCl_3$) δ 172.93, 130.53, 130.05, 127.10, 121.22, 120.93, 119.52, 53.42, 46.10, 29.70 ppm. IR (neat) ν 3020, 2920, 1690, 1432, 1276, 703 cm^{-1}.The ee value was determined by chiral HPLC analysis. Column (Chiral ID-3), UV detector 220 nm, eluent: *n*-Hexane/IPA = 5/1, Flow rate = 1.0 ml/min, tR = 19.6 min (major product), tR = 16.2 min (minor product). HRMS (DART) calcd for $C_{10}H_{11}N_1O_1$ [M+H]+: 162.0910 found: 162.0918.

(*S*)-6-Methoxy-2-methyl-3,8a-dihydrocyclohepta[c]pyrrol-1(2H)-one (58j)

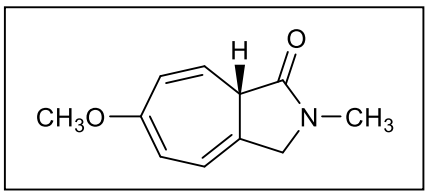

This compound was prepared according to the typical procedure for asymmetric Buchner ring expansion reaction of *N*,*N*-dibenzyl-2-diazoacetamide **57j** (44 mg, 0.2 mmol). The resulting mixture was purified by silica gel column

chromatography with *n*-Hexane/IPA as an eluent to give 6-methoxy-2-methyl-3,8a-dihydrocyclohepta[c]pyrrol-1(2H)-one **(58j)** as white powder (76% yield, 29 mg, 0.152 mmol), 99% ee. $[\alpha]^{23.2}_{D}$ = –9.5 (c 1, $CHCl_3$). ^{1}H NMR (500MHz, $CDCl_3$) δ 6.06–6.04 (m, 2H), 5.70 (d, *J* = 7.02 Hz, 1H), 5.47 (dd, *J* = 10.38, 4.27 Hz, 1H), 4.19 (d, *J* = 14.65 Hz, 1H), 4.13 (d, *J* = 14.65 Hz, 1H), 3.64 (s, 3H), 3.15 (s, 1H), 2.96 (s, 3H) ppm. ^{13}C NMR (125 MHz, $CDCl_3$) δ 174.08, 159.45, 125.18, 123.51, 123.40, 117.67, 102.84, 54.89, 53.28, 45.75, 29.72 ppm. IR (neat) ν 3011, 2956, 1697, 1433, 1218, 717 cm^{-1}. The ee value was determined by chiral HPLC analysis. Column (Chiral ID-3), UV detector 220 nm, eluent: *n*-Hexane/IPA = 5/1, Flow rate = 1.0 ml/min, tR = 31.8 min (major product), tR = 29.9 min (minor product). HRMS (DART) calcd for $C_{11}H_{13}N_1O_2$ [M+H]+: 192.1029 found: 192.1024.

(*S*)-2,6-Dimethyl-3,8a-dihydrocyclohepta[c]pyrrol-1(2H)-one (58k)

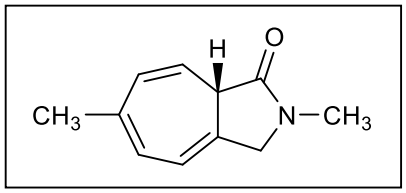

This compound was prepared according to the typical procedure for asymmetric Buchner ring expansion reaction of *N*,*N*-dibenzyl-2-diazoacetamide **57k** (40.6 mg, 0.2 mmol). The resulting mixture was purified by silica gel column chromatography with *n*-Hexane/IPA as an eluent to give 2,6-dimethyl-3,8a-dihydrocyclohepta[c]pyrrol-1(2H)-one **(58k)** as white powder (67% yield, 23.4 mg, 0.134 mmol), 99% ee. $[\alpha]^{23.3}_{D}$ = +32.6 (c 0.55, $CHCl_3$). ^{1}H NMR (500MHz, $CDCl_3$) δ 6.30 (d, *J* = 6.12 Hz, 1H), 6.05–6.01 (m, 2H), 5.28 (dd, *J* = 9.94, 4.20 Hz, 1H), 4.20 (d, *J* = 15.67 Hz, 1H), 4.15 (d, *J* = 15.67 Hz, 1H), 3.07 (s, 1H), 2.96 (s, 3H), 2.03 (s, 3H) ppm. ^{13}C NMR (125 MHz, $CDCl_3$) δ 174.35, 139.41, 130.25, 127.08, 126.82, 120.07, 119.13, 53.23, 45.78, 29.62, 24.82 ppm. IR (neat) ν 2921, 2857, 1681, 1400, 1255, 735 cm^{-1}. The ee value was determined by chiral HPLC analysis. Column (Chiral ID-3), UV detector 220 nm, eluent: *n*-Hexane/IPA = 5/1, Flow rate = 1.0 ml/min, tR = 17.7 min (major product), tR = 15.9 min (minor product). HRMS (DART) calcd for $C_{11}H_{13}N_1O_1$ [M+H]+: 176.1070 found: 176.1075.

(*S*)-6-Chloro-2-methyl-3,8a-dihydrocyclohepta[c]pyrrol-1(2H)-one (58l)

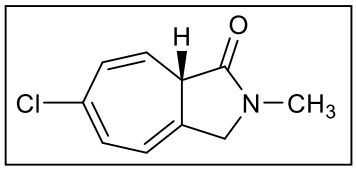

This compound was prepared according to the typical procedure for asymmetric Buchner ring expansion reaction of *N*,*N*-dibenzyl-2-diazoacetamide **57l** (44.7 mg, 0.2 mmol). The resulting mixture was

purified by silica gel column chromatography with *n*-Hexane/IPA as an eluent to give 6-chloro-2-methyl-3,8a-dihydrocyclohepta[c]pyrrol-1(2H)-one (**58l**) as white powder (61% yield, 23.9 mg, 0.122 mmol), 92% ee. $[\alpha]^{24.1}_{D}$ = +42.9 (c 0.1, $CHCl_3$). ^{1}HNMR (500MHz, $CDCl_3$) δ 6.70 (d, *J* = 6.88 Hz, 1H), 6.19 (dt, *J* = 9.94, 1.91 Hz, 1H), 6.08 (ddd., *J* = 4.59, 4.20, 1.91 Hz, 1H), 5.34 (dd, *J* = 9.94, 4.2 Hz, 1H), 4.22 (d, *J* = 15.67 Hz, 1H), 4.16 (d, *J* = 15.67 Hz, 1H), 3.20 (s, 1H), 2.97 (s, 1H) ppm. ^{13}C NMR (125 MHz, $CDCl_3$) δ 173.23, 135.24, 129.69, 128.92, 128.62, 122.69, 118.17, 53.26, 45.77, 29.73 ppm. IR (neat) ν 3036, 2920, 1694, 1486, 1268, 774 cm^{-1}. The ee value was determined by chiral HPLC analysis. Column (Chiral ID-3), UV detector 220 nm, eluent: *n*-Hexane/IPA = 5/1, Flow rate = 1.0 ml/min, tR = 32.6 min (major product), tR = 20.8 min (minor product). HRMS (DART) calcd for $C_{10}H_{10}Cl_1N_1O_1$ [M+H]+: 196.0527 found: 196.0529.

(*S*)-6-Bromo-2-methyl-3,8a-dihydrocyclohepta[c]pyrrol-1(2H)-one (58m)

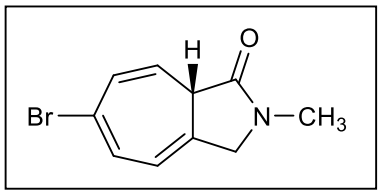

This compound was prepared according to the typical procedure for asymmetric Buchner ring expansion reaction of *N*,*N*-dibenzyl-2-diazoacetamide **57m** (53.6 mg, 0.2 mmol). The resulting mixture was purified by silica gel column chromatography with *n*-Hexane/IPA as an eluent to give 6-bromo-2-methyl-3,8a-dihydrocyclohepta[c]pyrrol-1(2H)-one (**51m**) as white powder (43% yield, 20.8 mg, 0.086 mmol), 96% ee. $[\alpha]^{24}_{D}$ = +34.5 (c 0.1, $CHCl_3$). ^{1}H NMR (500MHz, $CDCl_3$) δ 6.93 (d, *J* = 6.5 Hz, 1H), 6.31 (d, *J* = 9.94 Hz, 1H), 6.03 (ddd., *J* = 4.59, 4.20, 2.29, 1H), 5.25 (dd, *J* = 9.94, 4.20 Hz, 1H), 4.18 (d, *J* = 15.67 Hz, 1H), 4.13 (d, *J* = 15.67 Hz, 1H), 3.22 (s, 1H), 2.96 (s, 3H) ppm. ^{13}C NMR (125 MHz, $CDCl_3$) δ 173.16, 132.36, 130.86, 130.40, 124.66, 122.63, 118.99, 53.24, 45.82, 29.65 ppm. IR (neat) ν 3032, 2924, 1686, 1399, 1275, 774 cm^{-1}. The ee value was determined by chiral HPLC analysis. Column (Chiral ID-3), UV detector 220 nm, eluent: *n*-Hexane/IPA = 5/1, Flow rate = 1.0 ml/min, tR = 33.0 min (major product), tR = 23.4 min (minor product). HRMS (DART) calcd for $C_{10}H_{10}Br_1N_1O_1$ [M+H]+: 240.0023 found: 240.0024.

(*S*)-6-Fluoro-2-methyl-3,8a-dihydrocyclohepta[c]pyrrol-1(2H)-one (58n)

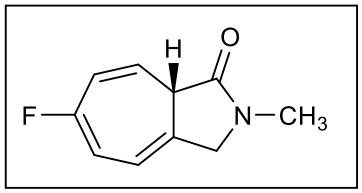

This compound was prepared according to the typical procedure for asymmetric Buchner ring expansion reaction of *N*,*N*-dibenzyl-2-diazoacetamide **57n** (41.4 mg, 0.2 mmol). The resulting mixture was purified by silica gel column chromatography with *n*-Hexane/IPA as an eluent to give 6-fluoro-2-methyl-3,8a-dihydrocyclohepta[c]pyrrol-1(2H)-one (**58n**) as colorless oil (44% yield, 15.6 mg, 0.088 mmol), 92% ee. $[\alpha]^{20.3}_{D}$ = –172.16 (c 0.6, $CHCl_3$). ^{1}H NMR (500MHz, $CDCl_3$) δ 6.25 (dd, *J* = 17.97, 8.03 Hz, 1H), 6.18 (tdd, *J* = 8.98, 2.29, 2.29 Hz, 1H), 6.09–6.05 (m, 1H), 5.46 (ddt, *J* = 9.94, 4.97, 4.97 Hz, 1H), 4.23 (d, *J* = 15.29 Hz, 1H), 4.14 (d, *J* = 15.29 Hz, 1H), 3.17 (s, 1H), 2.97 (s, 3H) ppm. ^{13}C NMR (125 MHz, $CDCl_3$) δ 173.34, 128.10, 125.86, 123.86, 122.17, 116.23, 110.58, 53.35, 45.99, 29.74 ppm. IR (neat) ν 3040, 2921, 1690, 1435, 1276, 715 cm^{-1}. The ee value was determined by chiral HPLC analysis. Column (Chiral ID-3), UV detector 220 nm, eluent: *n*-Hexane/IPA = 5/1, Flow rate = 1.0 ml/min, tR = 23.7 min (major product), tR = 17.6 min (minor product). HRMS (DART) calcd for $C_{10}H_{10}F_1N_1O_1$ [M+H]+: 180.0825 found: 180.0829.

IR SPECTRAL DATA

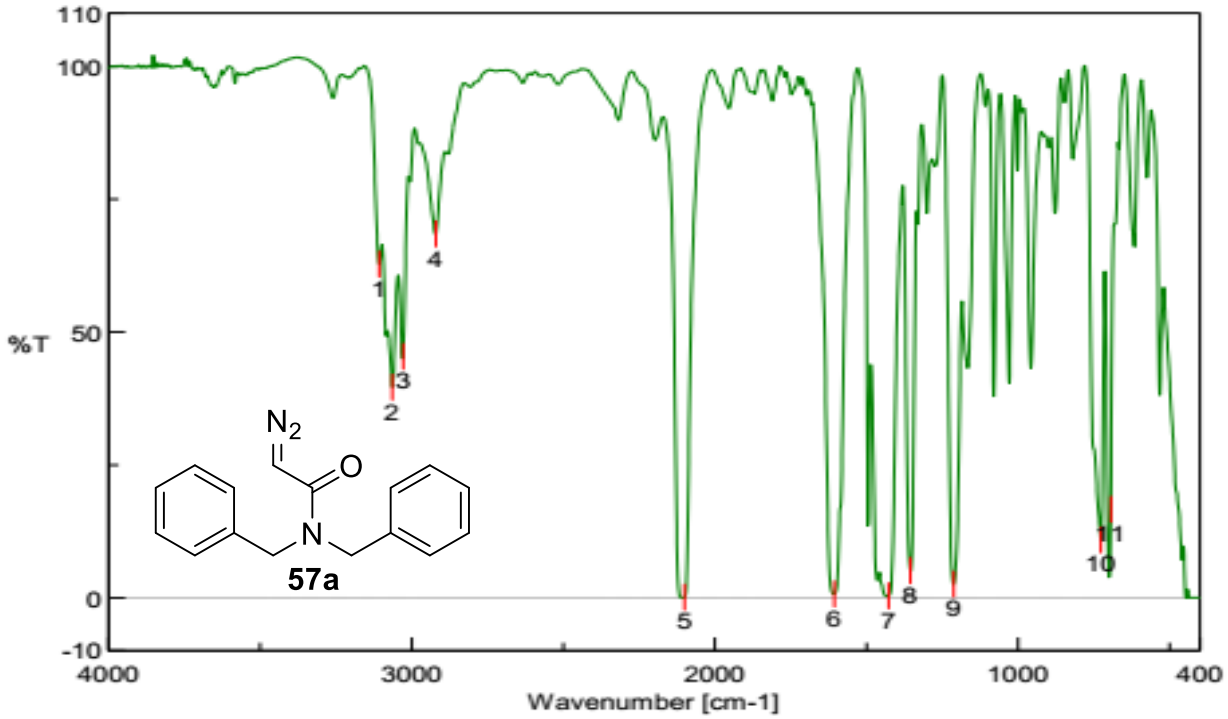

Figure 10. IR spectral of 2-diazo-*N*,*N*-dibenzylacetamide.

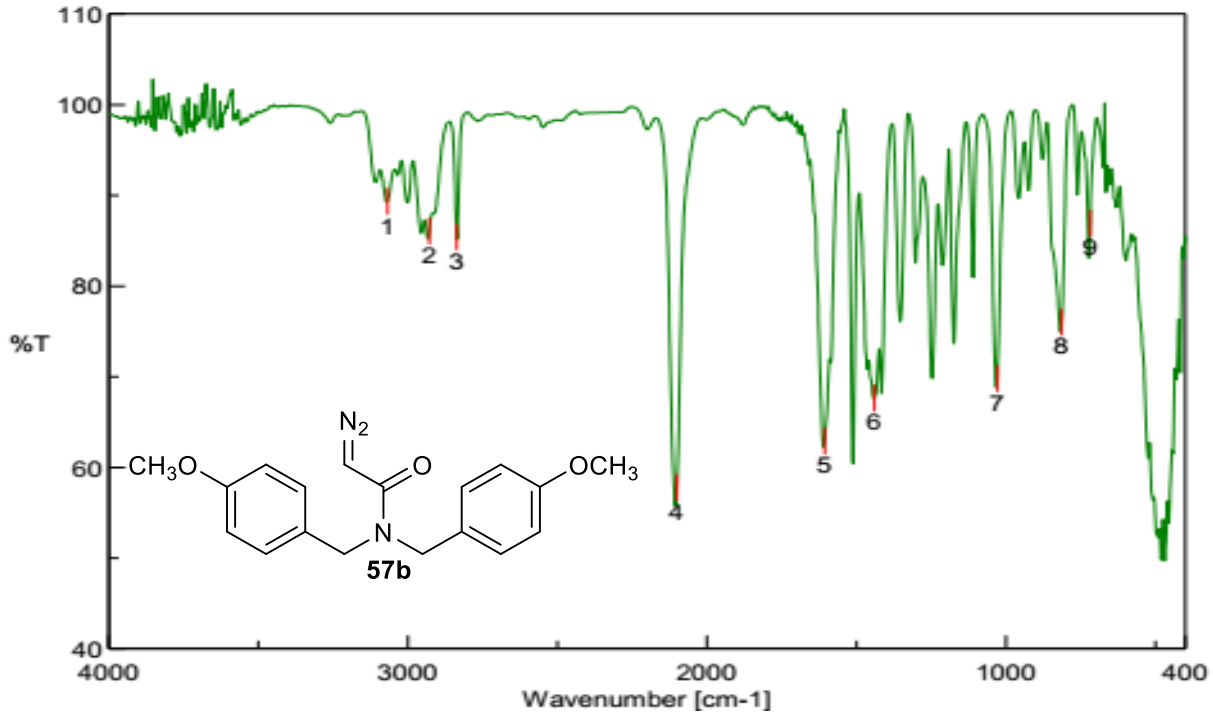

Figure 11. IR spectral of 2-diazo-*N*,*N*-bis(4-methoxybenzyl)acetamide.

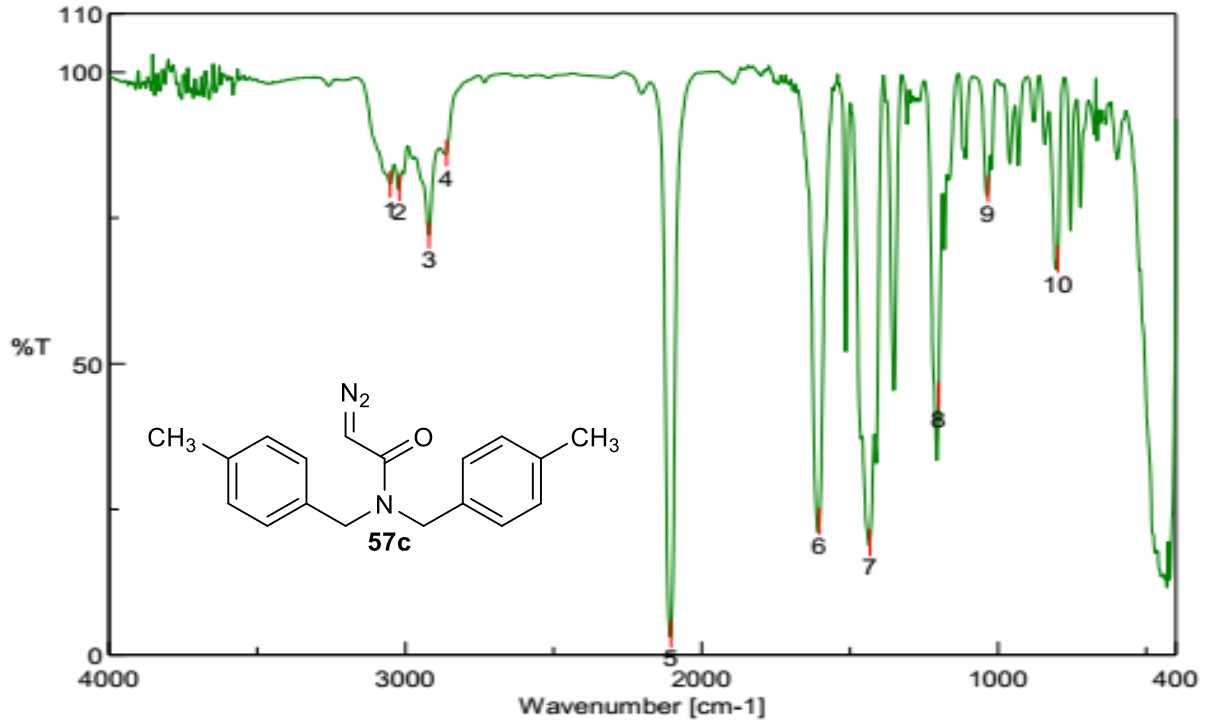

Figure 12. IR spectral of 2-diazo-*N*,*N*-bis(4-methylbenzyl)acetamide.

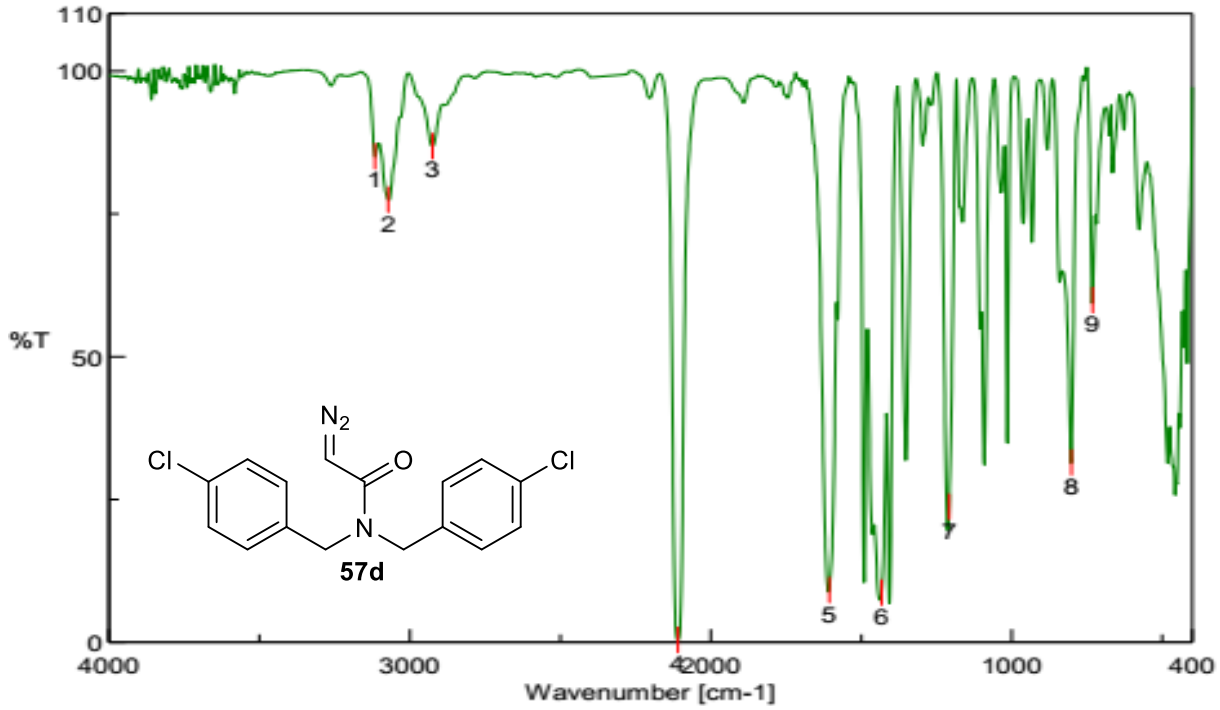

Figure 13. IR spectral of 2-diazo-*N*,*N*-bis(4-chlorobenzyl)acetamide.

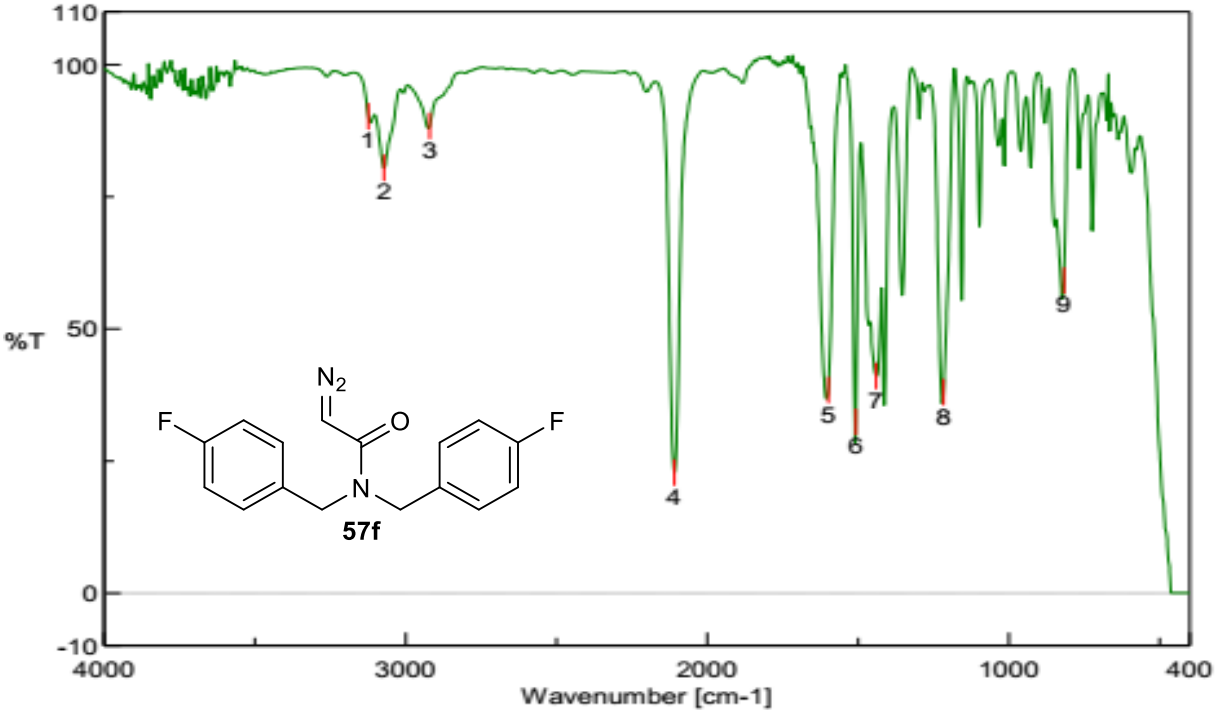

Figure 14. IR spectral of 2-diazo-*N*,*N*-bis(4-fluorobenzyl)acetamide.

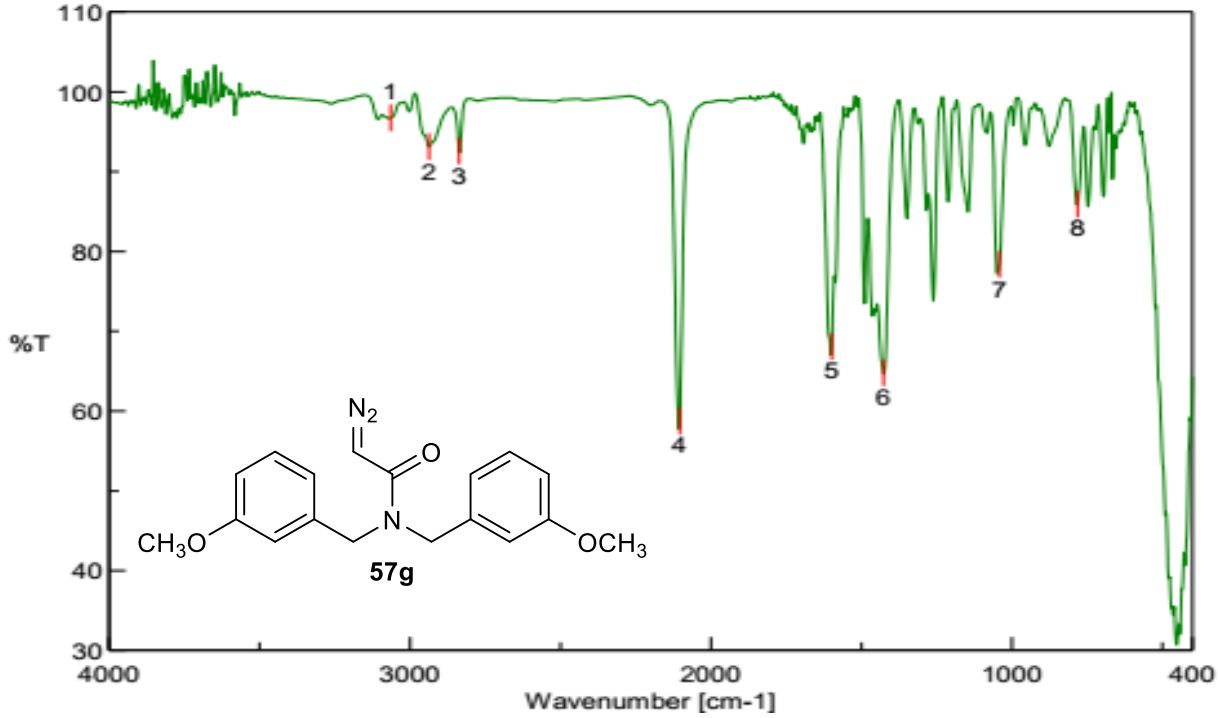

Figure 15. IR spectral of 2-diazo-*N*,*N*-bis(3-methoxybenzyl)acetamide.

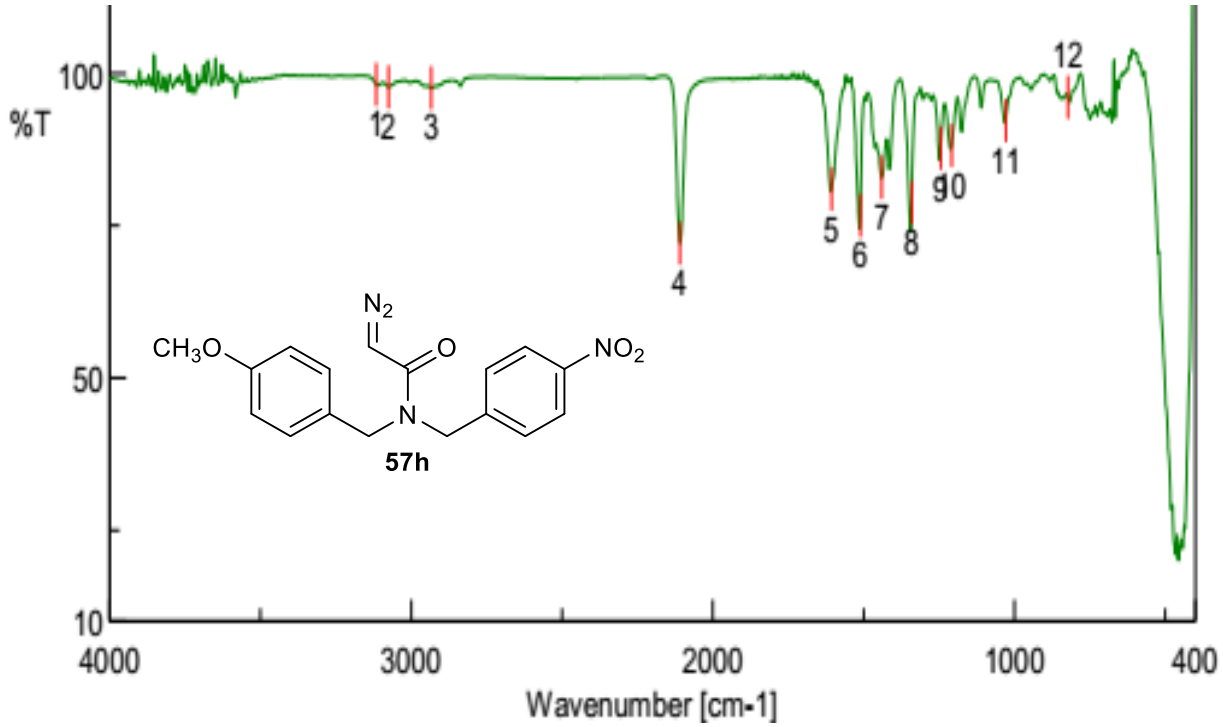

Figure 16. IR spectral of 2-diazo-*N*-(4-methoxybenzyl)-*N*-(4-nitrobenzyl)acetamide.

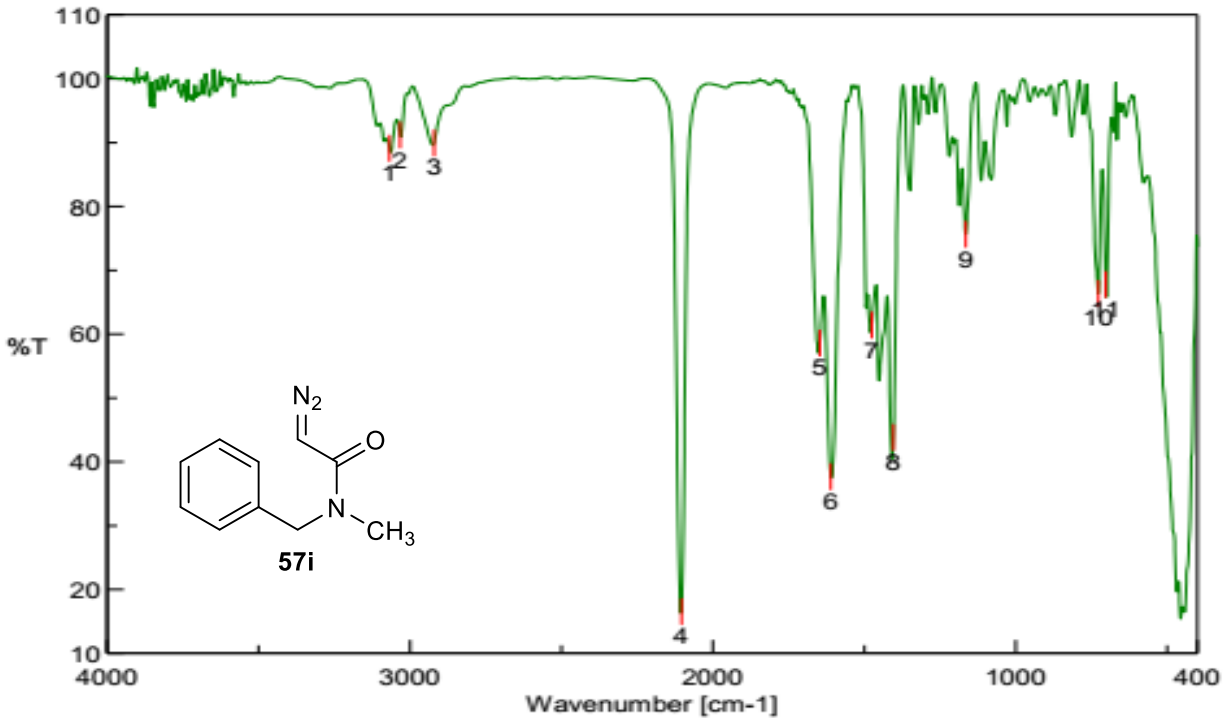

Figure 17. IR spectral of 2-diazo-*N*-benzyl-*N*-methylacetamide.

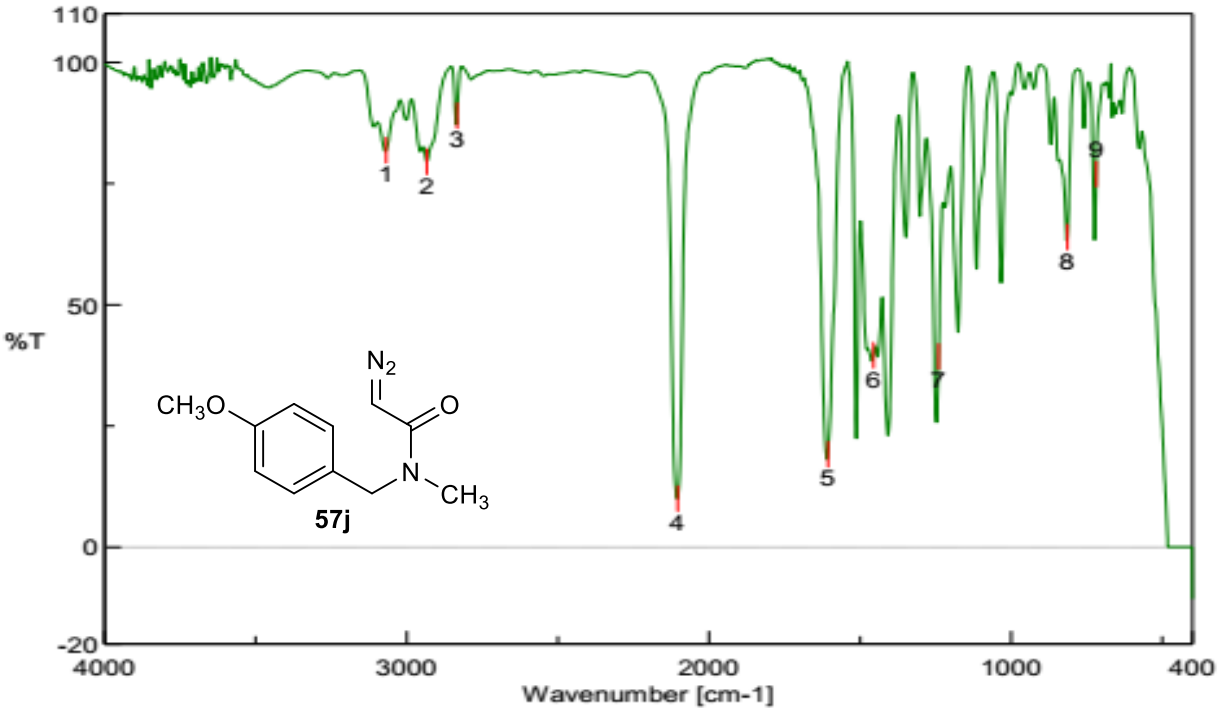

Figure 18. IR spectral of 2-diazo-*N*-(4-methoxybenzyl)-*N*-methylacetamide.

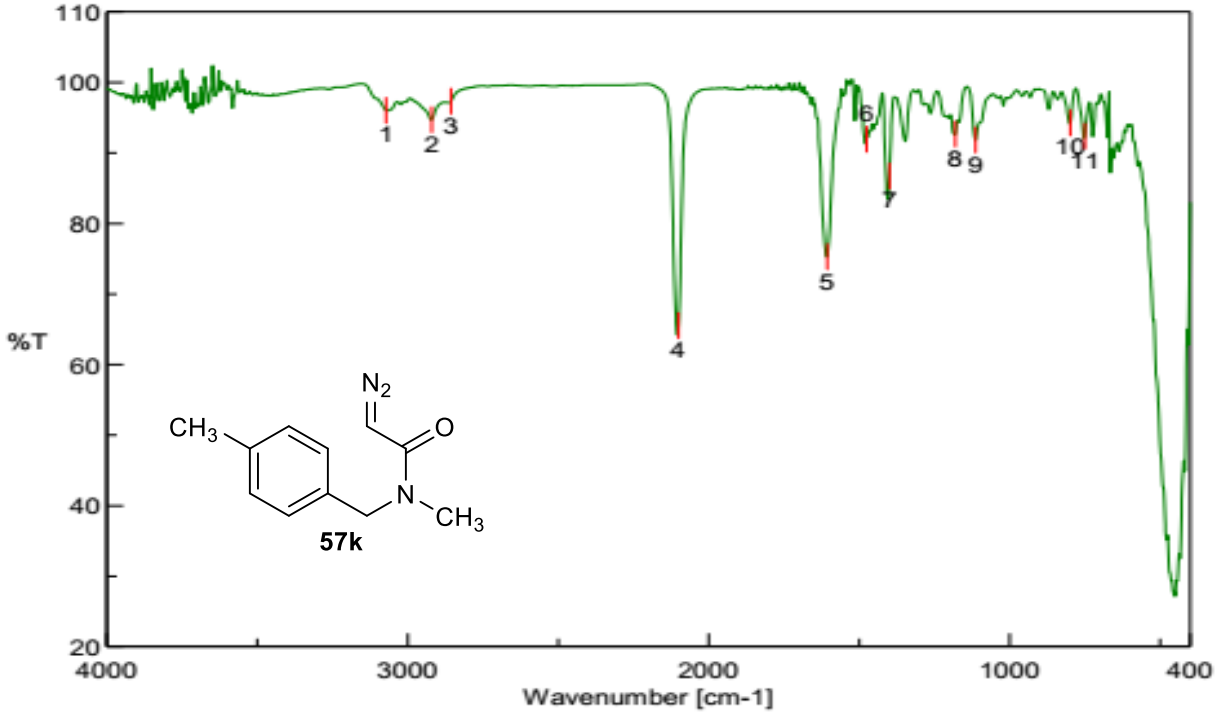

Figure 19. IR spectral of 2-diazo-*N*-(4-methylbenzyl)-*N*-methylacetamide.

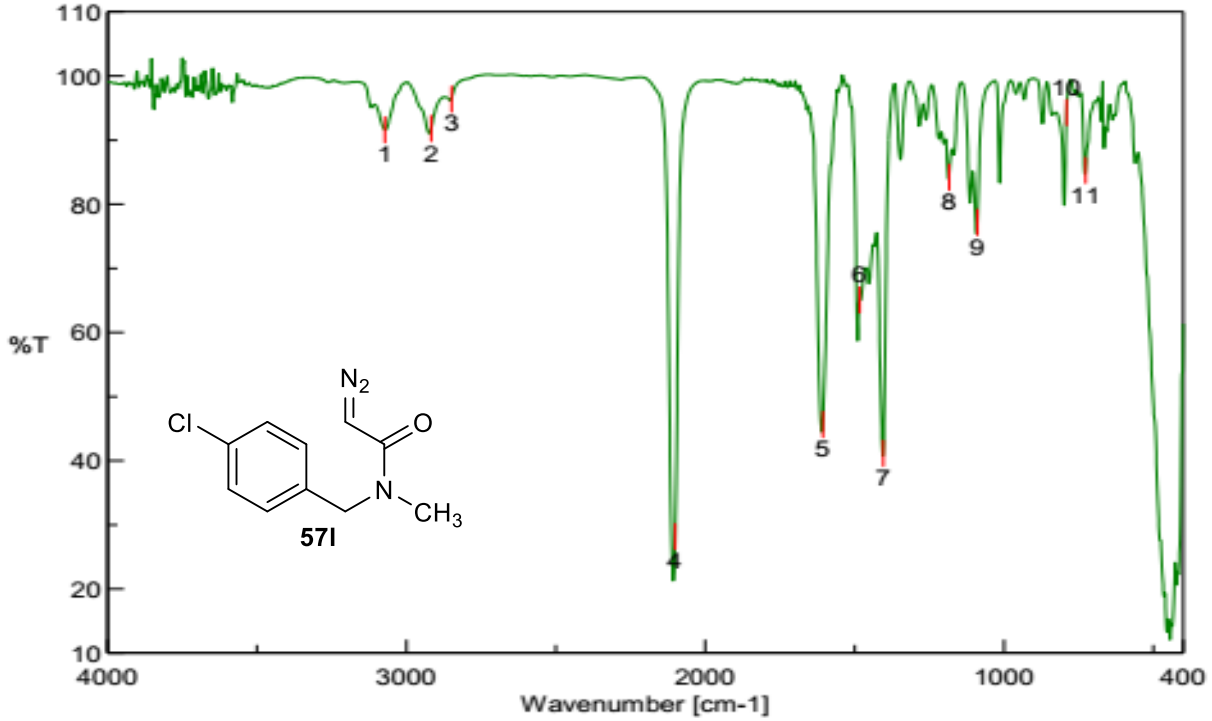

Figure 20. IR spectral of 2-diazo-*N*-(4-chlorobenzyl)-*N*-methylacetamide.

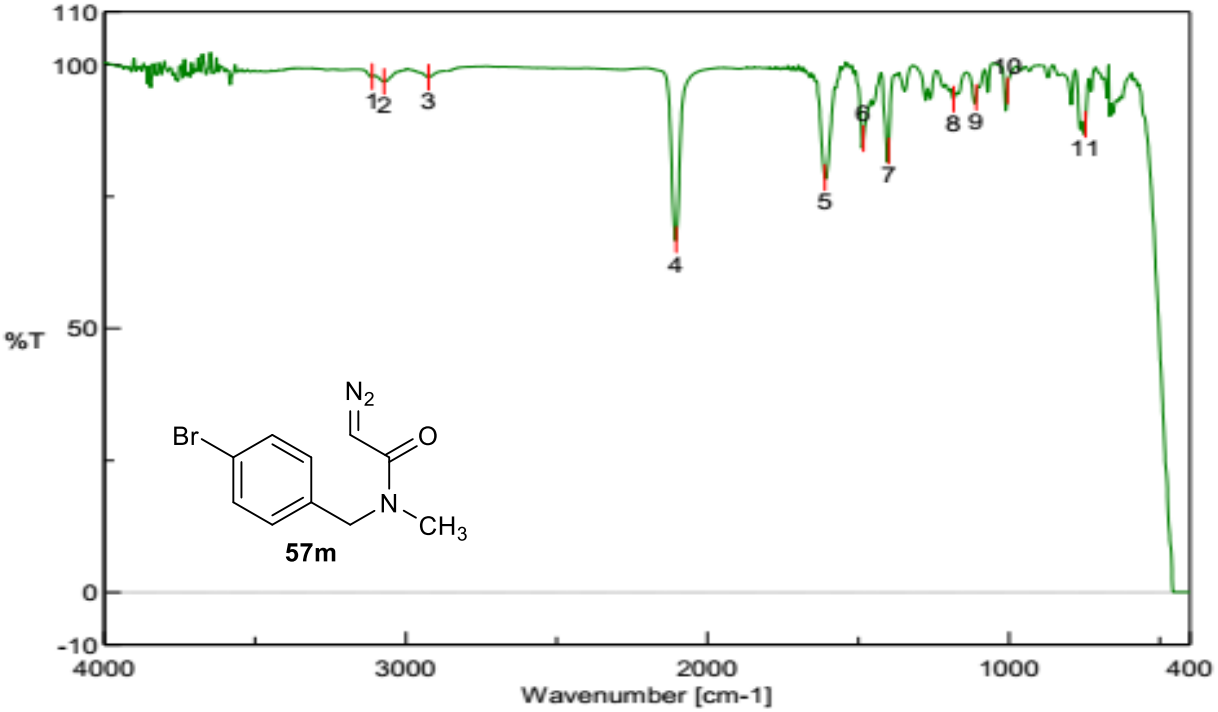

Figure 21. IR spectral of 2-diazo-*N*-(4-bromobenzyl)-*N*-methylacetamide.

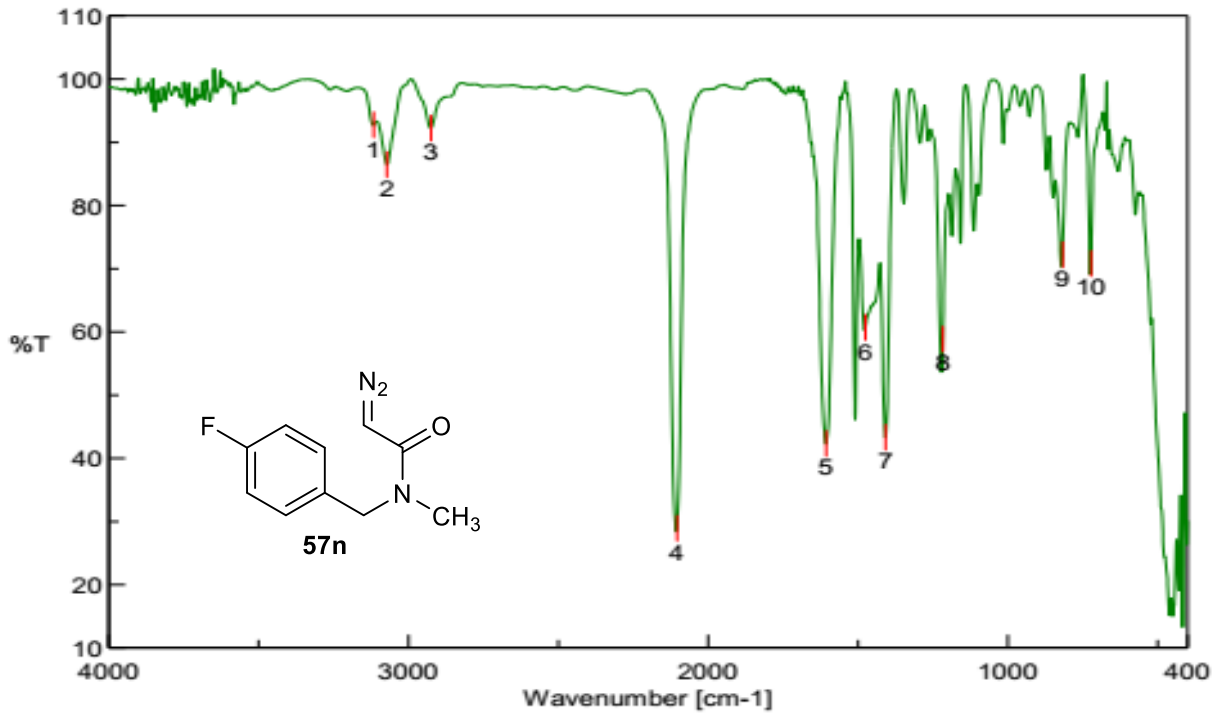

Figure 22. IR spectral of 2-diazo-*N*-(4-flourobenzyl)-*N*-methylacetamide.

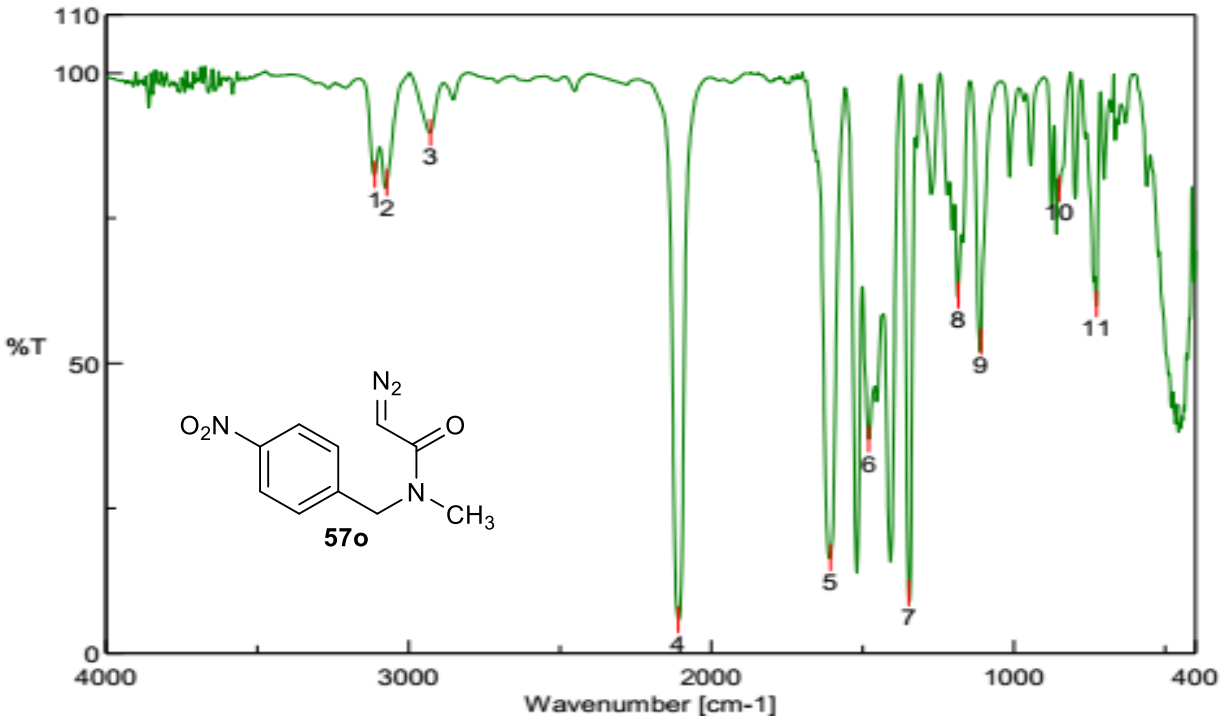

Figure 23. IR spectral of 2-diazo-N-(4-nitrobenzyl)-*N*-methylacetamide.

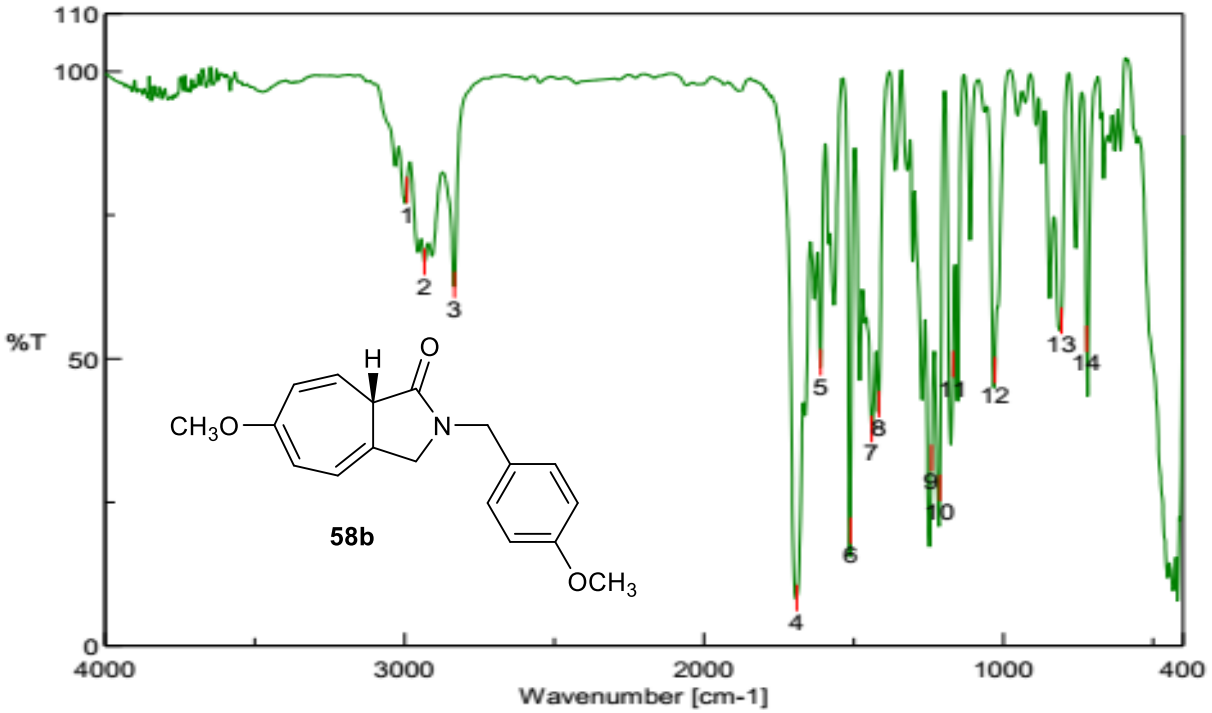

Figure 24. IR spectral of (*S*)-6-methoxy-2-(4-methoxybenzyl)-3,8a-dihydrocyclohepta [c]pyrrol-1(2H)-one.

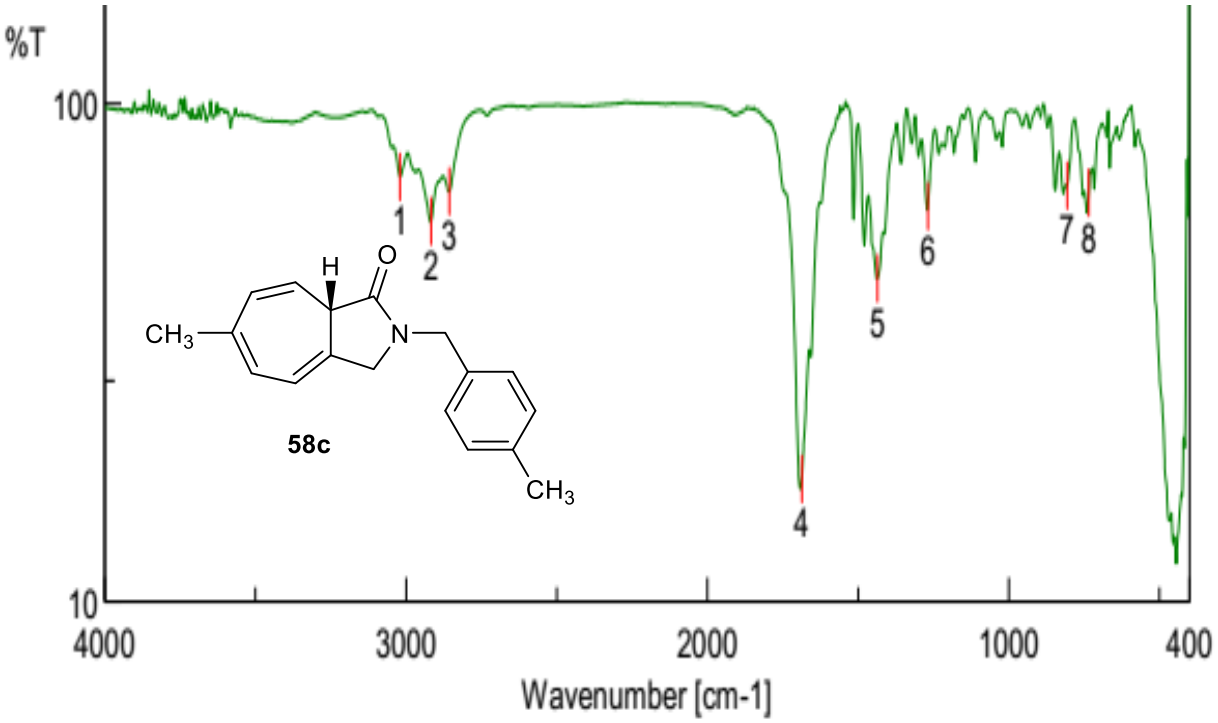

Figure 25. IR spectral of (*S*)-6-methyl-2-(4-methylbenzyl)-3,8a-dihydrocyclohepta [c]pyrrol-1(2H)-one.

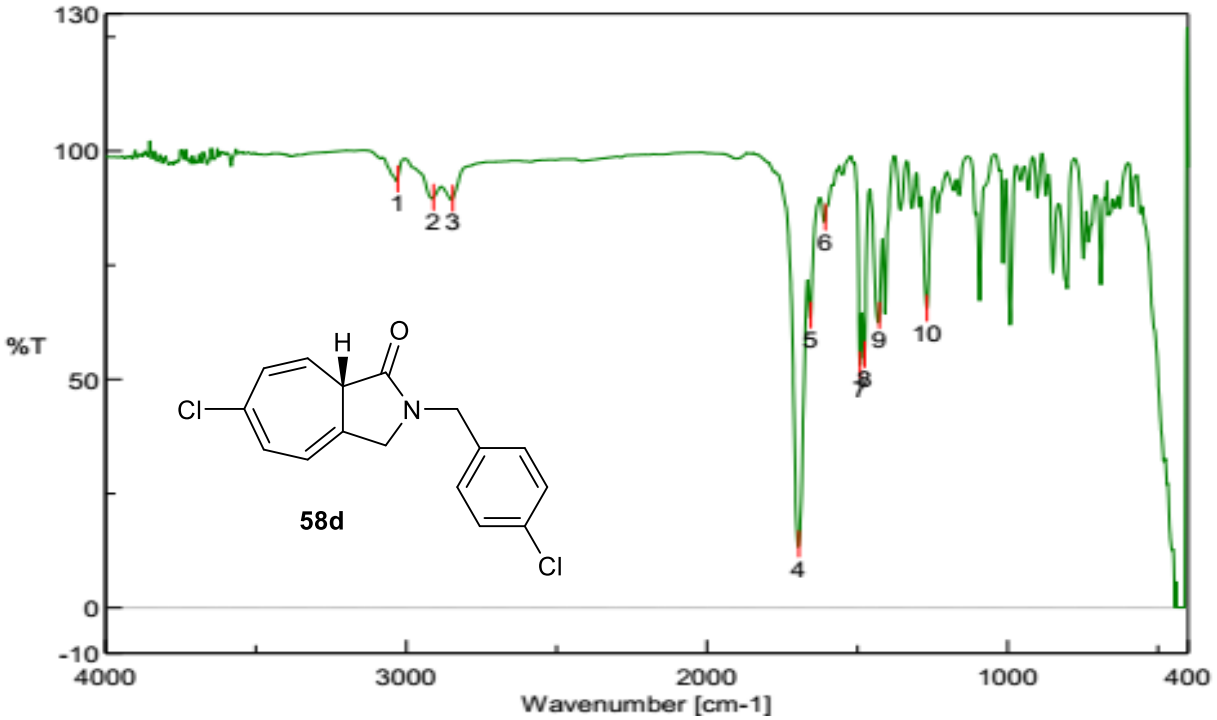

Figure 26. IR spectral of (*S*)-6-chloro-2-(4-chlorobenzyl)-3,8a-dihydrocyclohepta [c]pyrrol-1(2H)-one.

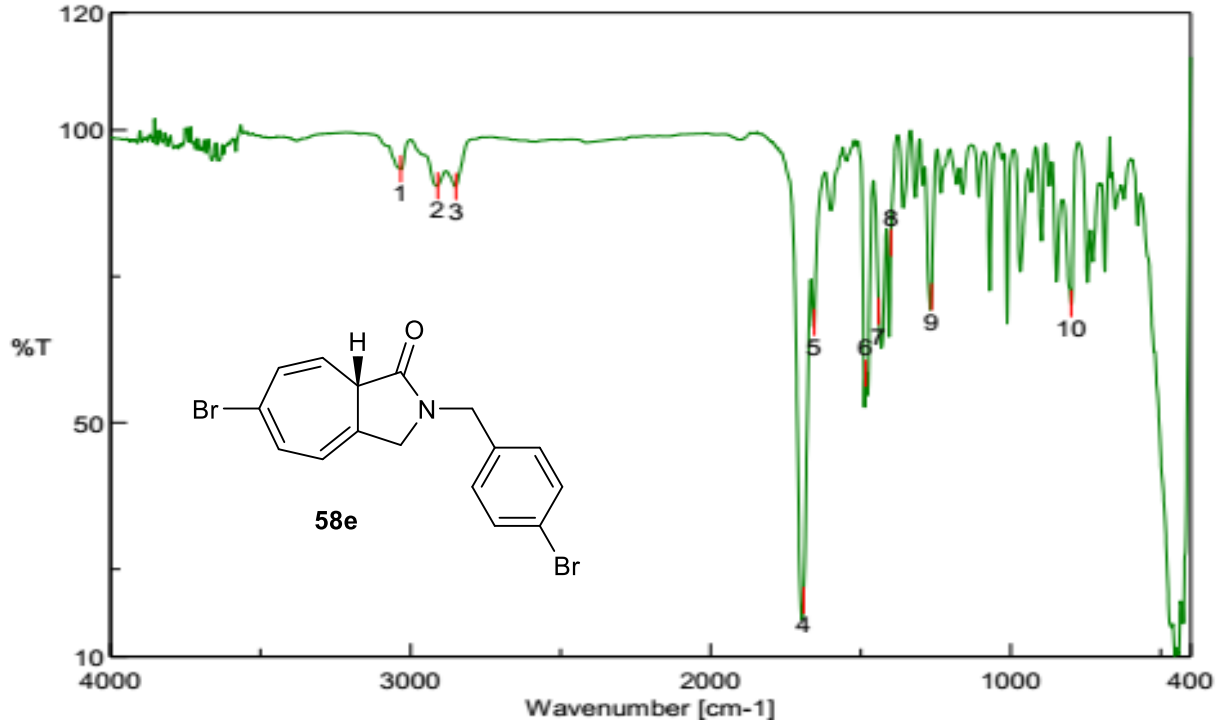

Figure 27. IR spectral of (*S*)-6-bromo-2-(4-bromobenzyl)-3,8a-dihydrocyclohepta [c]pyrrol-1(2H)-one.

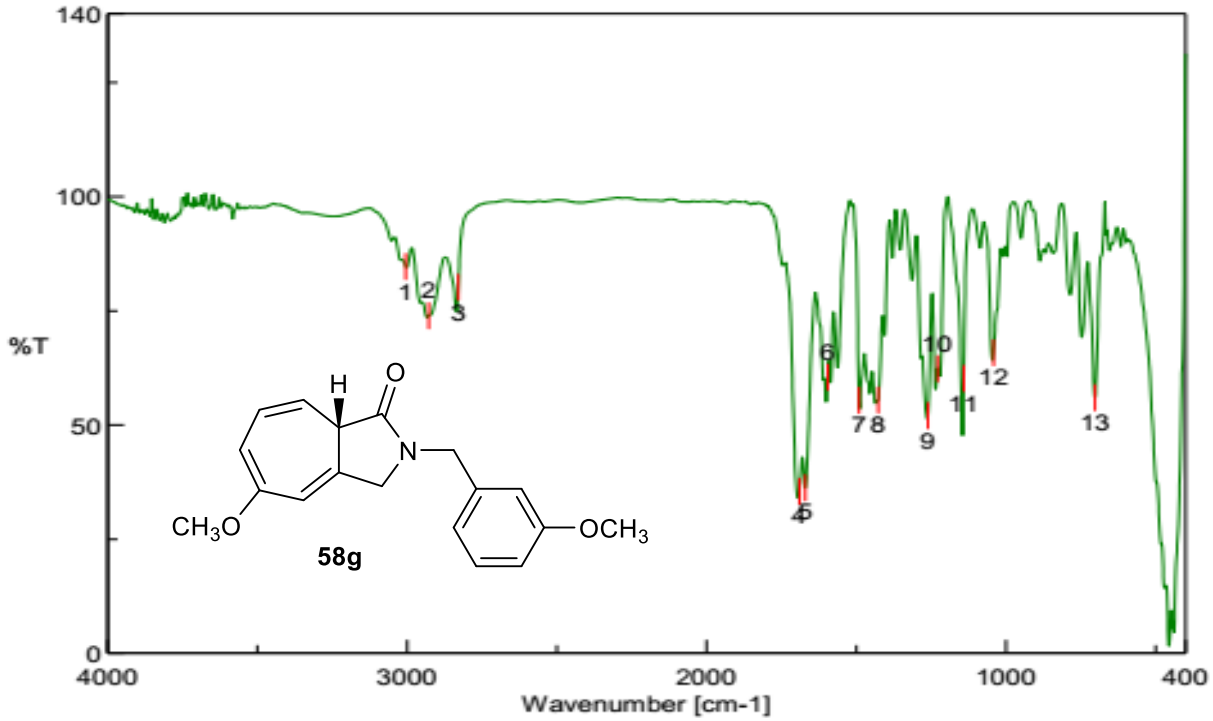

Figure 28. IR spectral of (*S*)-5-methoxy-2-(3-methoxybenzyl)-3,8a-dihydrocyclohepta [c]pyrrol-1(2H)-one.

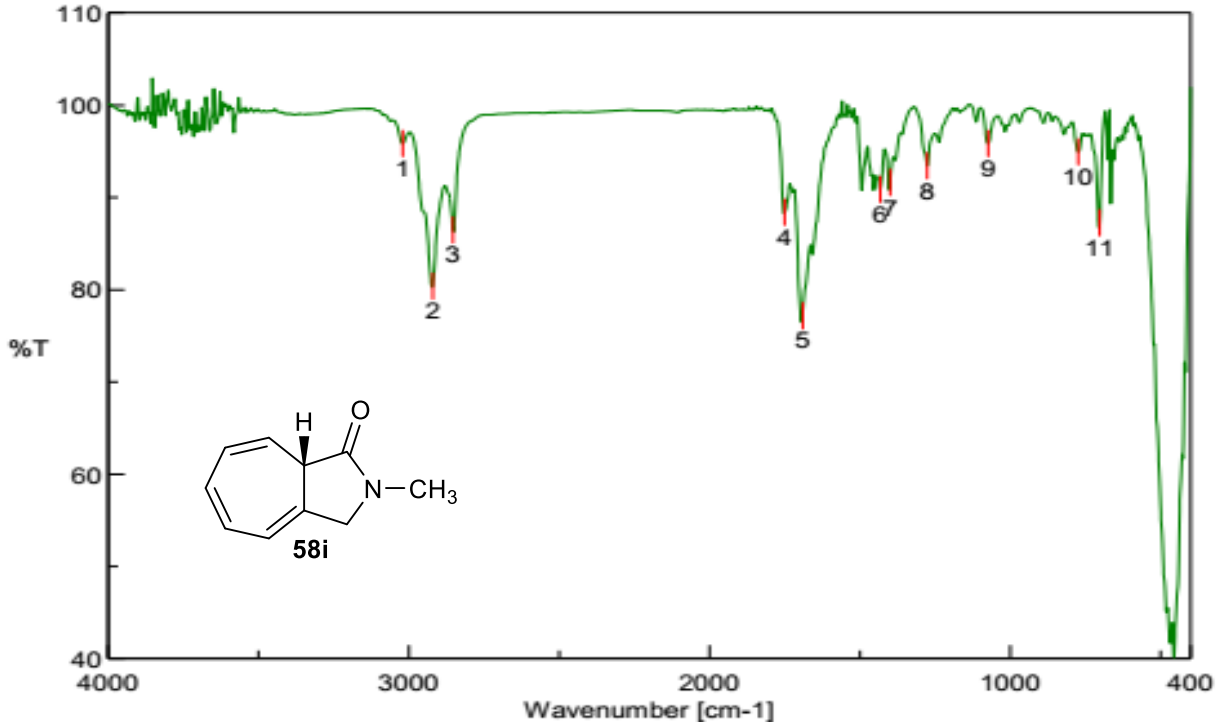

Figure 29. IR spectral of (*S*)-2-methyl-3,8a-dihydrocyclohepta[c]pyrrol-1(2H)-one.

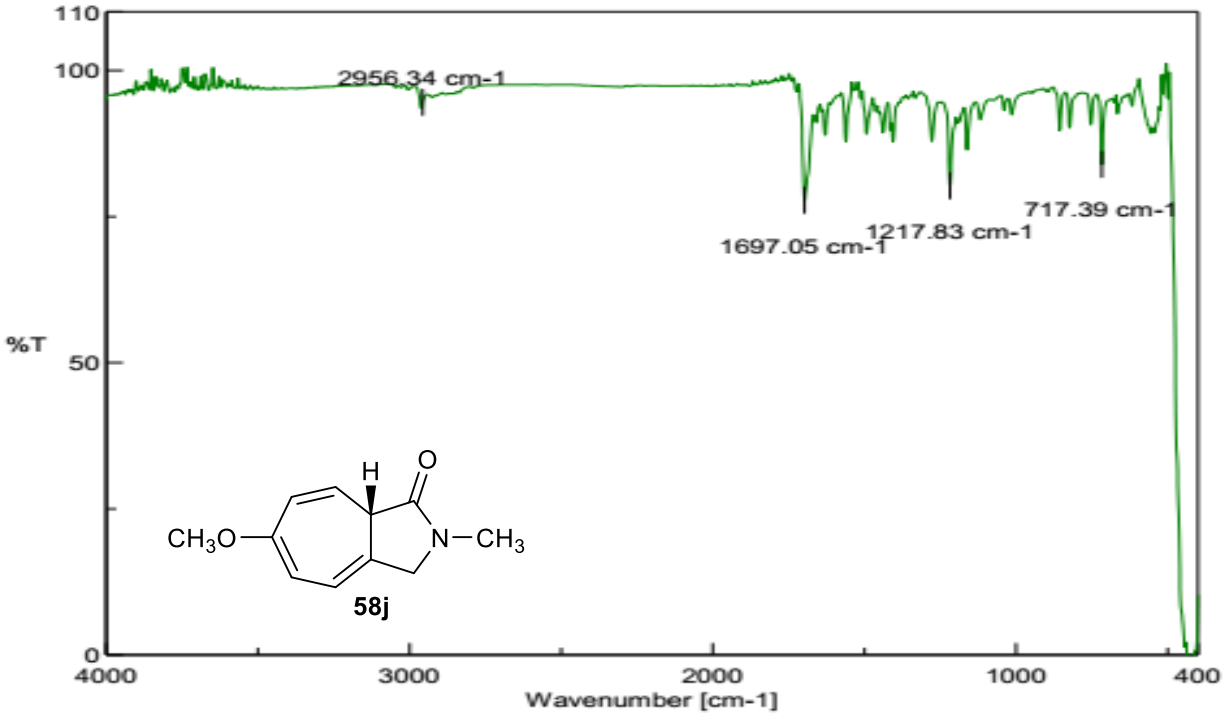

Figure 30. IR spectral of (*S*)-6-methoxy-2-methyl-3,8a-dihydrocyclohepta[c]pyrrol-1(2H)-one.

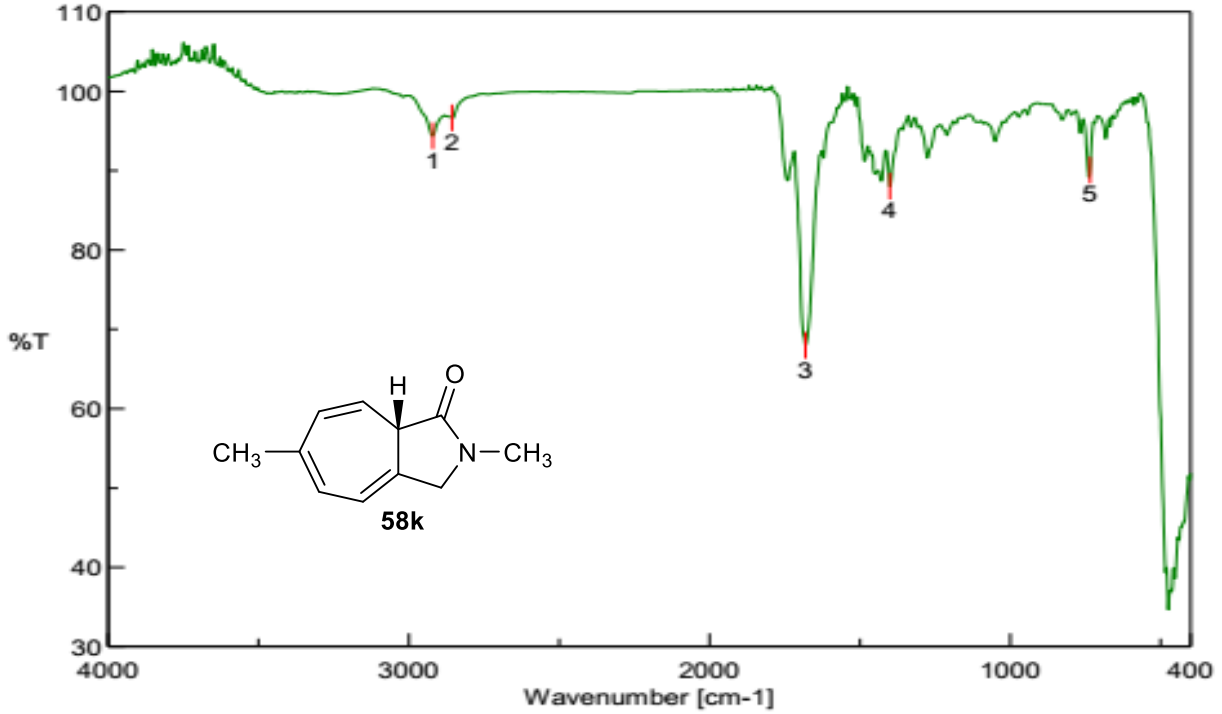

Figure 31. IR spectral of (*S*)-2,6-dimethyl-3,8a-dihydrocyclohepta[c]pyrrol-1(2H)-one.

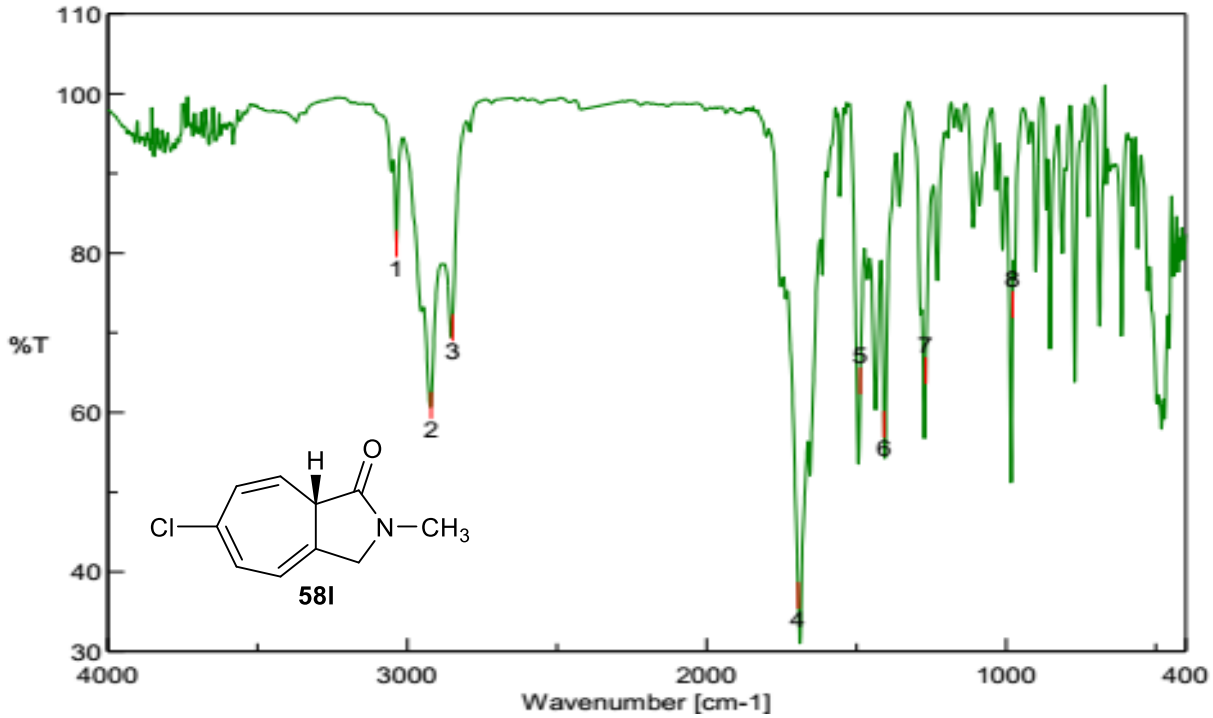

Figure 32. IR spectral of (*S*)-6-chloro-2-methyl-3,8a-dihydrocyclohepta[c]pyrrol-1(2H)-one.

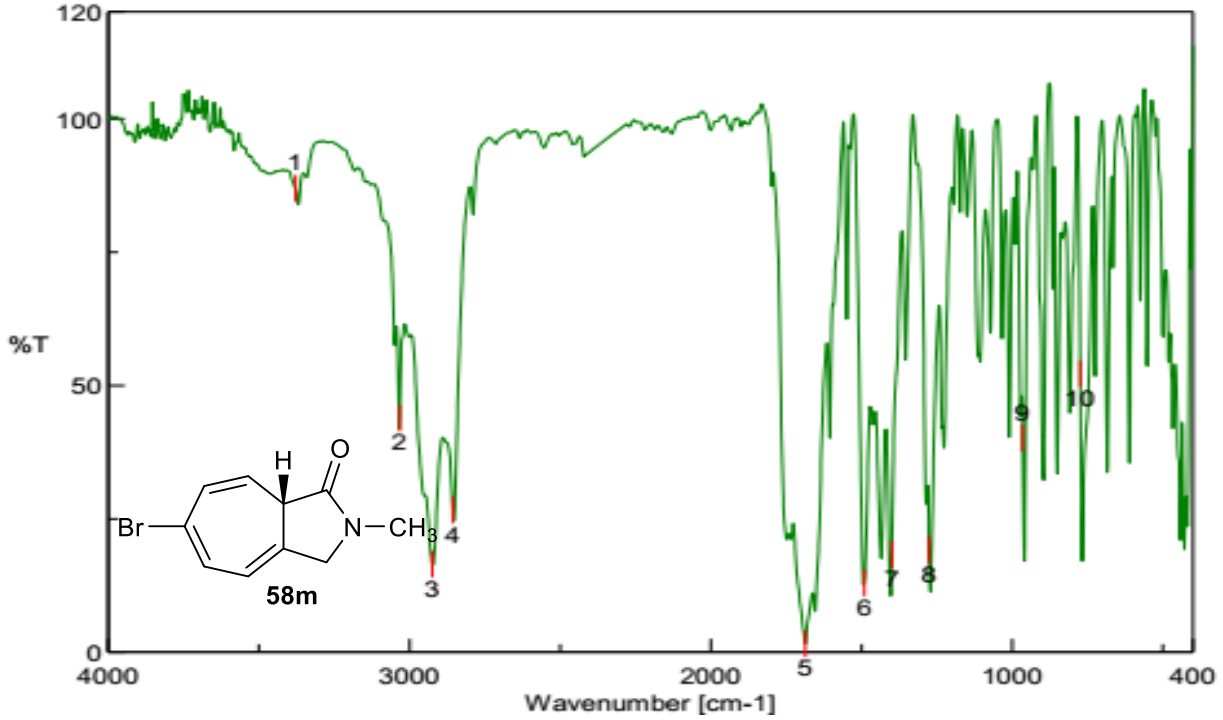

Figure 33. IR spectral of (*S*)-6-bromo-2-methyl-3,8a-dihydrocyclohepta[c]pyrrol-1(2H)-one.

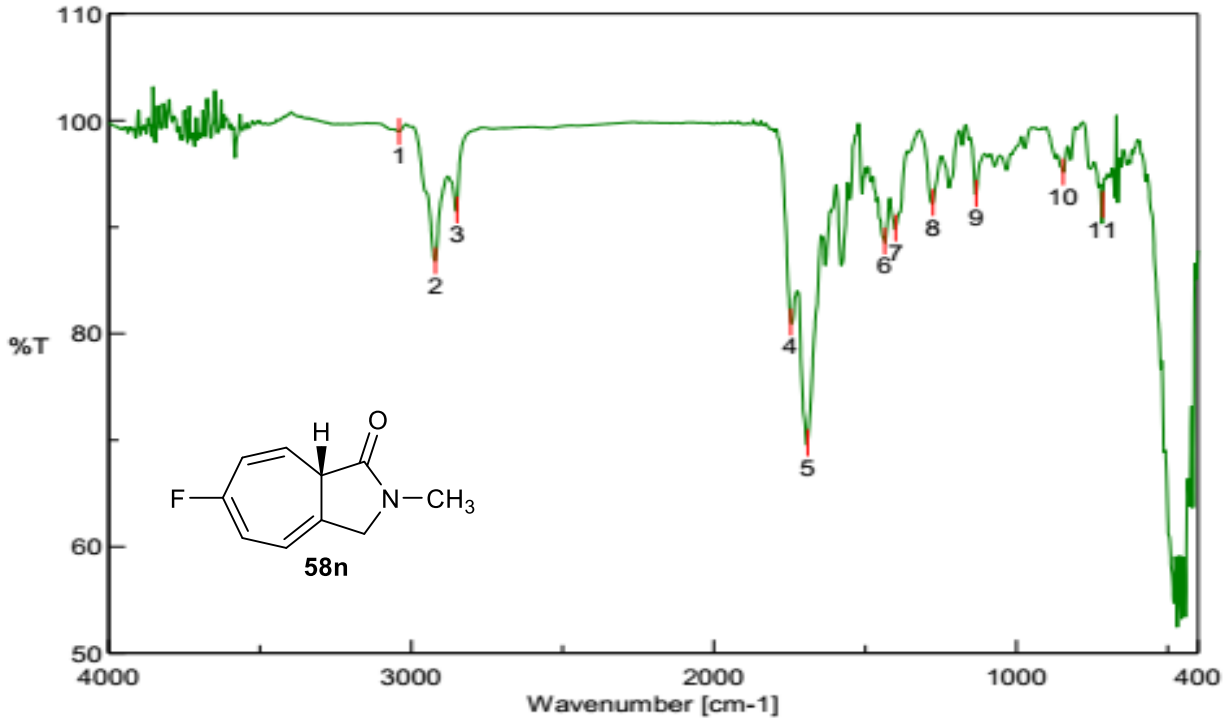

Figure 34. IR spectral of (*S*)-6-fluoro-2-methyl-3,8a-dihydrocyclohepta[c]pyrrol-1(2H)-one.

NMR SPECTRAL DATA

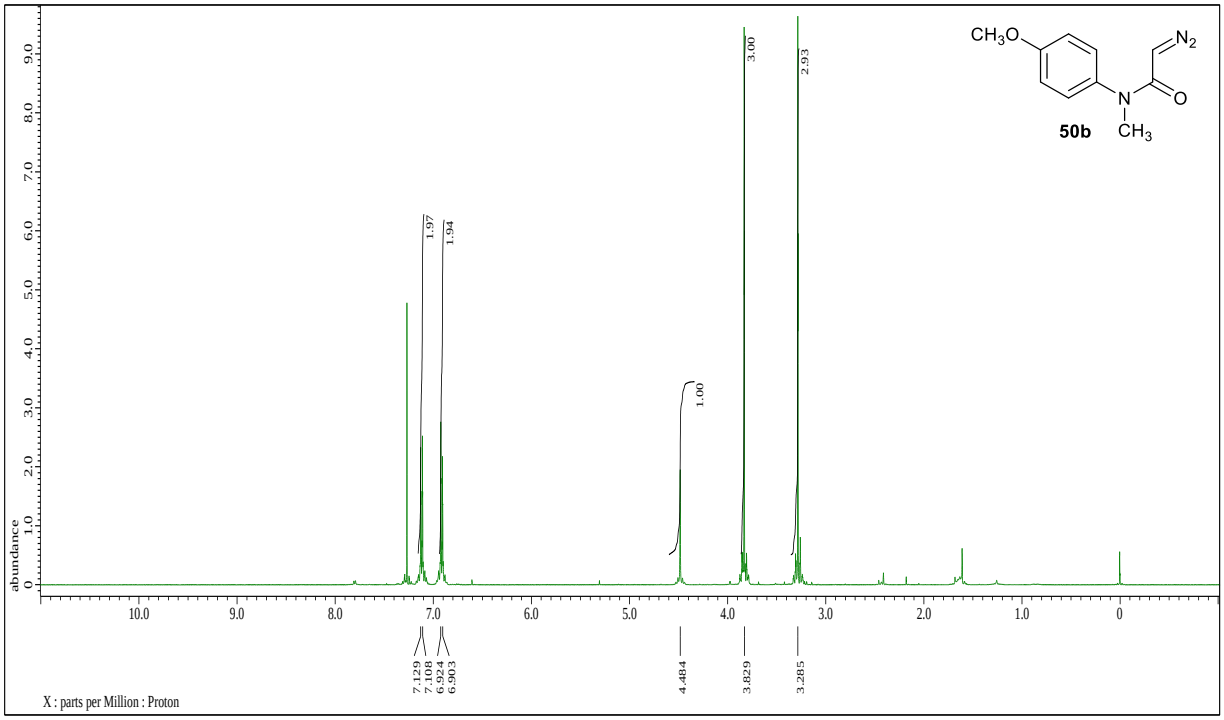

Figure 35. ^{1}HNMR spectral of 2-diazo-*N*-(4-methoxyphenyl)-*N*-methylacetamide.

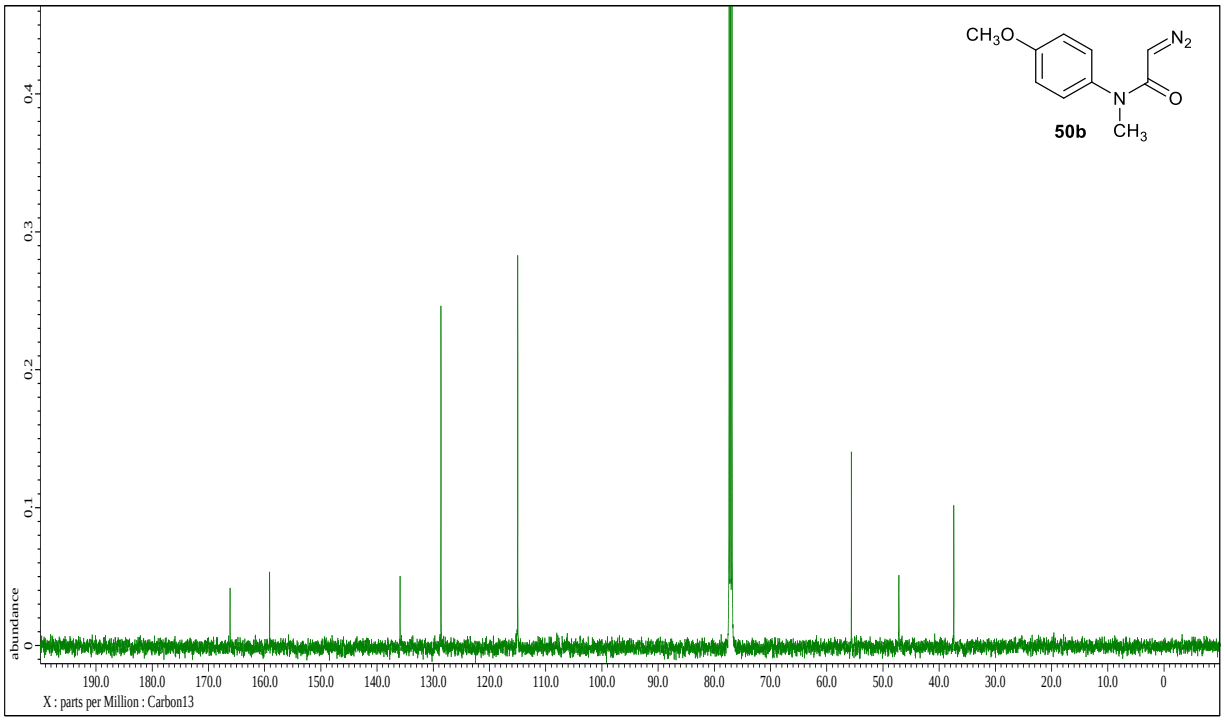

Figure 36. ^{13}CNMR spectral of 2-diazo-*N*-(4-methoxyphenyl)-*N*-methylacetamide.

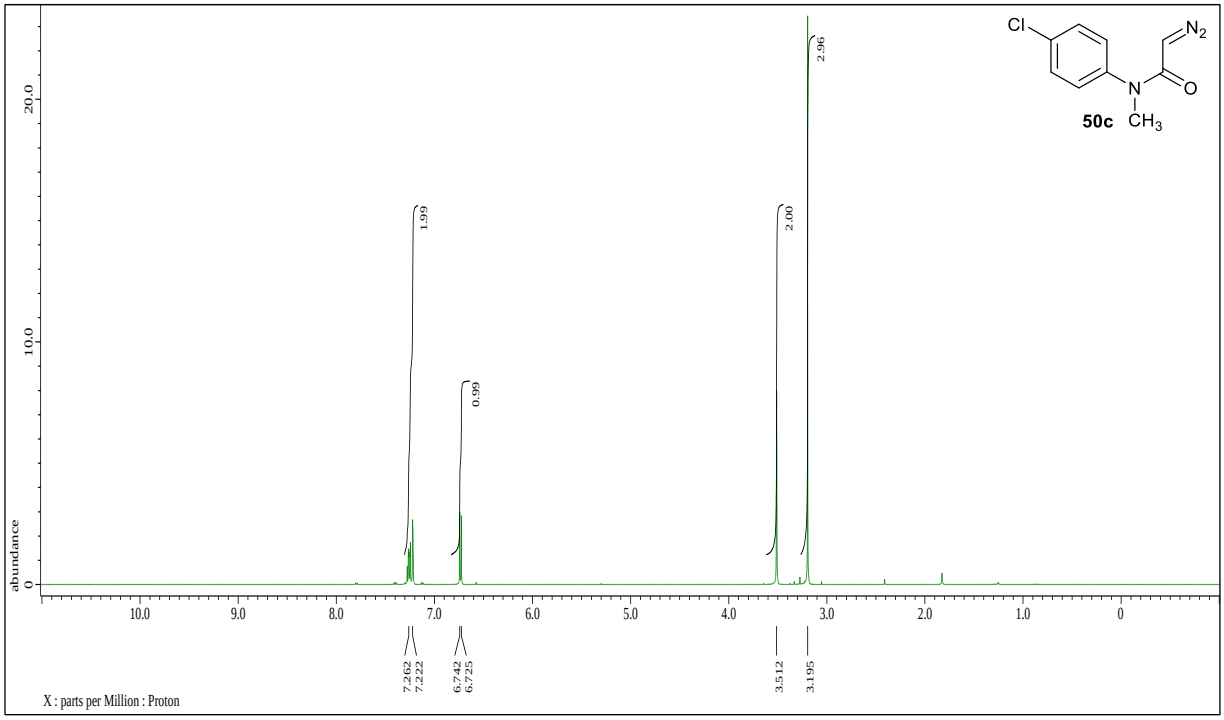

Figure 37. ^{1}HNMR spectral of 2-diazo-*N*-(4-chlorophenyl)-*N*-methylacetamide**.**

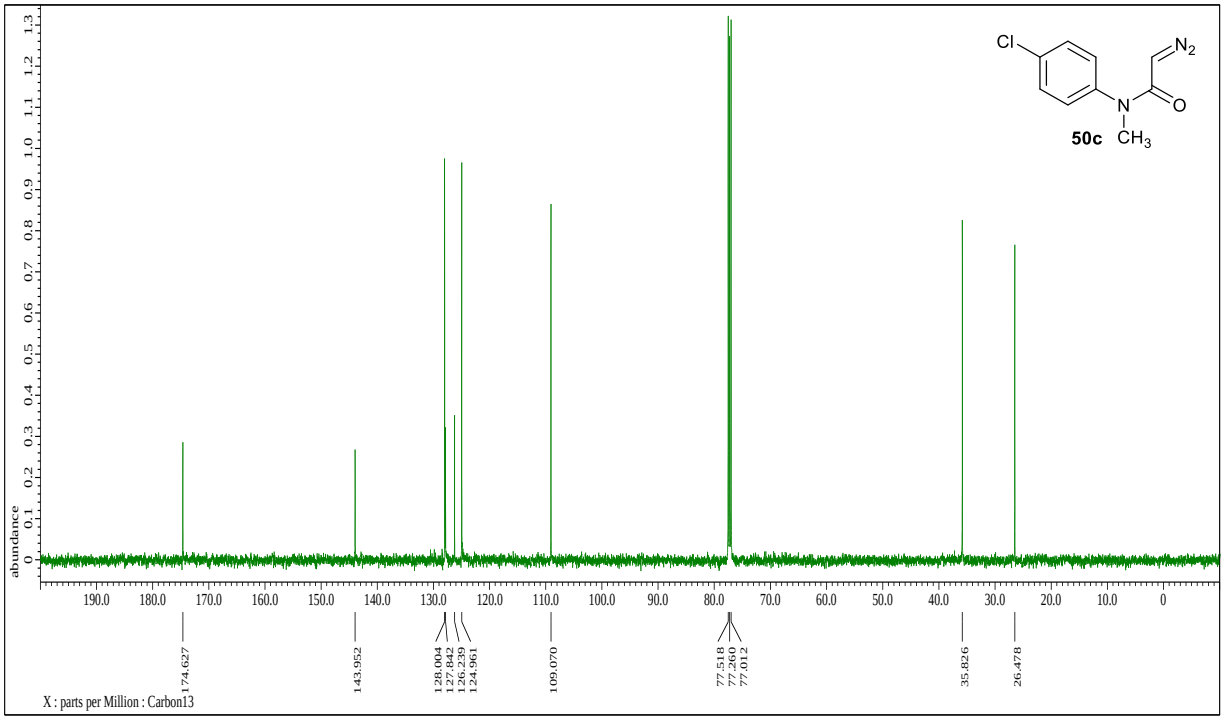

Figure 38. ^{13}CNMR spectral of 2-diazo-*N*-(4-chlorophenyl)-*N*-methylacetamide.

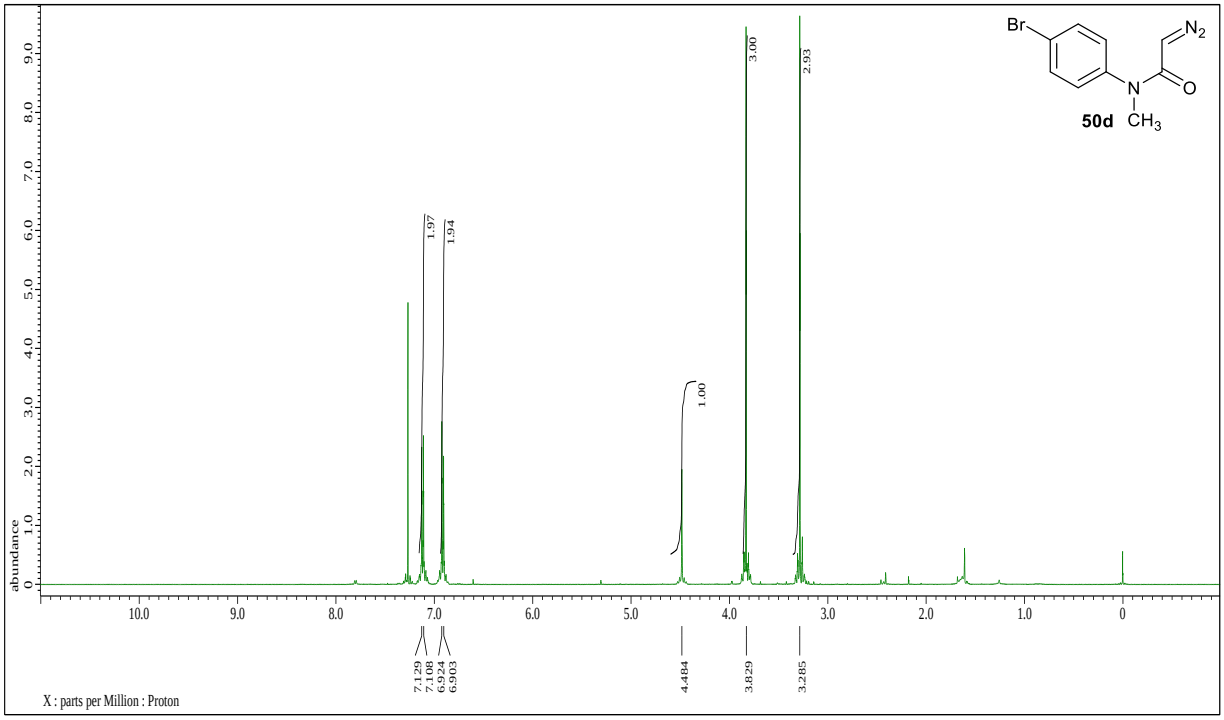

Figure 39. ^{1}HNMR spectral of 2-diazo-*N*-(4-bromophenyl)-*N*-methylacetamide.

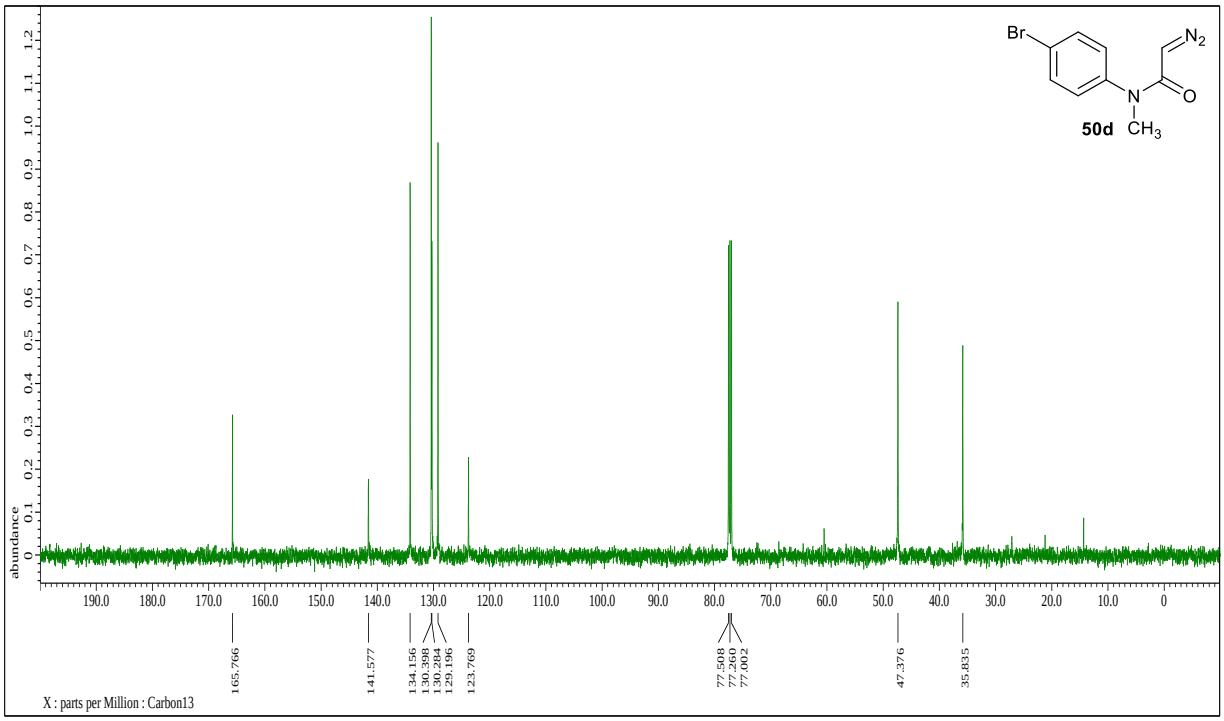

Figure 40. ^{13}CNMR spectral of 2-diazo-*N*-(4-bromophenyl)-*N*-methylacetamide.

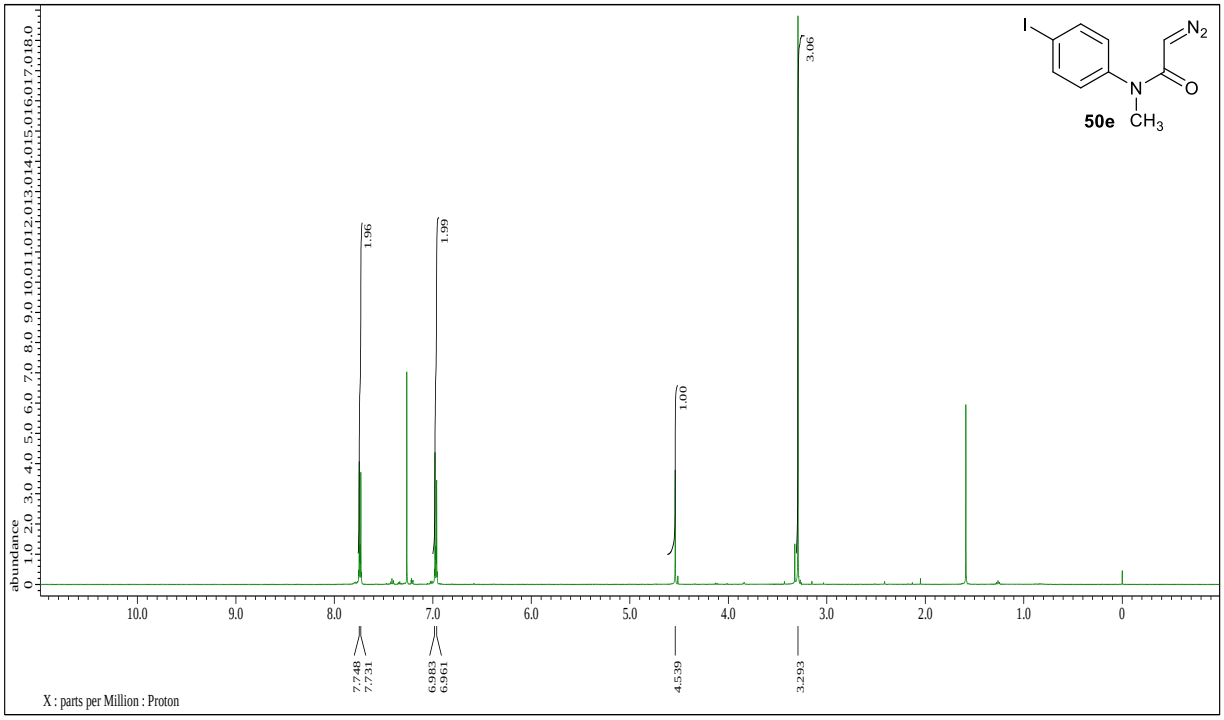

Figure 41. ^{1}HNMR spectral of 2-diazo-*N*-(4-iodophenyl)-*N*-methylacetamide.

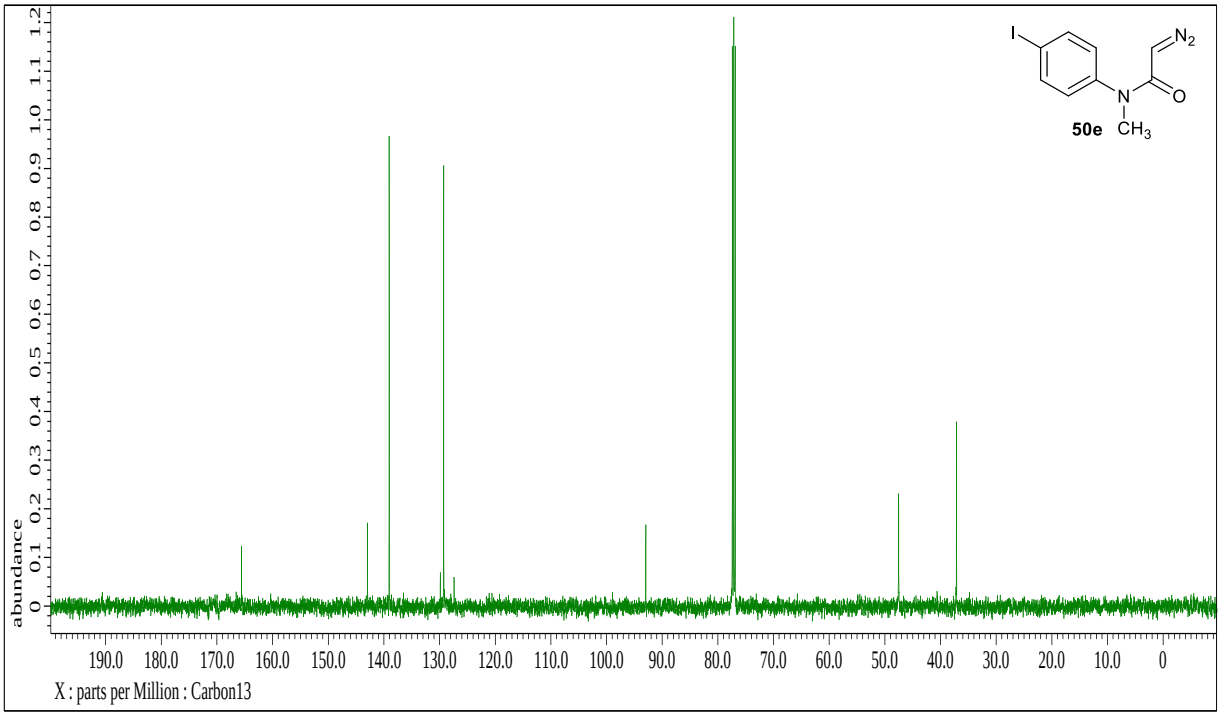

Figure 42. ^{13}CNMR spectral of 2-diazo-*N*-(4-iodophenyl)-*N*-methylacetamide.

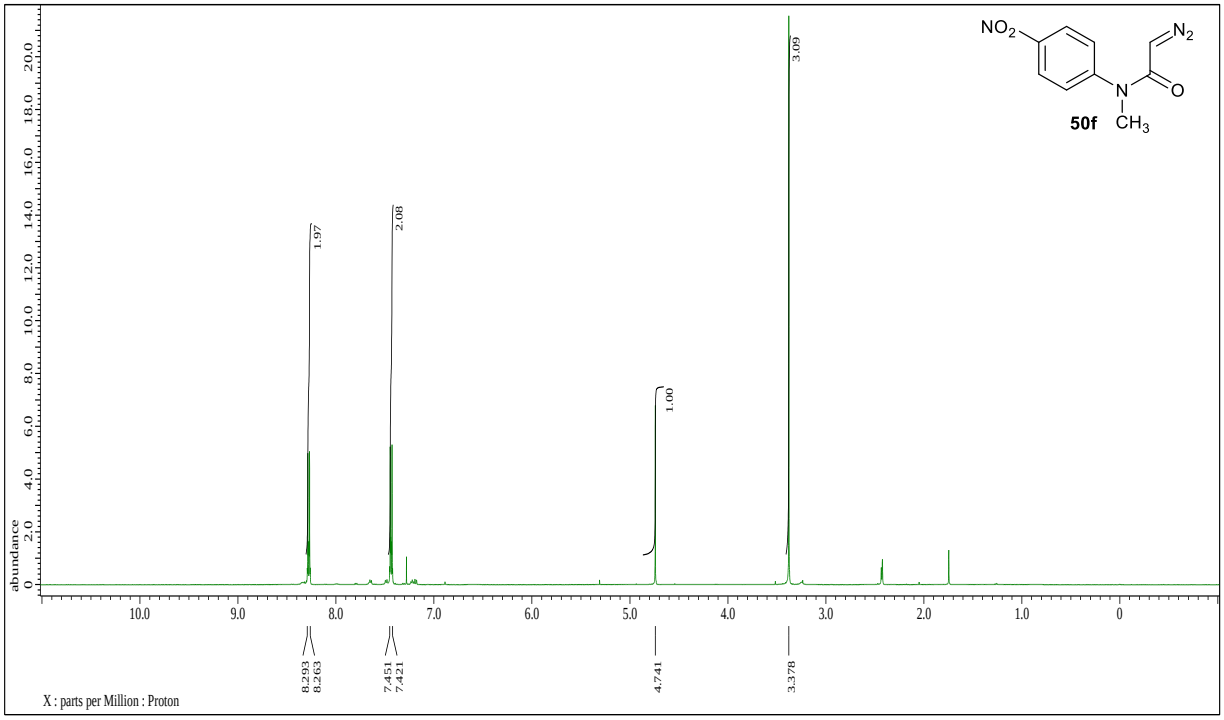

Figure 43. ^{1}HNMR spectral of 2-diazo-*N*-(4-nitrophenyl)-*N*-methylacetamide.

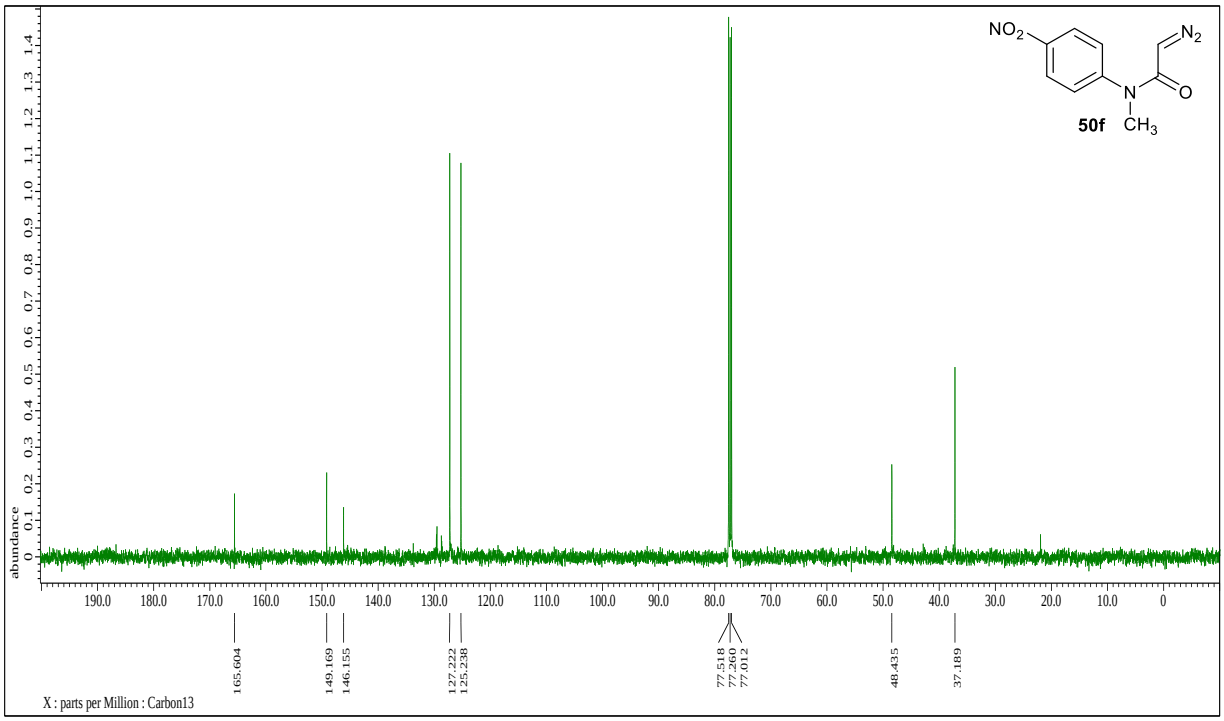

Figure 44. ^{13}CNMR spectral of 2-diazo-*N*-(4-nitrophenyl)-*N*-methylacetamide.

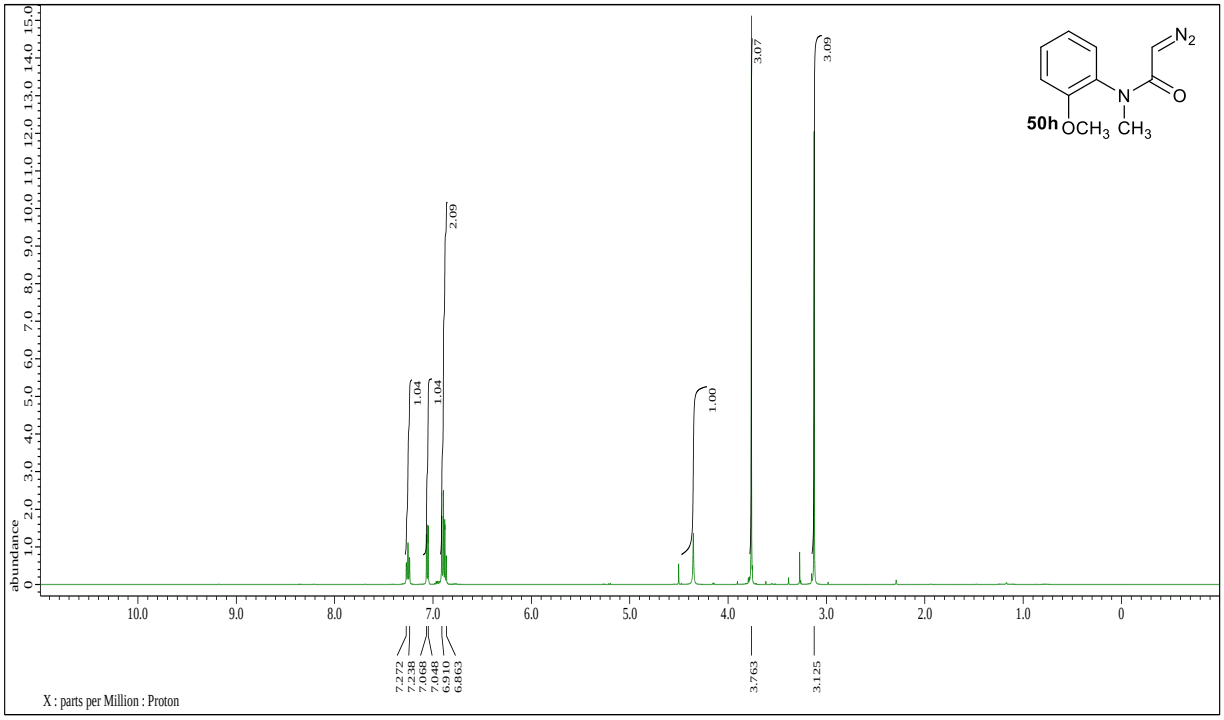

Figure 45. ^{1}HNMR spectral of 2-diazo-*N*-(2-methoxyphenyl)-*N*-methylacetamide.

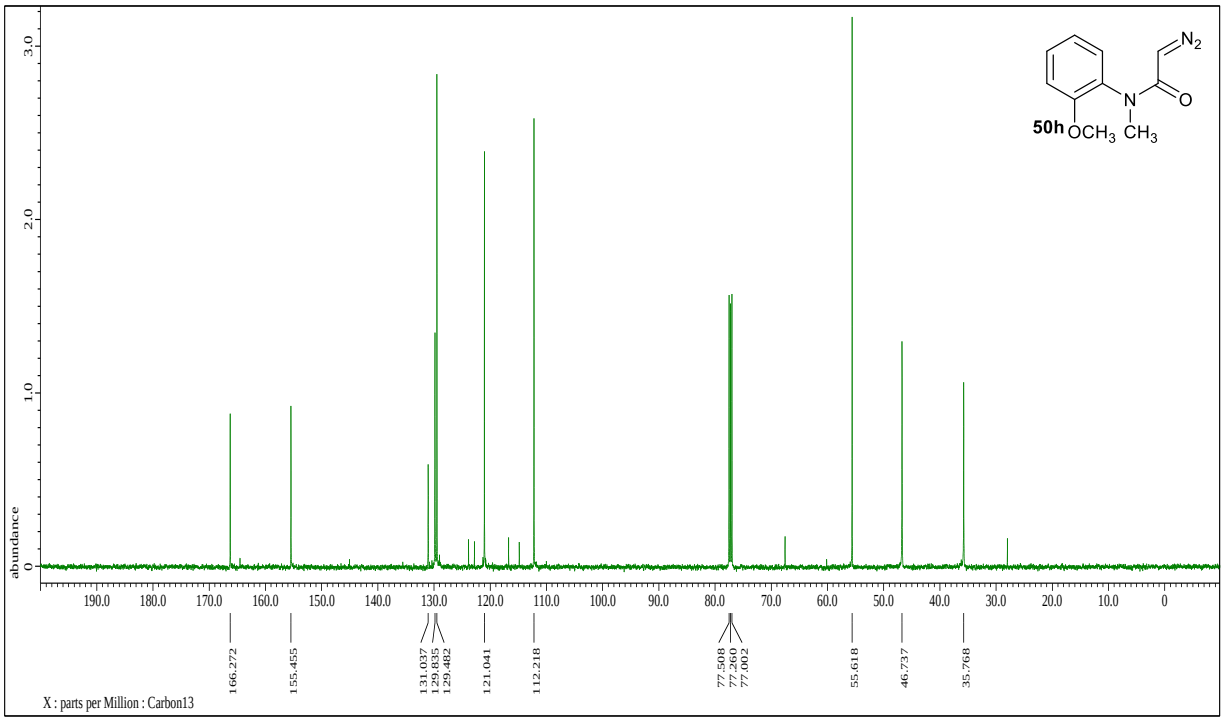

Figure 46. ^{13}CNMR spectral of 2-diazo-*N*-(2-methoxyphenyl)-*N*-methylacetamide.

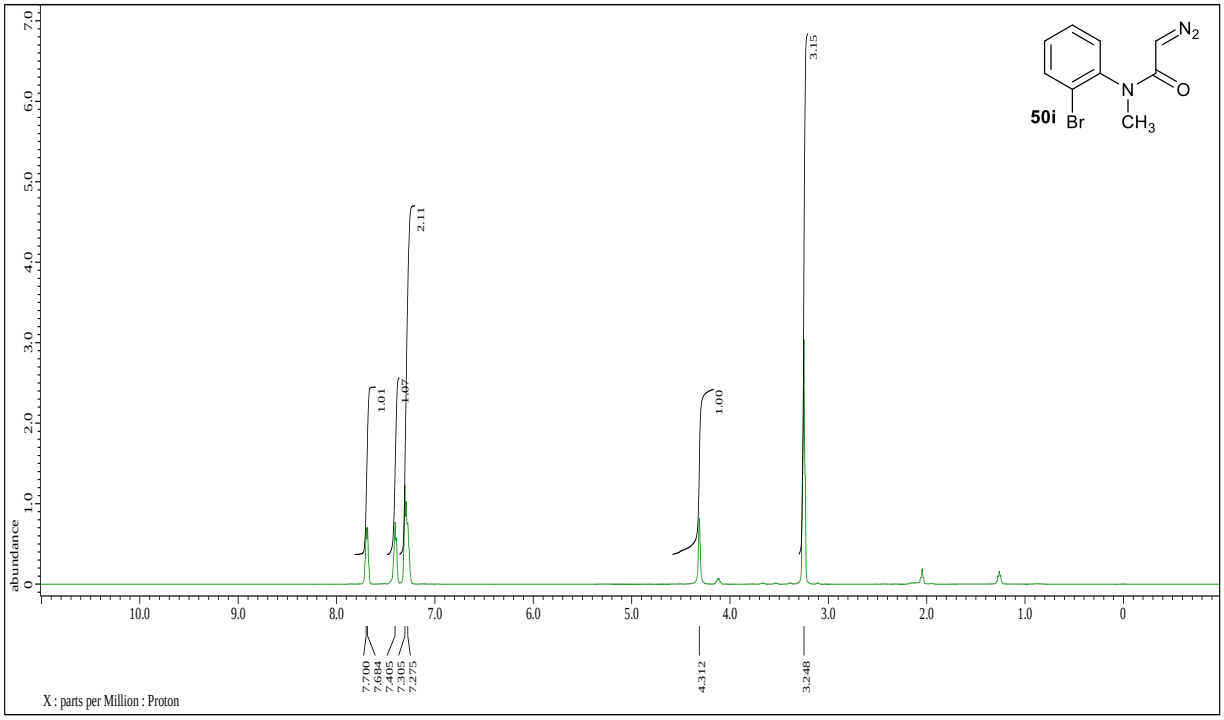

Figure 47. ^{1}HNMR spectral of 2-diazo-*N*-(2-bromophenyl)-*N*-methylacetamide.

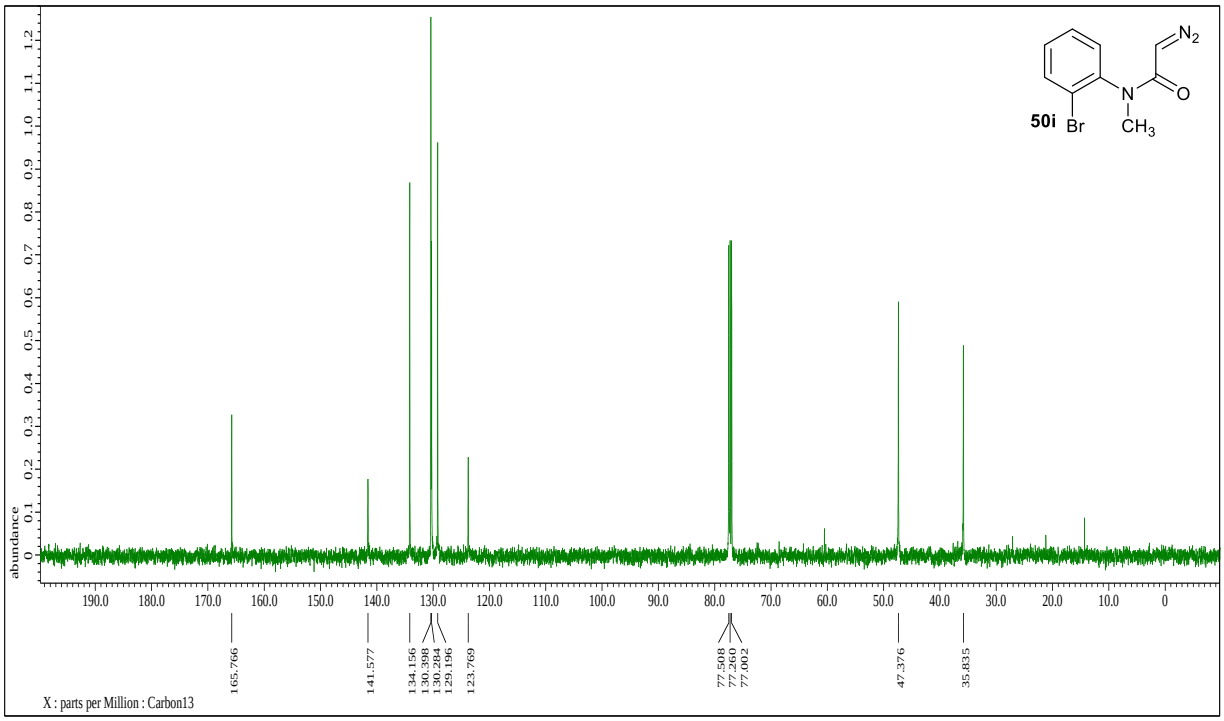

Figure 48. ^{13}CNMR spectral of 2-diazo-*N*-(2-bromophenyl)-*N*-methylacetamide.

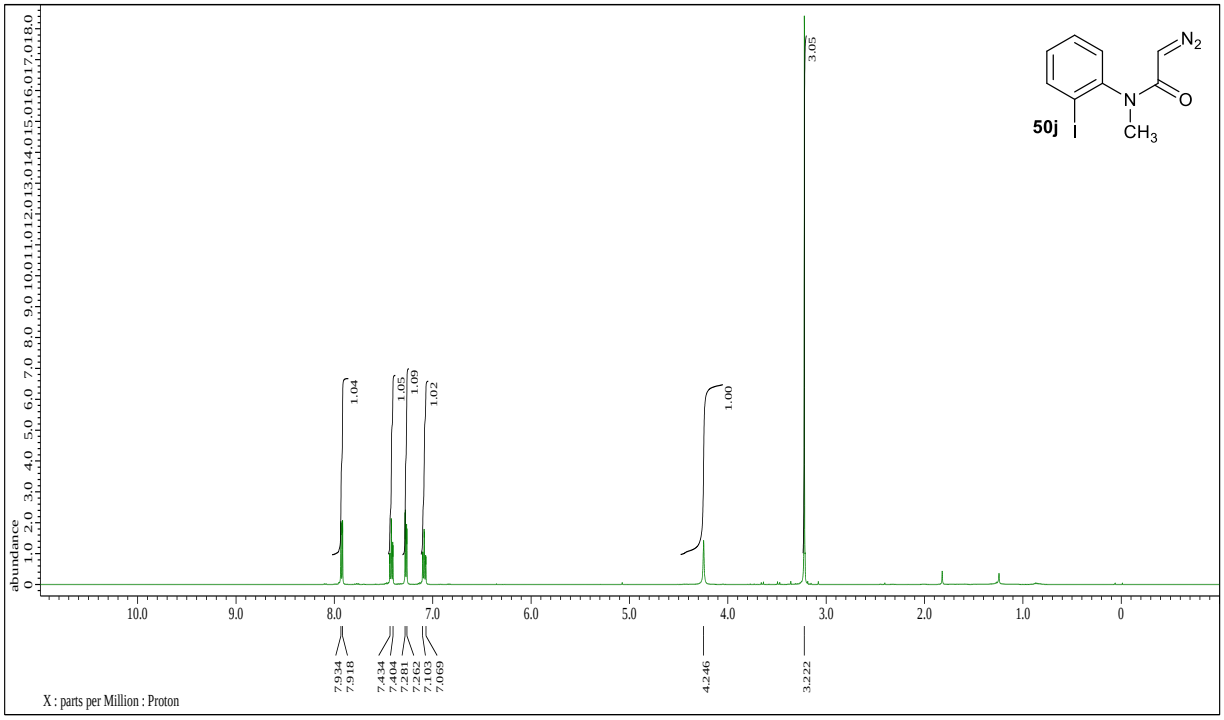

Figure 49. ^{1}HNMR spectral of 2-diazo-*N*-(2-iodophenyl)-*N*-methylacetamide.

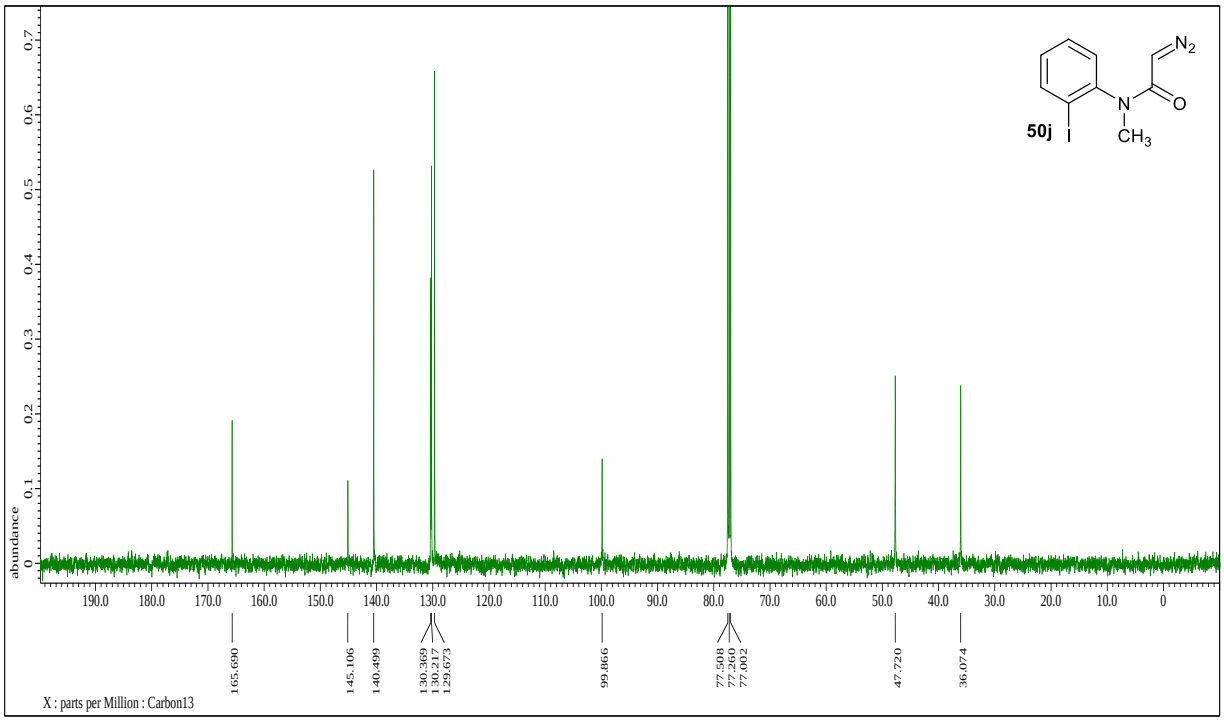

Figure 50. ^{13}CNMR spectral of 2-diazo-*N*-(2-iodophenyl)-*N*-methylacetamide.

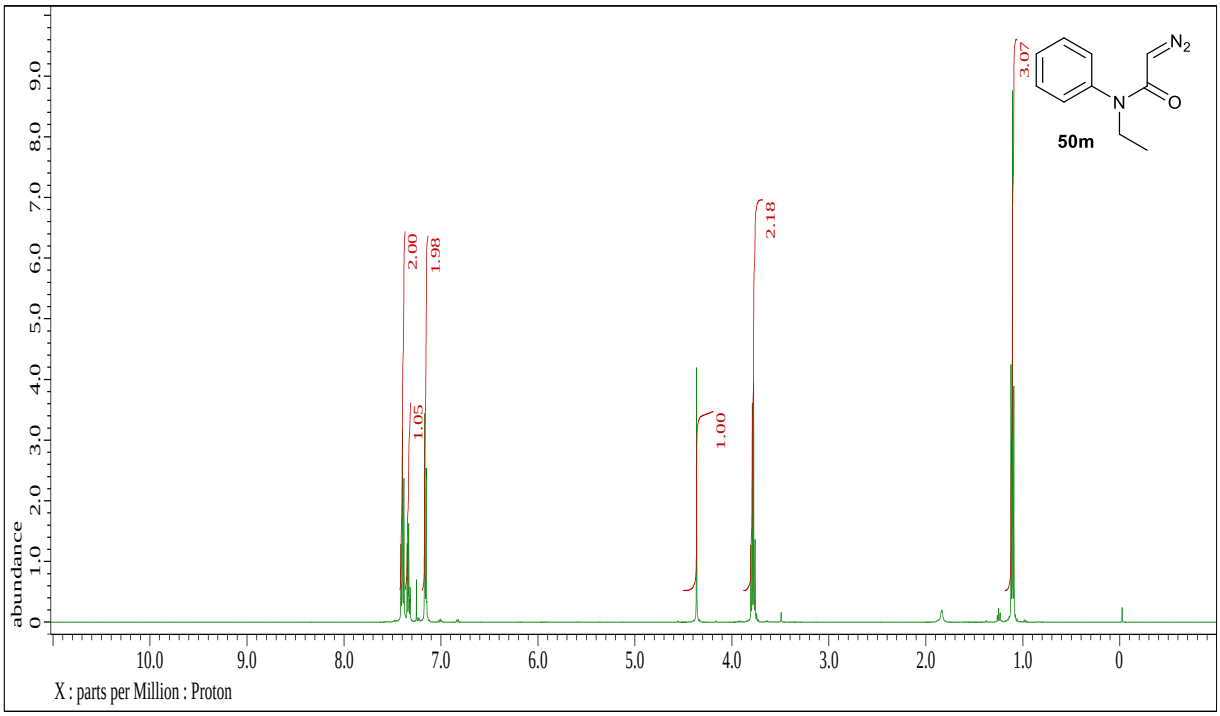

Figure 51. ^{1}HNMR spectral of 2-diazo-*N*-ethyl-*N*-phenylacetamide.

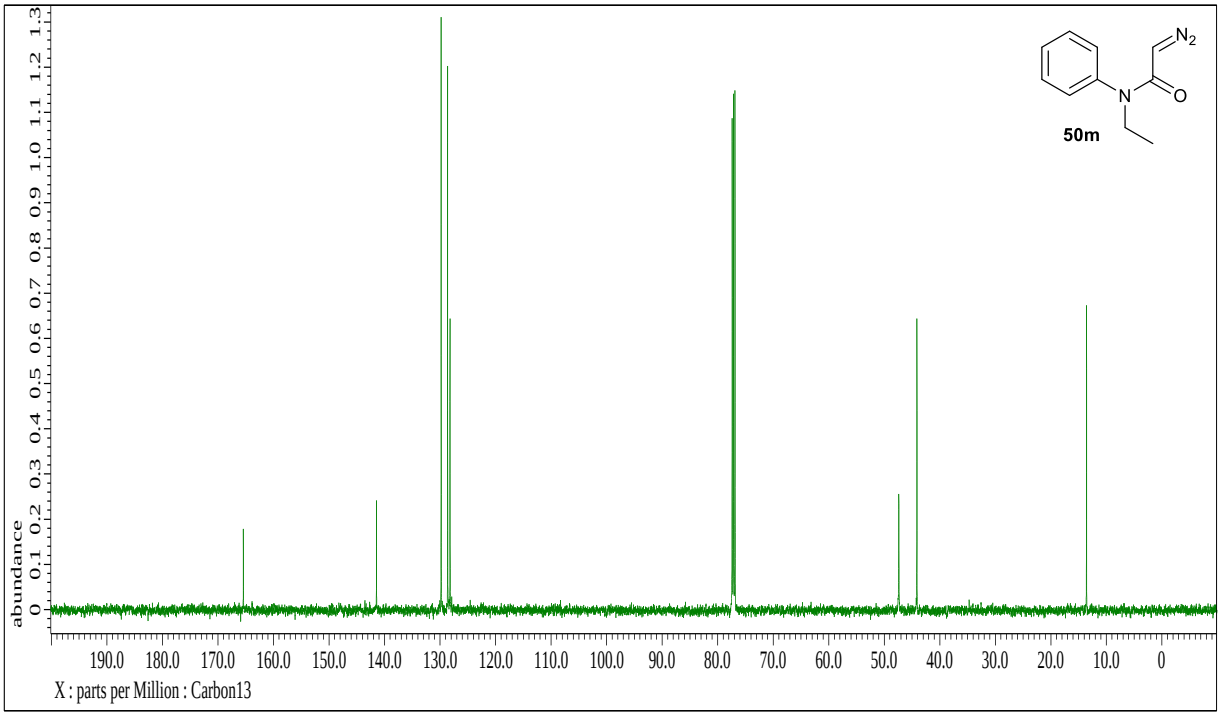

Figure 52. ^{13}CNMR spectral of 2-diazo-*N*-ethyl-*N*-phenylacetamide.

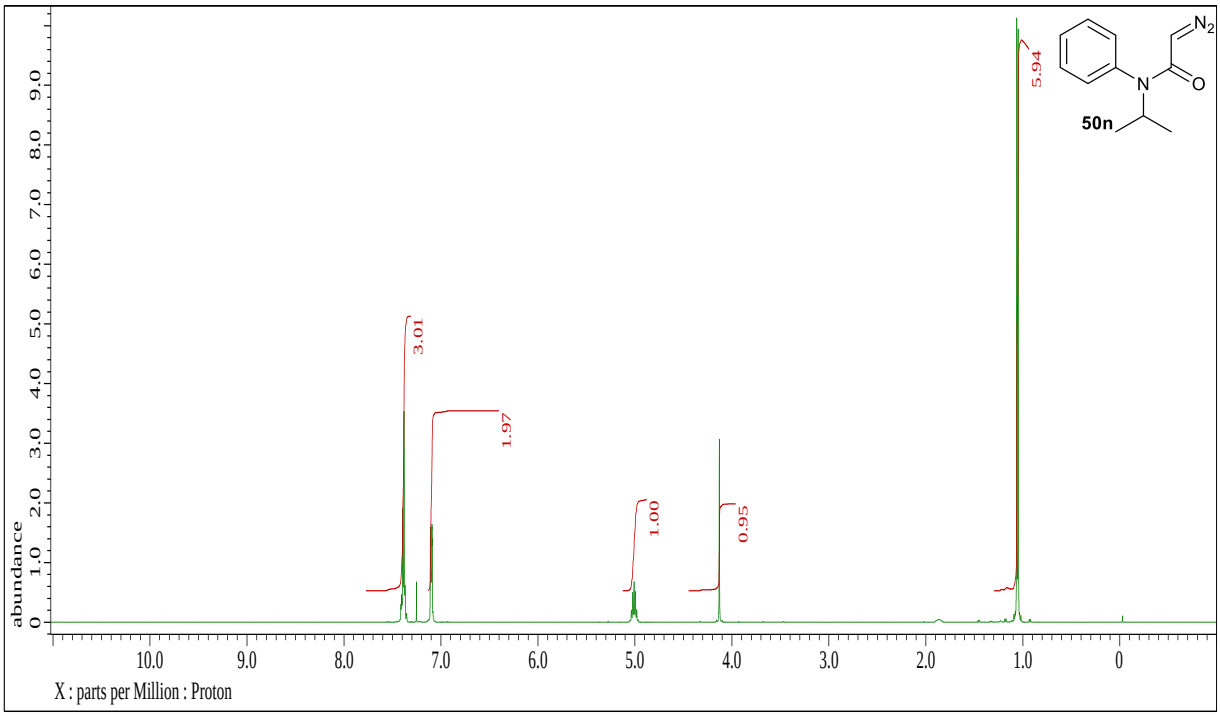

Figure 53. ^{1}HNMR spectral of 2-diazo-*N*-isopropyl-*N*-phenylacetamide.

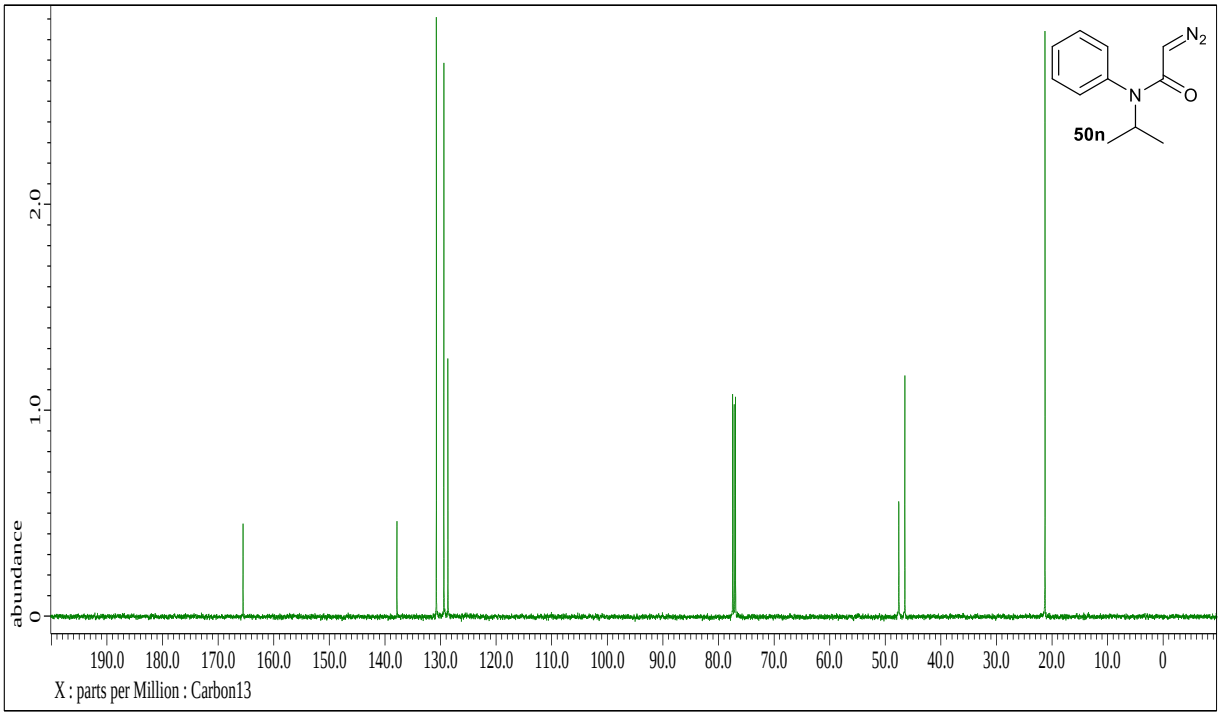

Figure 54. ^{13}CNMR spectral of 2-diazo-*N*-isopropyl-*N*-phenylacetamide.

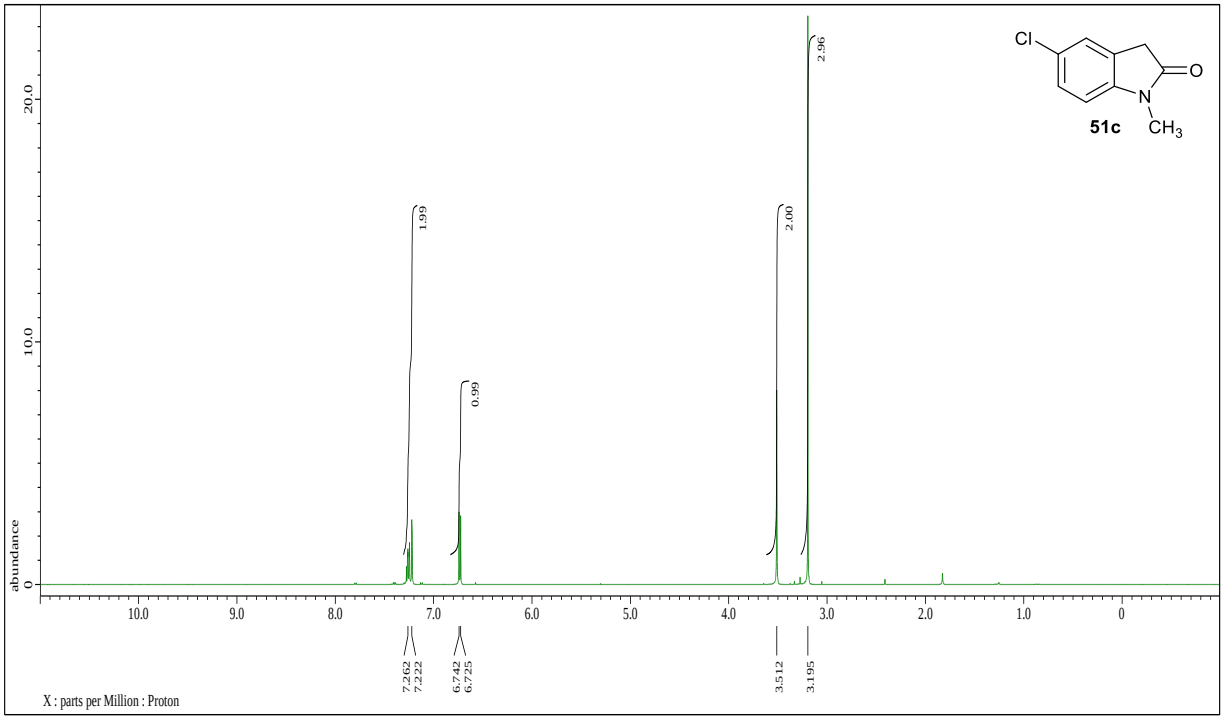

Figure 55. ^{1}HNMR spectral of 5-chloro-1-methylindolin-2-one.

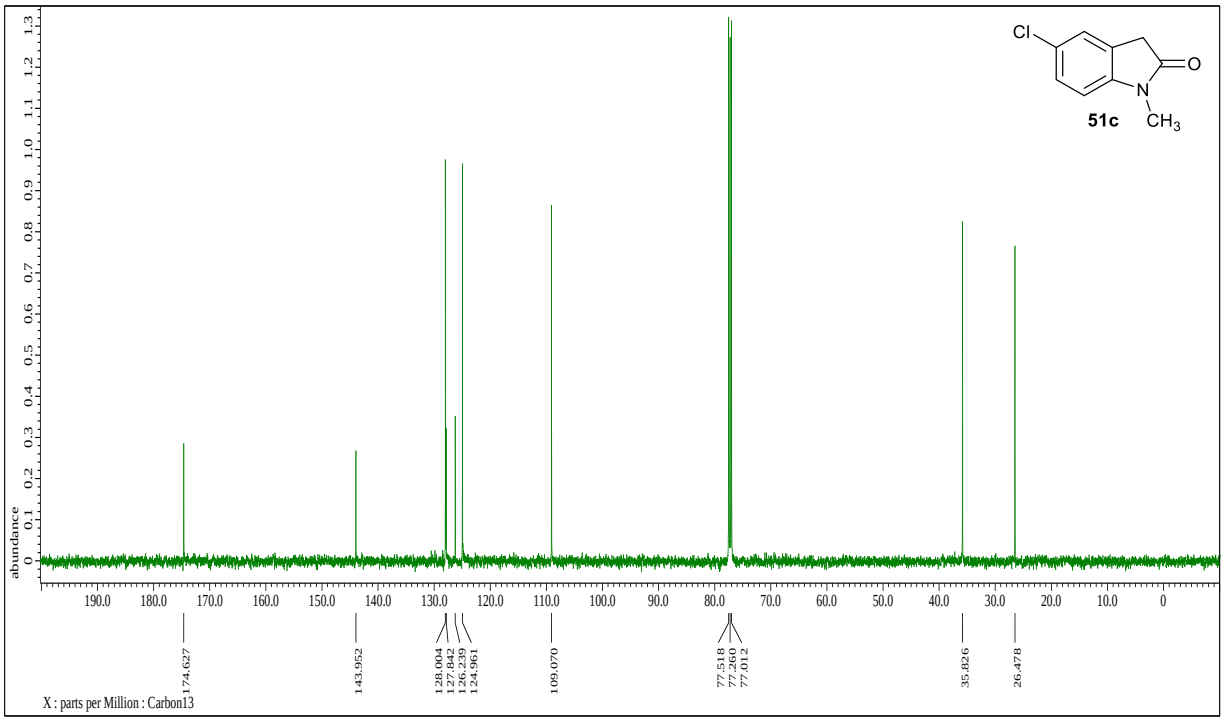

Figure 56. ^{13}CNMR spectral of 5-chloro-1-methylindolin-2-one.

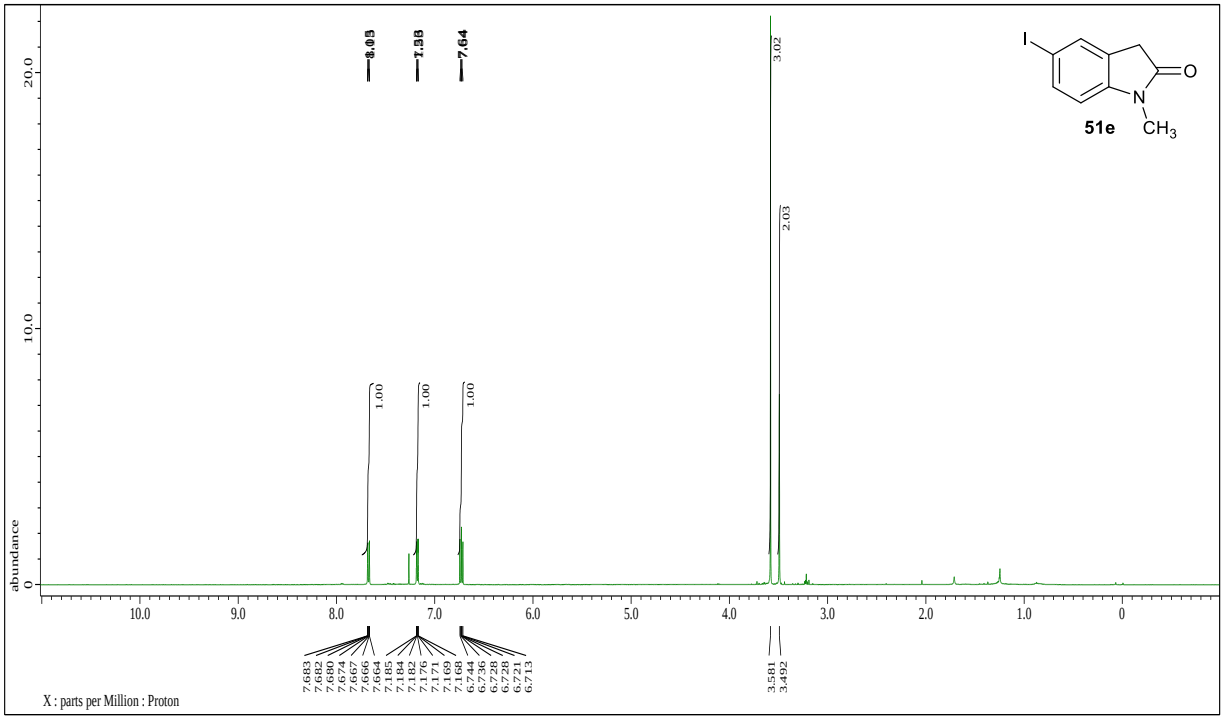

Figure 57. ^{1}HNMR spectral of 5-iodo-1-methylindolin-2-one.

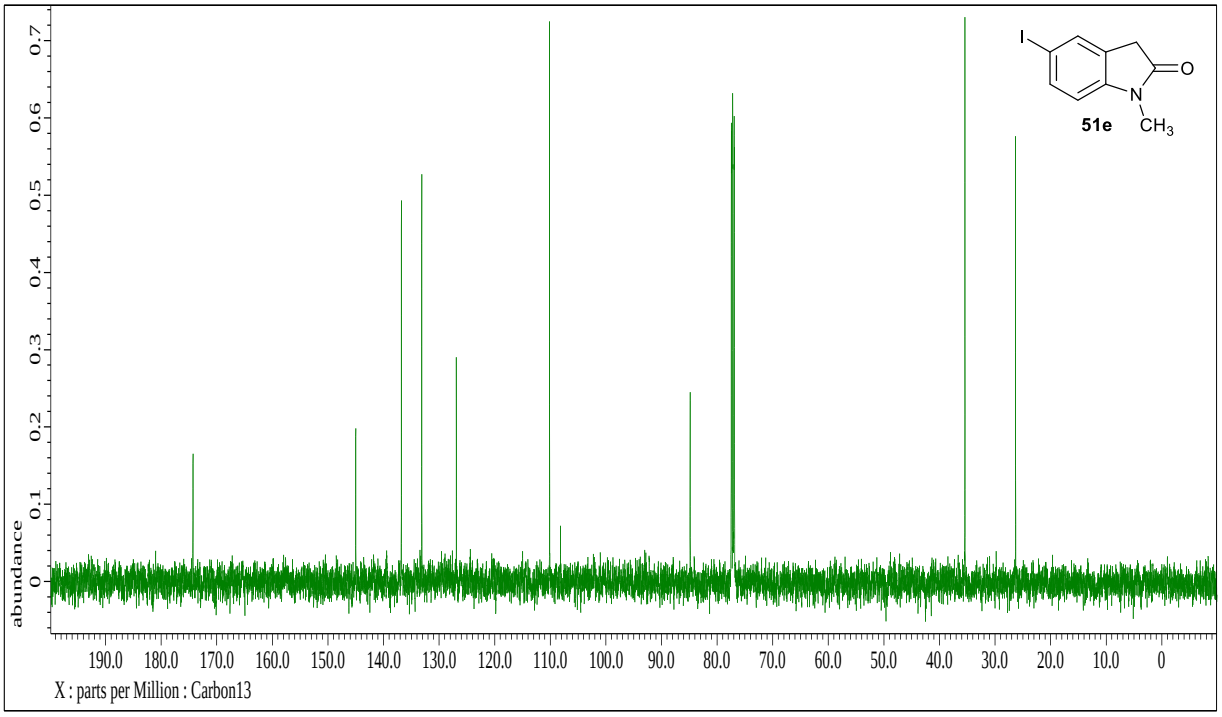

Figure 58. ^{13}CNMR spectral of 5-iodo-1-methylindolin-2-one.

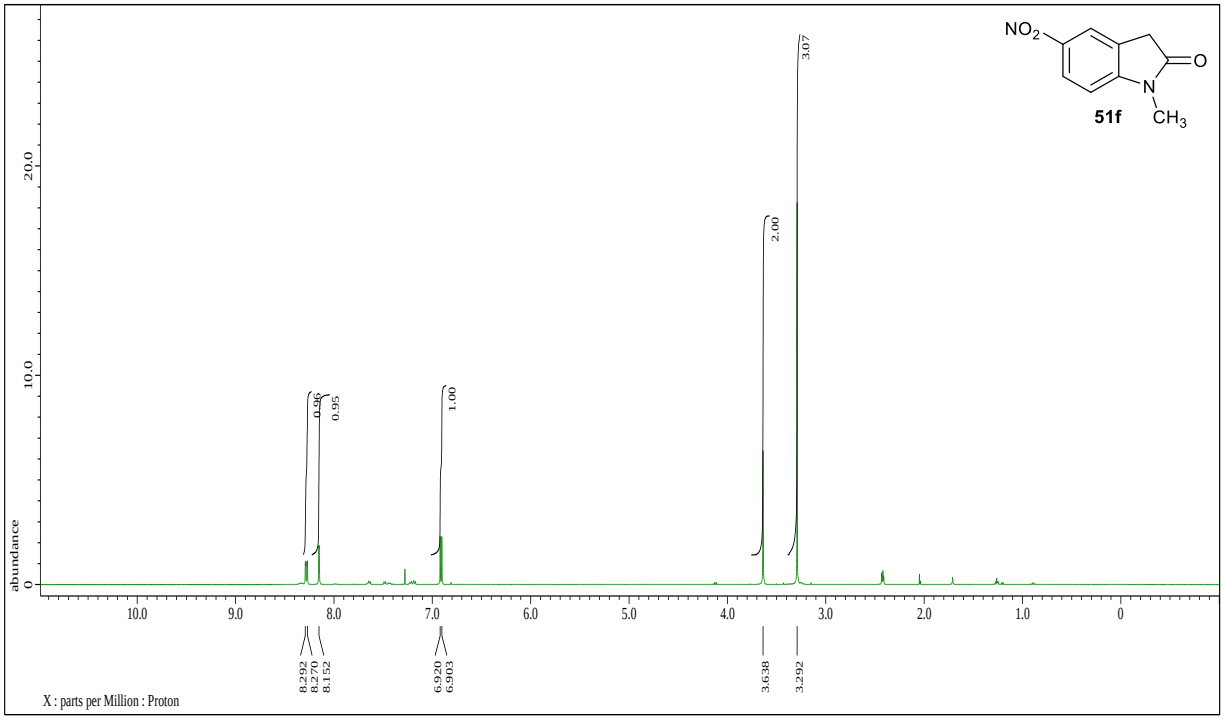

Figure 59. ^{1}HNMR spectral of 5-nitro-1-methylindolin-2-one.

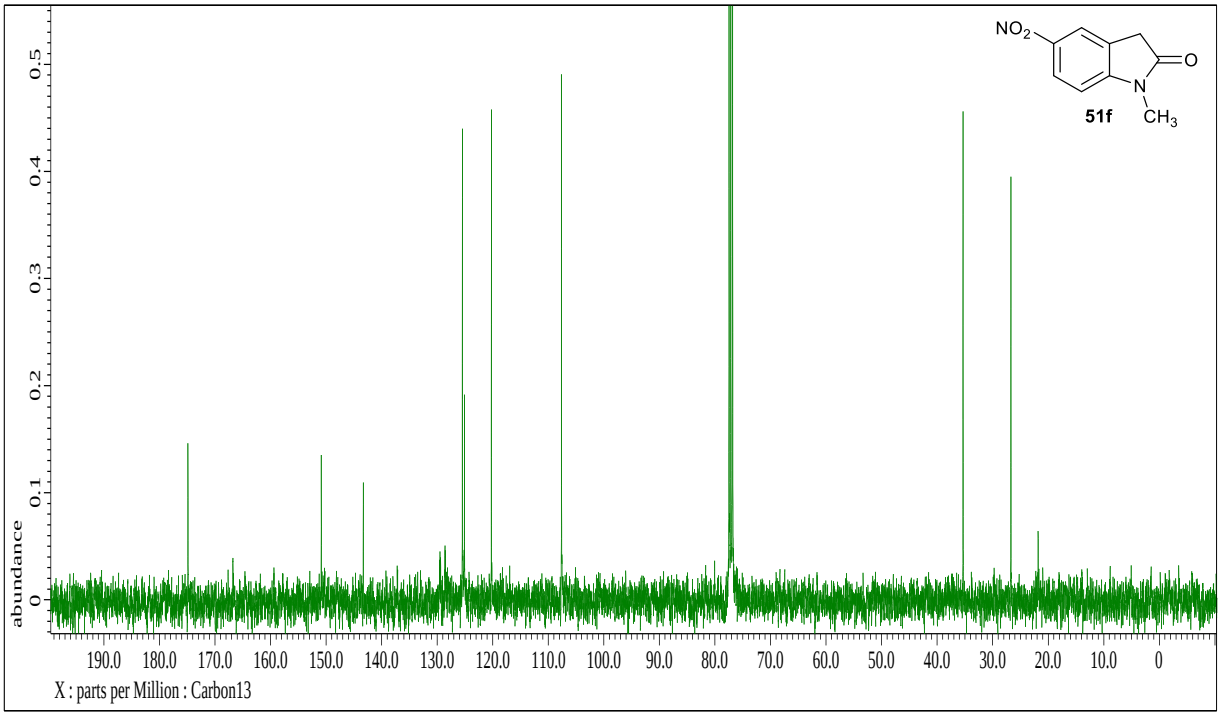

Figure 60. ^{13}CNMR spectral of 5-nitro-1-methylindolin-2-one.

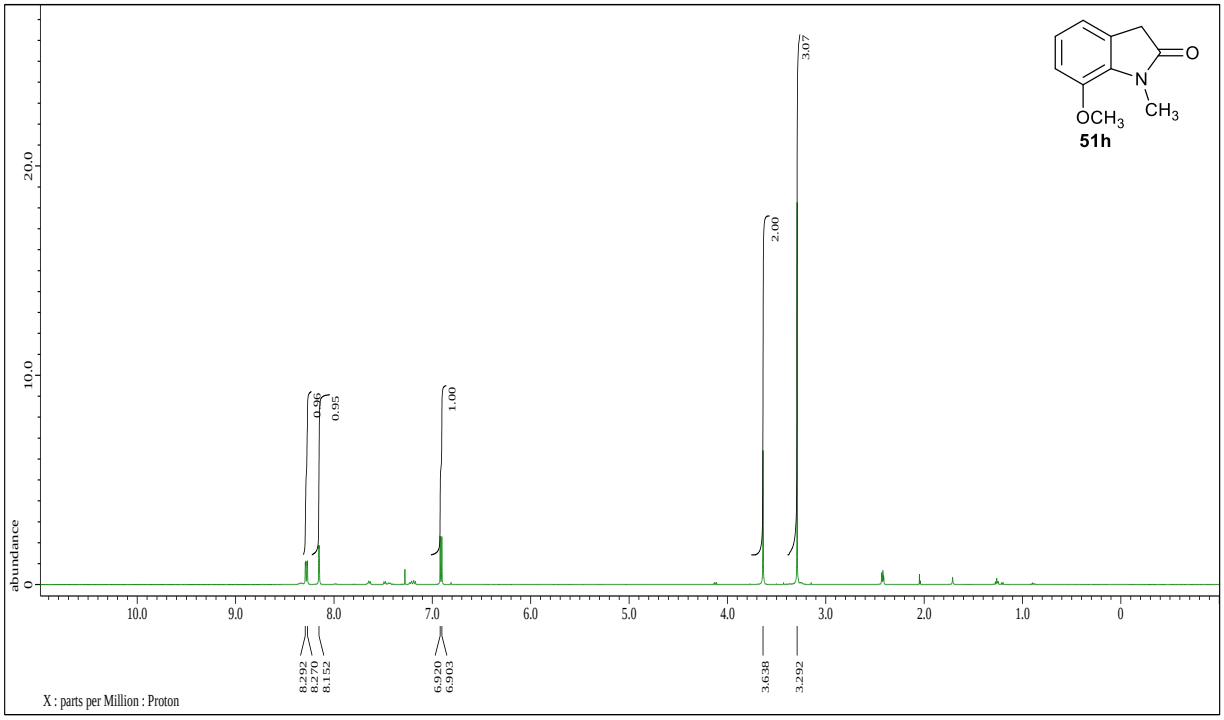

Figure 61. ^{1}HNMR spectral of 7-methoxy-1-methylindolin-2-one.

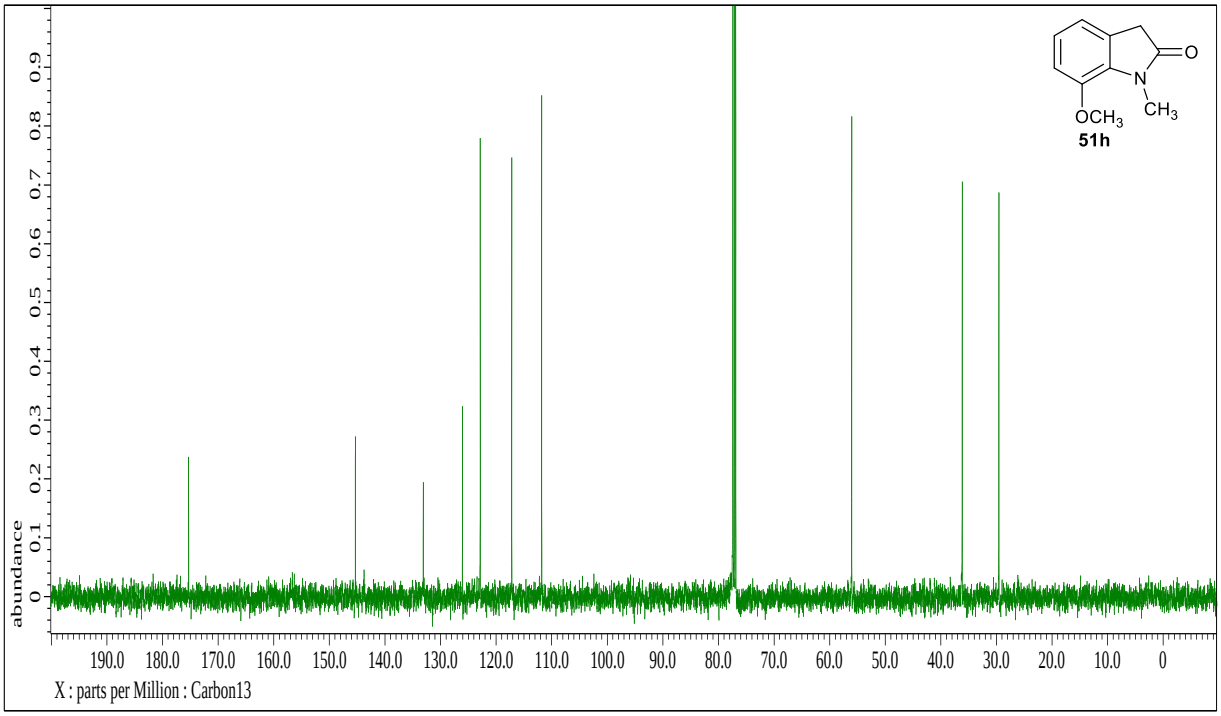

Figure 62. ^{13}CNMR spectral of 7-methoxy-1-methylindolin-2-one.

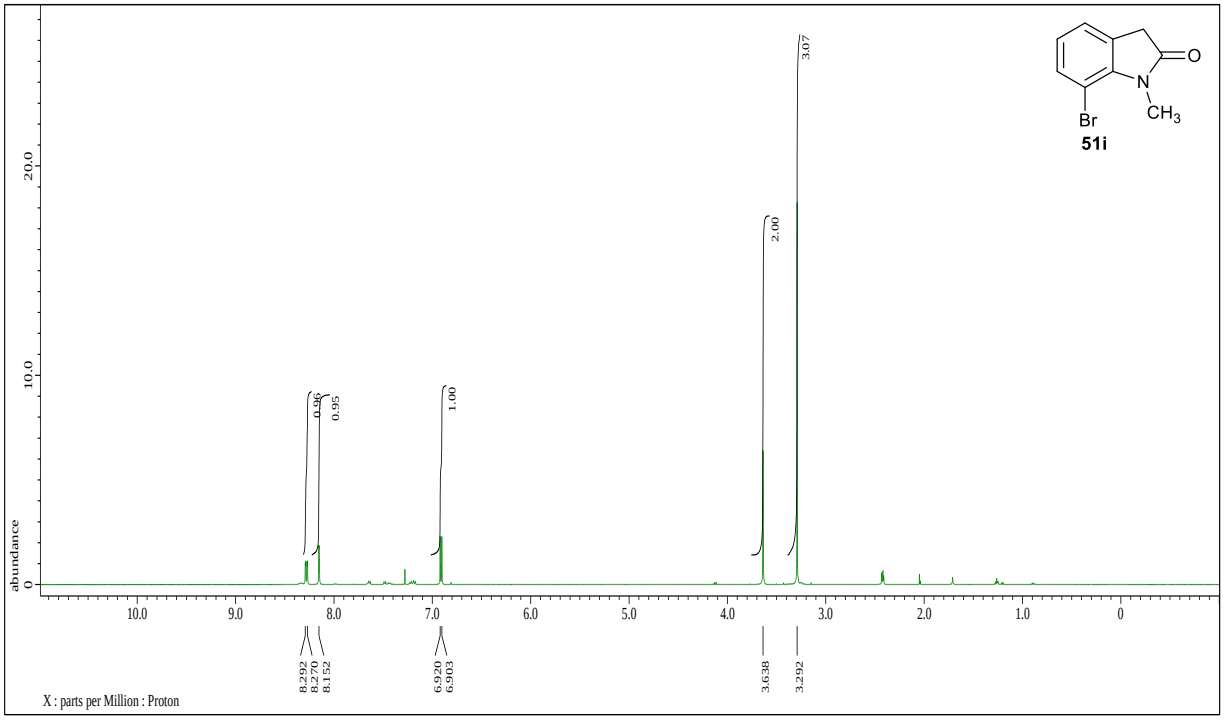

Figure 63. ^{1}HNMR spectral of 7-bromo-1-methylindolin-2-one.

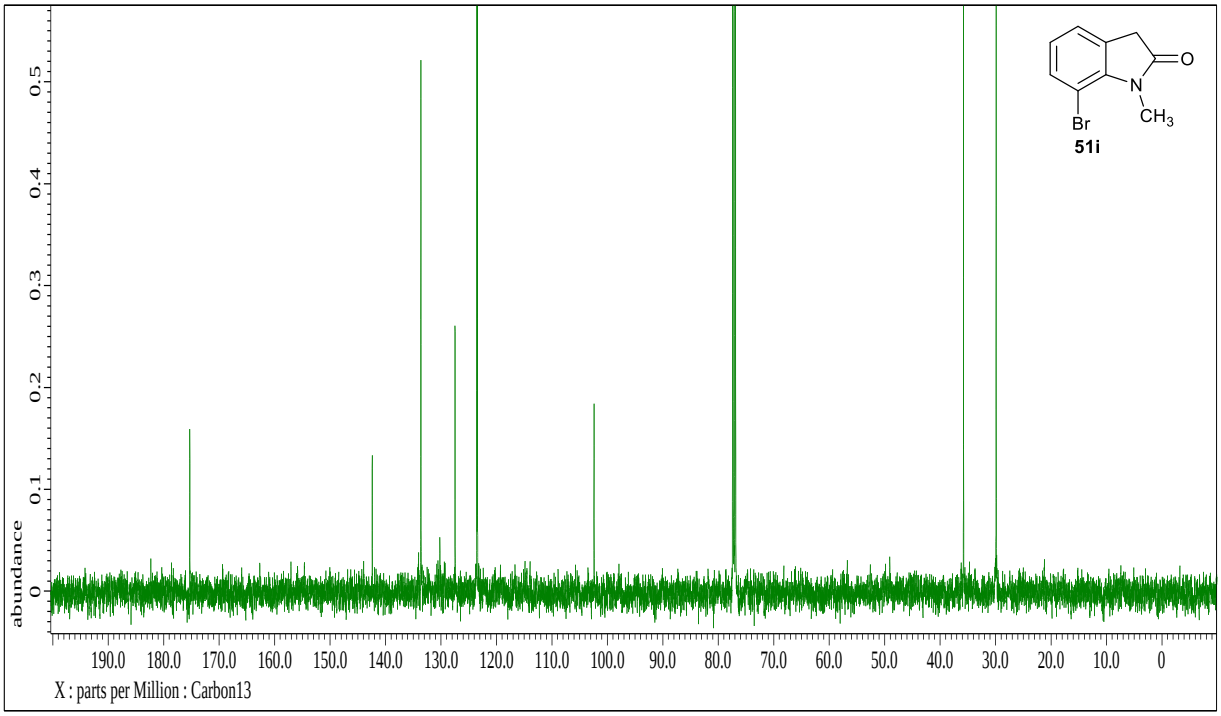

Figure 64. ^{13}CNMR spectral of 7-bromo-1-methylindolin-2-one.

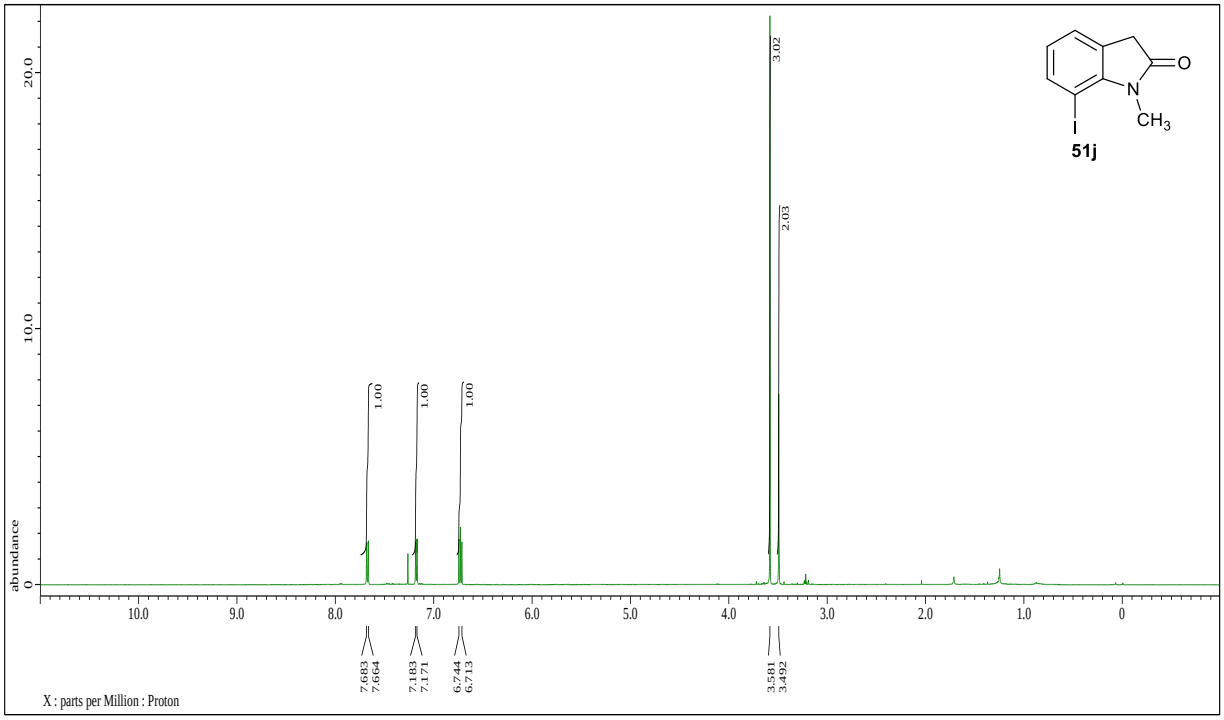

Figure 65. ^{1}HNMR spectral of 7-iodo-1-methylindolin-2-one.

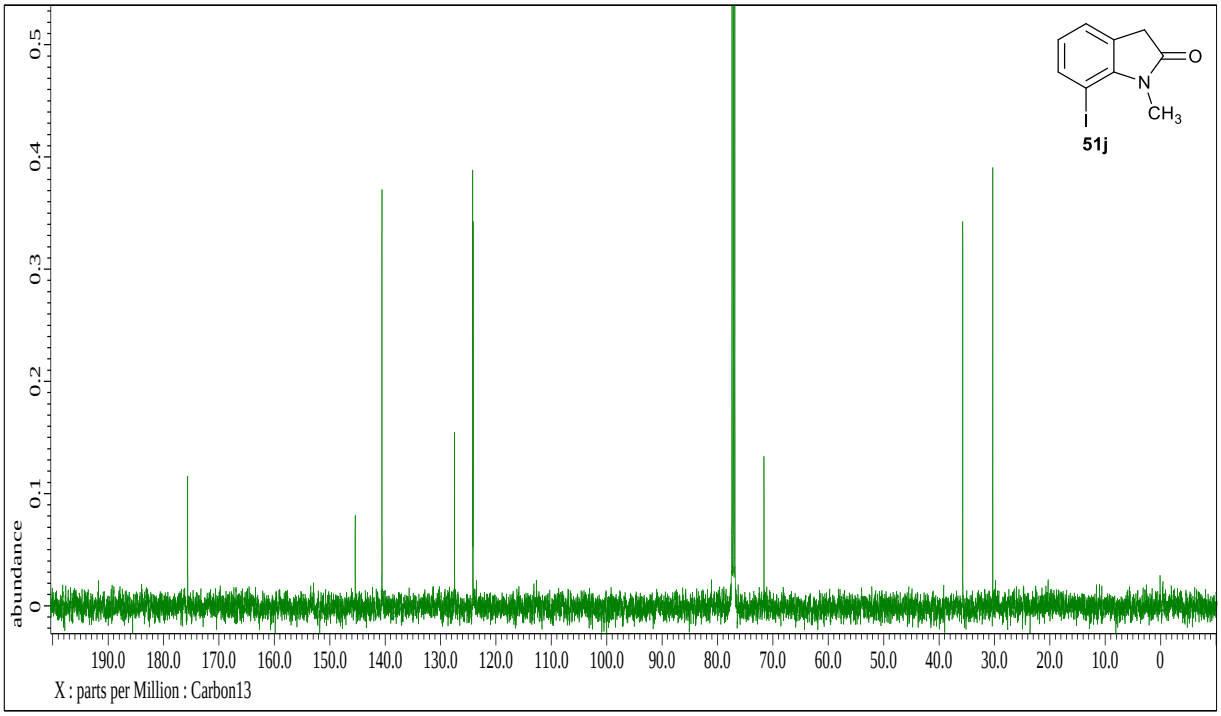

Figure 66. ^{13}CNMR spectral of 7-iodo-1-methylindolin-2-one.

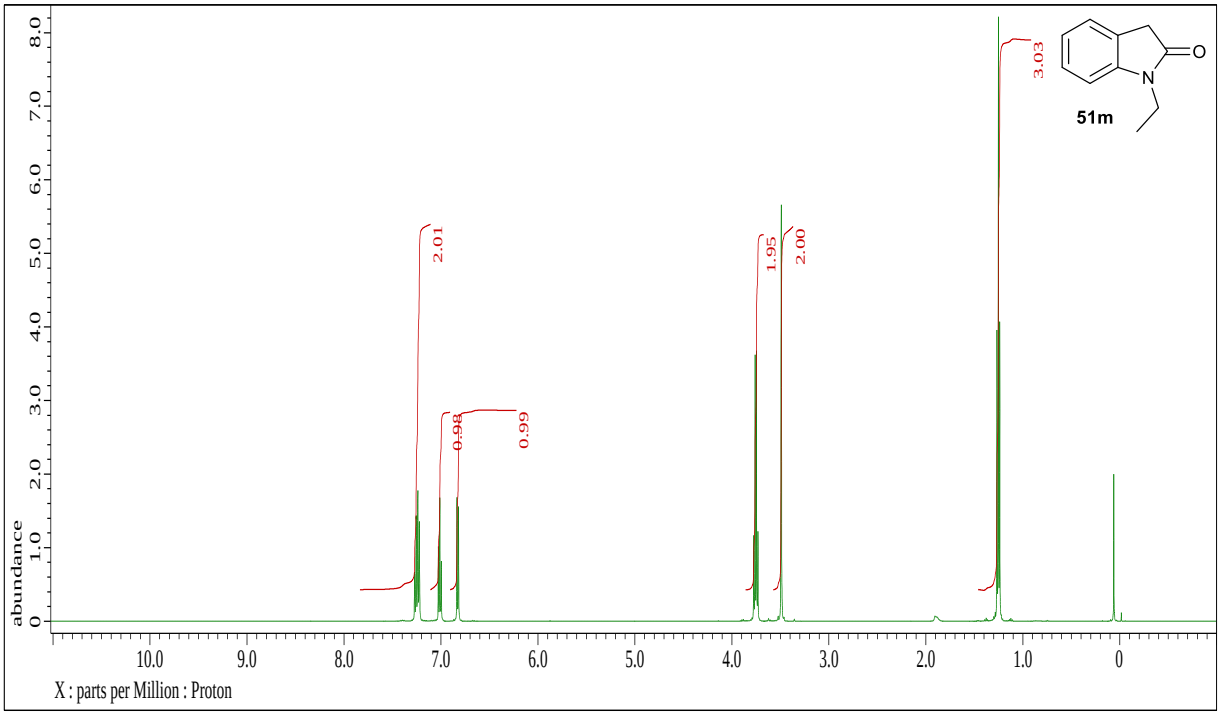

Figure 67. ^{1}HNMR spectral of 1-ethylindolin-2-one.

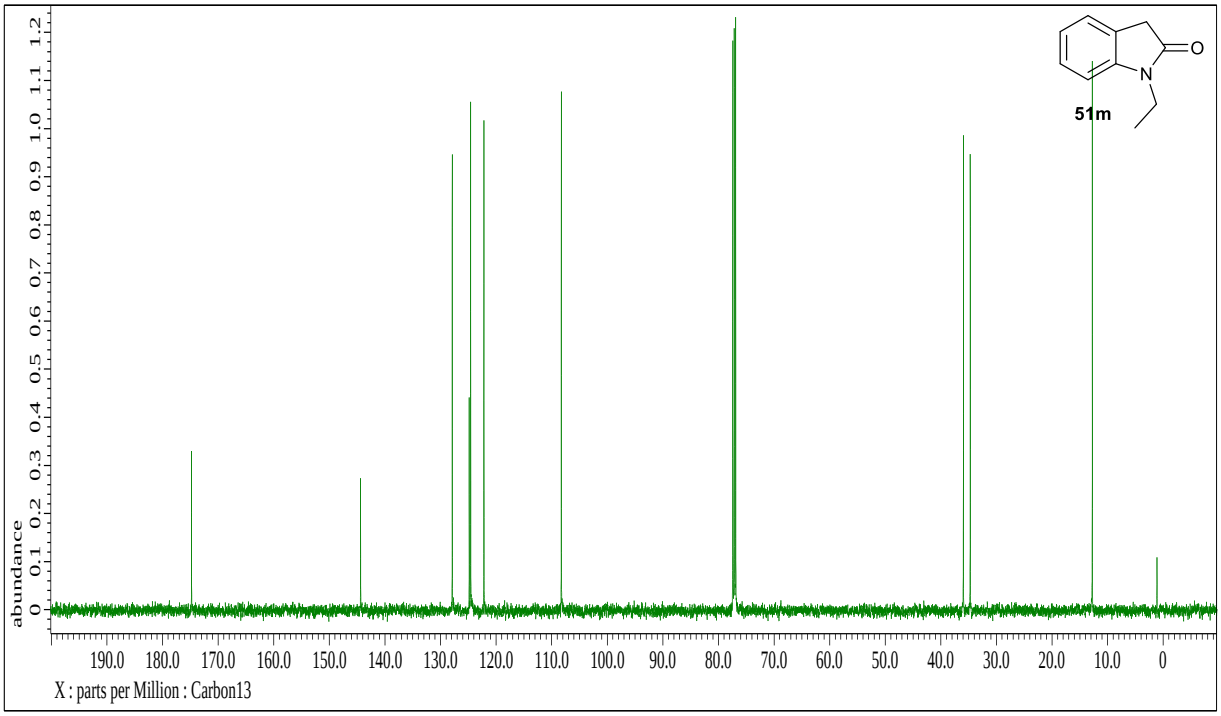

Figure 68. ^{13}CNMR spectral of 1-ethylindolin-2-one.

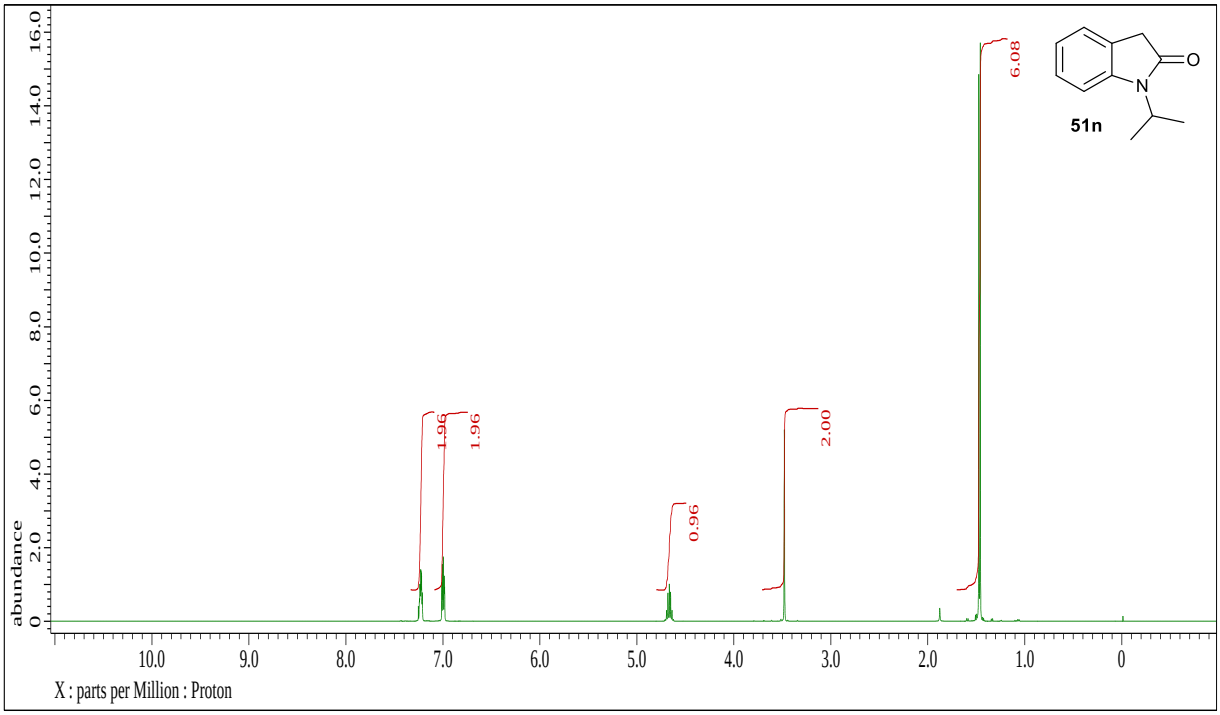

Figure 69. ^{1}HNMR spectral of 1-isopropylindolin-2-one.

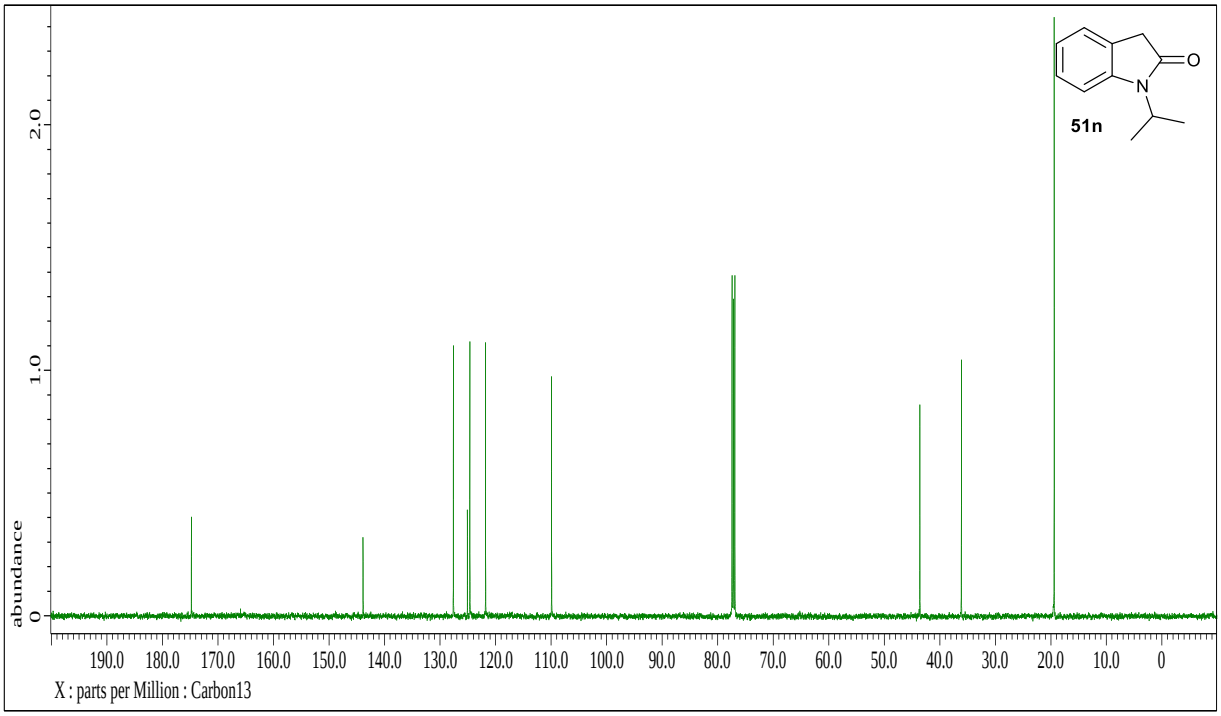

Figure 70. ^{13}CNMR spectral of 1-isopropylindolin-2-one.

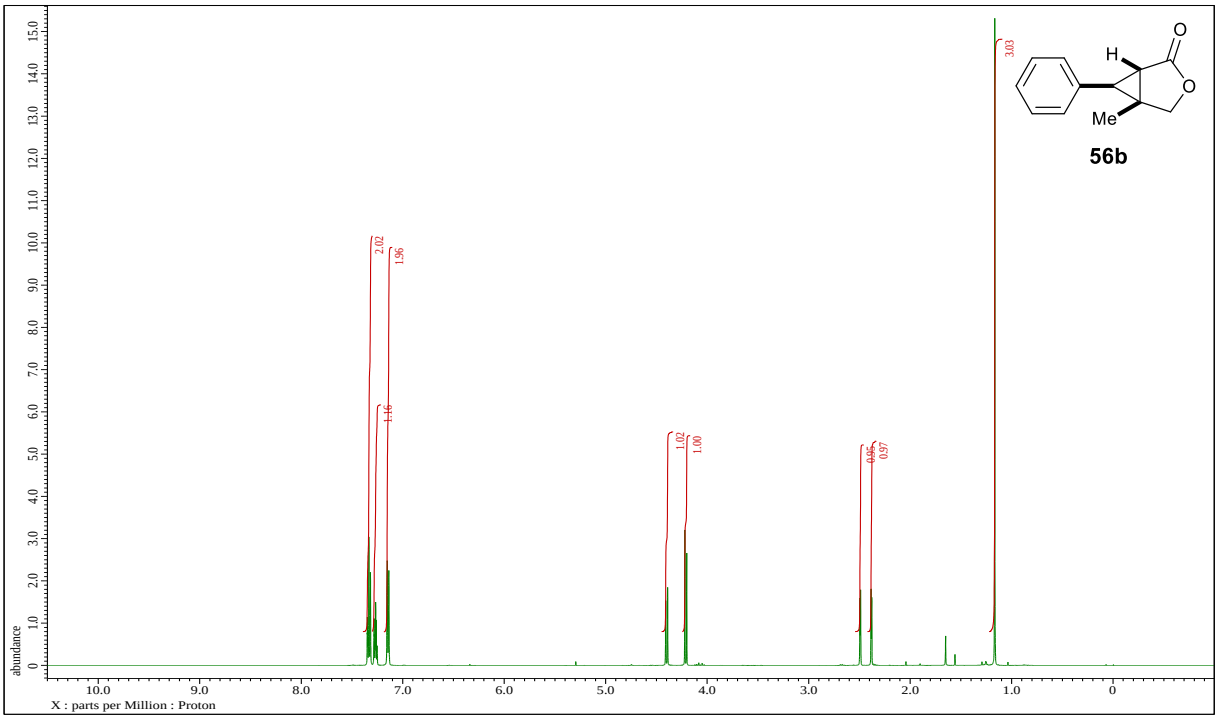

Figure 71. ^{1}HNMR spectral of (*1S,5R,6R*)-5-Methyl-6-phenyl-3-oxabicyclo[3.1.0]hexan-2-one.

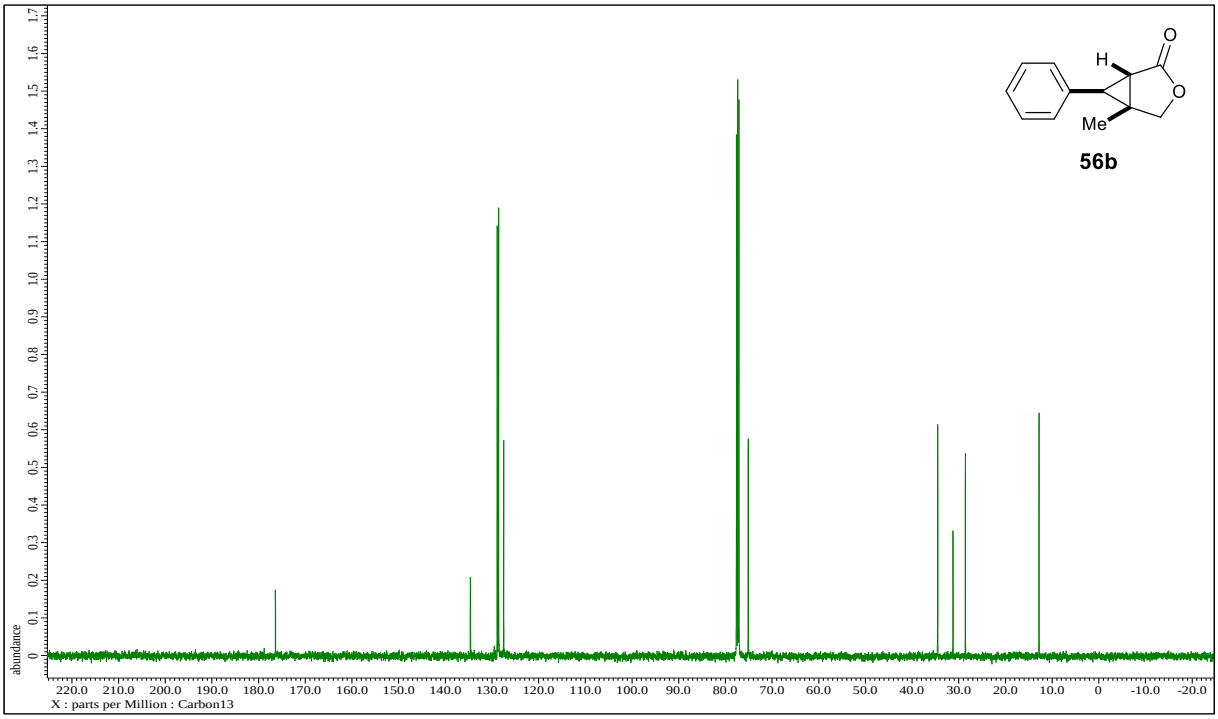

Figure 72. ^{13}CNMR spectral of (*1S,5R,6R*)-5-Methyl-6-phenyl-3-oxabicyclo[3.1.0]hexan-2-one.

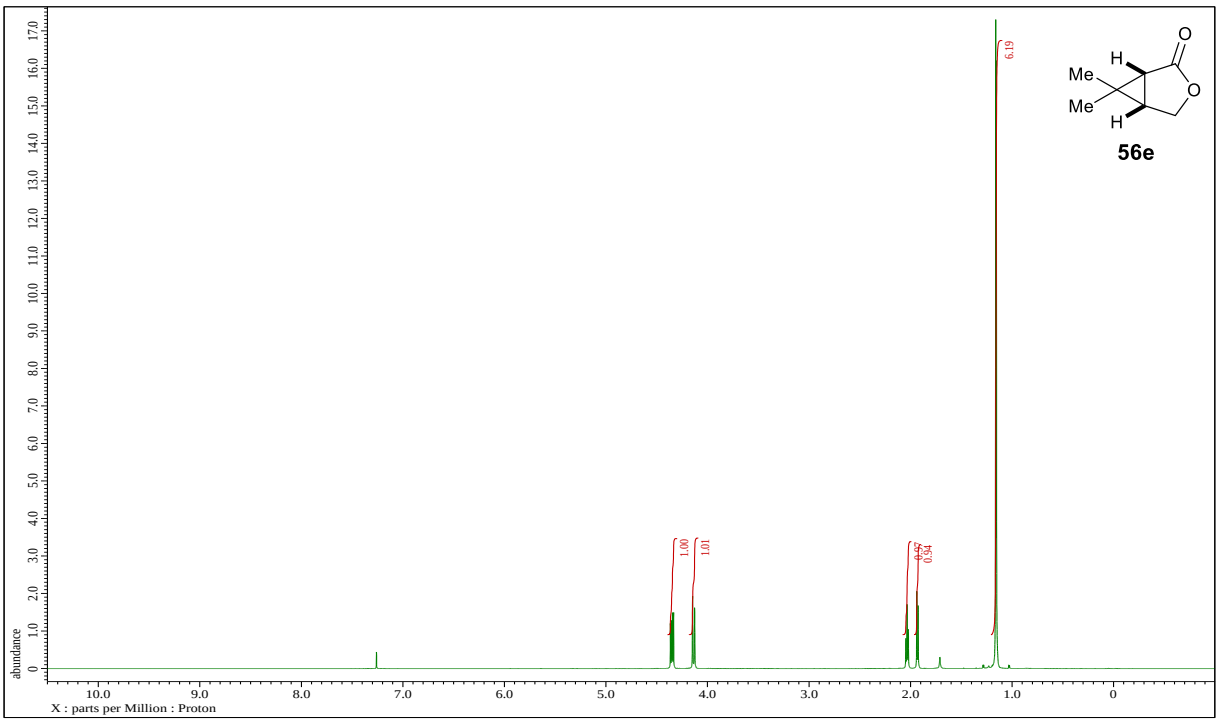

Figure 73. ^{1}HNMR spectral of (1*R*,5*S*)-6,6-dimethyl-3-oxabicyclo[3.1.0]hexan-2-one.

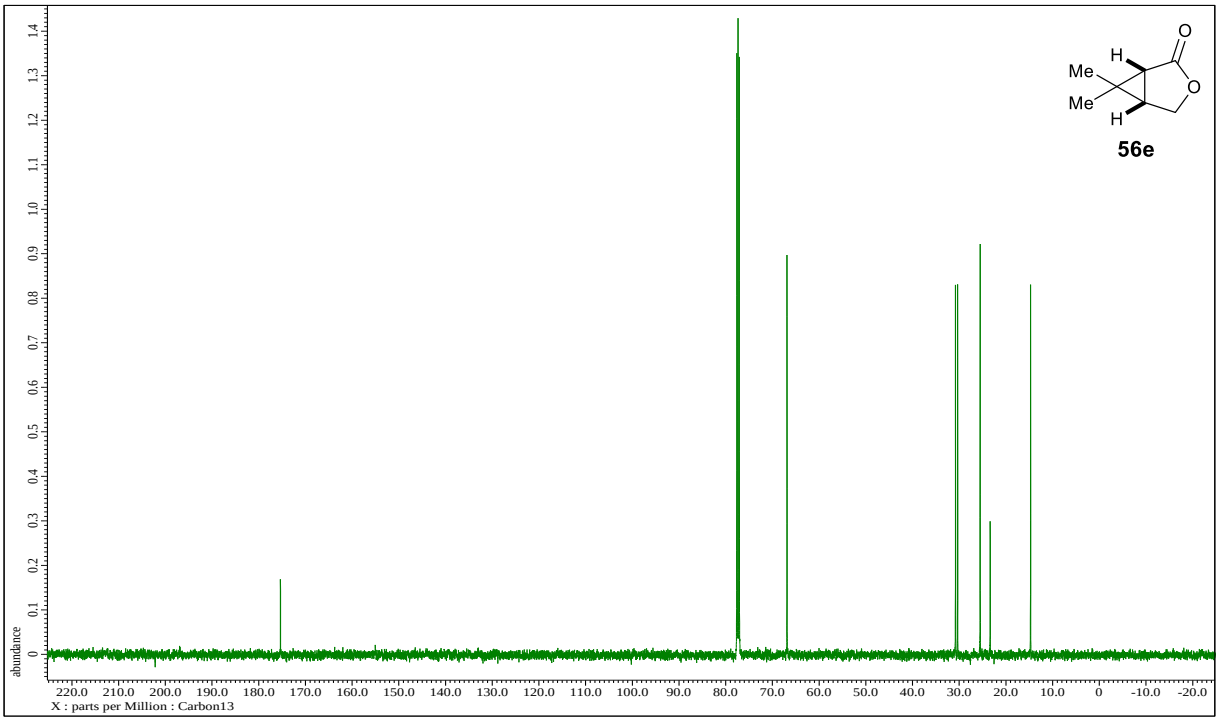

Figure 74. ^{13}CNMR spectral of (1*R*,5*S*)-6,6-dimethyl-3-oxabicyclo[3.1.0]hexan-2-one.

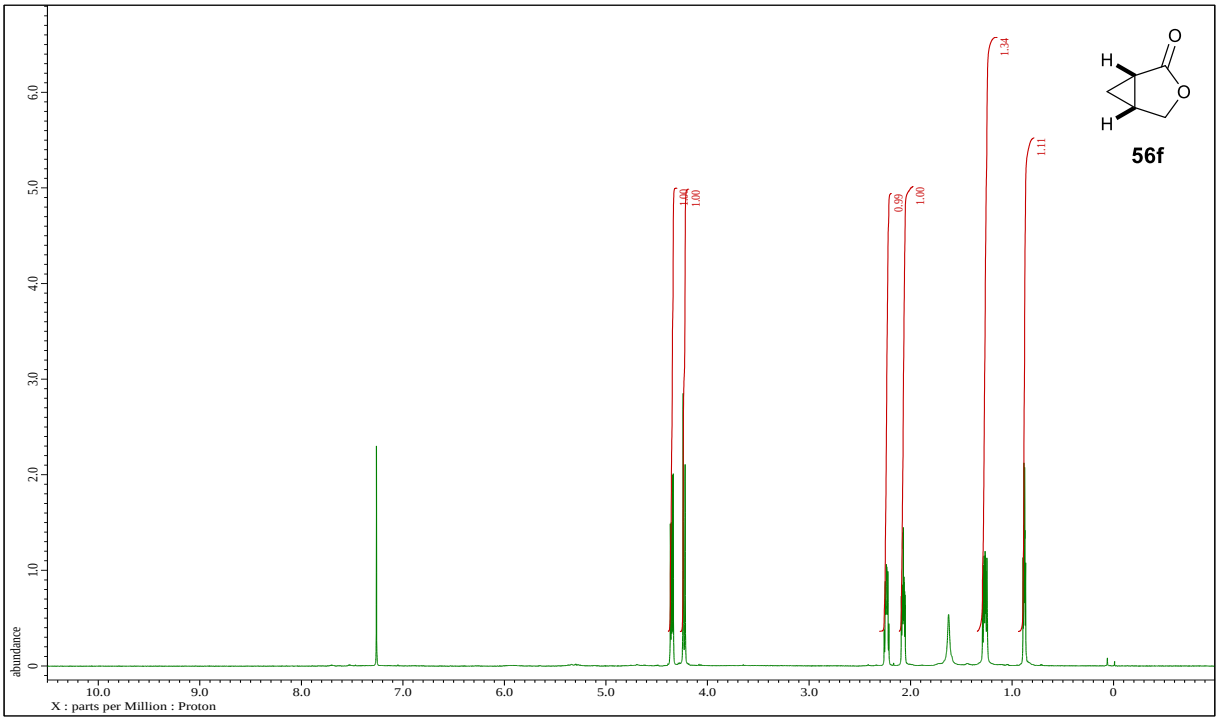

Figure 75. ^{1}HNMR spectral of (1*S*,5*R*)-3-oxabicyclo[3.1.0]hexan-2-one.

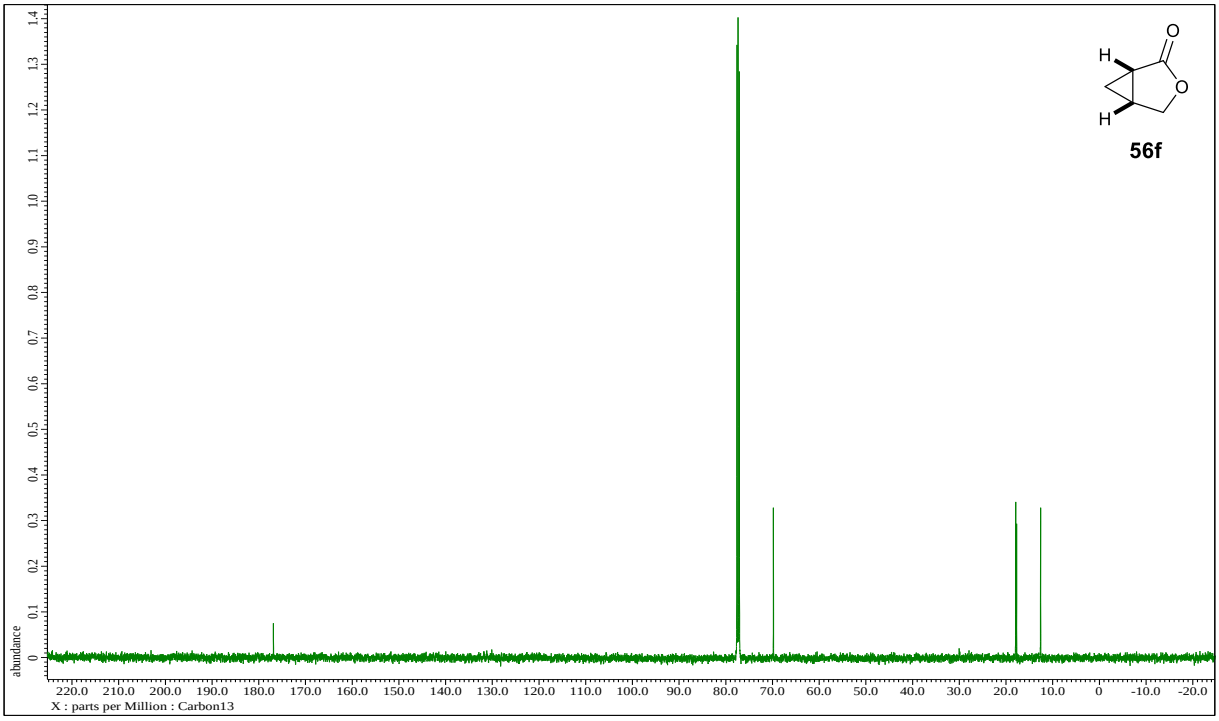

Figure 76. ^{13}CNMR spectral of (1*S*,5*R*)-3-oxabicyclo[3.1.0]hexan-2-one.

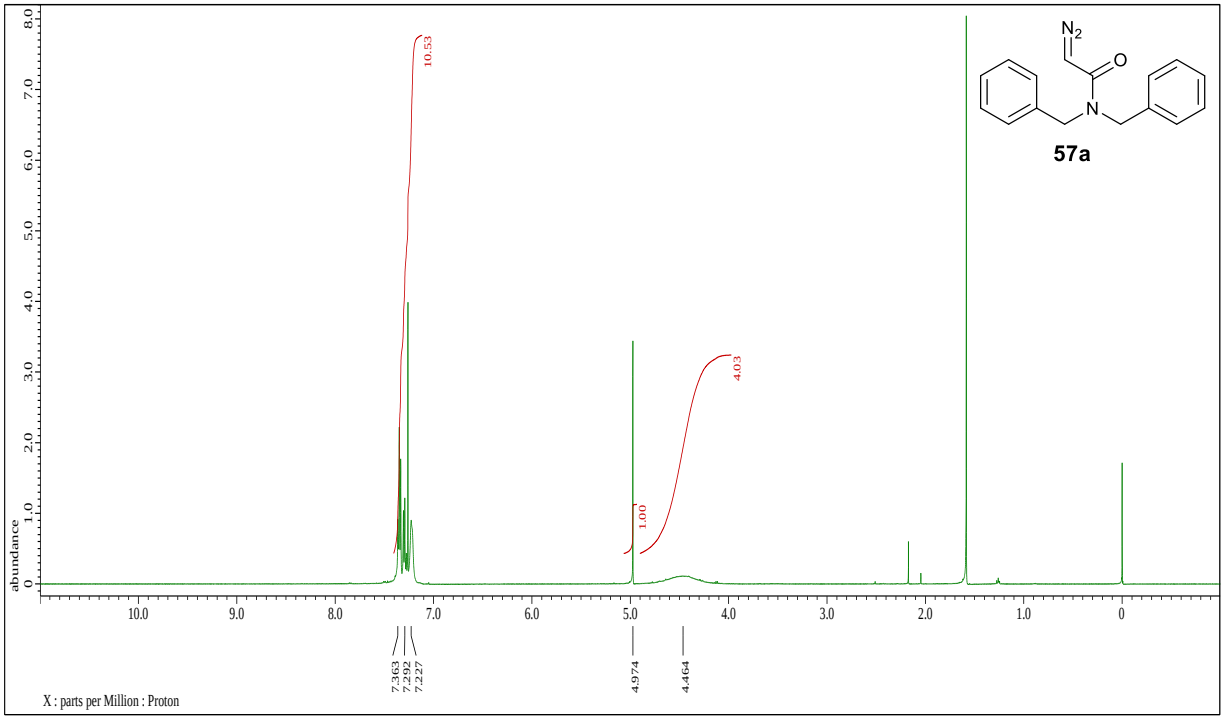

Figure 77. ^{1}HNMR spectral of 2-diazo-*N*,*N*-dibenzylacetamide.

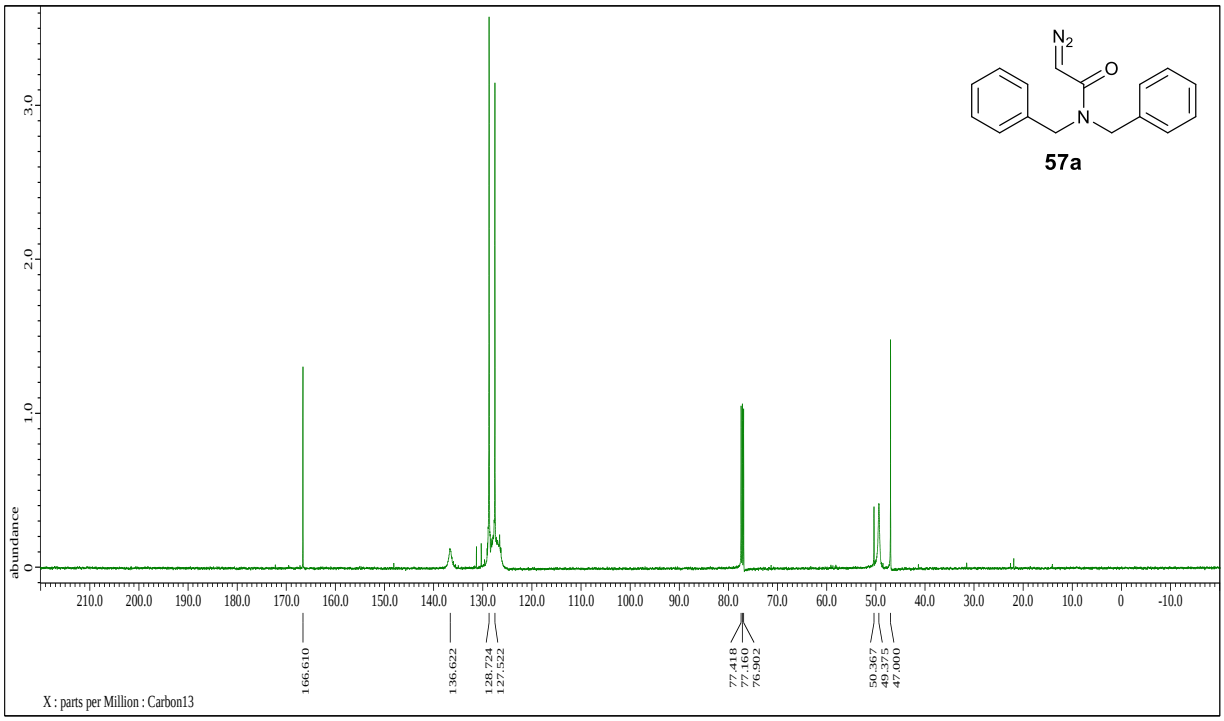

Figure 78. ^{13}CNMR spectral of 2-diazo-*N*,*N*-dibenzylacetamide.

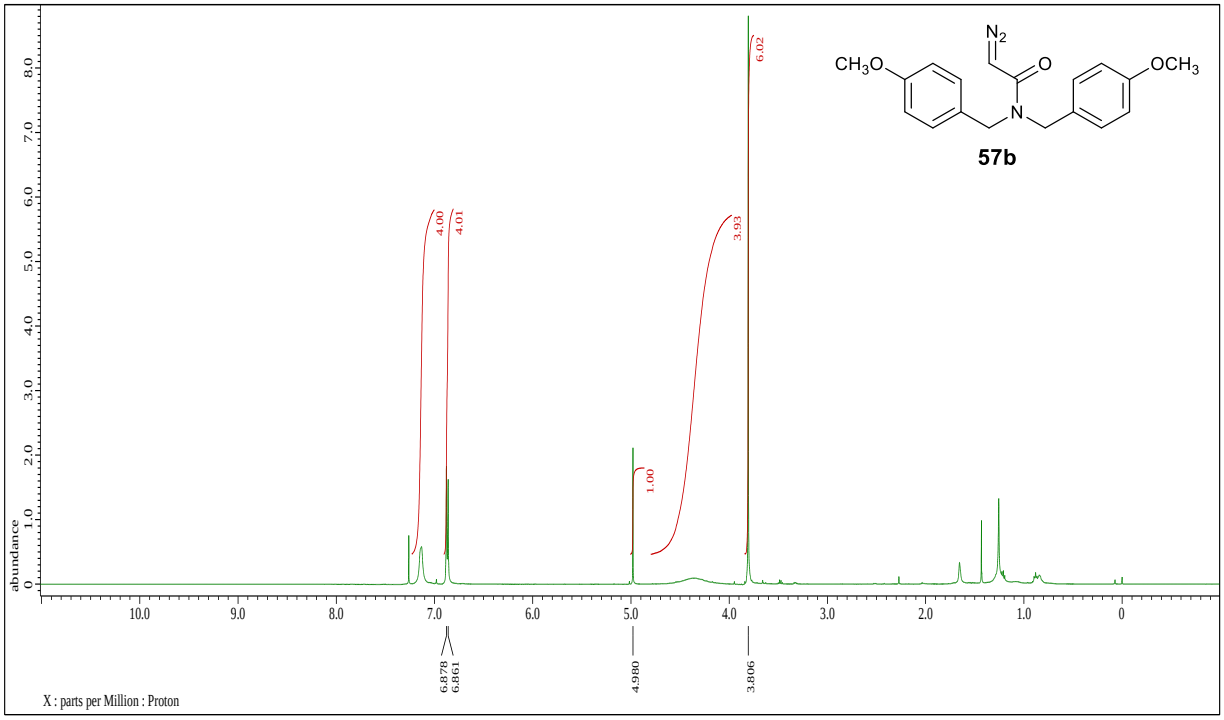

Figure 79. ^{1}HNMR spectral of 2-diazo-*N*,*N*-bis(4-methoxybenzyl)acetamide.

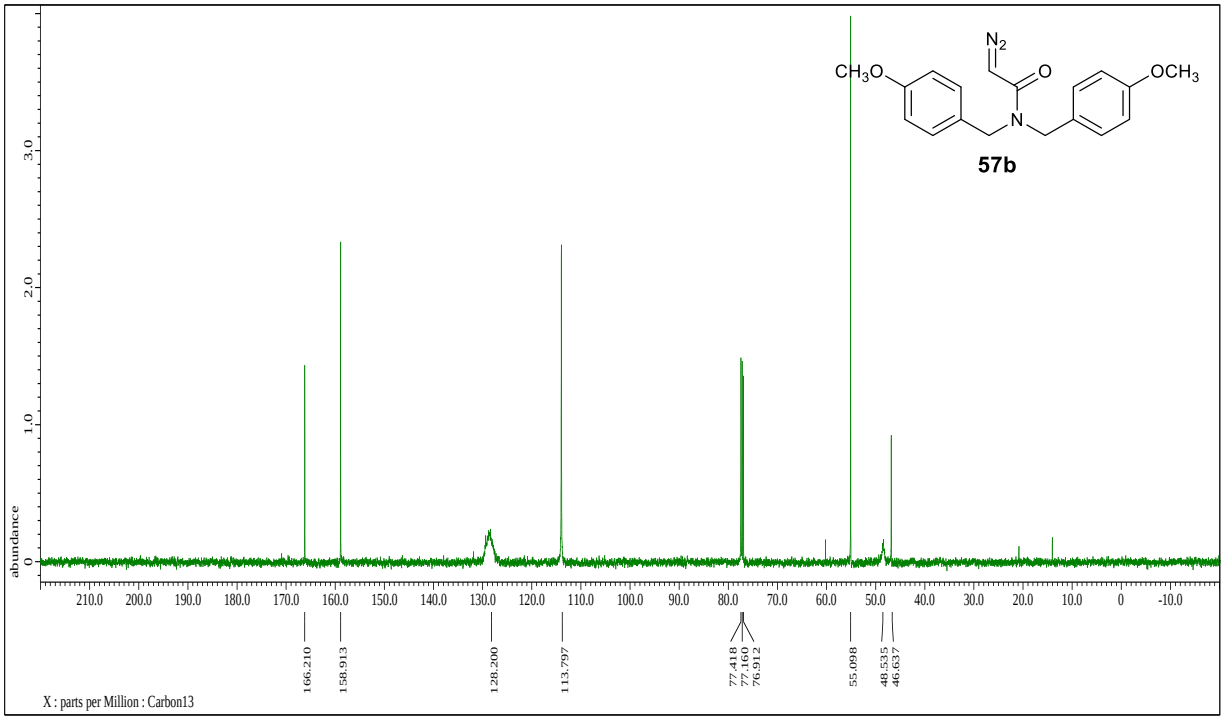

Figure 80. ^{13}CNMR spectral of 2-diazo-*N*,*N*-bis(4-methoxybenzyl)acetamide.

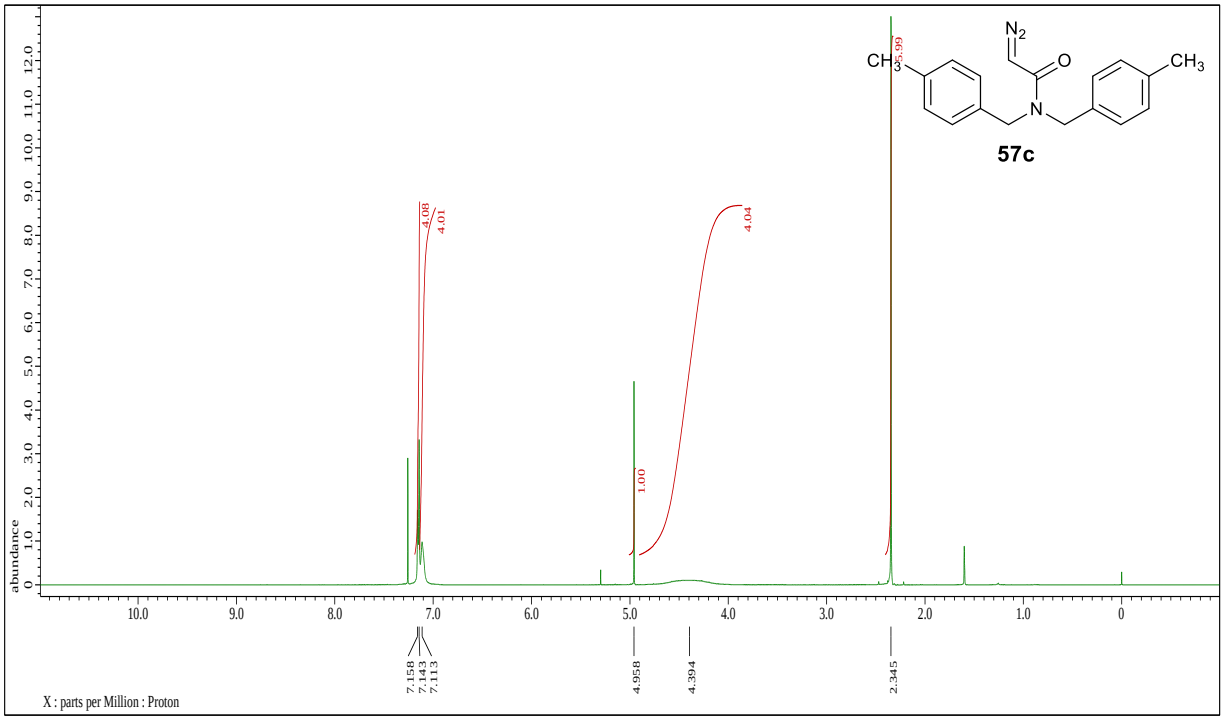

Figure 81. ^{1}HNMR spectral of 2-diazo-*N*,*N*-bis(4-methylbenzyl)acetamide.

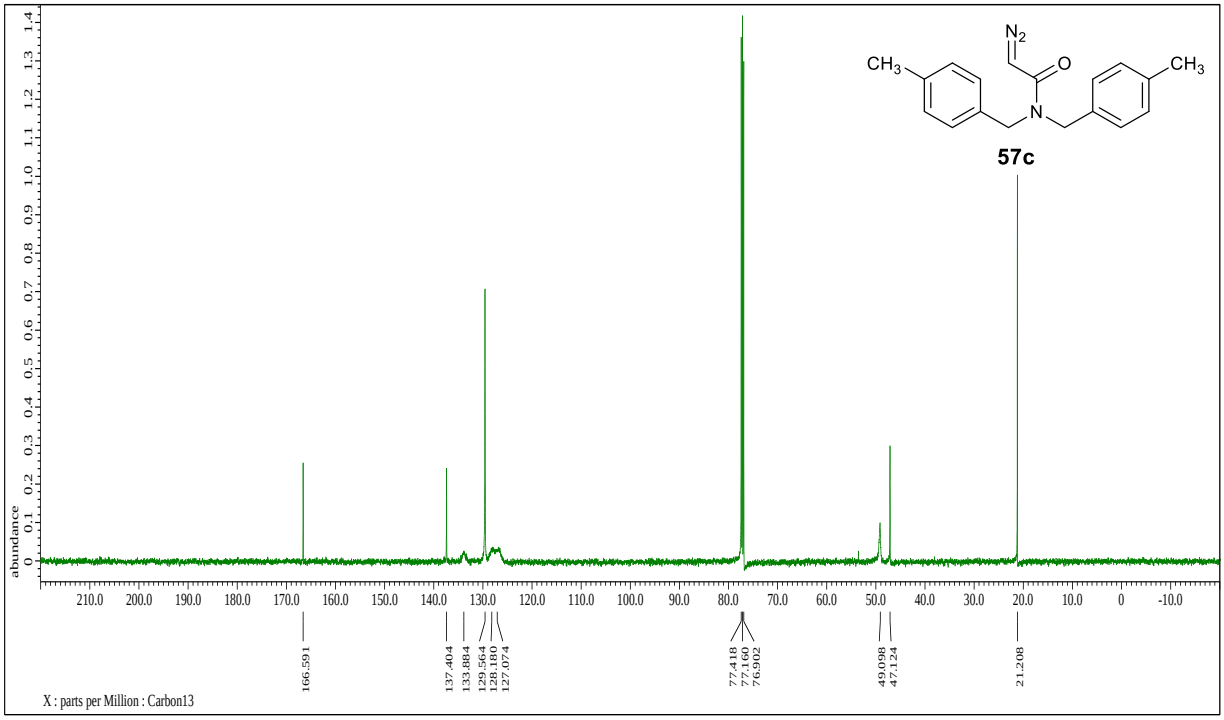

Figure 82. ^{13}CNMR spectral of 2-diazo-*N*,*N*-bis(4-methylbenzyl)acetamide.

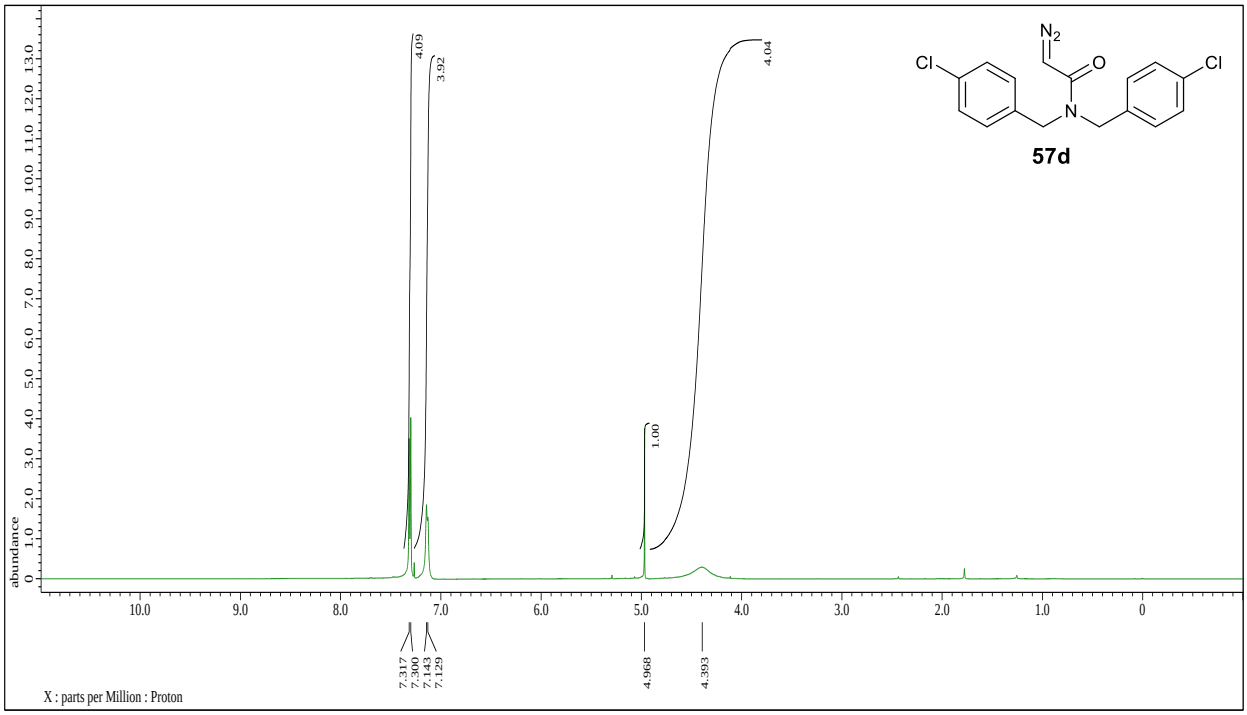

Figure 83. ^{1}HNMR spectral of 2-diazo-*N*,*N*-bis(4-chlorobenzyl)acetamide.

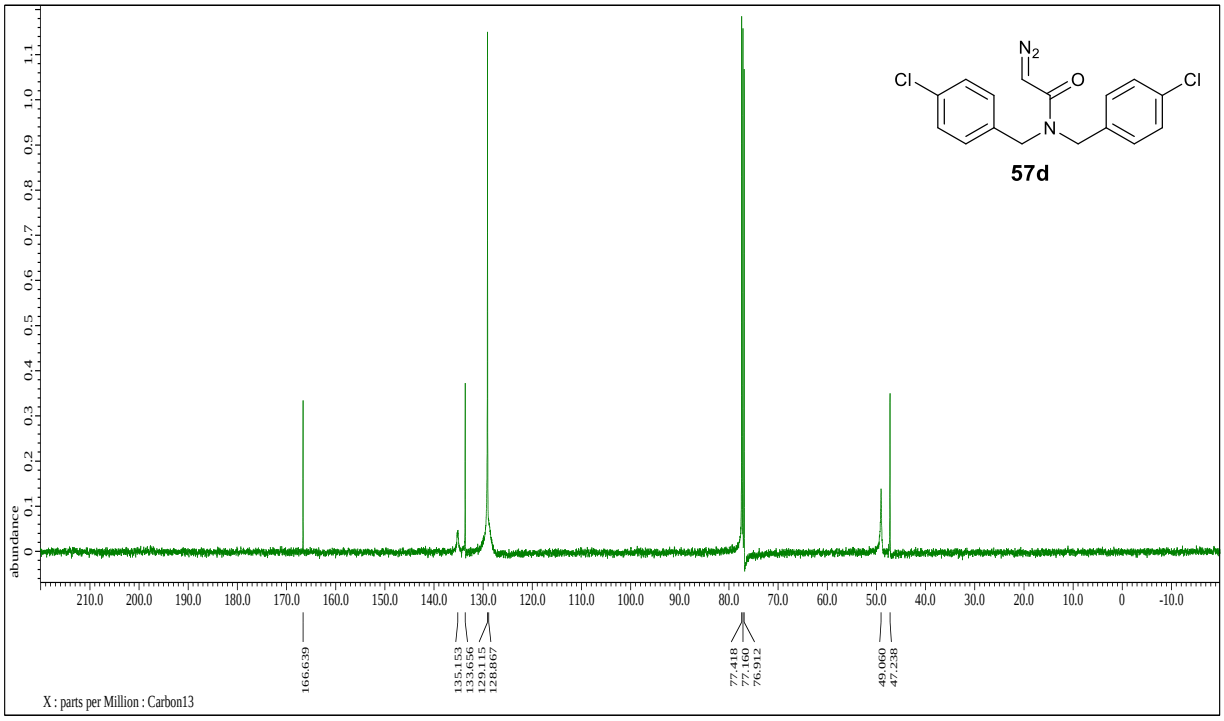

Figure 84. ^{13}CNMR spectral of 2-diazo-*N*,*N*-bis(4-chlorobenzyl)acetamide.

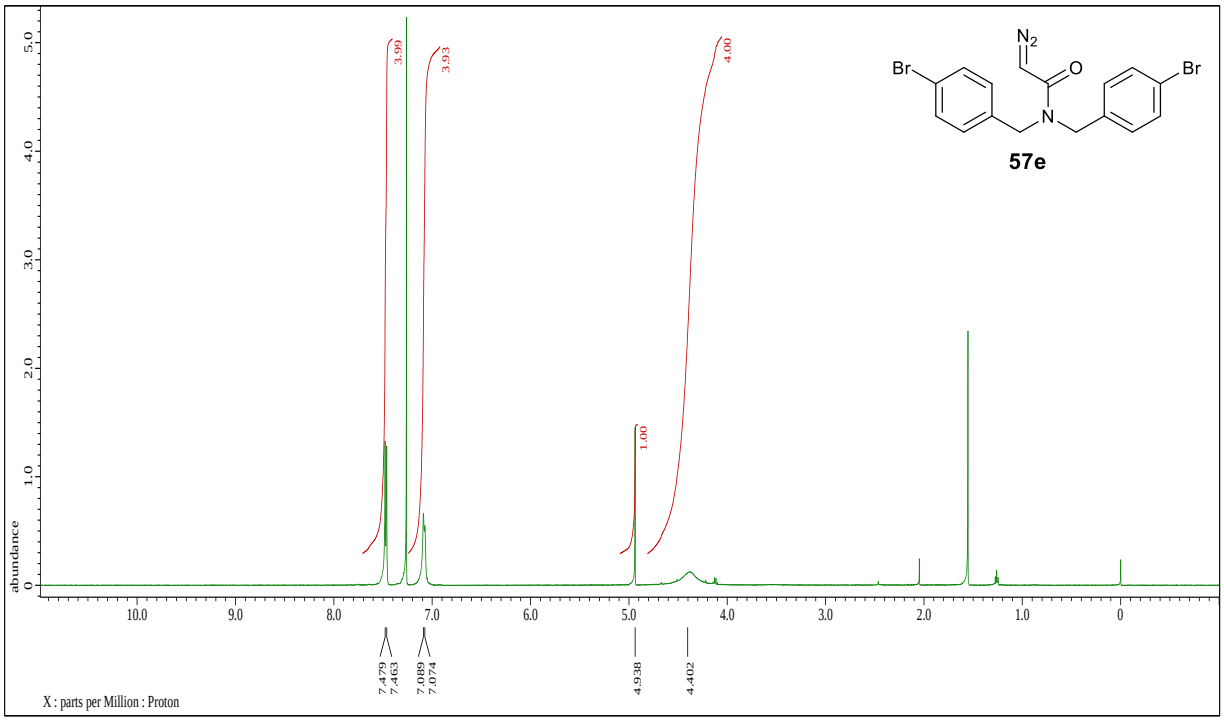

Figure 85. ^{1}HNMR spectral of 2-diazo-*N*,*N*-bis(4-bromobenzyl)acetamide.

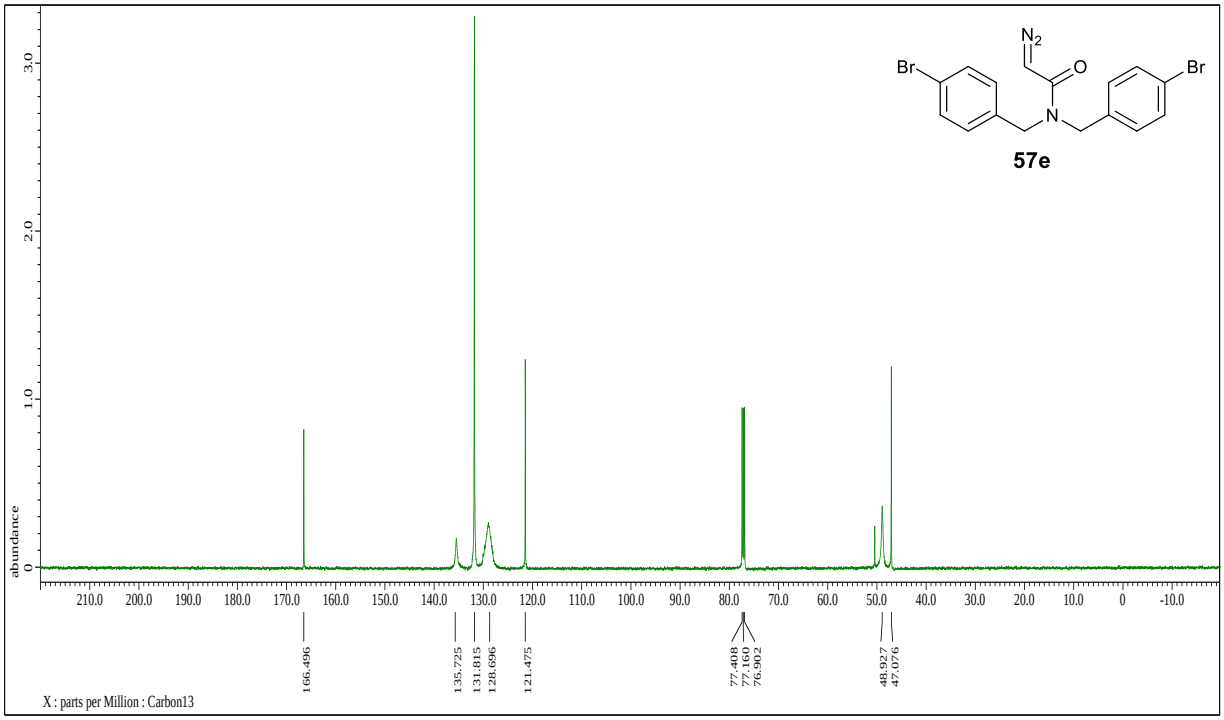

Figure 86. ^{13}CNMR spectral of 2-diazo-*N*,*N*-bis(4-bromobenzyl)acetamide.

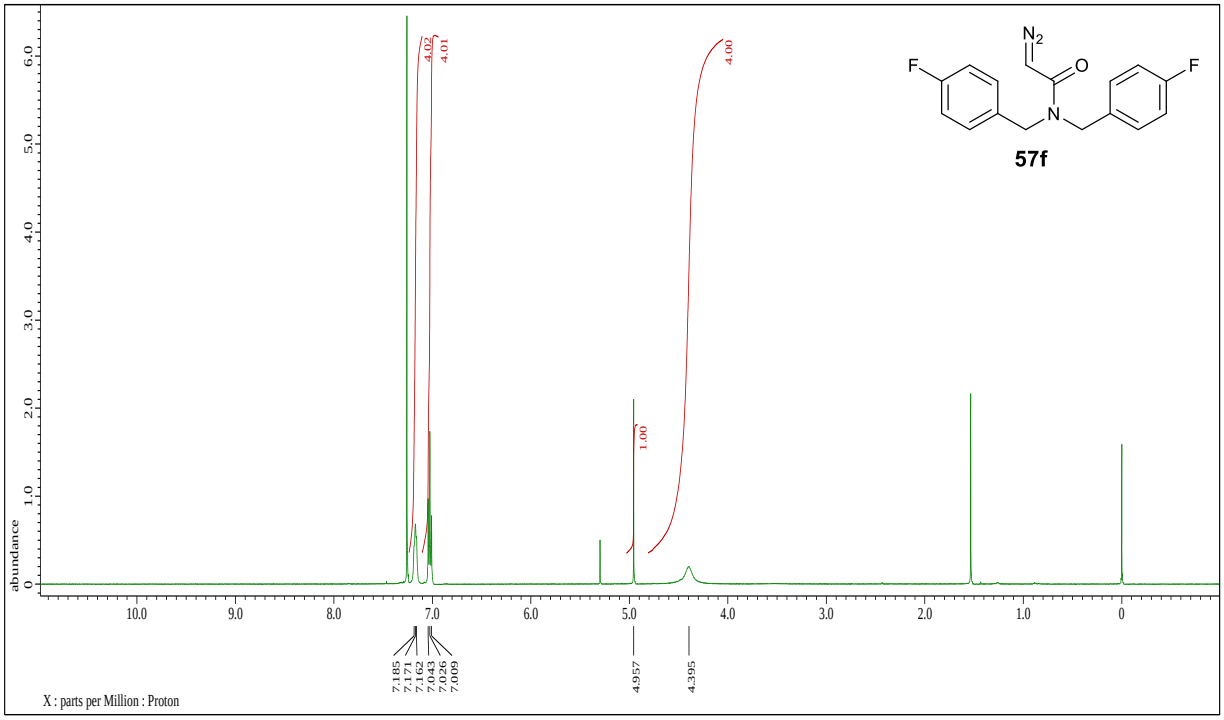

Figure 87. ^{1}HNMR spectral of 2-diazo-*N*,*N*-bis(4-fluorobenzyl)acetamide.

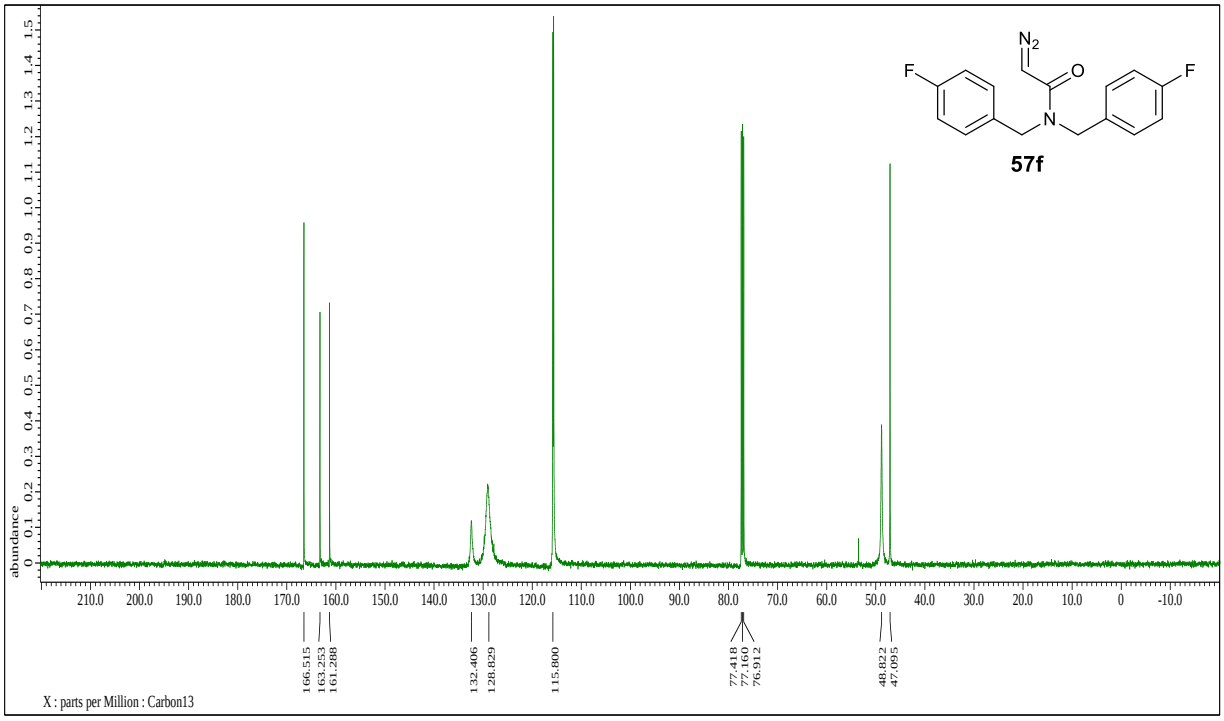

Figure 88. ^{13}CNMR spectral of 2-diazo-*N*,*N*-bis(4-fluorobenzyl)acetamide.

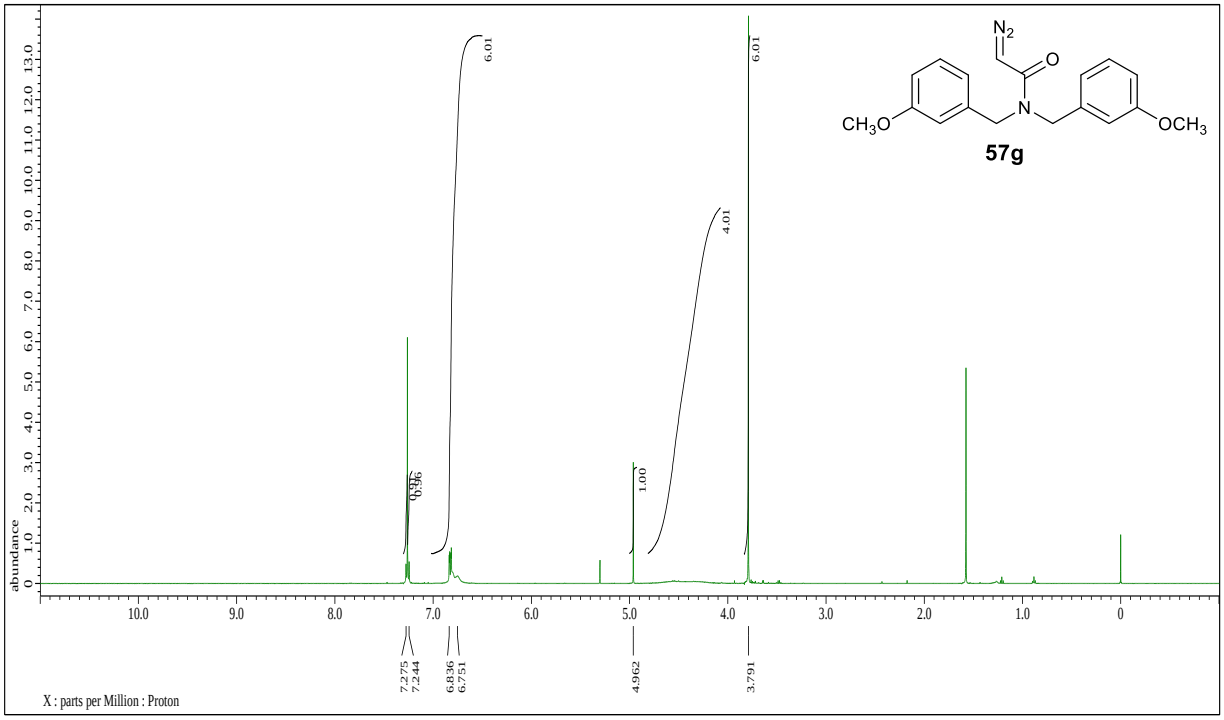

Figure 89. ^{1}HNMR spectral of 2-diazo-*N*,*N*-bis(3-methoxybenzyl)acetamide.

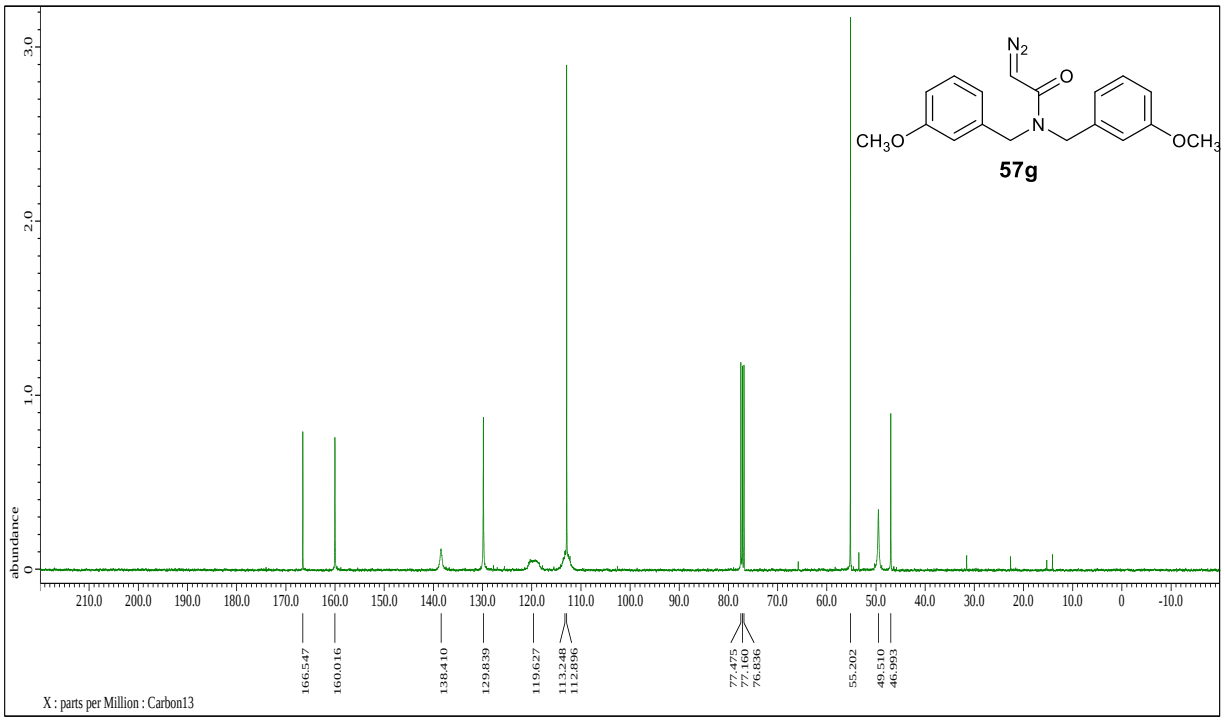

Figure 90. ^{13}CNMR spectral of 2-diazo-*N*,*N*-bis(3-methoxybenzyl)acetamide.

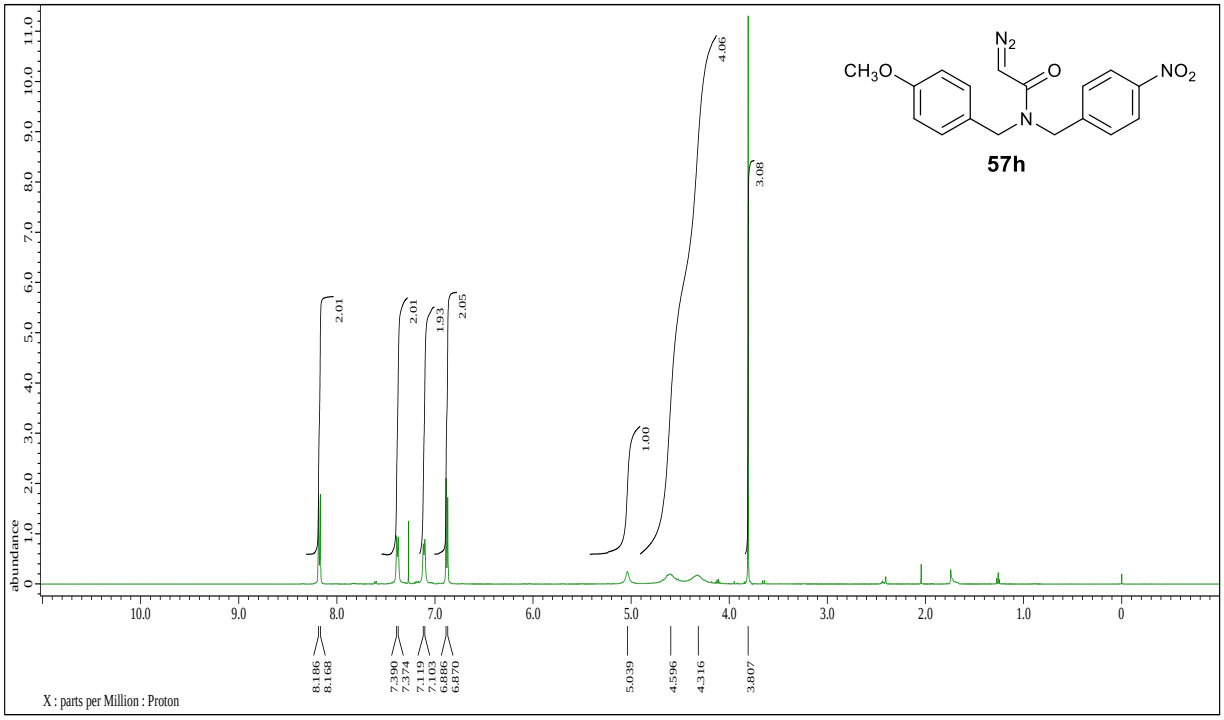

Figure 91. ^{1}HNMR spectral of 2-diazo-*N*-(4-methoxybenzyl)-*N*-(4-nitrobenzyl)acetamide.

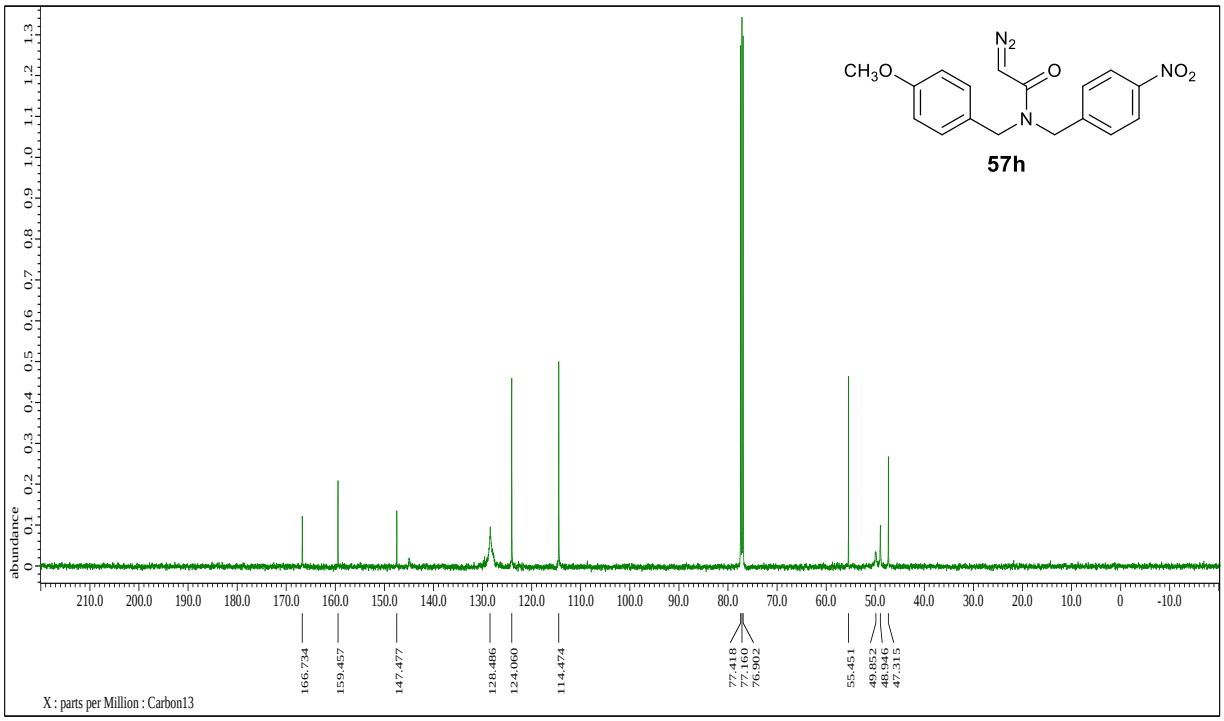

Figure 92. ^{13}CNMR spectral of 2-diazo-*N*-(4-methoxybenzyl)-*N*-(4-nitrobenzyl)acetamide.

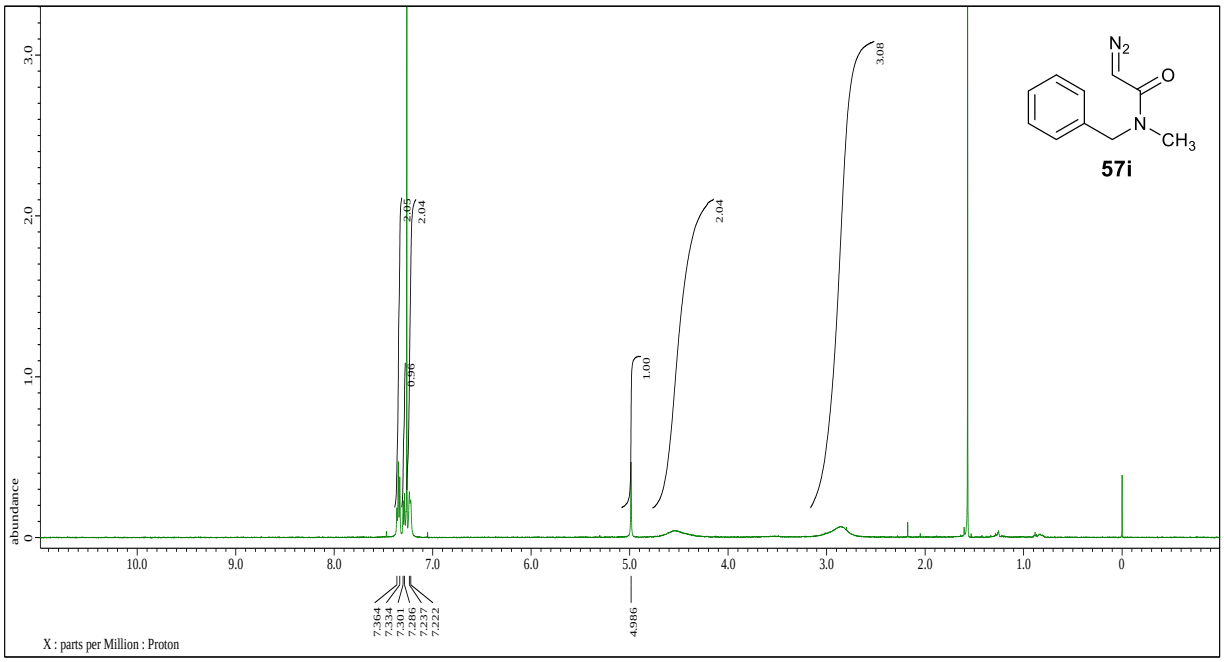

Figure 93. ^{1}HNMR spectral of 2-diazo-*N*-benzyl-*N*-methylacetamide.

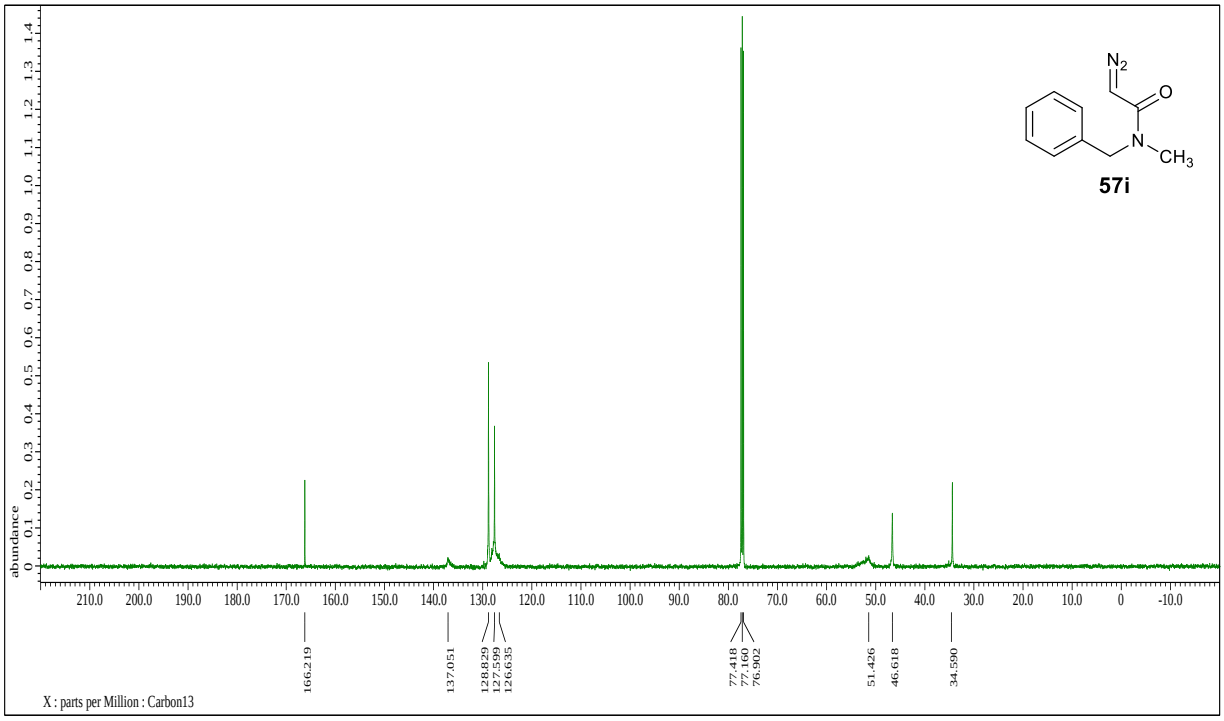

Figure 94. ^{13}CNMR spectral of 2-diazo-*N*-benzyl-*N*-methylacetamide.

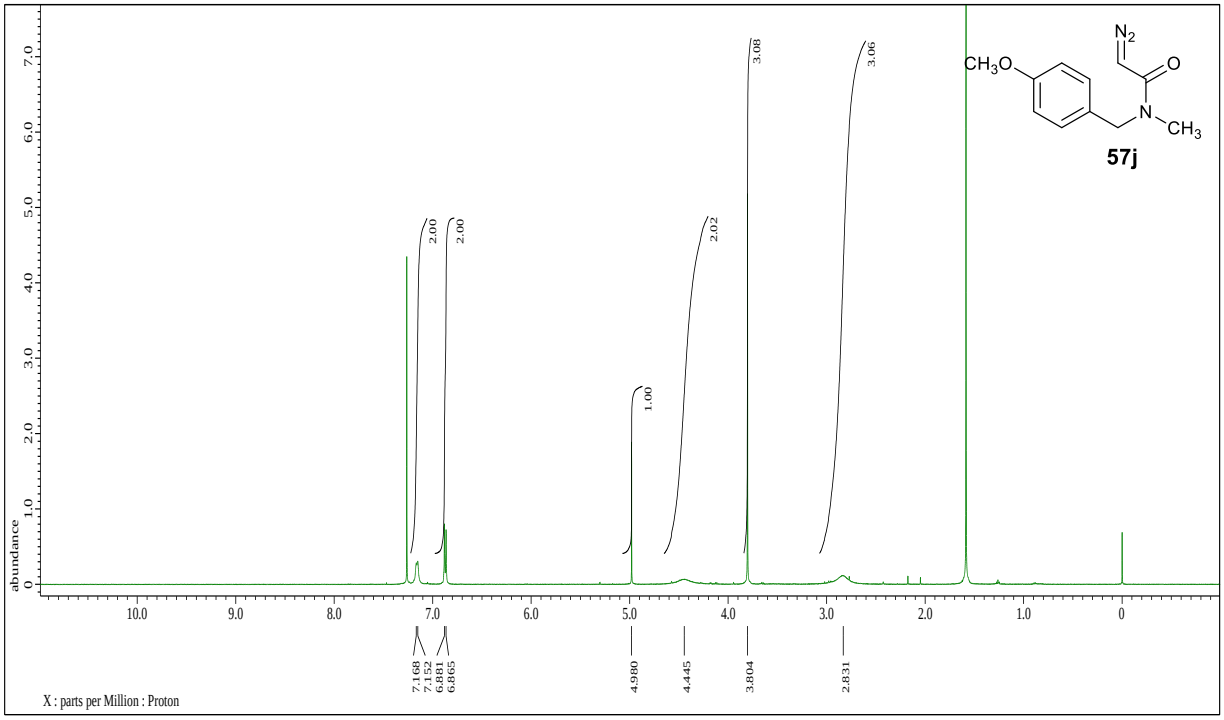

Figure 95. ^{1}HNMR spectral of 2-diazo-*N*-(4-methoxybenzyl)-*N*-methylacetamide.

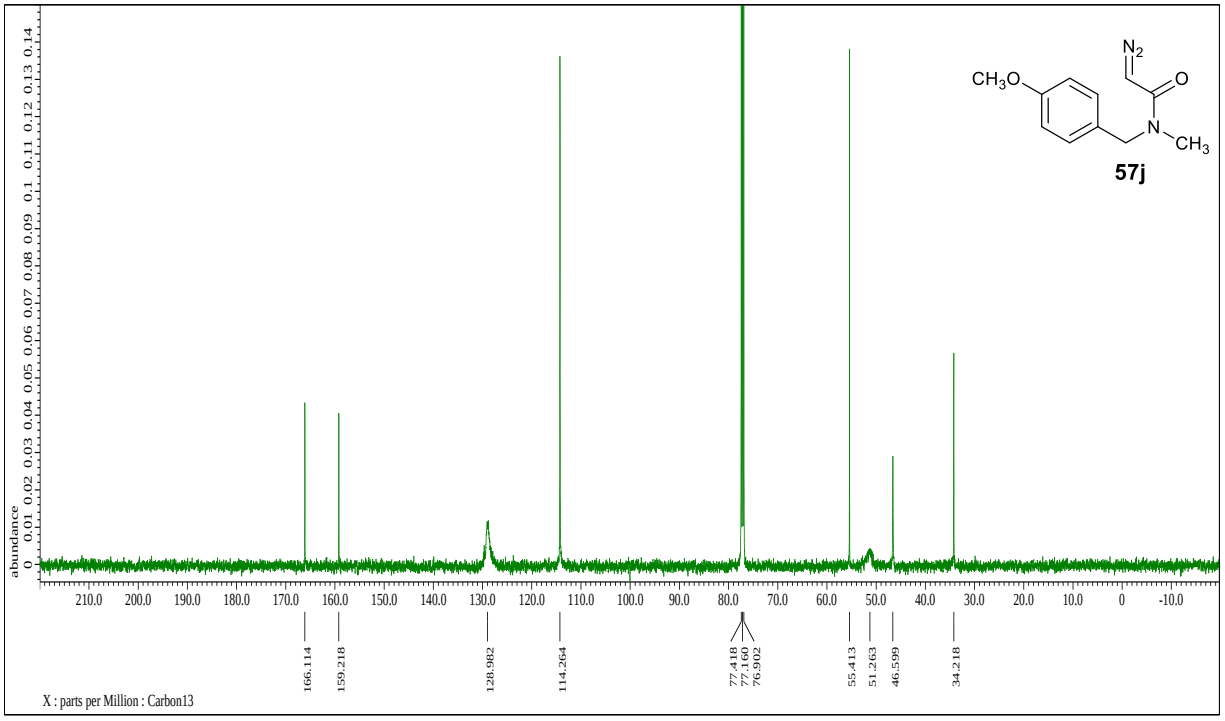

Figure 96. ^{13}CNMR spectral of 2-diazo-*N*-(4-methoxybenzyl)-*N*-methylacetamide.

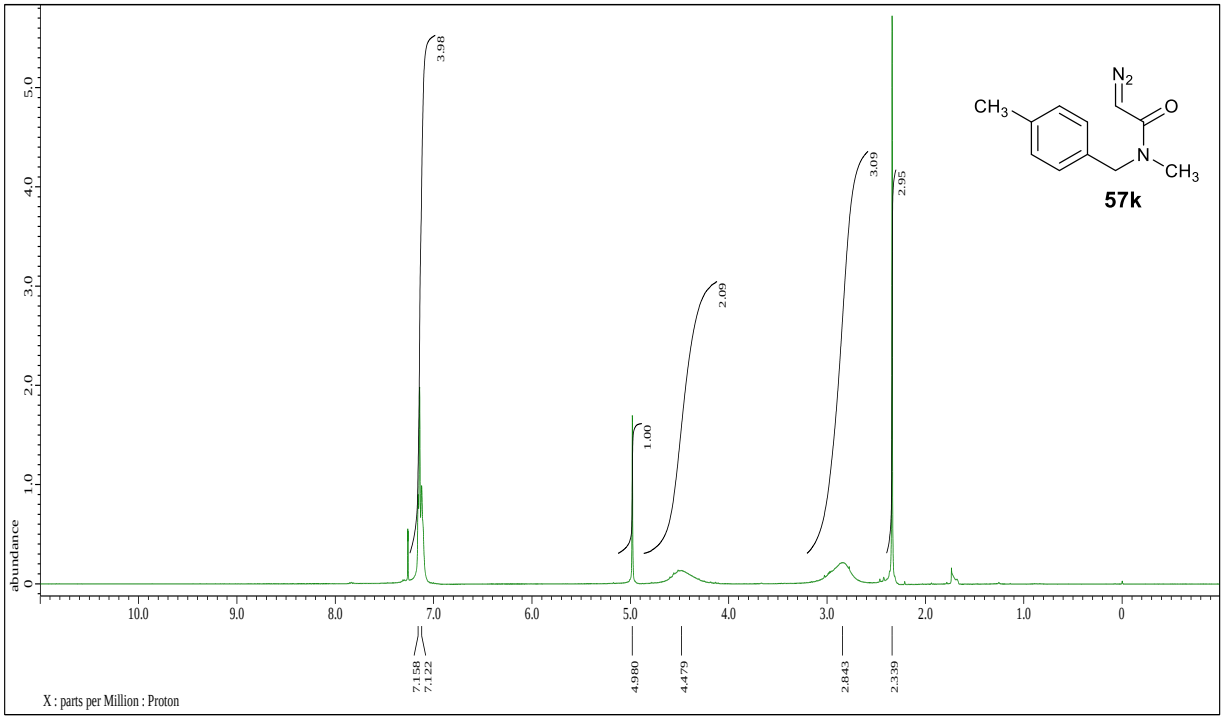

Figure 97. ^{1}HNMR spectral of 2-diazo-*N*-(4-methylbenzyl)-*N*-methylacetamide.

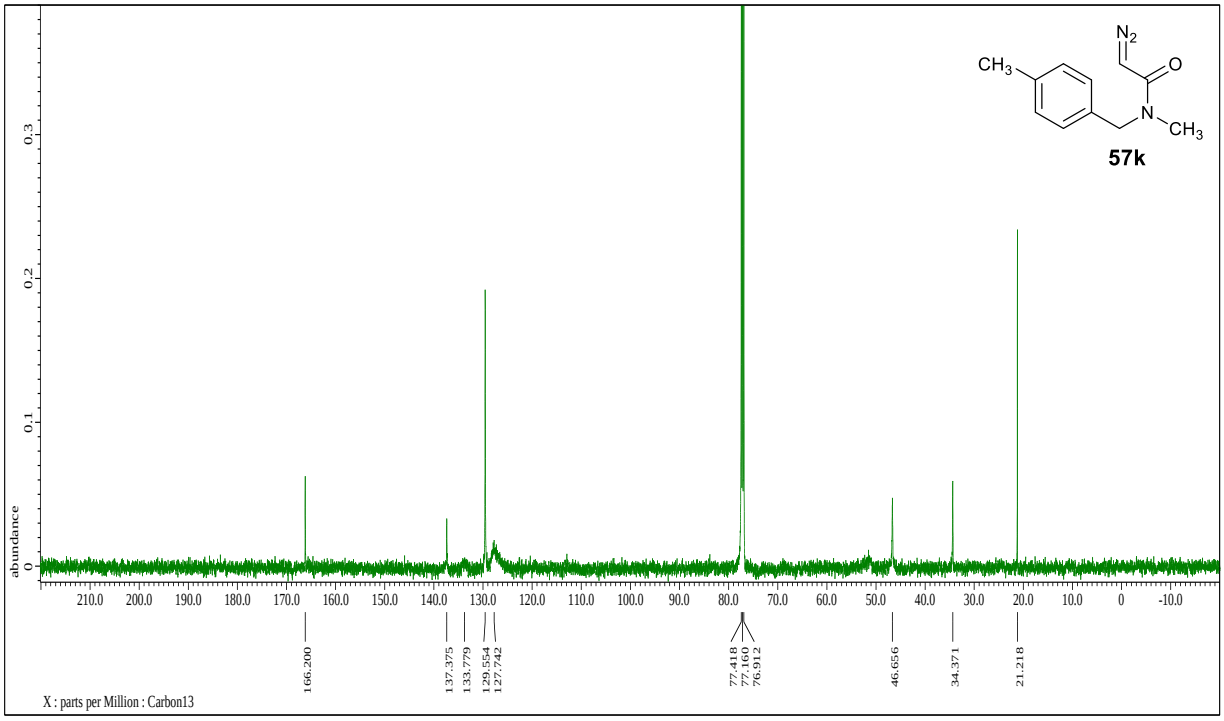

Figure 98. ^{13}CNMR spectral of 2-diazo-*N*-(4-methylbenzyl)-*N*-methylacetamide.

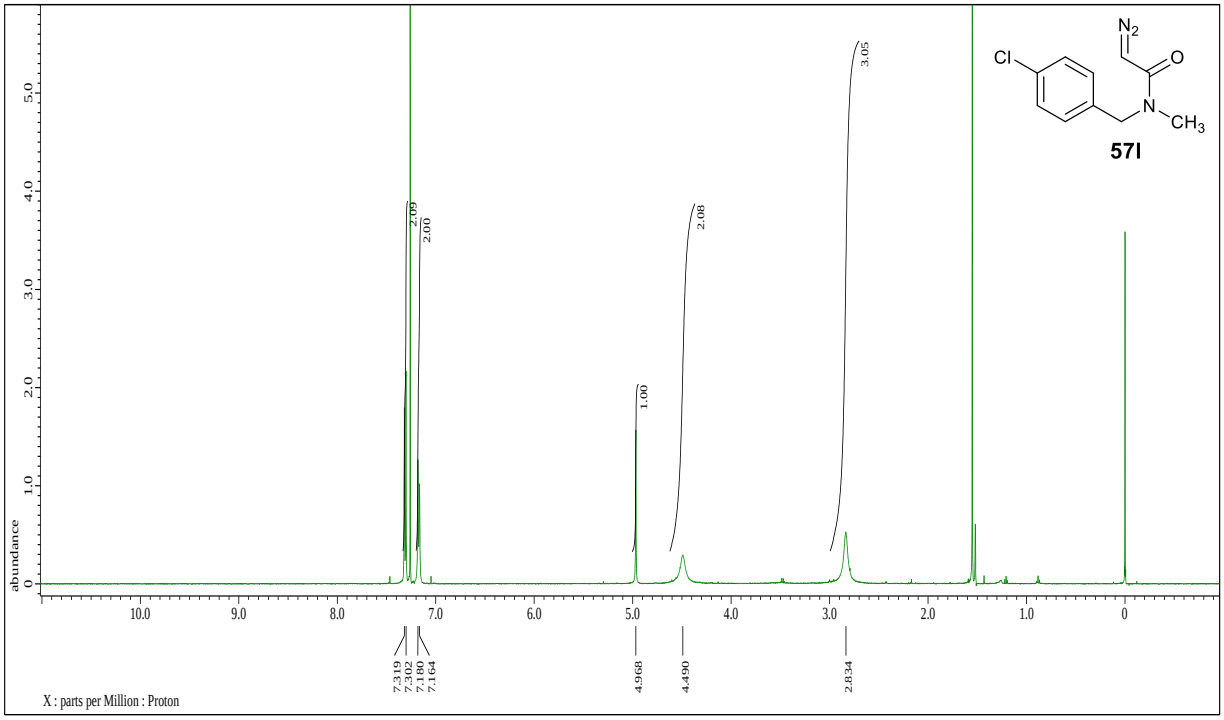

Figure 99. ^{1}HNMR spectral of 2-diazo-*N*-(4-chlorobenzyl)-*N*-methylacetamide.

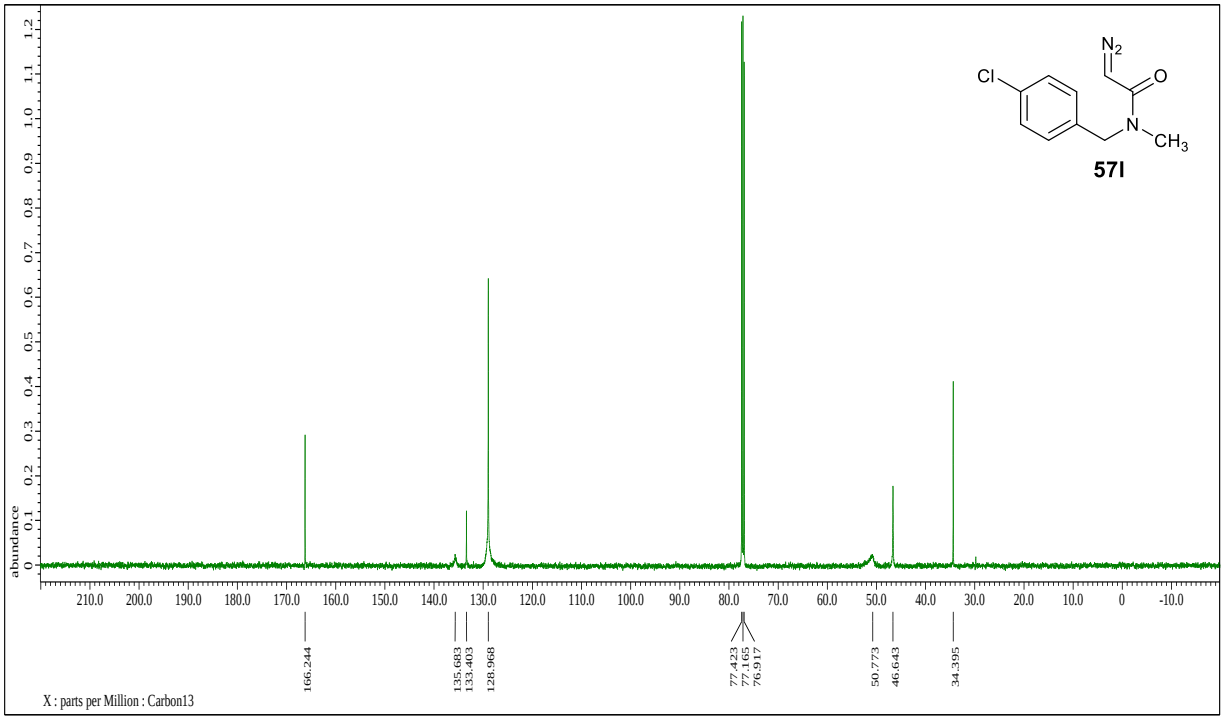

Figure 100. ^{13}CNMR spectral of 2-diazo-*N*-(4-chlorobenzyl)-*N*-methylacetamide

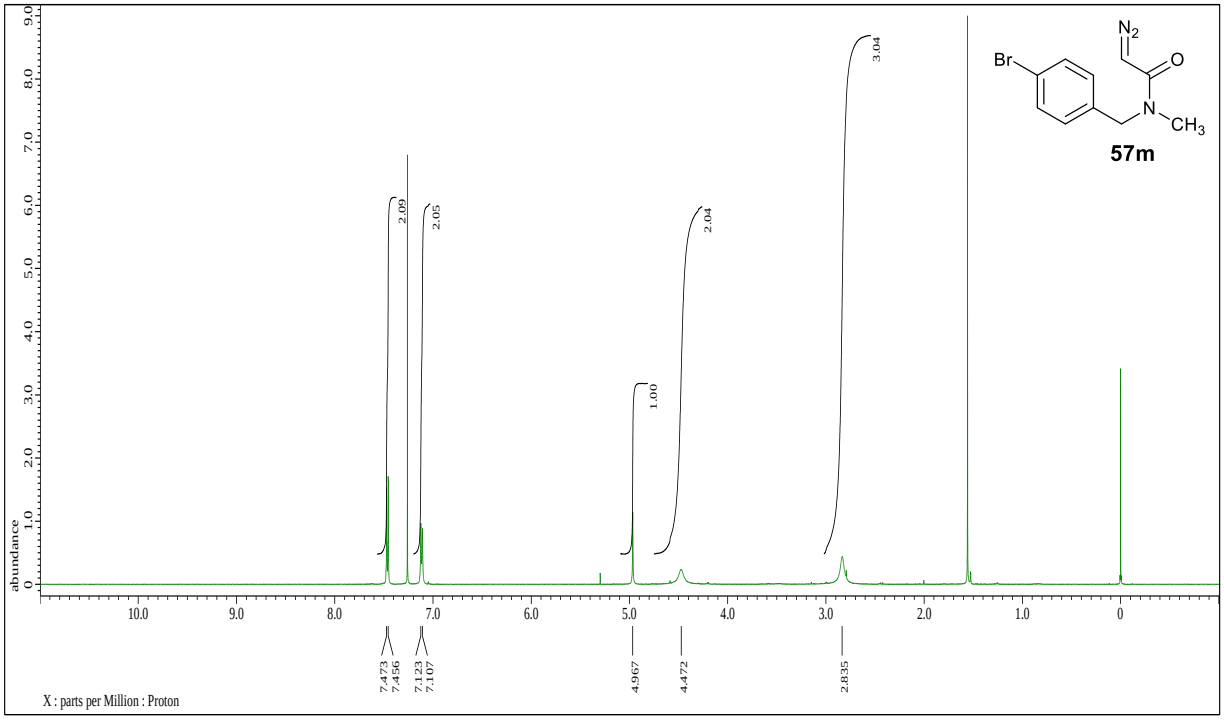

Figure 101. ^{1}HNMR spectral of 2-diazo-*N*-(4-bromobenzyl)-*N*-methylacetamide.

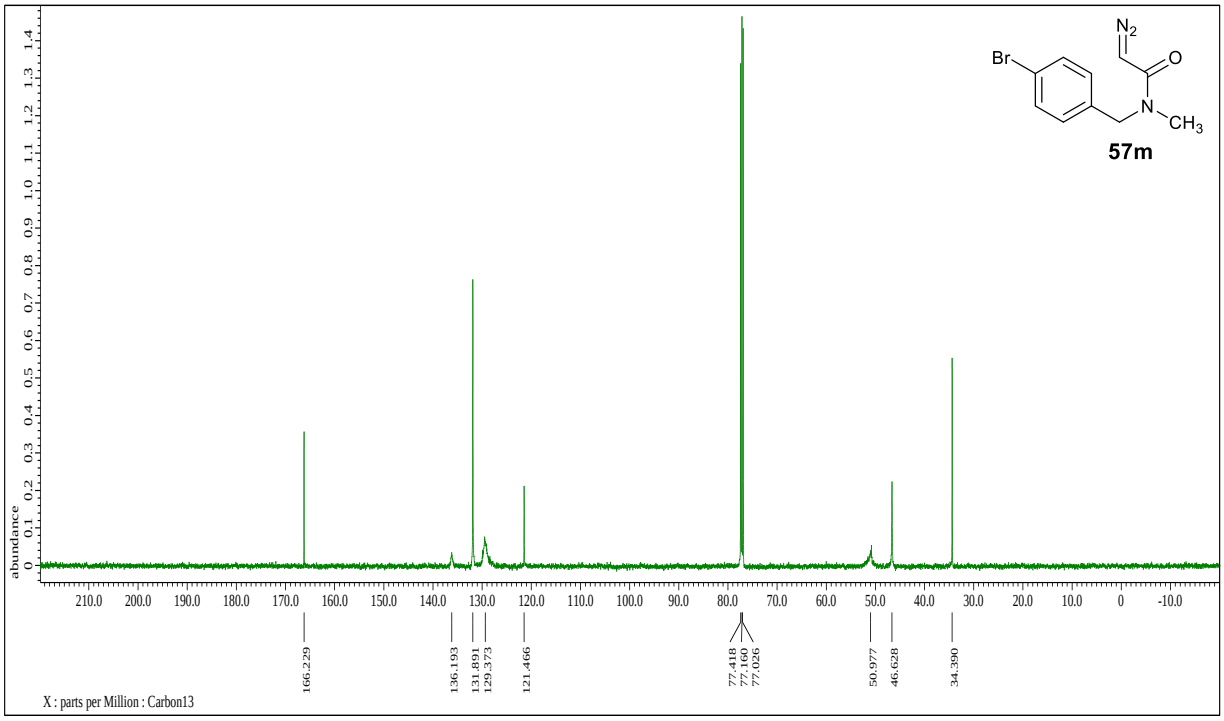

Figure 102. ^{13}CNMR spectral of 2-diazo-*N*-(4-bromobenzyl)-*N*-methylacetamide.

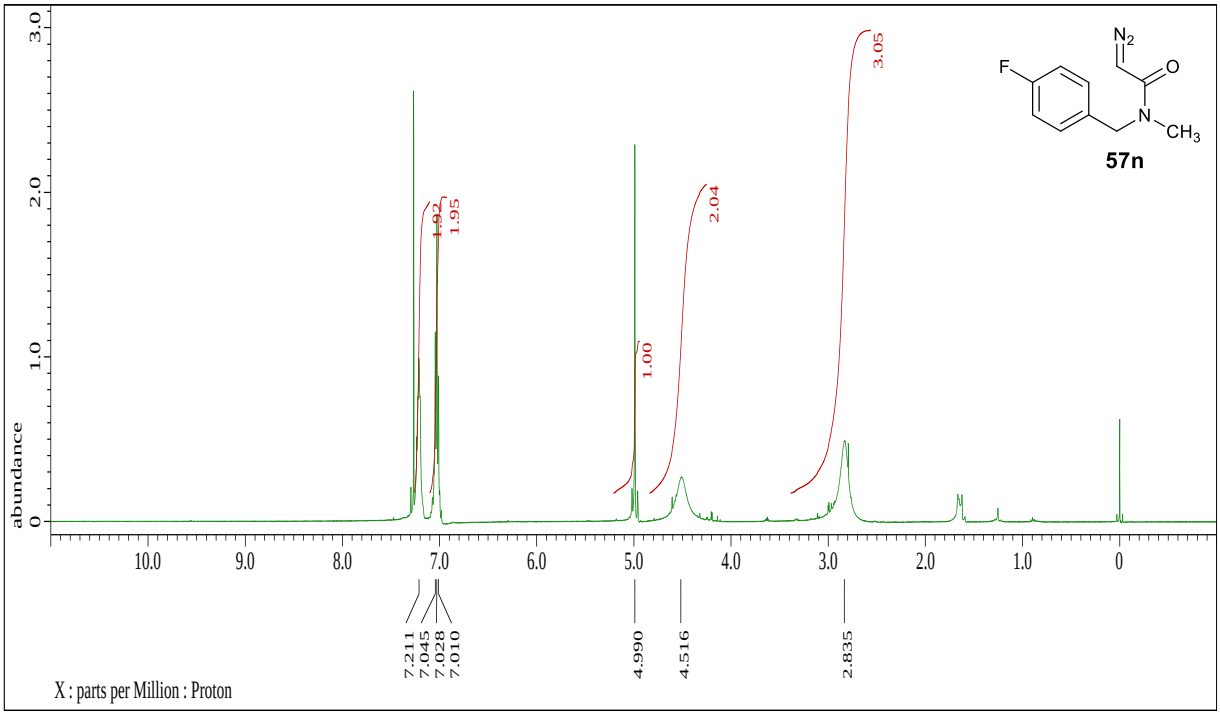

Figure 103. ^{1}HNMR spectral of 2-diazo-*N*-(4-flourobenzyl)-*N*-methylacetamide.

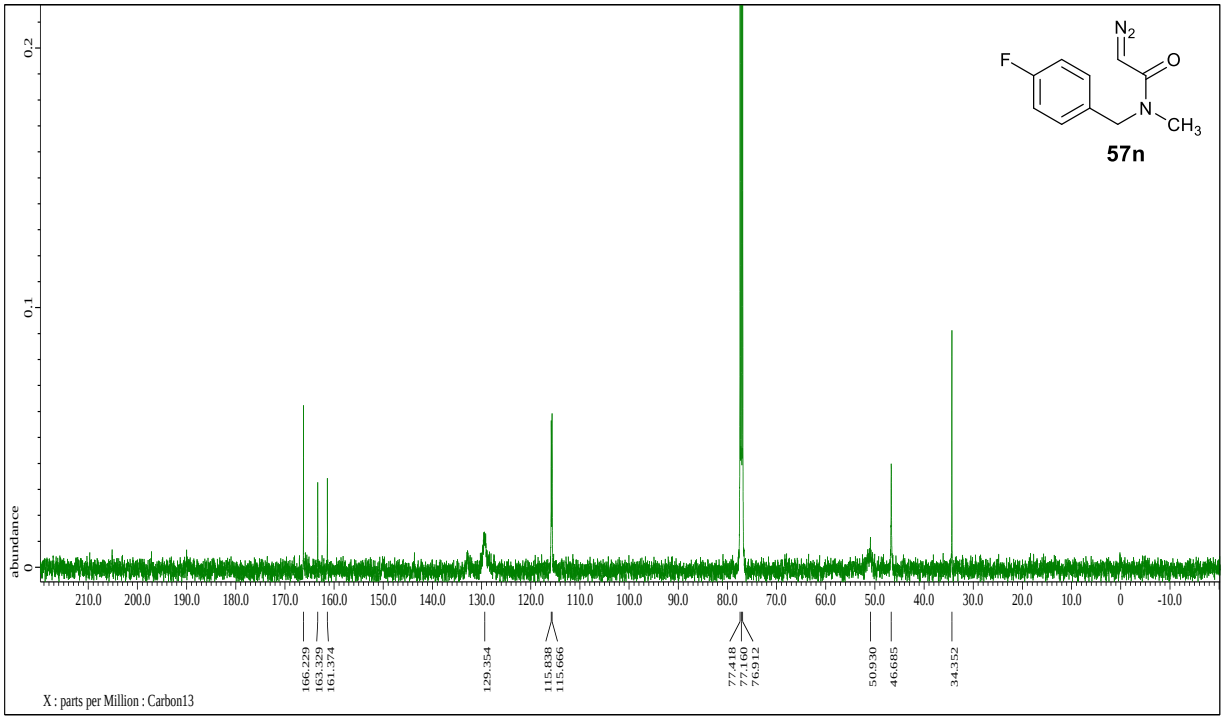

Figure 104. ^{13}CNMR spectral of 2-diazo-*N*-(4-flourobenzyl)-*N*-methylacetamide.

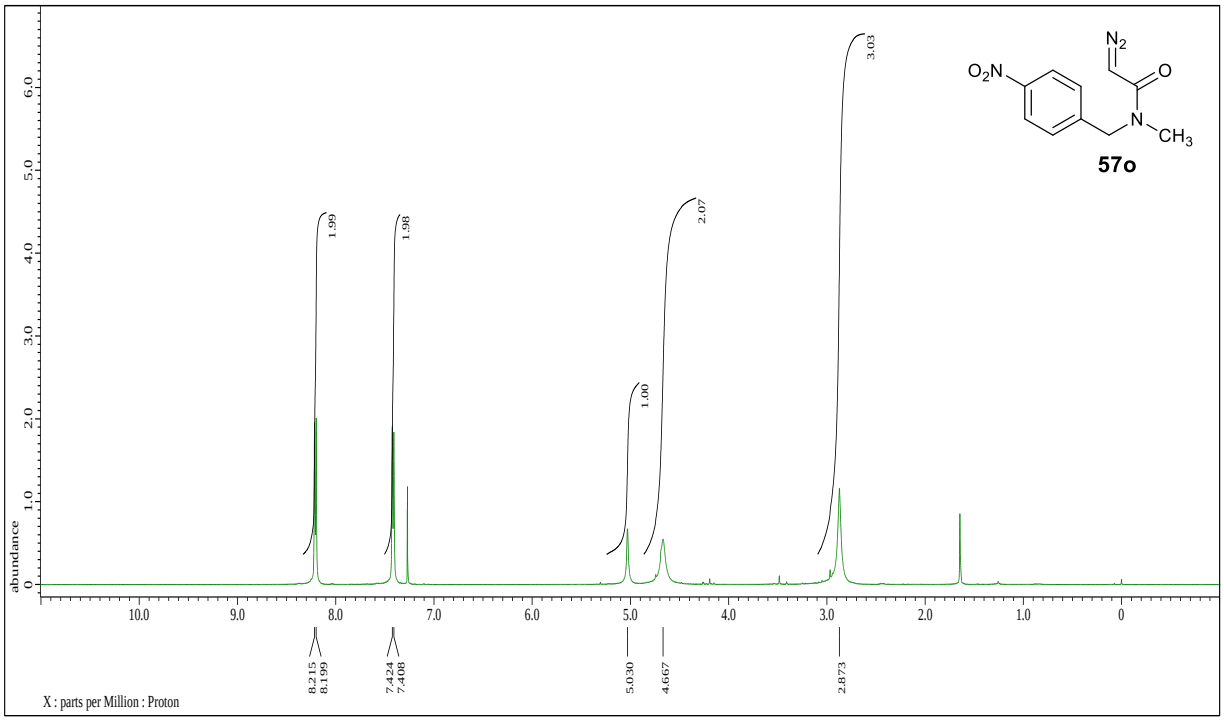

Figure 105. ^{1}HNMR spectral of 2-diazo-N-(4-nitrobenzyl)-*N*-methylacetamide.

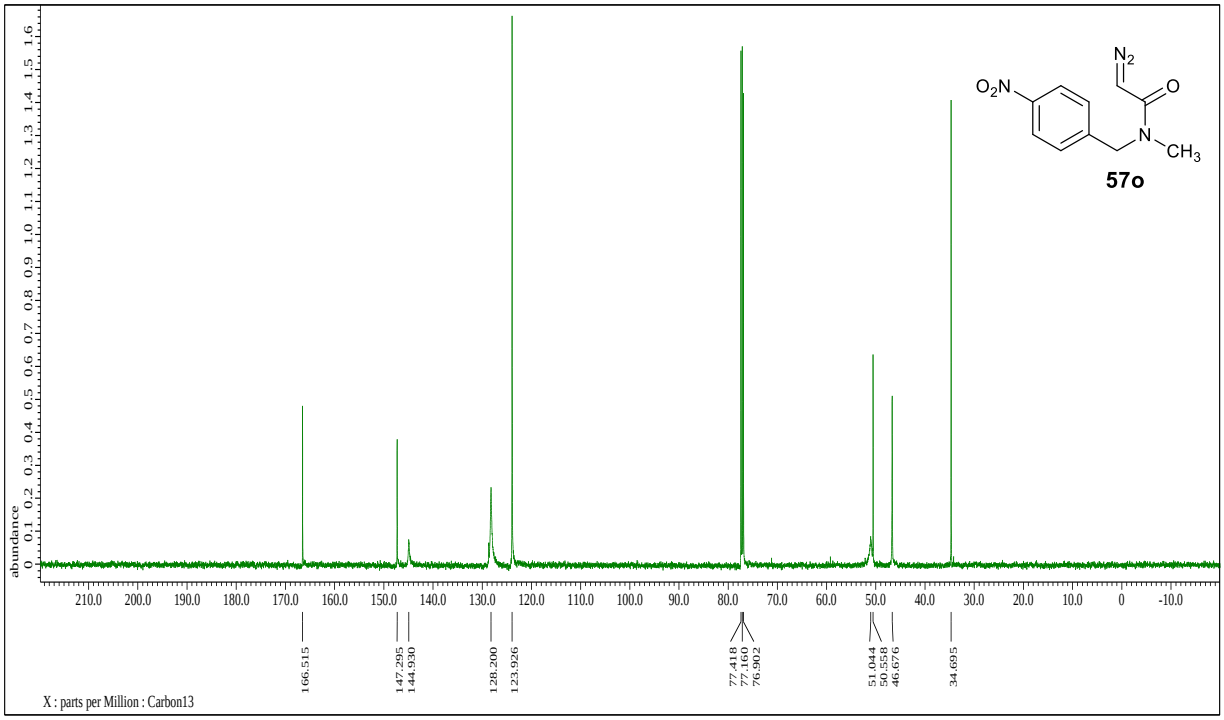

Figure 106. ^{13}CNMR spectral of 2-diazo-N-(4-nitrobenzyl)-*N*-methylacetamide.

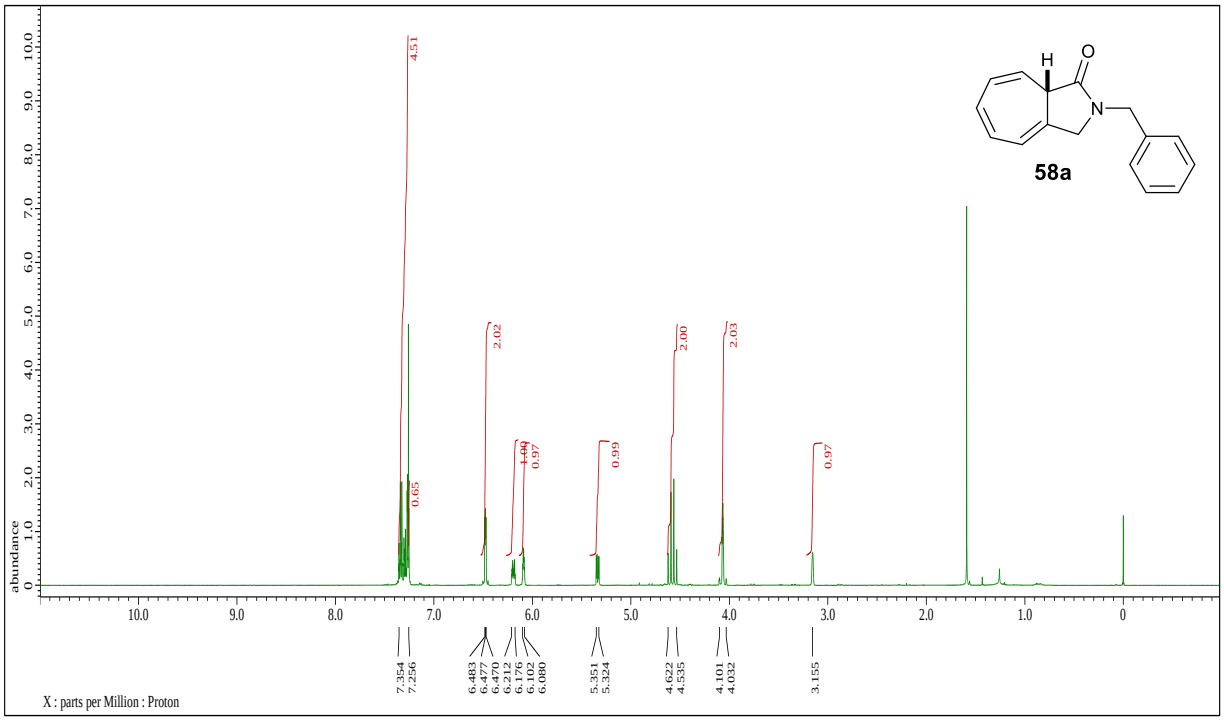

Figure 107. ^{1}HNMR spectral of (*S*)-2-benzyl-3,8a-dihydrocyclohepta[c]pyrrol-1(2H)-one.

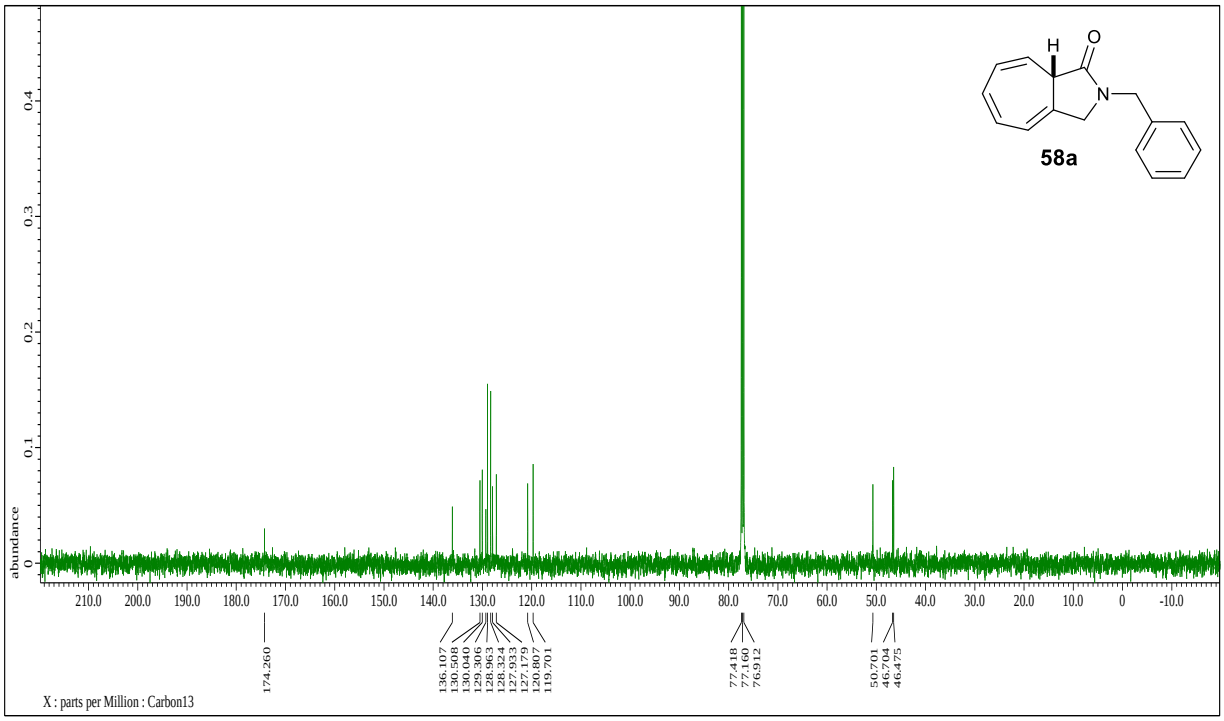

Figure 108. ^{13}CNMR spectral of (*S*)-2-benzyl-3,8a-dihydrocyclohepta[c]pyrrol-1(2H)-one.

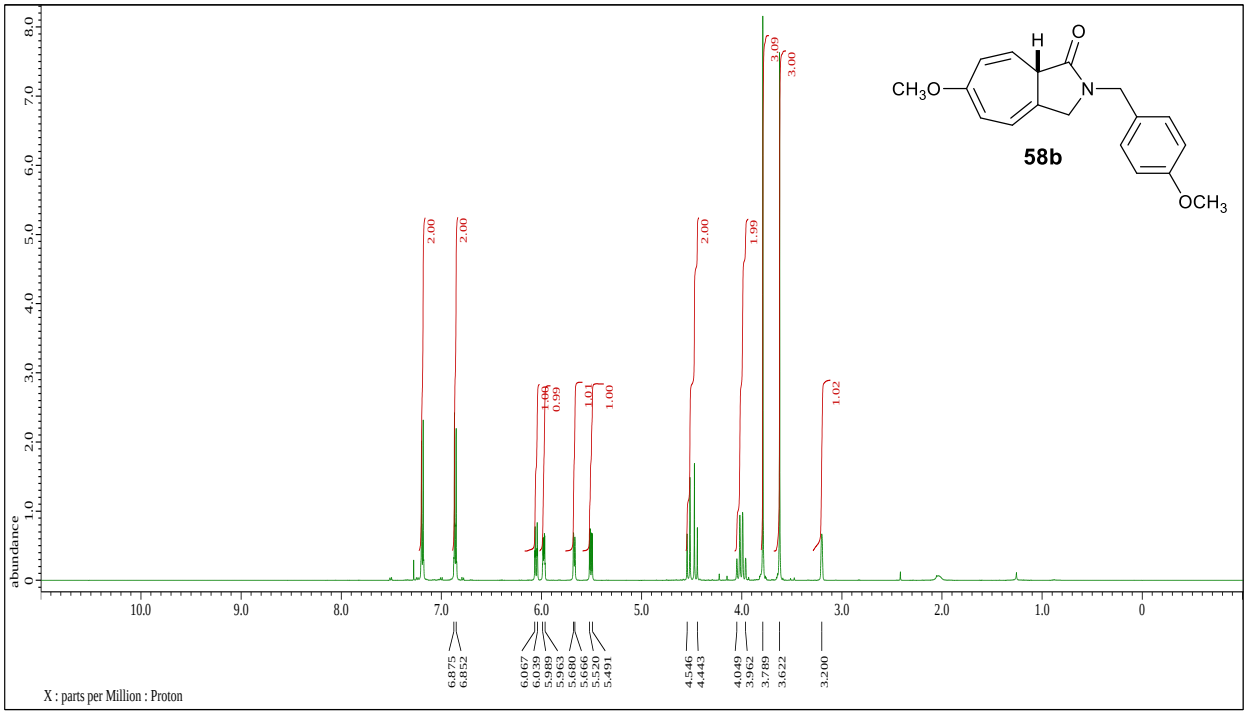

Figure 109. ^{1}HNMR spectral of (*S*)-6-methoxy-2-(4-methoxybenzyl)-3,8a-dihydrocyclohepta [c]pyrrol-1(2H)-one.

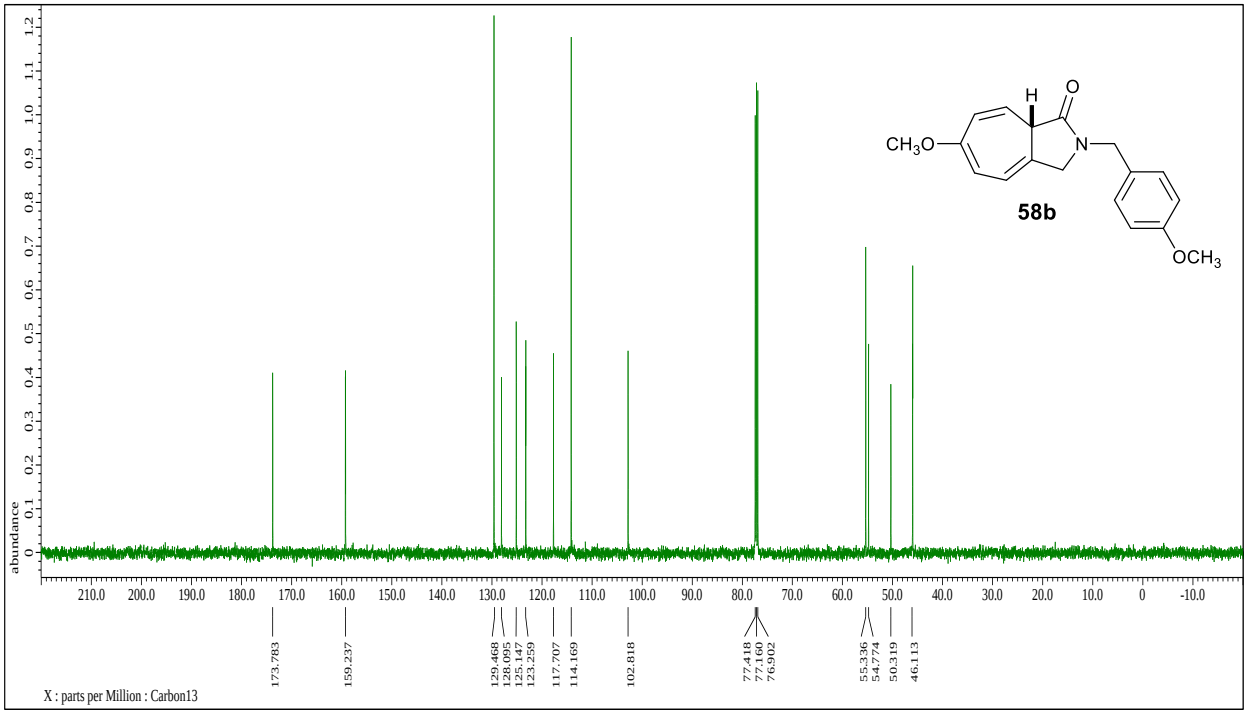

Figure 110. ^{13}CNMR spectral of (*S*)-6-methoxy-2-(4-methoxybenzyl)-3,8a-dihydrocyclohepta [c]pyrrol-1(2H)-one.

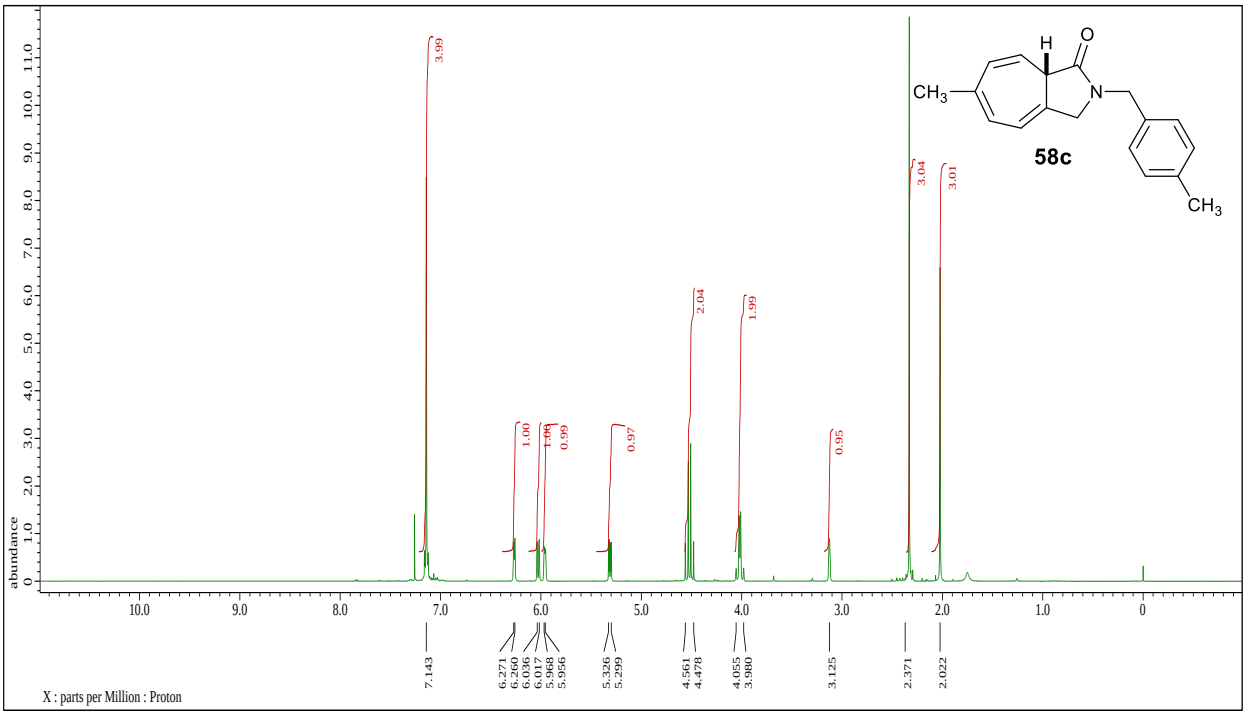

Figure 111. ^{1}HNMR spectral of (*S*)-6-methyl-2-(4-methylbenzyl)-3,8a-dihydrocyclohepta [c]pyrrol-1(2H)-one.

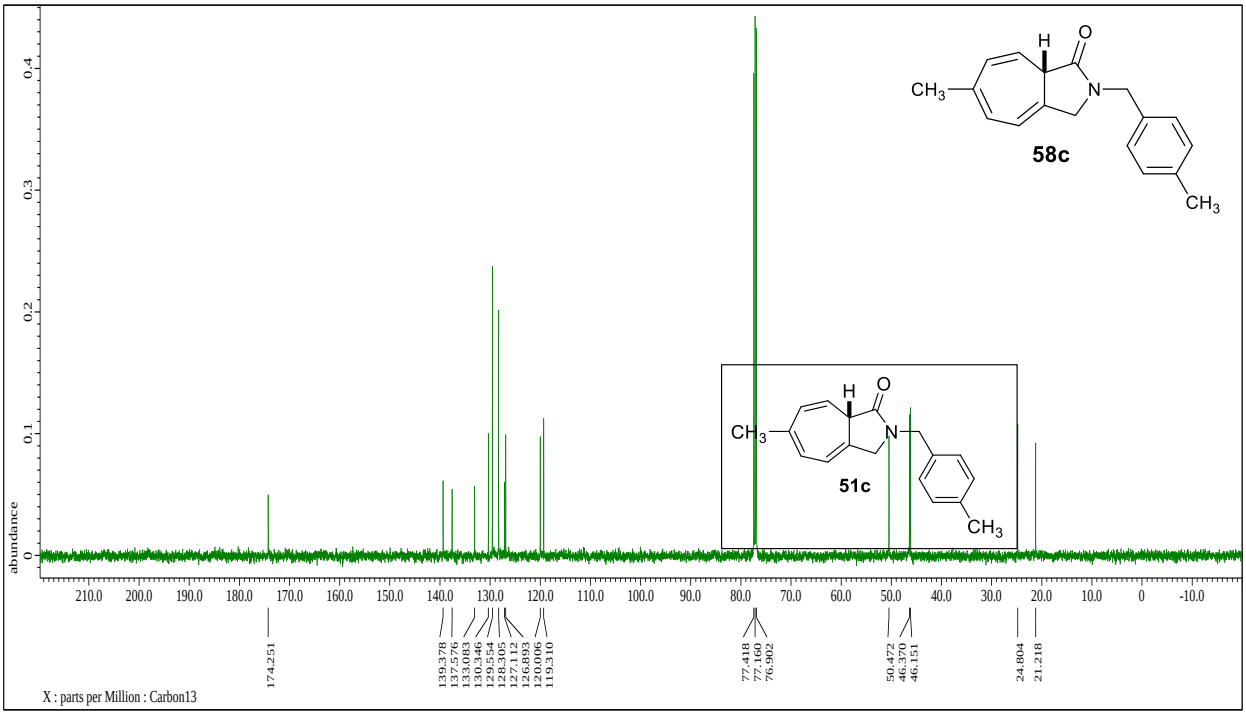

Figure 112. ^{13}CNMR spectral of (*S*)-6-methyl-2-(4-methylbenzyl)-3,8a-dihydrocyclohepta[c] pyrrol-1(2H)-one.

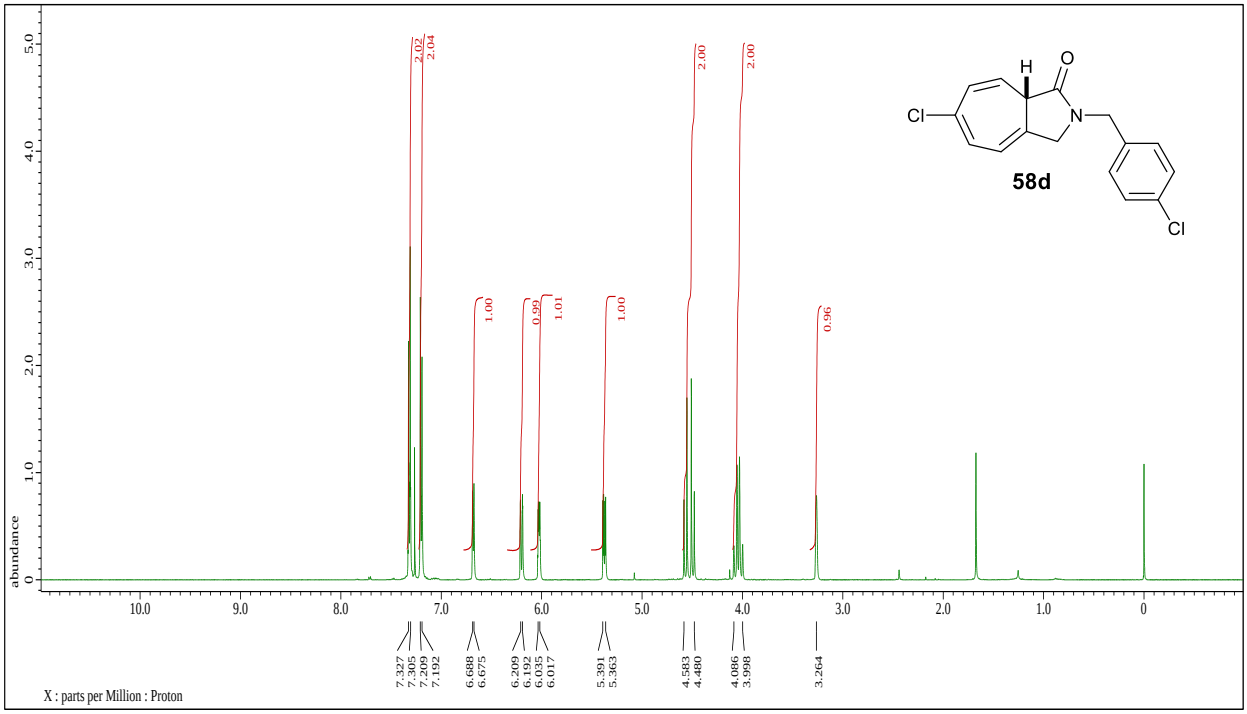

Figure 113. ^{1}HNMR spectral of (*S*)-6-chloro-2-(4-chlorobenzyl)-3,8adihydrocyclohepta[c]pyrrol -1(2H)-one.

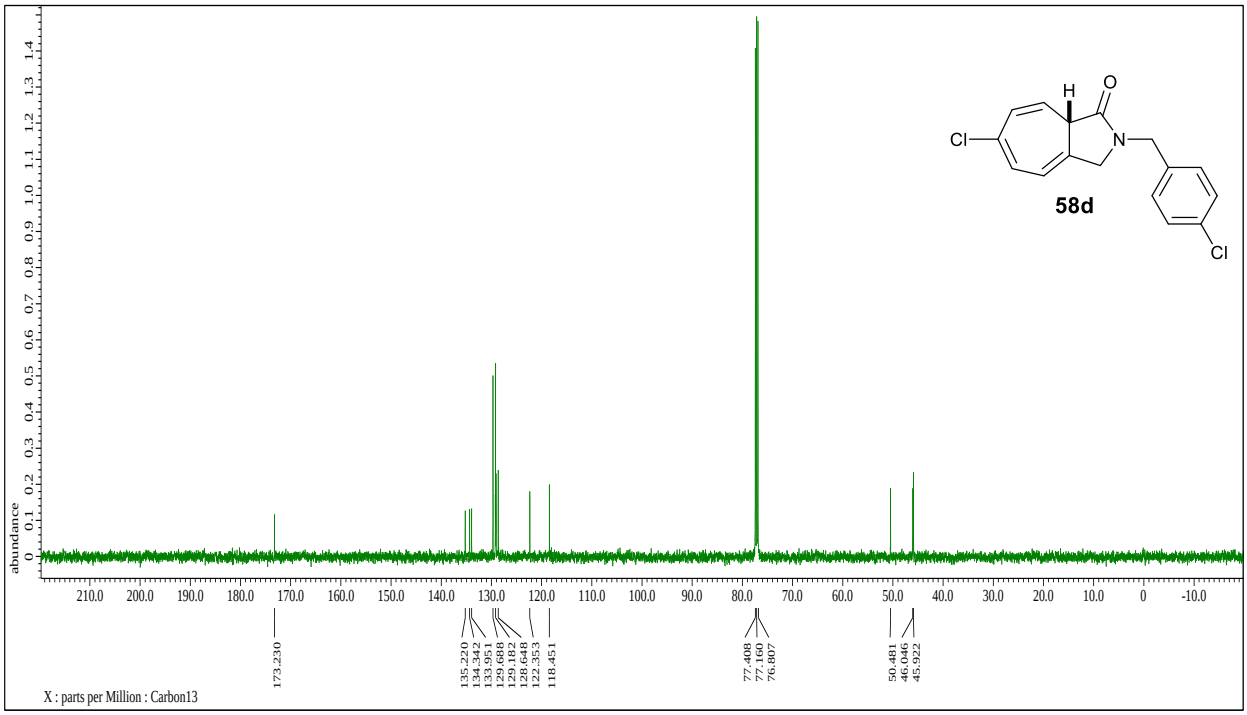

Figure 114. ^{13}CNMR spectral of (*S*)-6-chloro-2-(4-chlorobenzyl)-3,8adihydrocyclohepta[c] pyrrol-1(2H)-one.

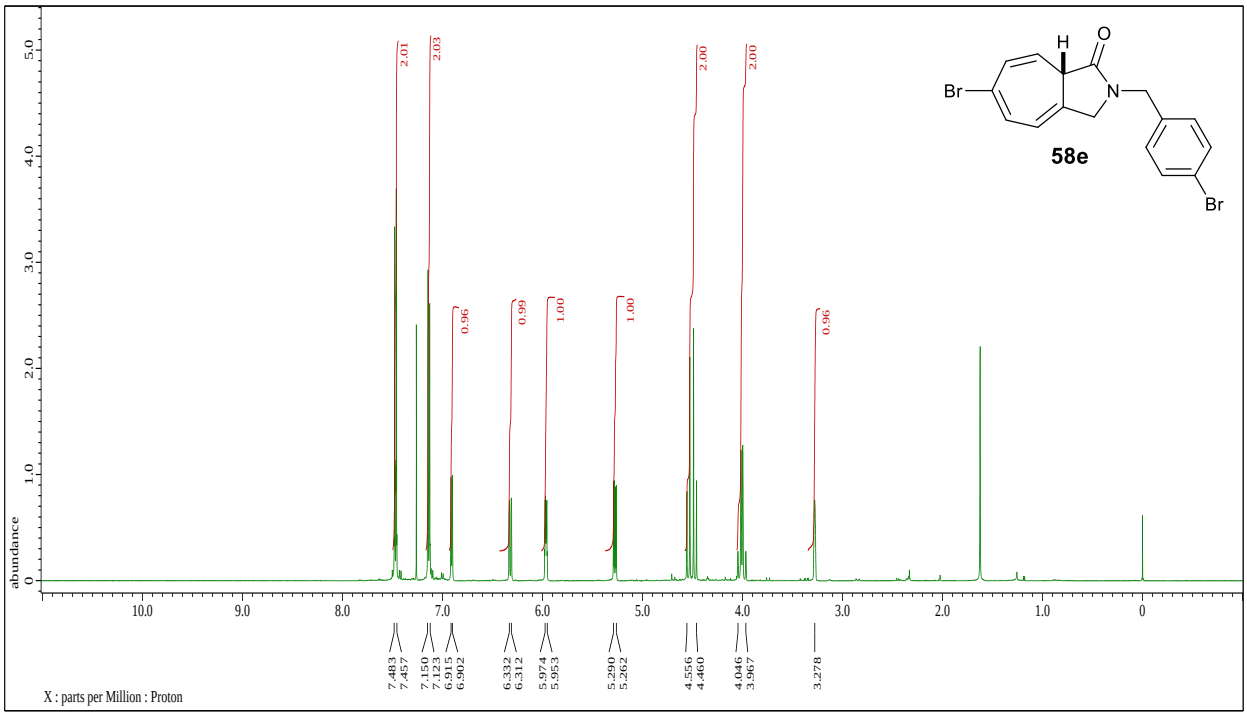

Figure 115. ^{1}HNMR spectral of (*S*)-6-bromo-2-(4-bromobenzyl)-3,8a-dihydrocyclohepta[c] pyrrol-1(2H)-one.

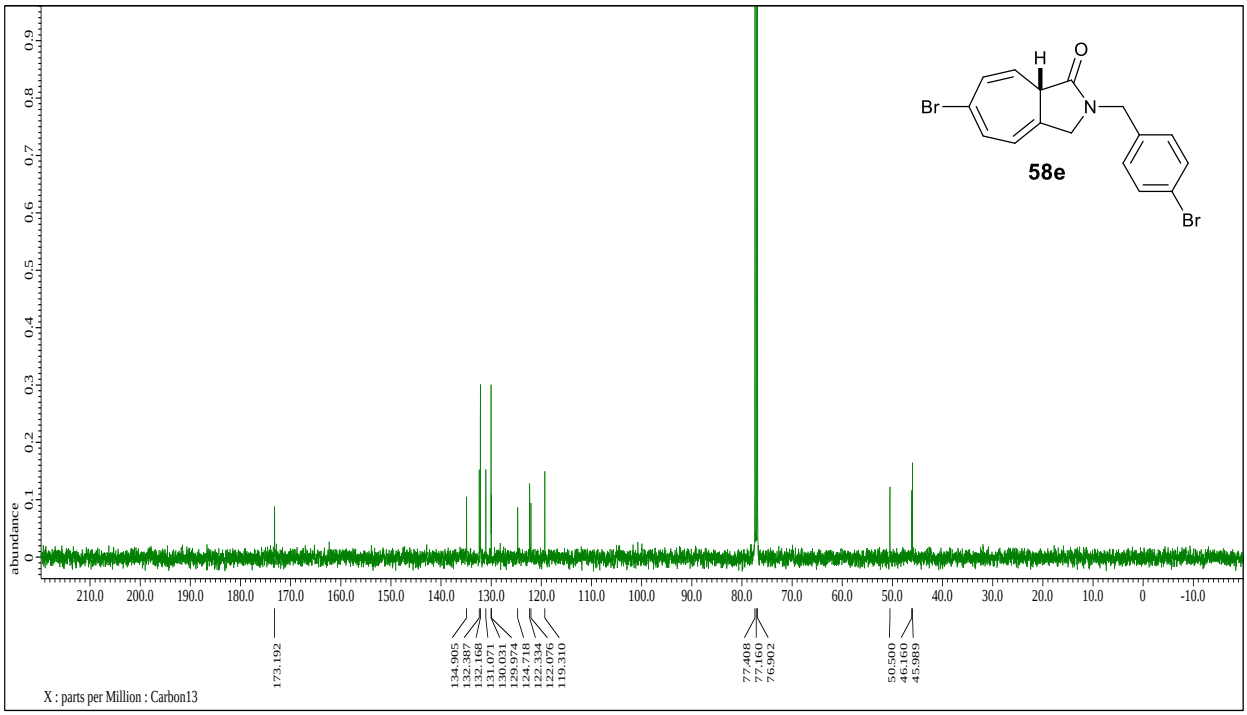

Figure 116. ^{13}CNMR spectral of(*S*)-6-bromo-2-(4-bromobenzyl)-3,8a-dihydrocyclohepta[c] pyrrol-1(2H)-one.

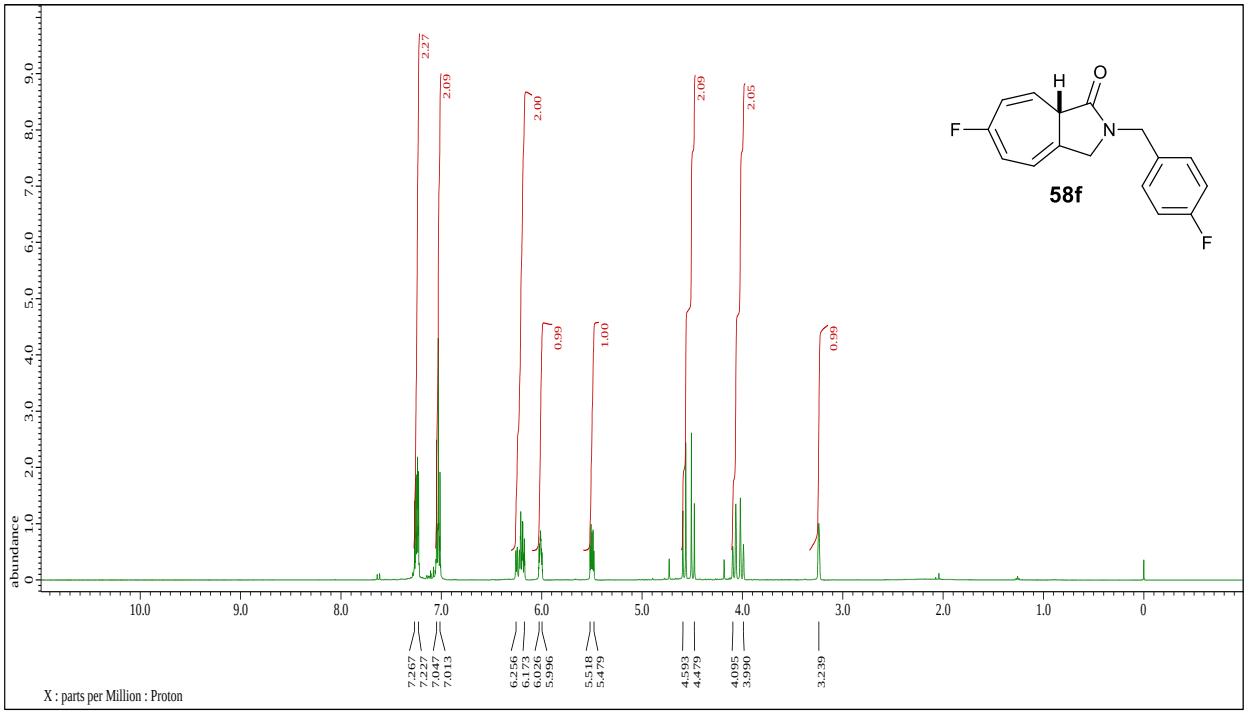

Figure 117. ^{1}HNMR spectral of (*S*)-6-fluoro-2-(4-fluorobenzyl)-3,8a-dihydrocyclohepta[c] pyrrol-1(2H)-one.

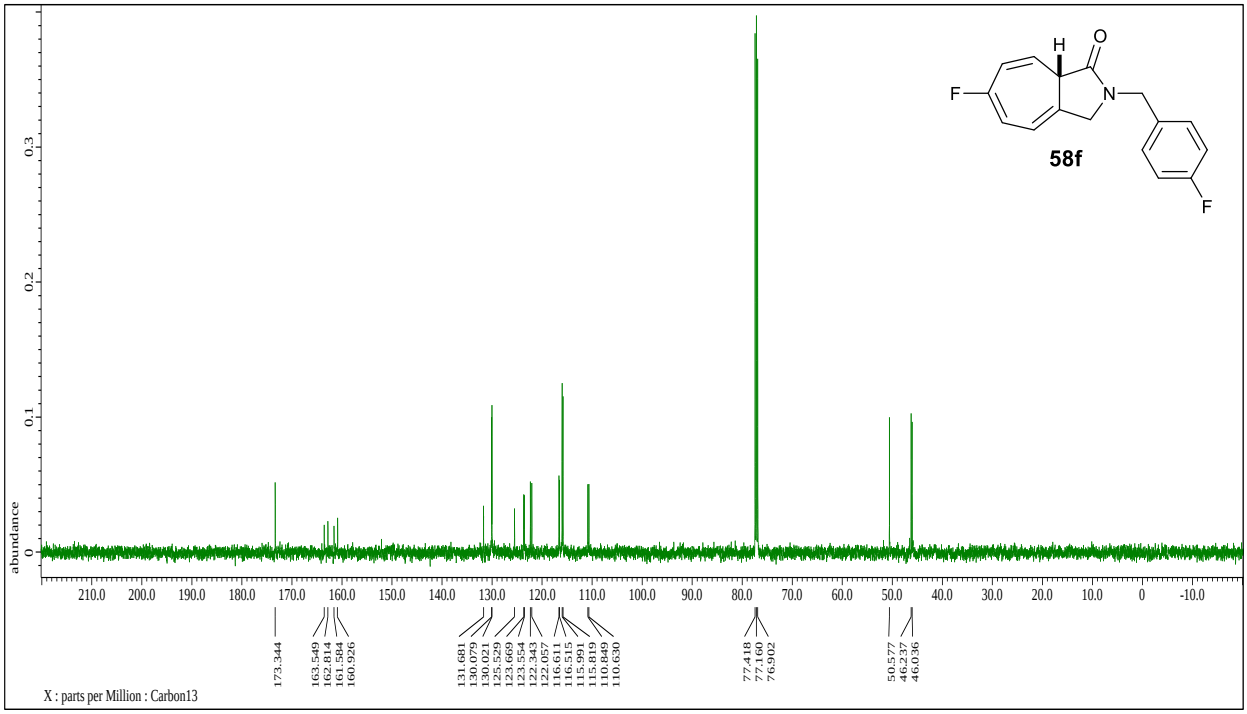

Figure 118. ^{13}CNMR spectral of (*S*)-6-fluoro-2-(4-fluorobenzyl)-3,8a-dihydrocyclohepta[c] pyrrol-1(2H)-one.

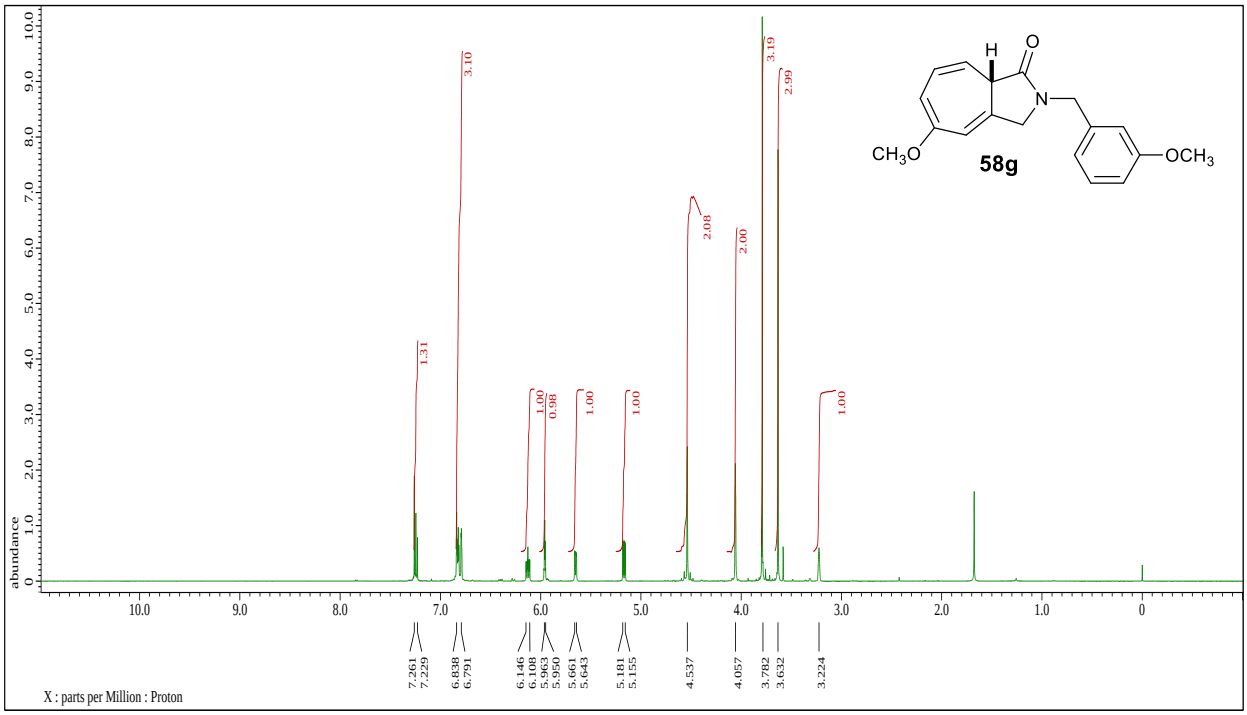

Figure 119. ^{1}HNMR spectral of (*S*)-5-Methoxy-2-(3-methoxybenzyl)-3,8a-dihydrocyclohepta[c] pyrrol-1(2H)-one.

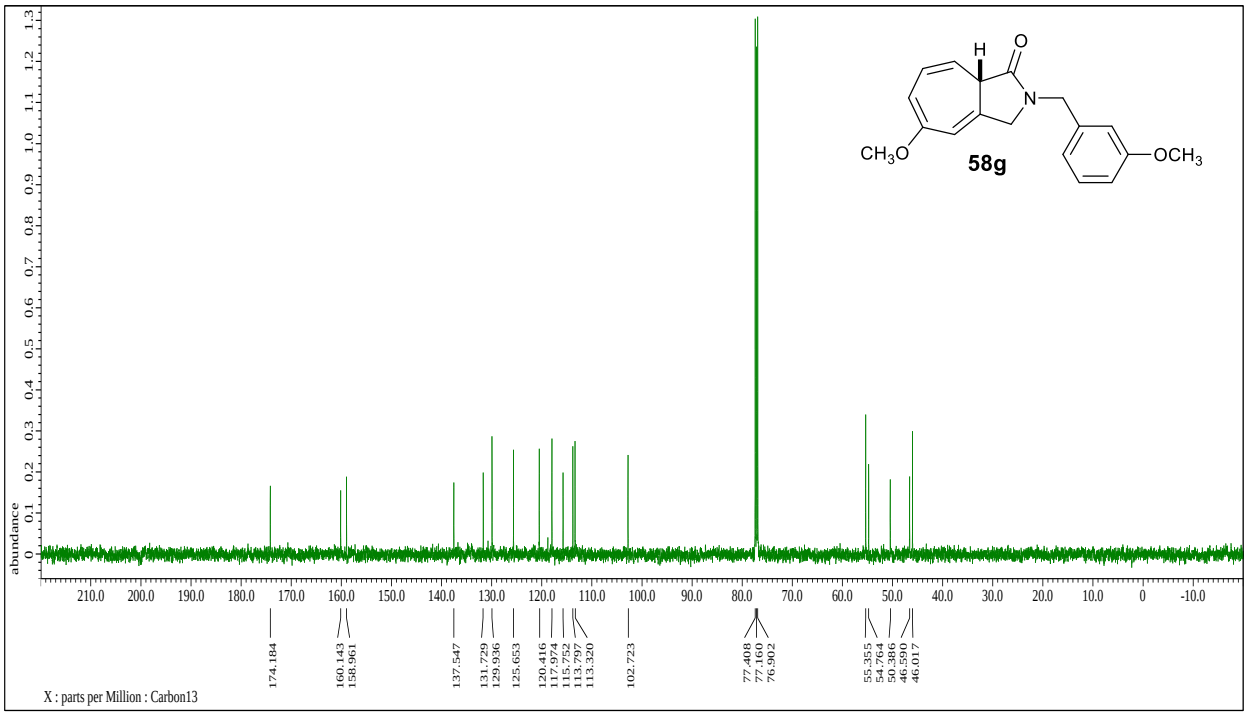

Figure 120. ^{13}CNMR spectral of (*S*)-5-Methoxy-2-(3-methoxybenzyl)-3,8a-dihydrocyclohepta [c]pyrrol-1(2H)-one.

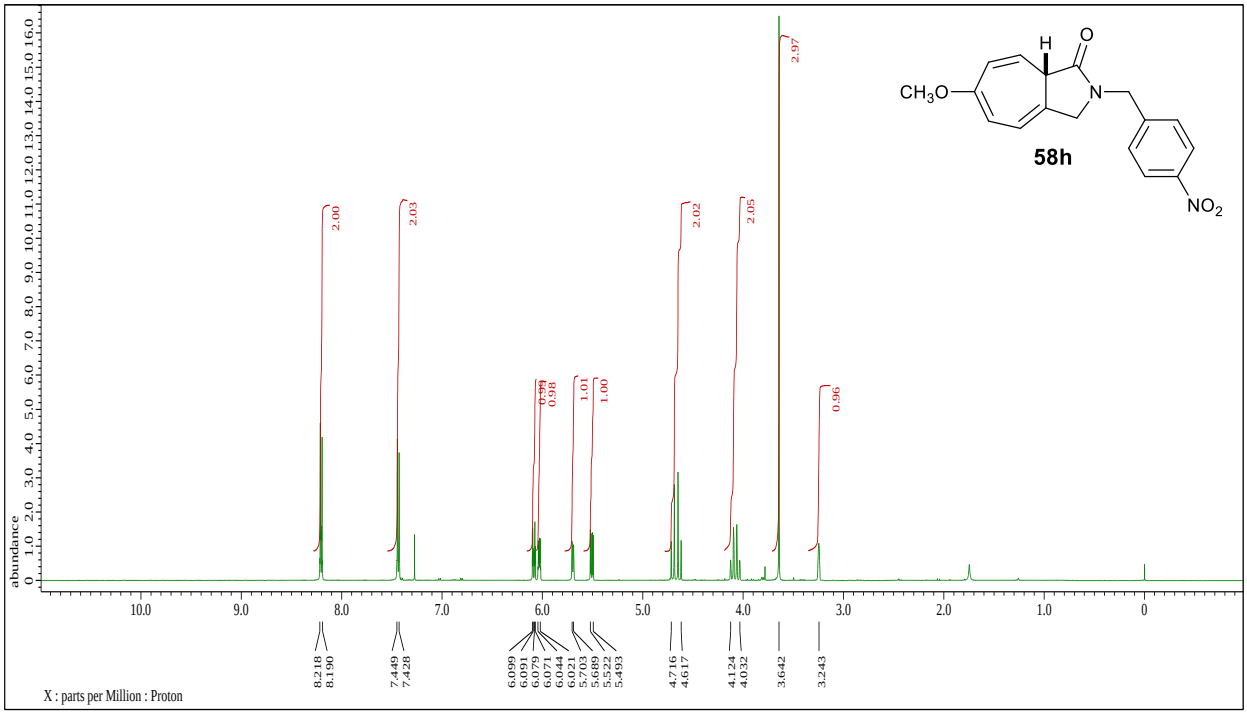

Figure 121. ^{1}HNMR spectral of (*S*)-6-methoxy-2-(4-nitrobenzyl)-3,8a-dihydrocyclohepta[c] pyrrol-1(2H)-one.

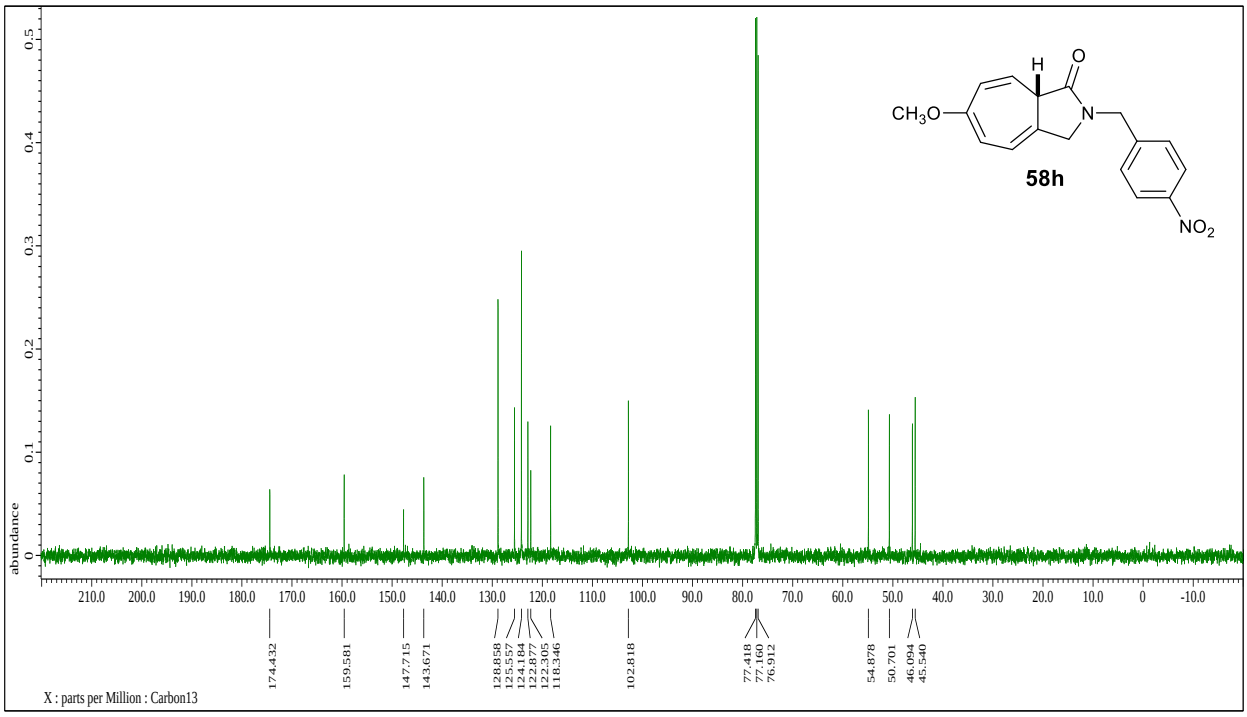

Figure 122. ^{13}CNMR spectral of (*S*)-6-methoxy-2-(4-nitrobenzyl)-3,8a-dihydrocyclohepta[c] pyrrol-1(2H)-one.

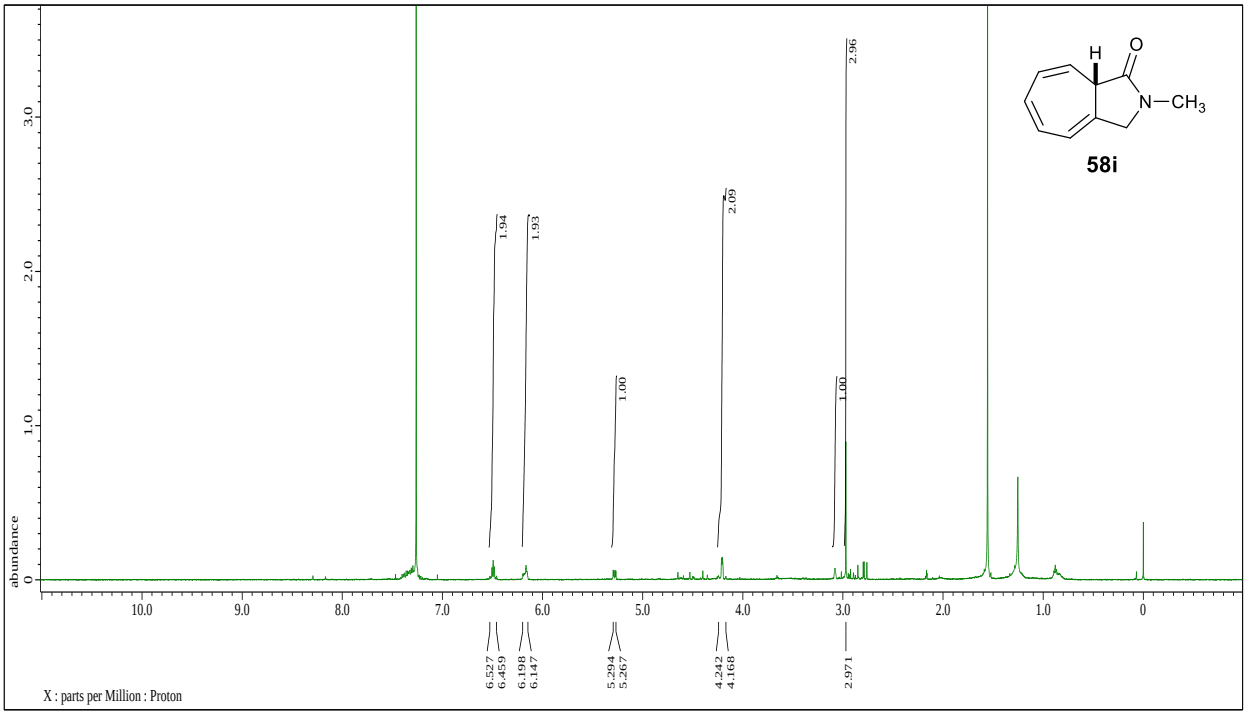

Figure 123. ^{1}HNMR spectral of (*S*)-2-methyl-3,8a-dihydrocyclohepta[c]pyrrol-1(2H)-one.

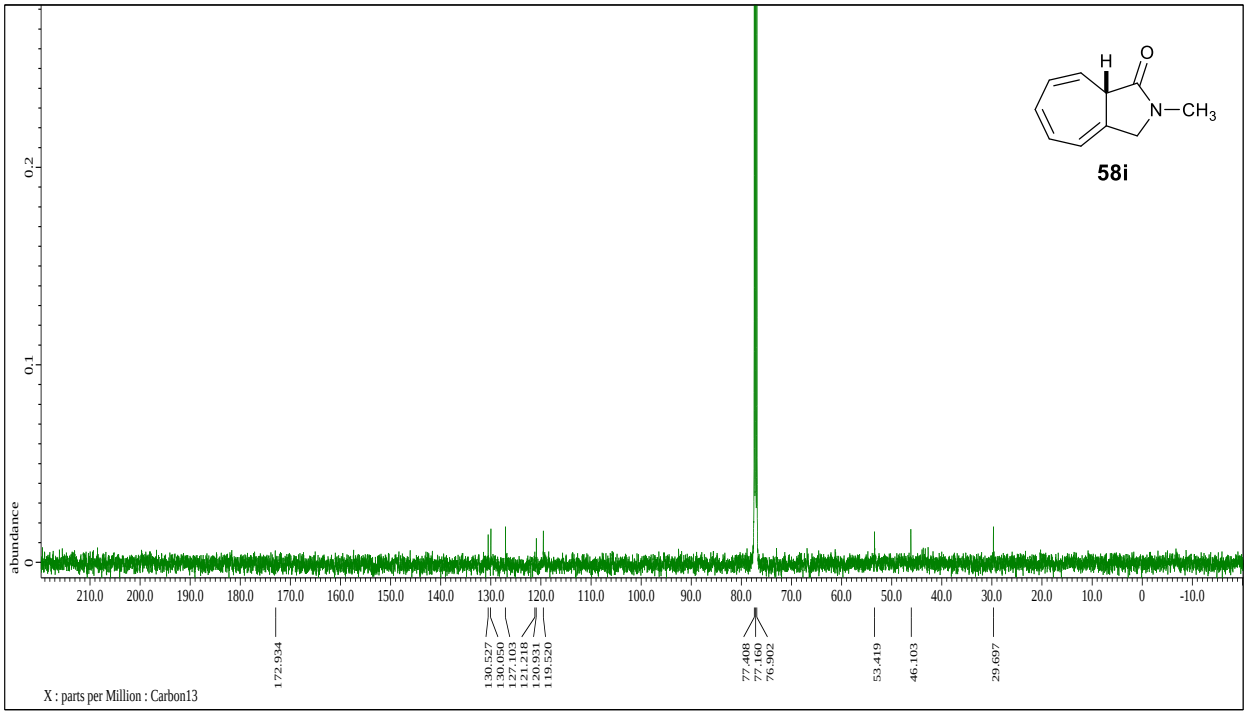

Figure 124. ^{13}CNMR spectral of (*S*)-2-methyl-3,8a-dihydrocyclohepta[c]pyrrol-1(2H)-one.

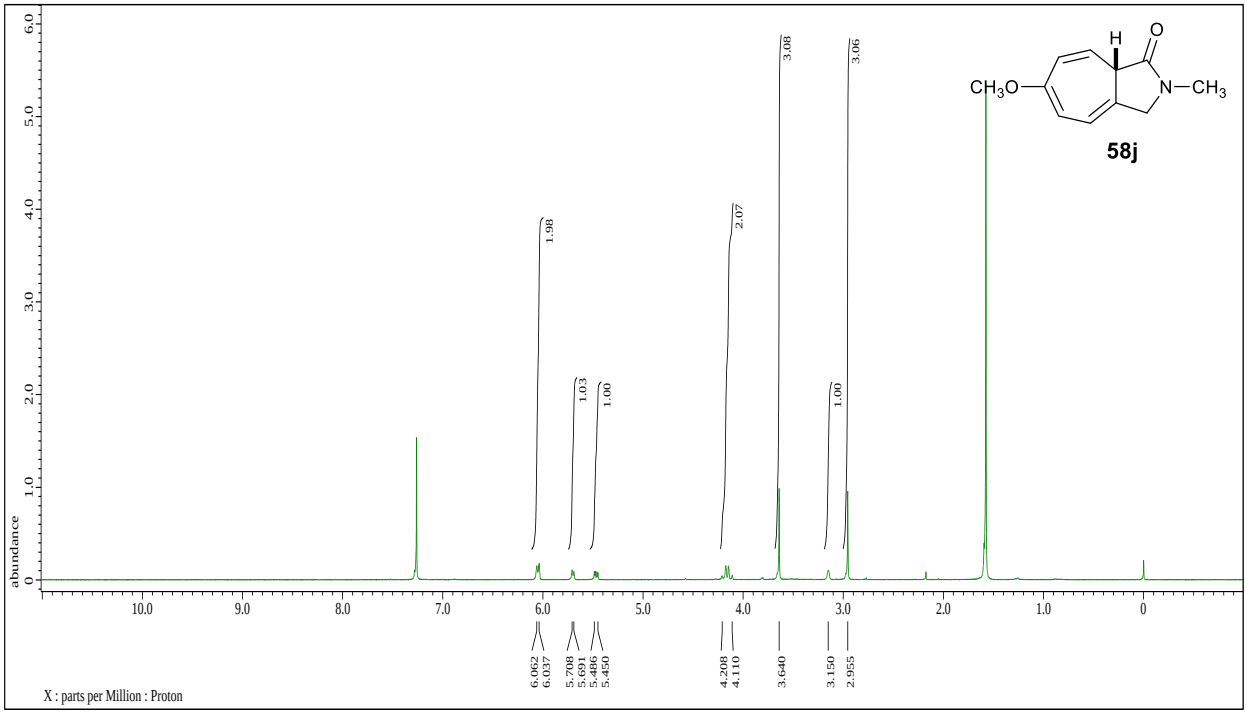

Figure 125. ^{1}HNMR spectral of (*S*)-6-methoxy-2-methyl-3,8a-dihydrocyclohepta[c]pyrrol-1(2H)-one.

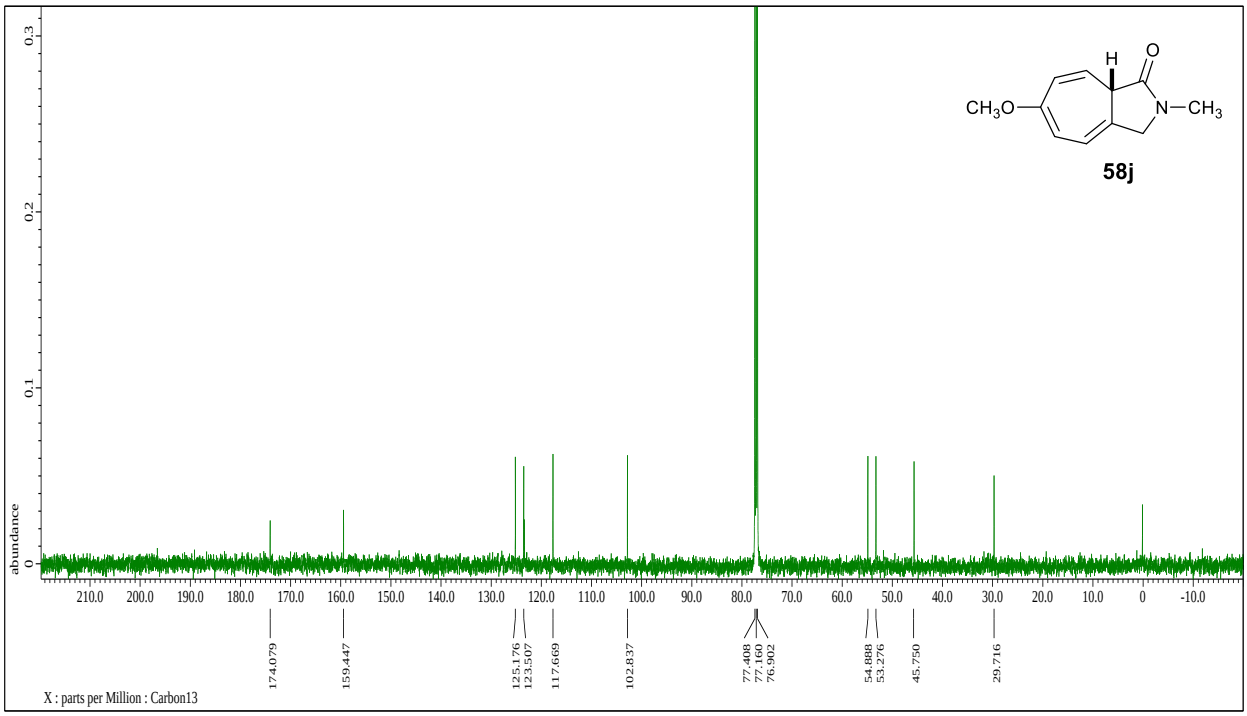

Figure 126. ^{13}CNMR spectral of (*S*)-6-methoxy-2-methyl-3,8a-dihydrocyclohepta[c]pyrrol-1(2H)-one.

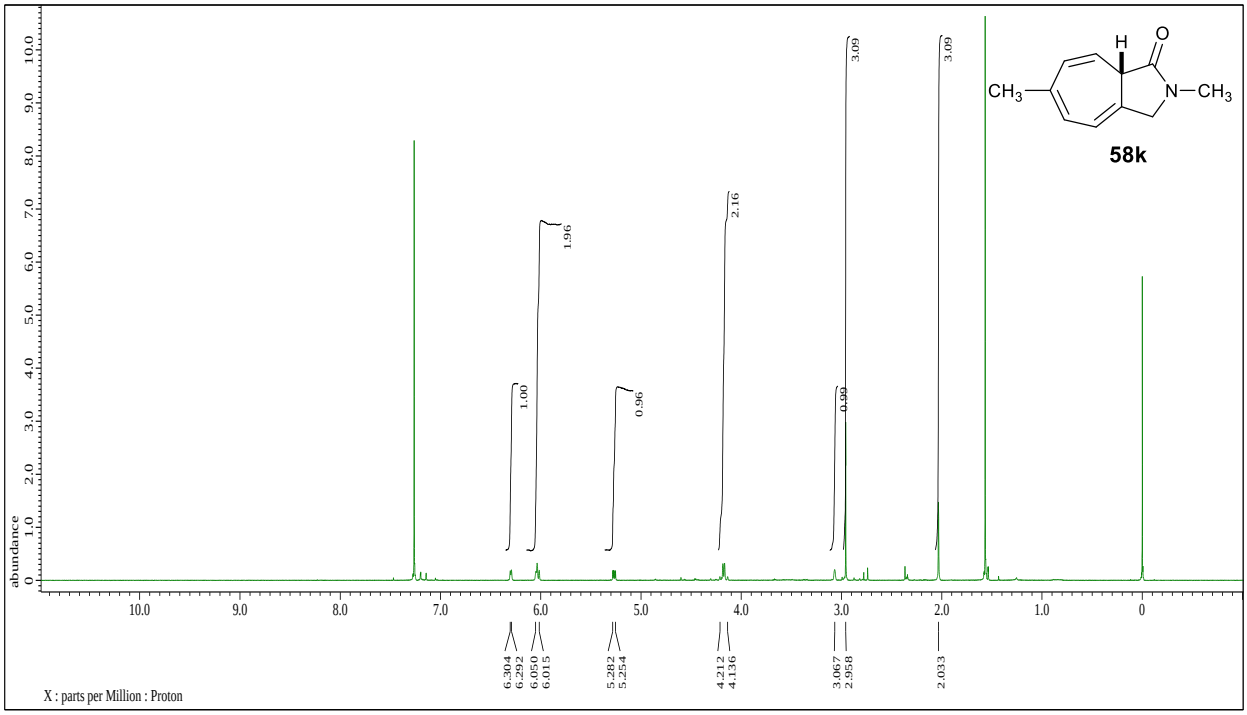

Figure 127. ^{1}HNMR spectral of **(*S*)**-2,6-dimethyl-3,8a-dihydrocyclohepta[c]pyrrol-1(2H)-one.

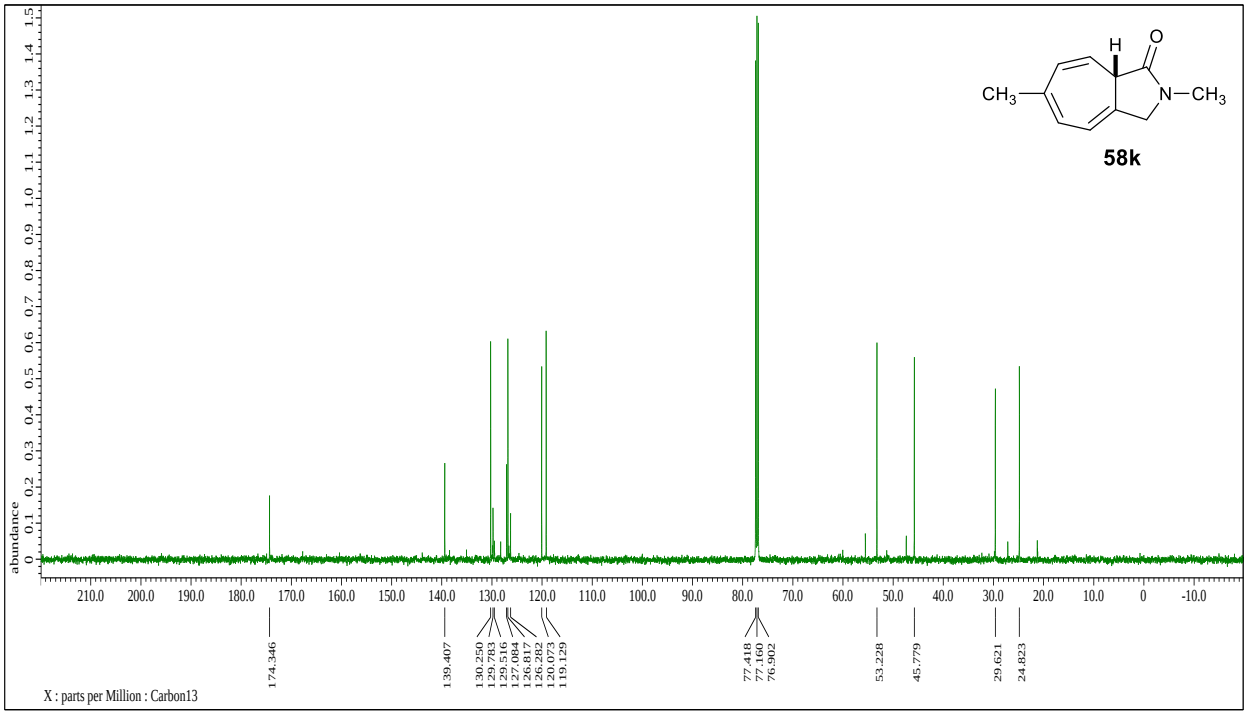

Figure 128. ^{13}CNMR spectral of **(*S*)**-2,6-dimethyl-3,8a-dihydrocyclohepta[c]pyrrol-1(2H)-one.

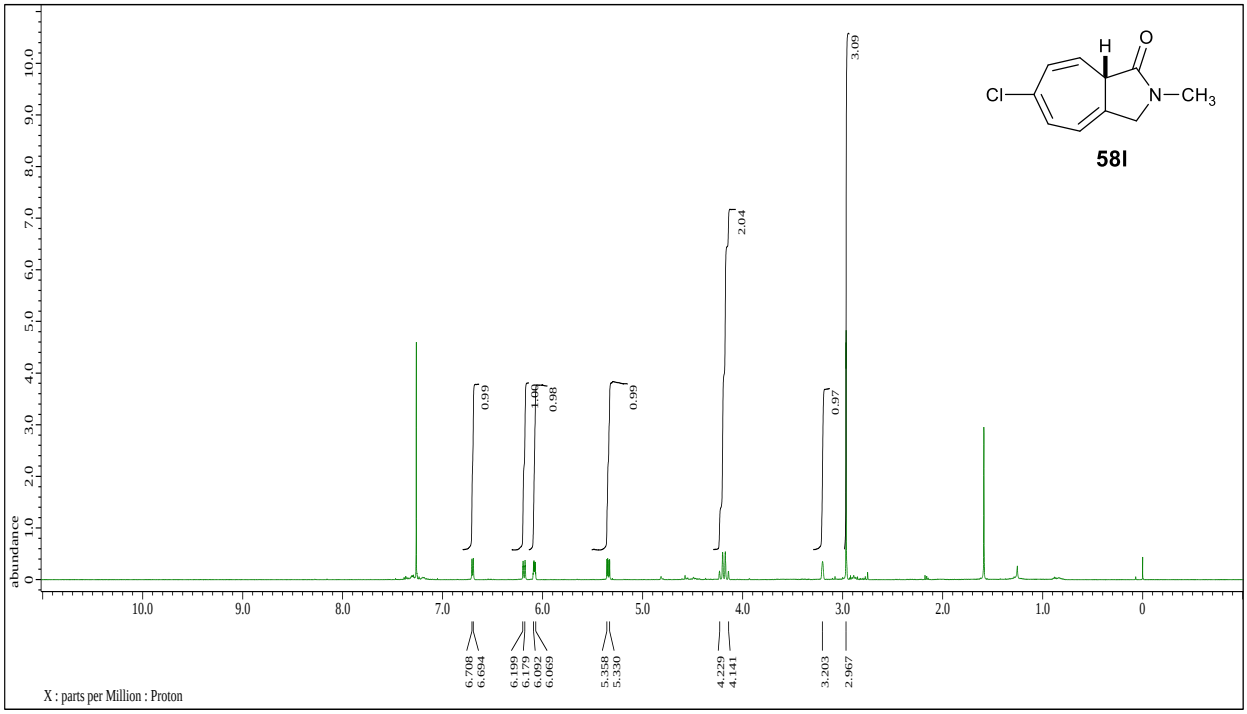

Figure 129. ^{1}HNMR spectral of (*S*)-6-Chloro-2-methyl-3,8a-dihydrocyclohepta[c]pyrrol-1(2H)-one.

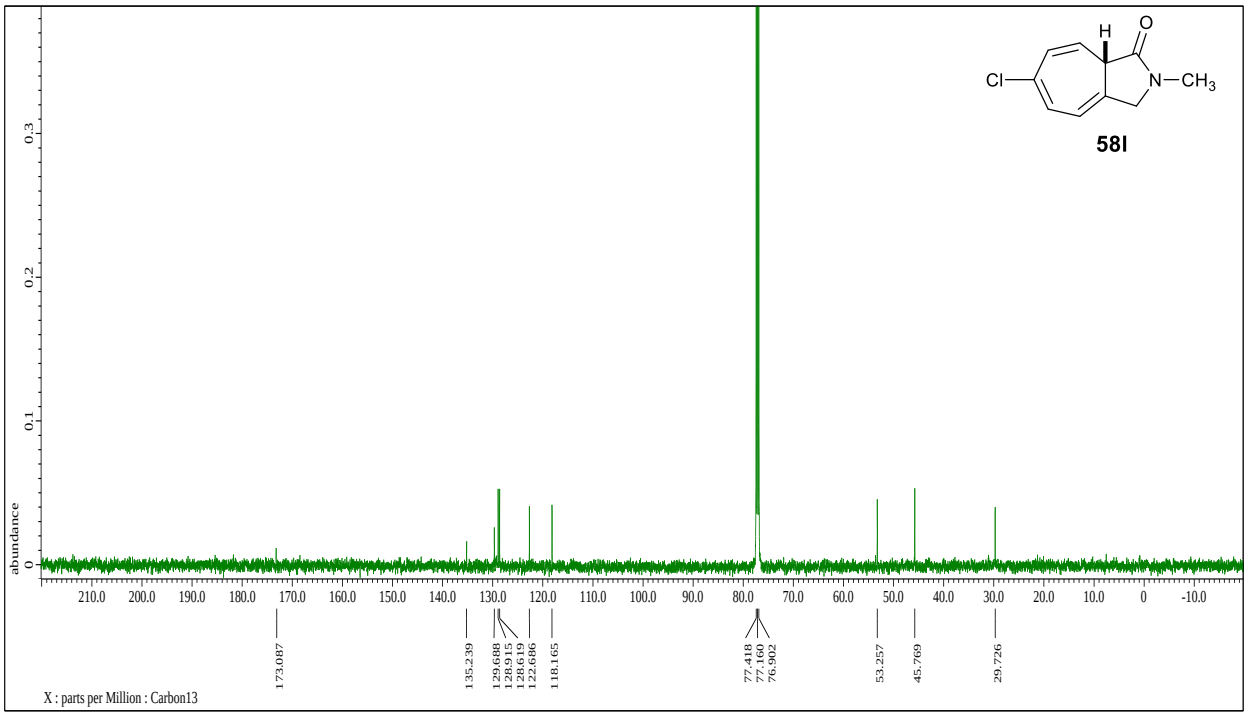

Figure 130. ^{13}CNMR spectral of (*S*)-6-Chloro-2-methyl-3,8a-dihydrocyclohepta[c]pyrrol-1(2H)-one.

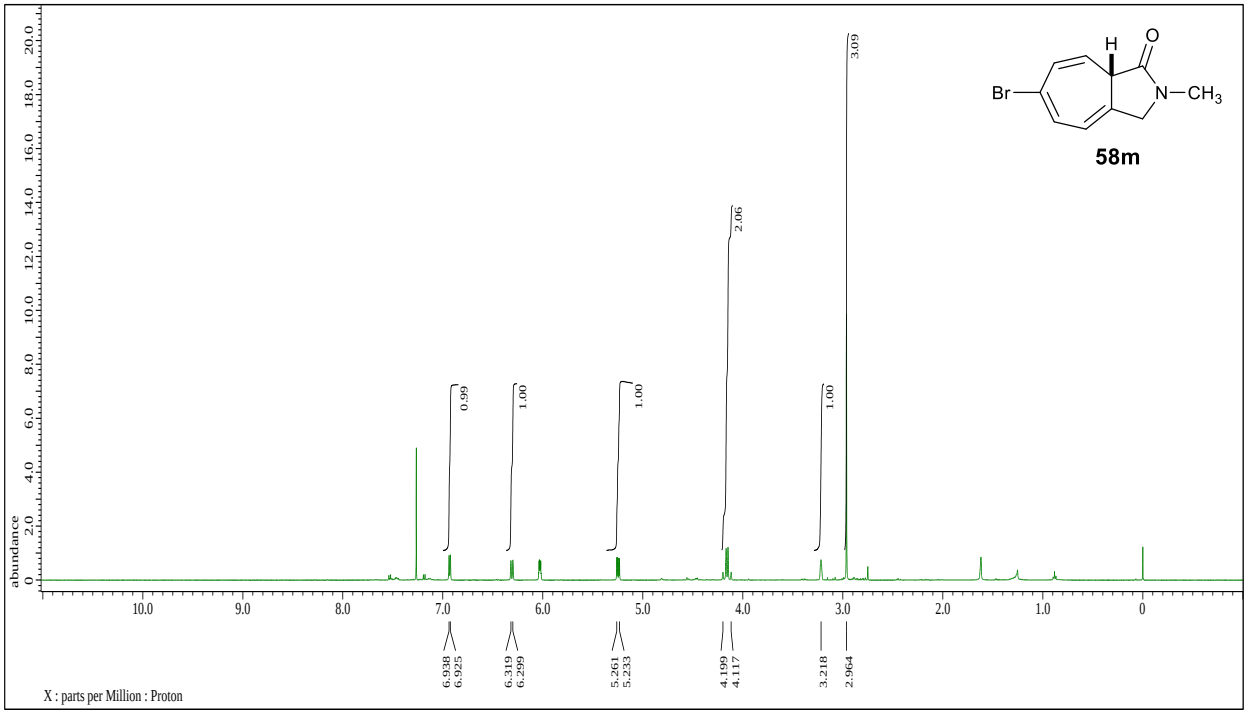

Figure 131. ^{1}HNMR spectral of (*S*)-6-bromo-2-methyl-3,8a-dihydrocyclohepta[c]pyrrol-1(2H)-one.

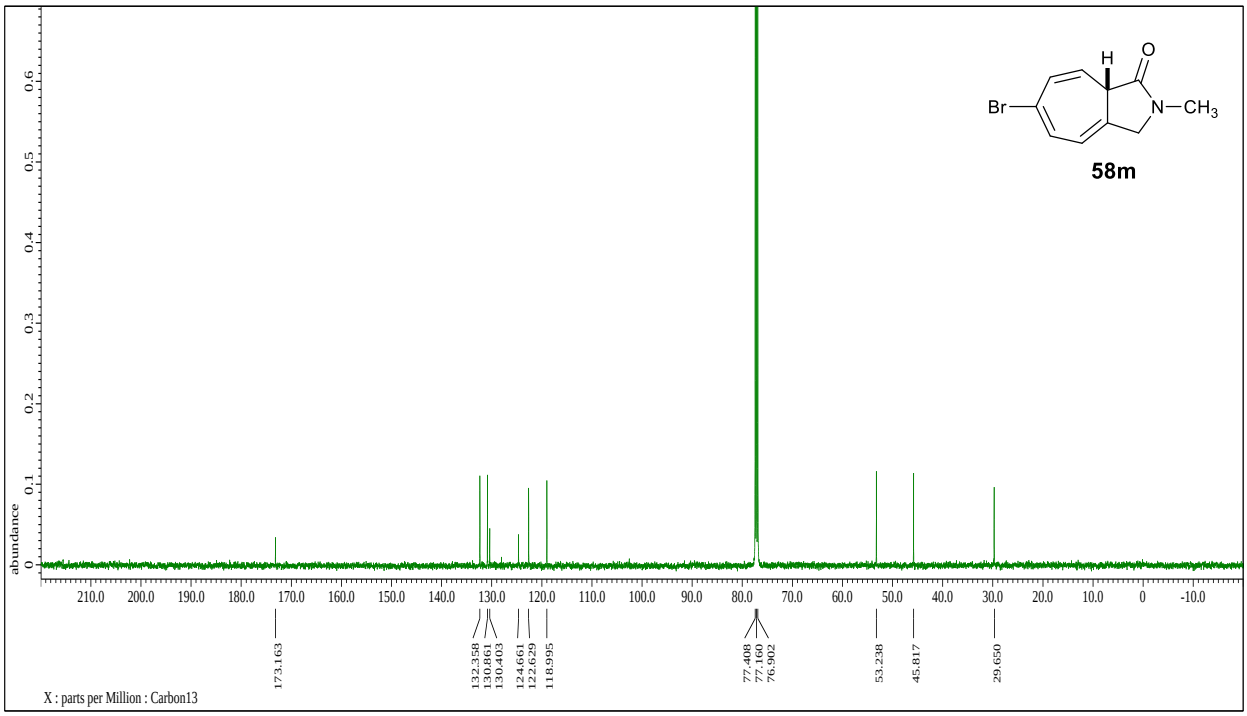

Figure 132. ^{13}CNMR spectral of (*S*)-6-bromo-2-methyl-3,8a-dihydrocyclohepta[c]pyrrol-1(2H)-one.

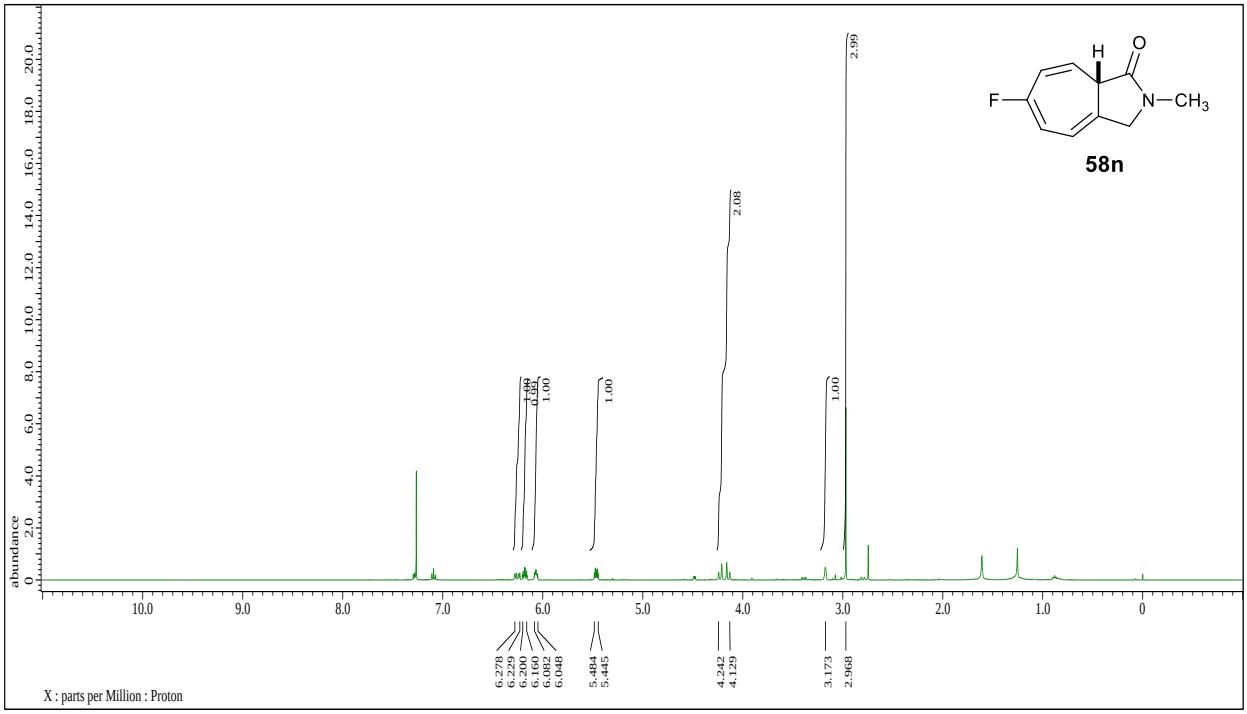

Figure 133. ^{1}HNMR spectral of **(*S*)**-6-fluoro-2-methyl-3,8a-dihydrocyclohepta[c]pyrrol-1(2H)-one.

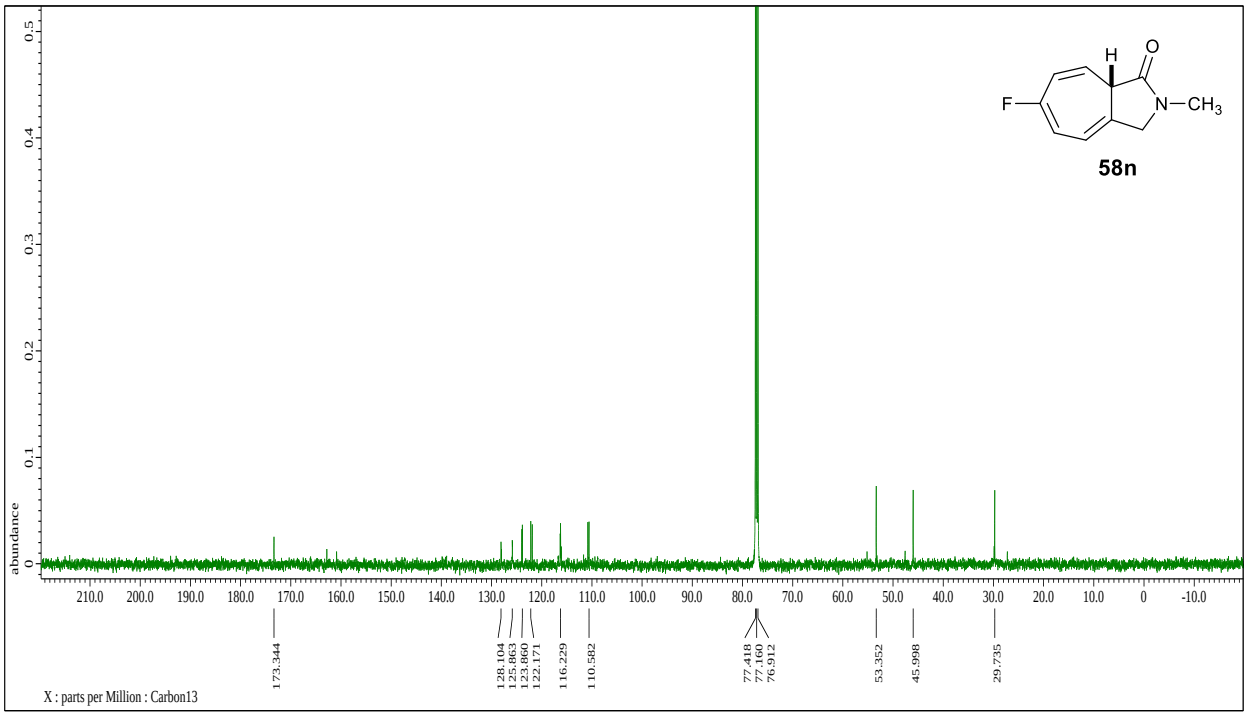

Figure 134. ^{13}CNMR spectral of **(*S*)**-6-fluoro-2-methyl-3,8a-dihydrocyclohepta[c]pyrrol-1(2H)-one.

HPLC DATA

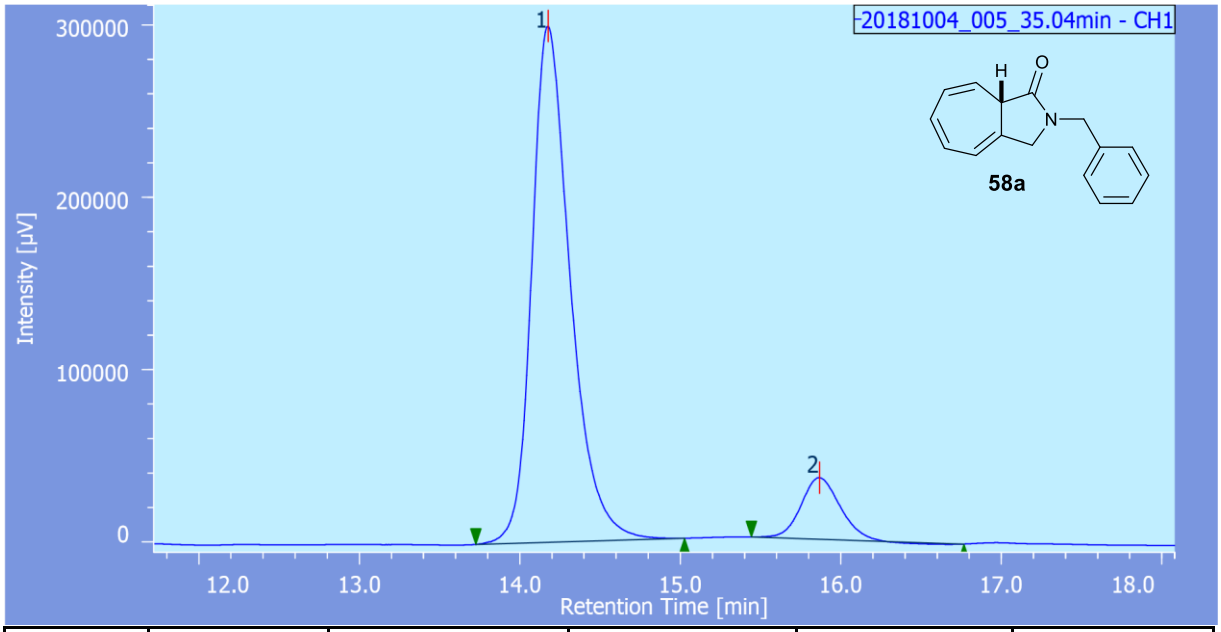

PEAK	RT [min]	AREA [µV-sec]	HEIGHT [µV]	AREA%	HEIGHT%
1	14.175	4998378	299334	89.146	89.343
2	15.867	608581	35704	10.854	10.657

Figure 135. HPLC data of chiral (***S***)-2-benzyl-3,8a-dihydrocyclohepta[c]pyrrol-1(2H)-one.

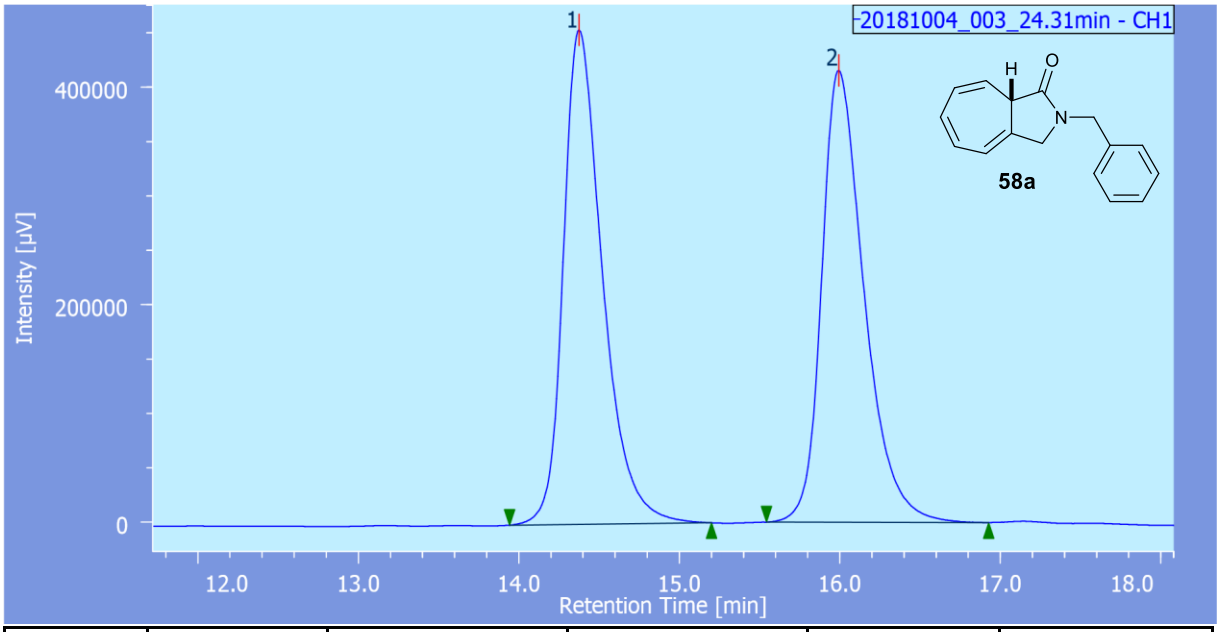

PEAK	RT [min]	AREA [µV-sec]	HEIGHT [µV]	AREA%	HEIGHT%
1	14.375	7722581	454495	50.284	52.250
2	15.992	7635293	415356	49.716	47.750

Figure 136. HPLC data of racemic 2-benzyl-3,8a-dihydrocyclohepta[c]pyrrol-1(2H)-one.

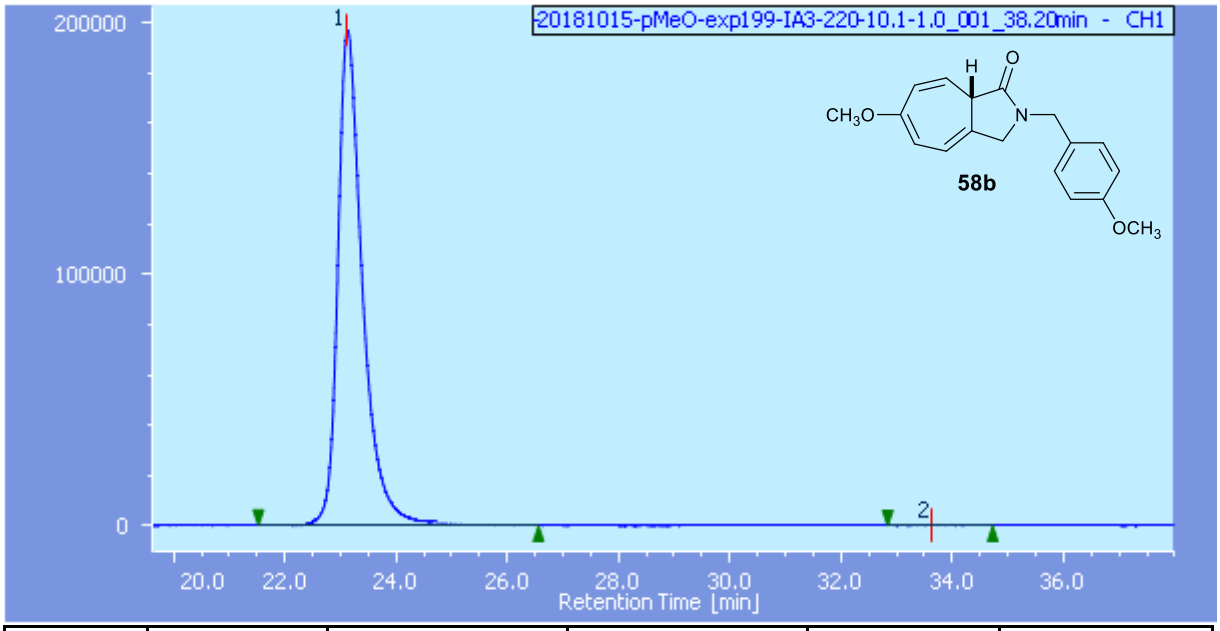

PEAK	RT [min]	AREA [µV-sec]	HEIGHT [µV]	AREA%	HEIGHT%
1	23.125	6146103	196853	99.840	99.845
2	15.992	7635293	415356	49.716	47.750

Figure 137. HPLC data of chiral (*S*)-6-Methoxy-2-(4-methoxybenzyl)-3,8a-dihydrocyclohepta [c]pyrrol-1(2H)-one.

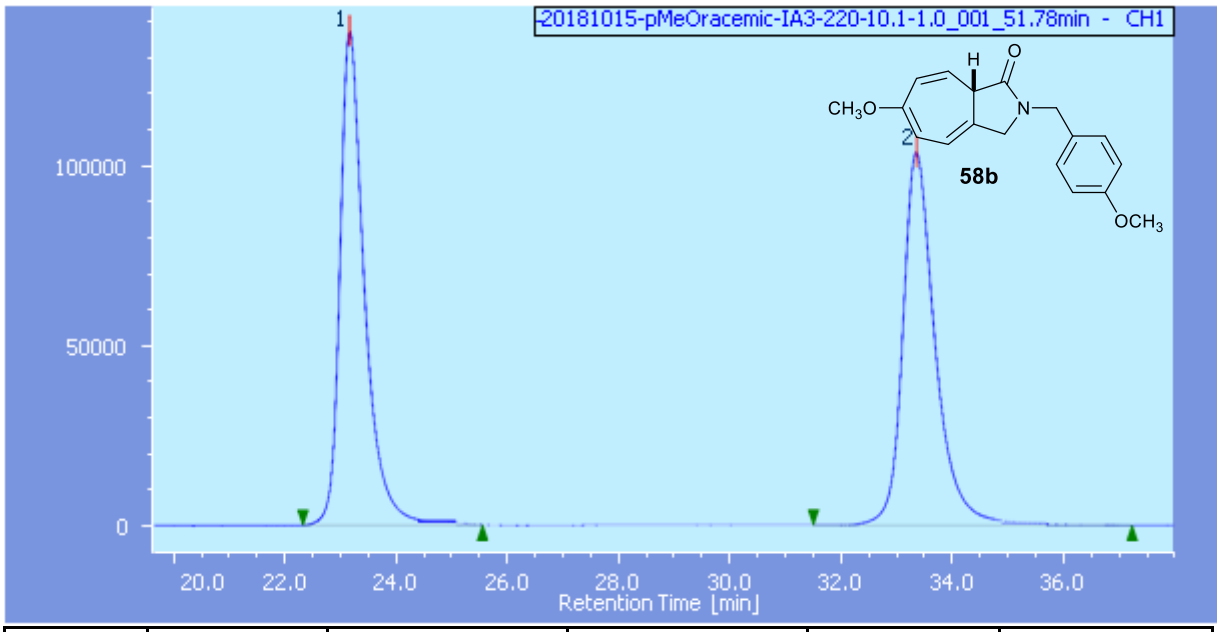

PEAK	RT [min]	AREA [µV-sec]	HEIGHT [µV]	AREA%	HEIGHT%
1	23.133	4234078	137212	50.121	56.990
2	15.992	7635293	415356	49.716	47.750

Figure 138. HPLC data of racemic 6-Methoxy-2-(4-methoxybenzyl)-3,8a-dihydrocyclohepta [c]pyrrol-1(2H)-one.

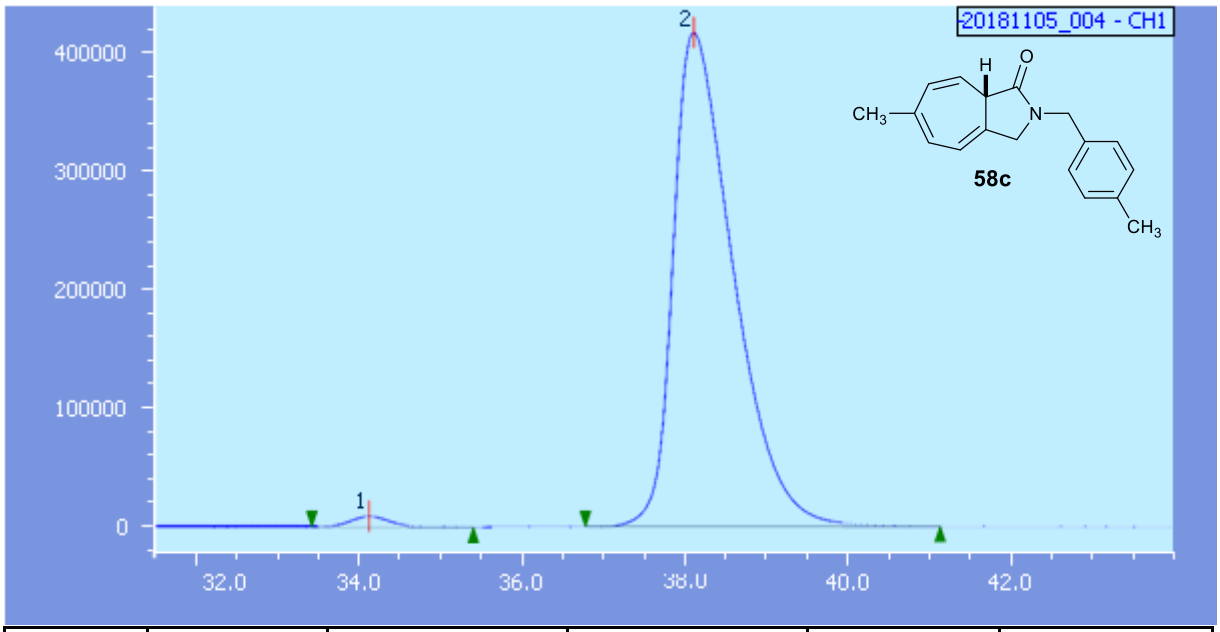

PEAK	RT [min]	AREA [µV-sec]	HEIGHT [µV]	AREA%	HEIGHT%
1	34.125	295038	8787	1.361	2.064
2	38.108	21383869	416923	98.639	97.936

Figure 139. HPLC data of chiral (*S*)-6-methyl-2-(4-methylbenzyl)-3,8a-dihydrocyclohepta [c]pyrrol-1(2H)-one.

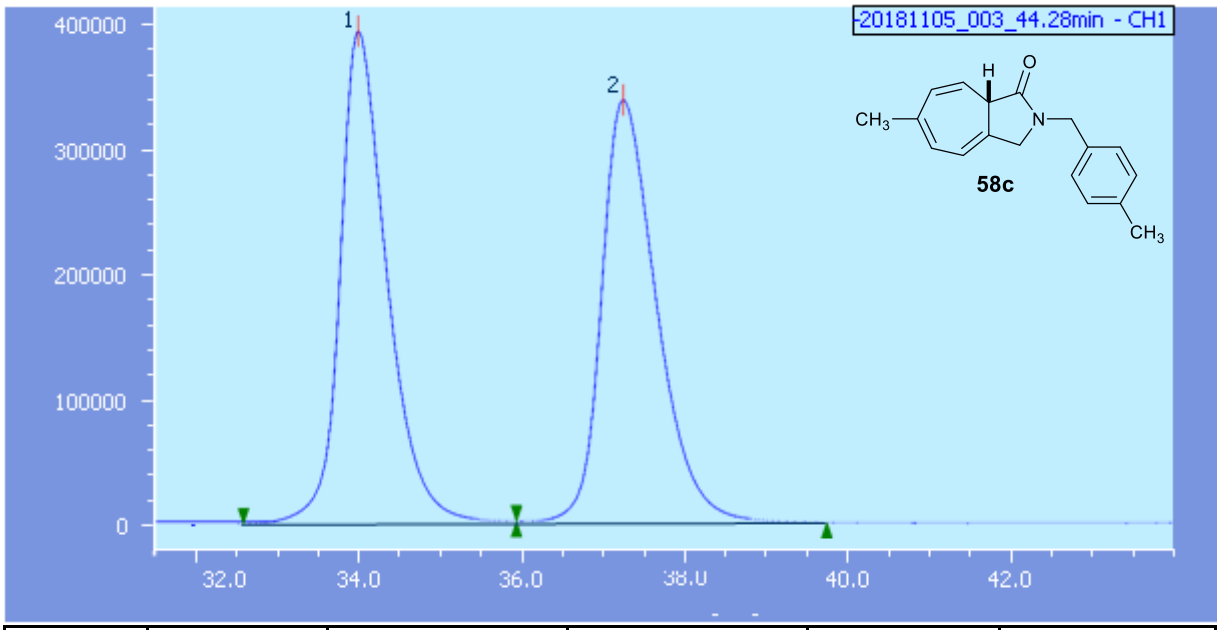

PEAK	RT [min]	AREA [µV-sec]	HEIGHT [µV]	AREA%	HEIGHT%
1	33.967	15960801	394027	49.677	53.750
2	37.217	16168539	339041	50.323	46.250

Figure 140. HPLC data of racemic 6-methyl-2-(4-methylbenzyl)-3,8a-dihydrocyclohepta [c]pyrrol-1(2H)-one.

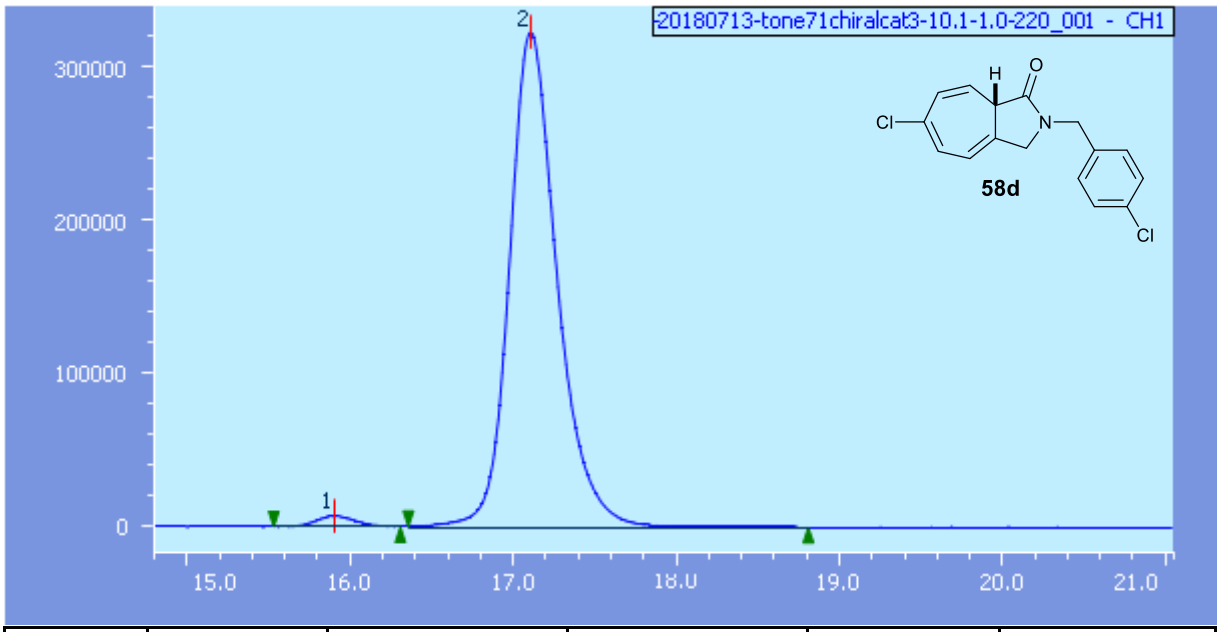

PEAK	RT [min]	AREA [µV-sec]	HEIGHT [µV]	AREA%	HEIGHT%
1	15.908	123785	7090	1.851	2.148
2	17.108	6565407	323049	98.149	97.852

Figure 141. HPLC data of chiral (*S*)-6-chloro-2-(4-chlorobenzyl)-3,8a-dihydrocyclohepta[c] pyrrol-1(2H)-one.

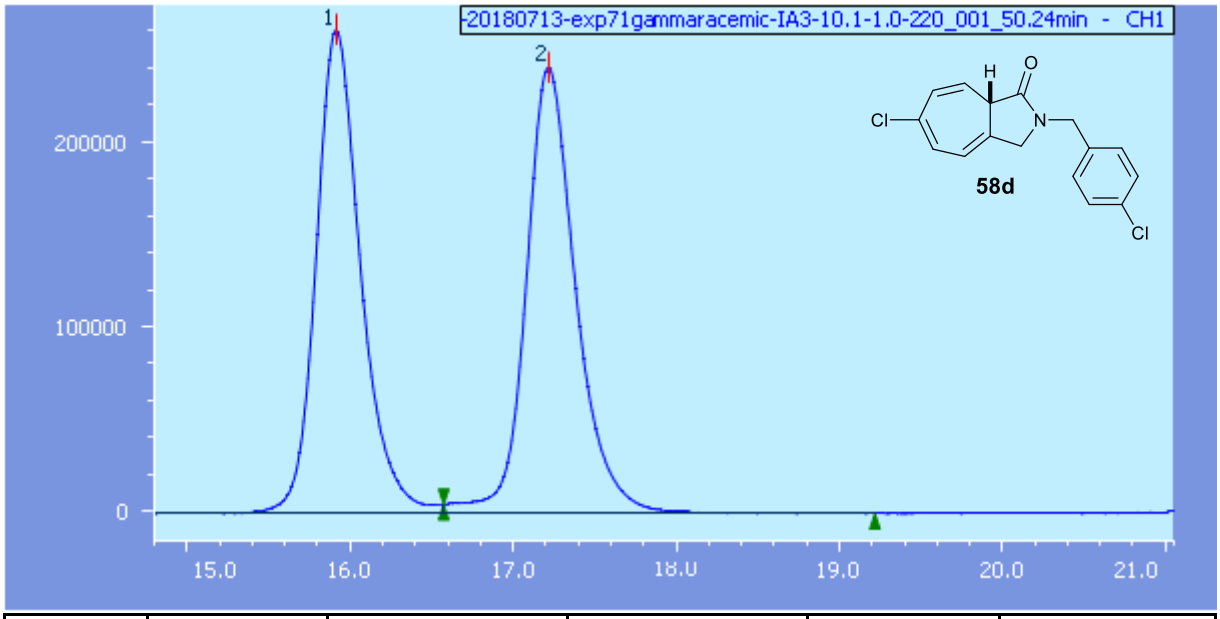

PEAK	RT [min]	AREA [µV-sec]	HEIGHT [µV]	AREA%	HEIGHT%
1	15.917	4998114	261500	49.299	52.029
2	17.217	5140338	241108	50.701	47.971

Figure 142. HPLC data of racemic 6-chloro-2-(4-chlorobenzyl)-3,8a-dihydrocyclohepta[c] pyrrol-1(2H)-one.

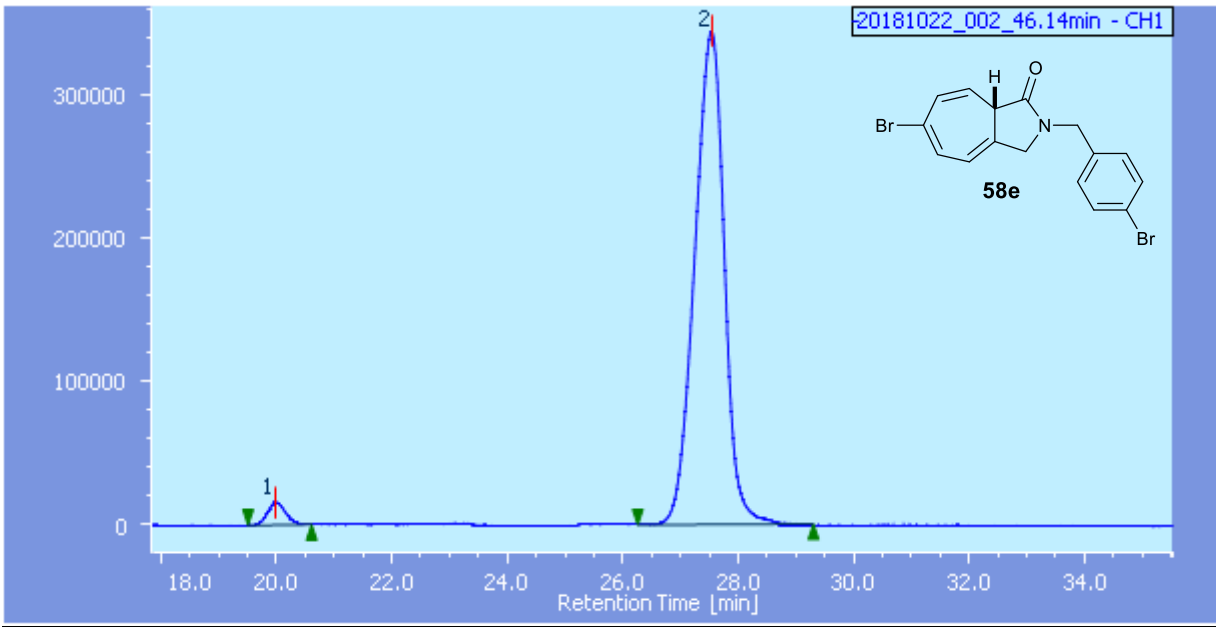

PEAK	RT [min]	AREA [µV-sec]	HEIGHT [µV]	AREA%	HEIGHT%
1	19.992	342399	15821	2.722	4.406
2	27.533	12237527	343240	97.278	95.594

Figure 143. HPLC data of chiral (*S*)-6-bromo-2-(4-bromobenzyl)-3,8a-dihydrocyclohepta[c] pyrrol-1(2H)-one.

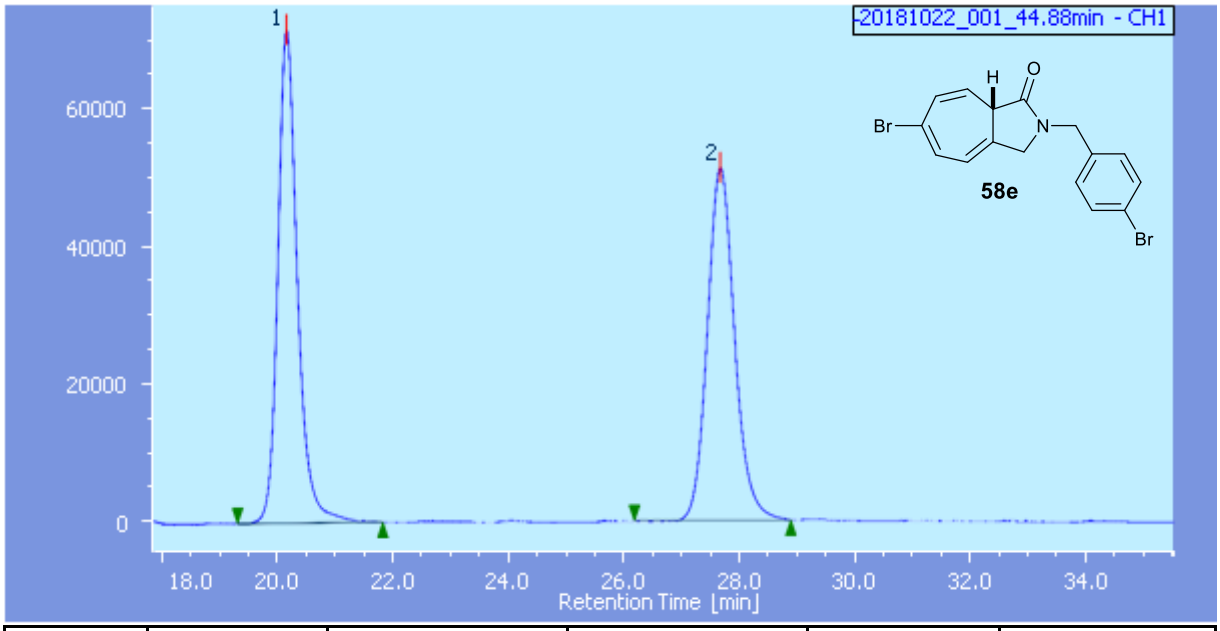

PEAK	RT [min]	AREA [µV-sec]	HEIGHT [µV]	AREA%	HEIGHT%
1	20.133	1689569	71715	50.168	58.329
2	27.642	1678278	51234	49.832	41.671

Figure 144. HPLC data of racemic 6-bromo-2-(4-bromobenzyl)-3,8a-dihydrocyclohepta[c] pyrrol-1(2H)-one.

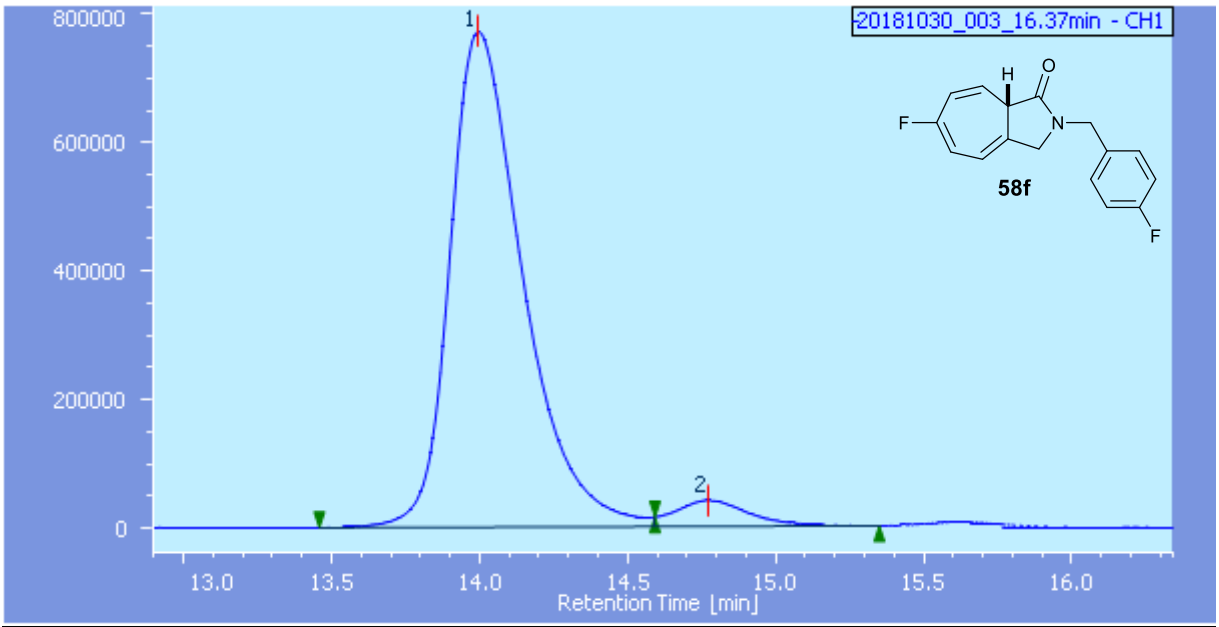

PEAK	RT [min]	AREA [µV-sec]	HEIGHT [µV]	AREA%	HEIGHT%
1	13.992	13211783	769810	95.041	95.032
2	14.775	689306	40241	4.959	4.968

Figure 145. HPLC data of chiral (*S*)-6-fluoro-2-(4-fluorobenzyl)-3,8a-dihydrocyclohepta[c] pyrrol-1(2H)-one.

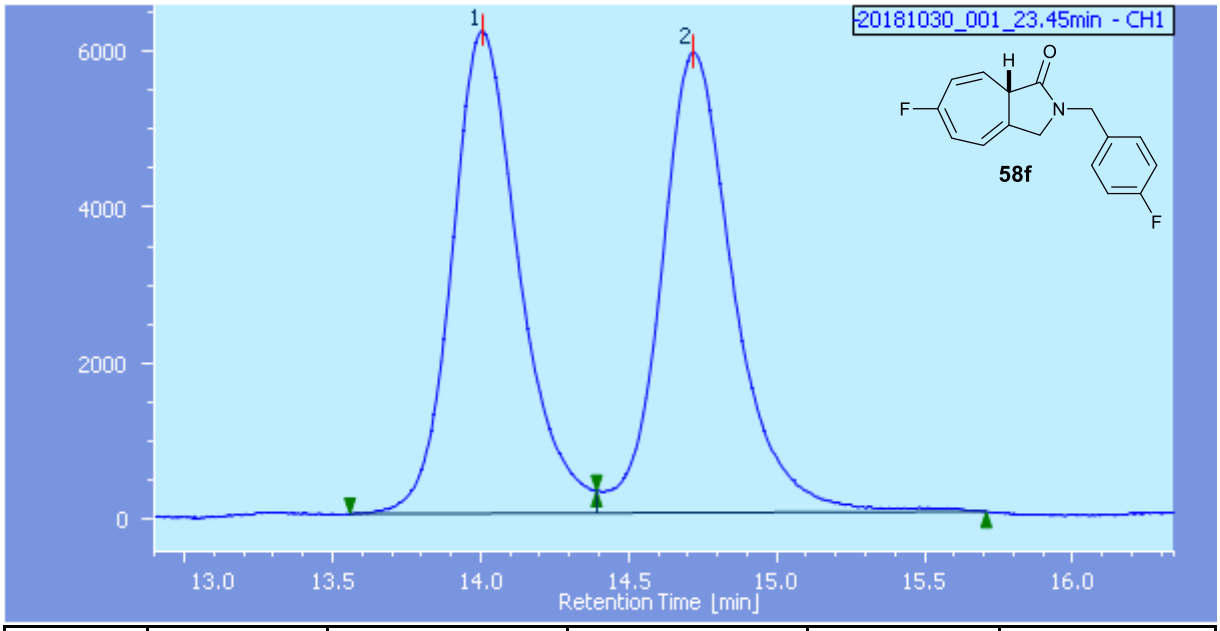

PEAK	RT [min]	AREA [µV-sec]	HEIGHT [µV]	AREA%	HEIGHT%
1	14.008	98046	6202	49.186	51.143
2	14.717	101291	5925	50.814	48.857

Figure 146. HPLC data of racemic 6-fluoro-2-(4-fluorobenzyl)-3,8a-dihydrocyclohepta[c] pyrrol-1(2H)-one.

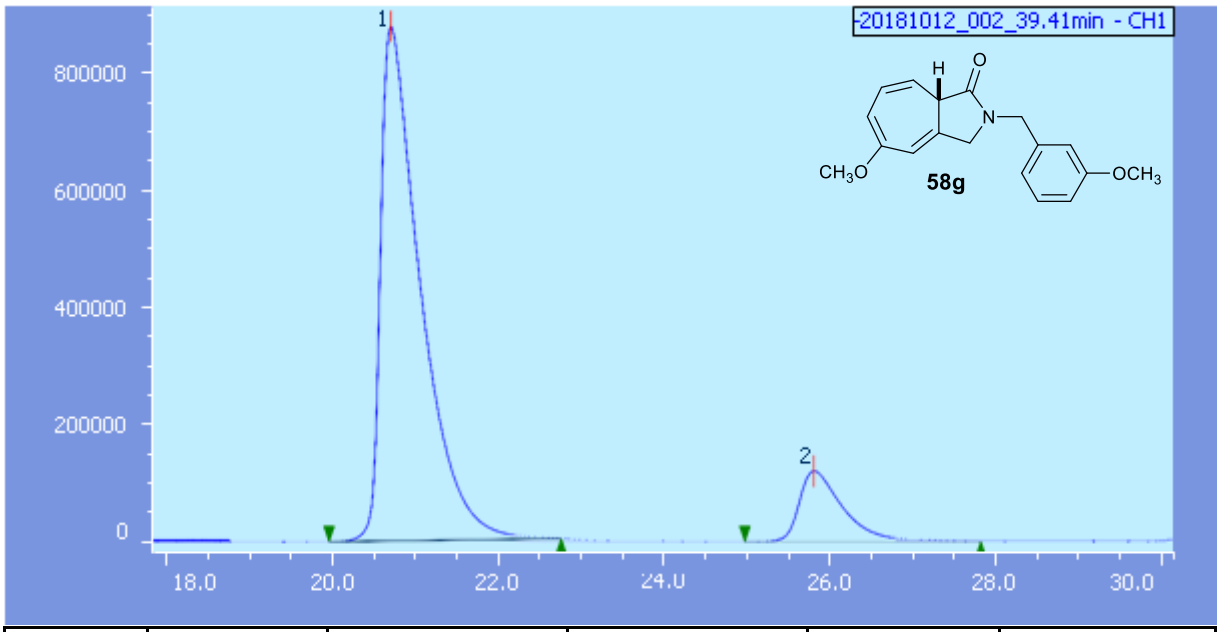

PEAK	RT [min]	AREA [µV-sec]	HEIGHT [µV]	AREA%	HEIGHT%
1	20.700	29448287	876831	86.893	87.930
2	25.808	4441998	120360	13.107	12.070

Figure 147. HPLC data of chiral (*S*)-5-methoxy-2-(3-methoxybenzyl)-3,8a-dihydrocyclohepta[c] pyrrol-1(2H)-one.

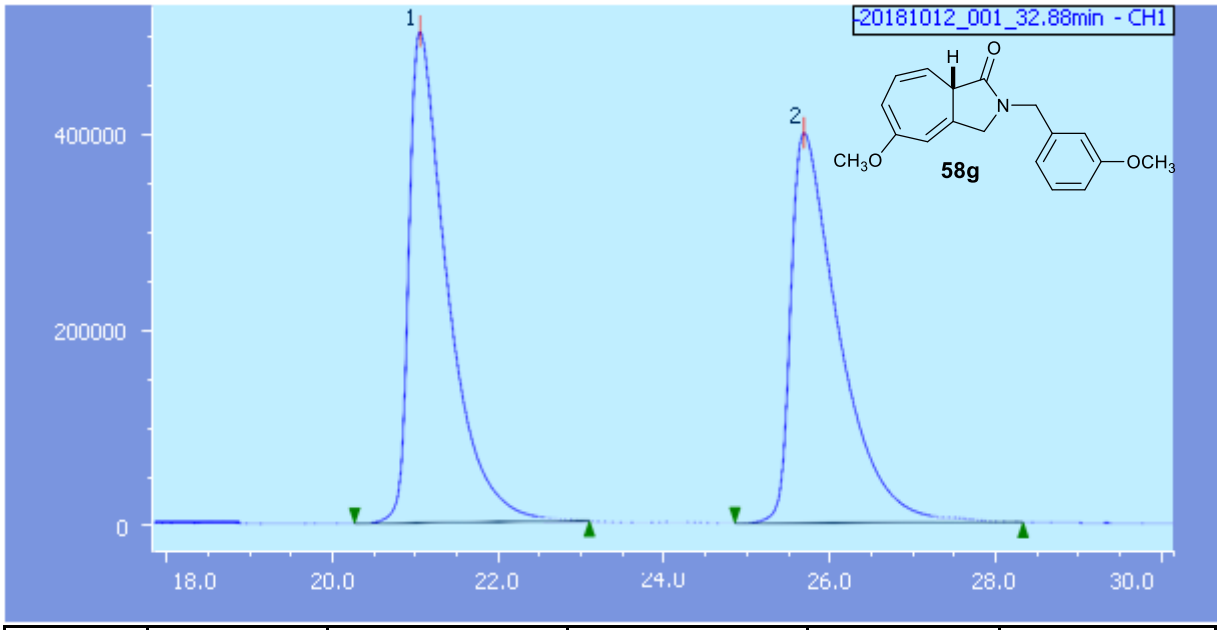

PEAK	RT [min]	AREA [µV-sec]	HEIGHT [µV]	AREA%	HEIGHT%
1	21.033	16376122	503364	50.237	55.731
2	25.667	16221879	399841	49.763	44.269

Figure 148. HPLC data of racemic 5-methoxy-2-(3-methoxybenzyl)-3,8a-dihydrocyclohepta[c] pyrrol-1(2H)-one.

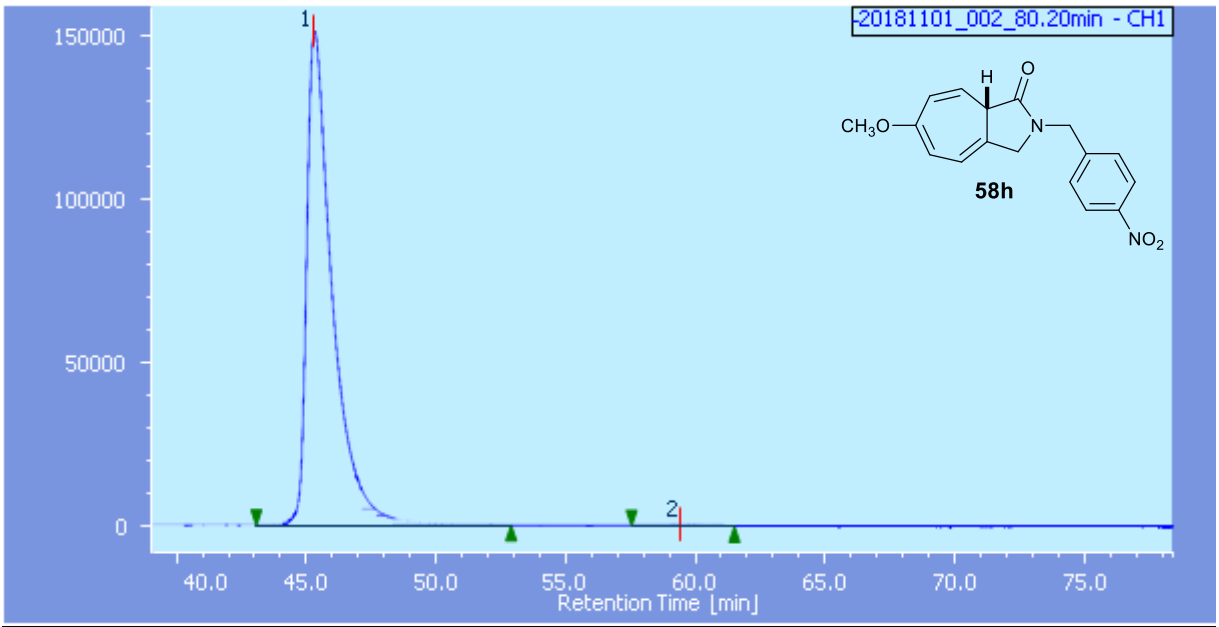

PEAK	RT [min]	AREA [µV-sec]	HEIGHT [µV]	AREA%	HEIGHT%
1	45.267	10518585	151022	99.593	99.630
2	59.375	43024	561	0.407	0.370

Figure 149. HPLC data of chiral (*S*)-6-methoxy-2-(4-nitrobenzyl)-3,8a-dihydrocyclohepta[c] pyrrol-1(2H)-one.

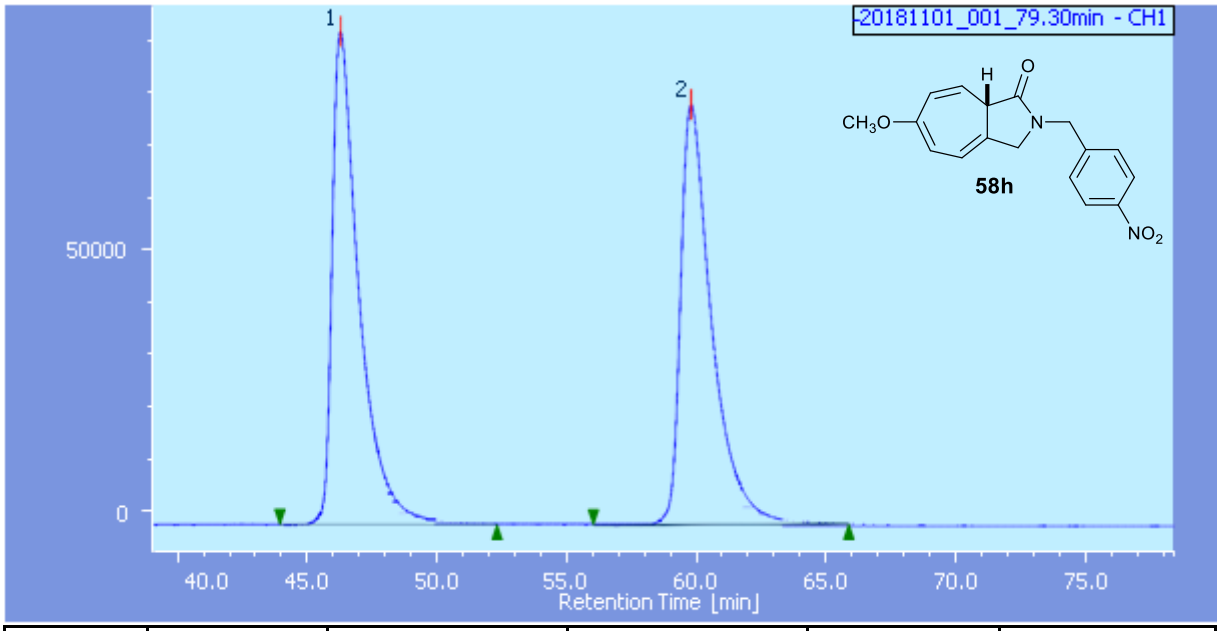

PEAK	RT [min]	AREA [µV-sec]	HEIGHT [µV]	AREA%	HEIGHT%
1	46.208	6857632	94333	50.173	53.968
2	59.725	6810218	80461	49.827	46.032

Figure 150. HPLC data of racemic 6-methoxy-2-(4-nitrobenzyl)-3,8a-dihydrocyclohepta[c] pyrrol-1(2H)-one.

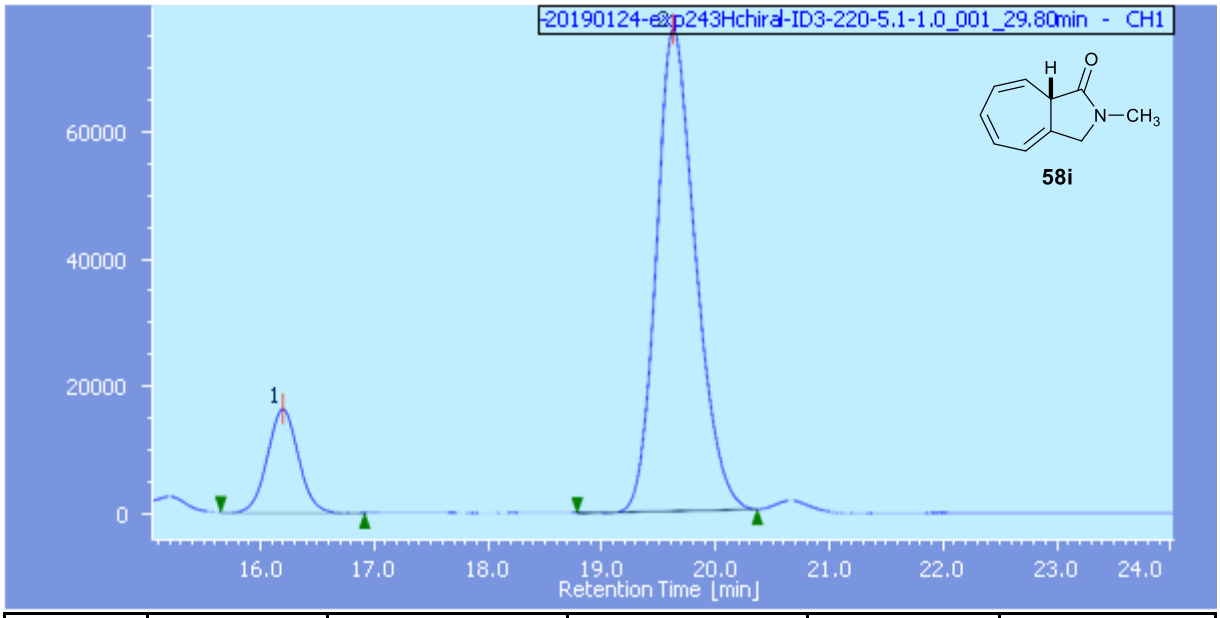

PEAK	RT [min]	AREA [µV-sec]	HEIGHT [µV]	AREA%	HEIGHT%
1	16.192	306518	16310	14.422	17.682
2	19.617	1818808	75934	85.578	82.318

Figure 151. HPLC data of chiral (*S*)-2-methyl-3,8a-dihydrocyclohepta[c]pyrrol-1(2H)-one.

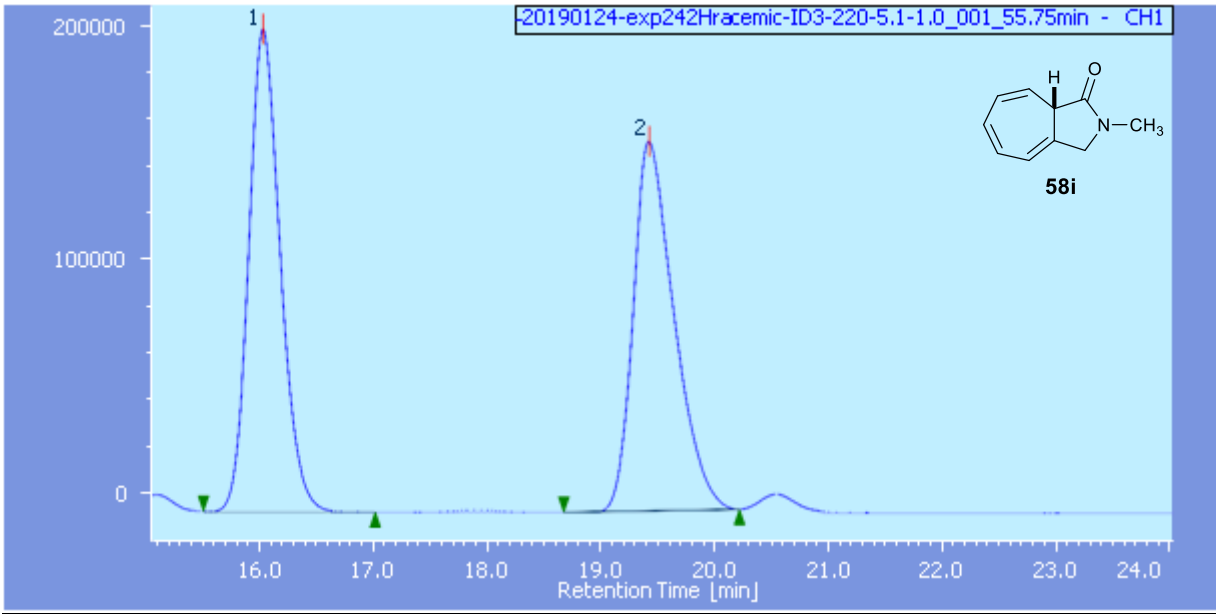

PEAK	RT [min]	AREA [µV-sec]	HEIGHT [µV]	AREA%	HEIGHT%
1	16.025	3954021	205833	50.172	56.646
2	19.417	3926904	157533	49.828	43.354

Figure 152. HPLC data of racemic 2-methyl-3,8a-dihydrocyclohepta[c]pyrrol-1(2H)-one.

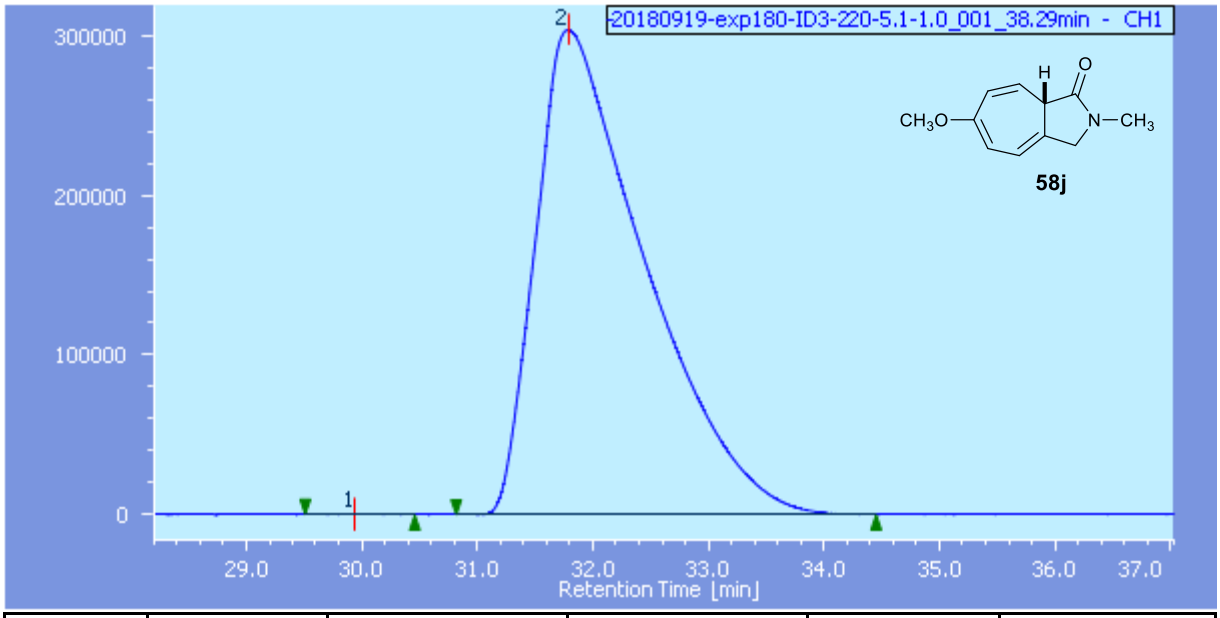

PEAK	RT [min]	AREA [µV-sec]	HEIGHT [µV]	AREA%	HEIGHT%
1	29.942	15701	530	0.078	0.174
2	31.783	20074522	304757	99.922	99.826

Figure 153. HPLC data of chiral (*S*)-6-methoxy-2-methyl-3,8a-dihydrocyclohepta[c]pyrrol-1(2H)-one.

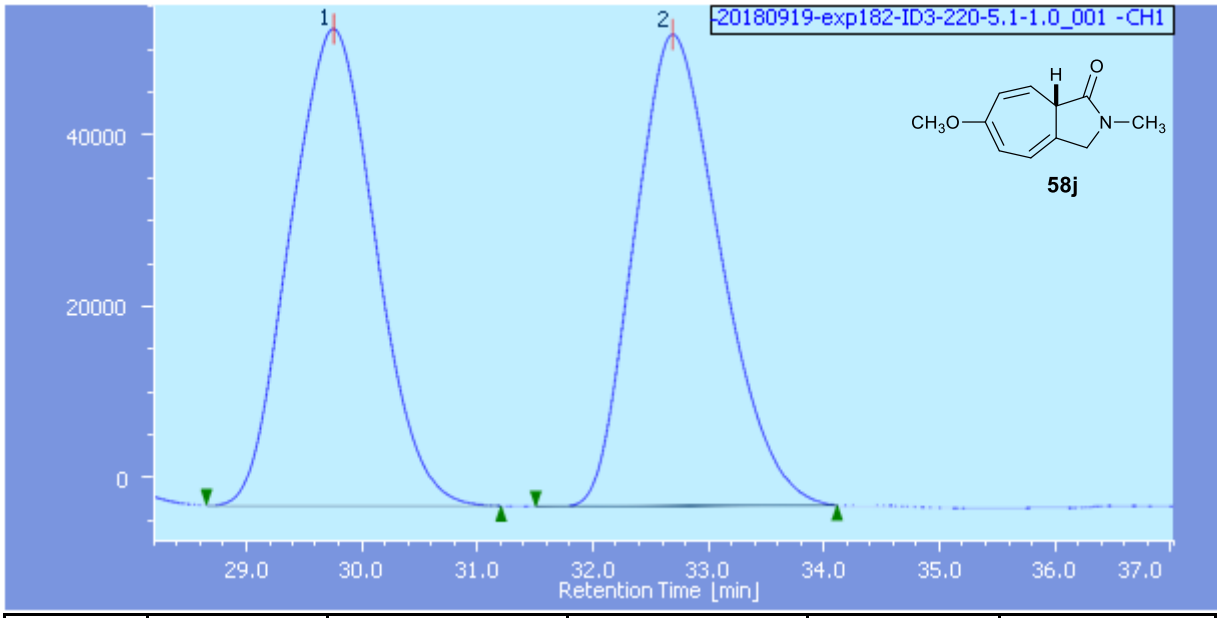

PEAK	RT [min]	AREA [µV-sec]	HEIGHT [µV]	AREA%	HEIGHT%
1	29.742	2845125	55576	50.019	50.264
2	32.675	2842914	54992	49.981	49.736

Figure 154. HPLC data of racemic 6-methoxy-2-methyl-3,8a-dihydrocyclohepta[c]pyrrol-1(2H)-one.

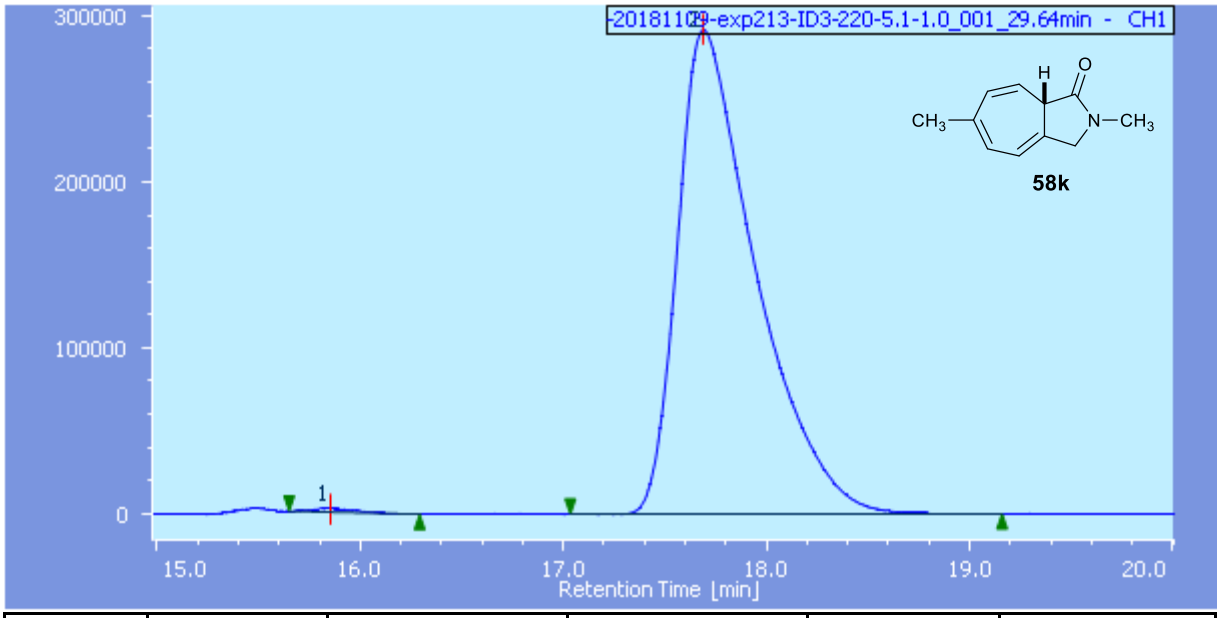

PEAK	RT [min]	AREA [µV-sec]	HEIGHT [µV]	AREA%	HEIGHT%
1	15.850	28737	1989	0.368	0.677
2	17.692	7782124	291612	99.632	99.323

Figure 155. HPLC data of chiral (*S*)-2,6-dimethyl-3,8a-dihydrocyclohepta[c]pyrrol-1(2H)-one.

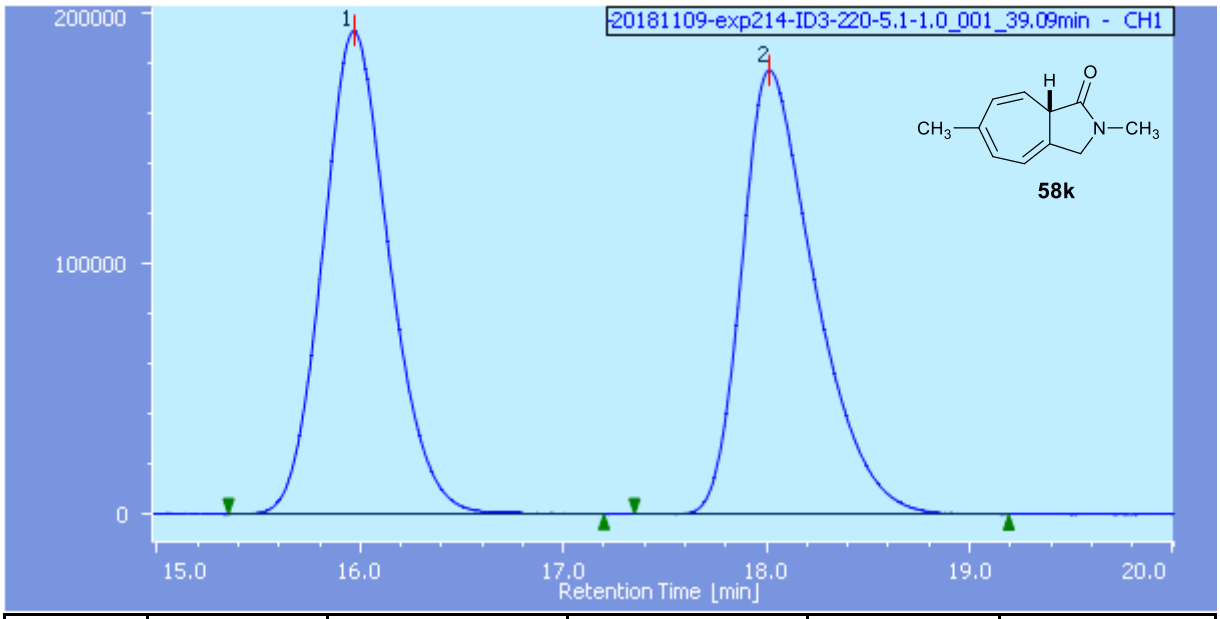

PEAK	RT [min]	AREA [µV-sec]	HEIGHT [µV]	AREA%	HEIGHT%
1	15.967	4407082	192794	49.790	52.096
2	18.017	4444247	177287	50.210	47.904

Figure 156. HPLC data of racemic 2,6-dimethyl-3,8a-dihydrocyclohepta[c]pyrrol-1(2H)-one.

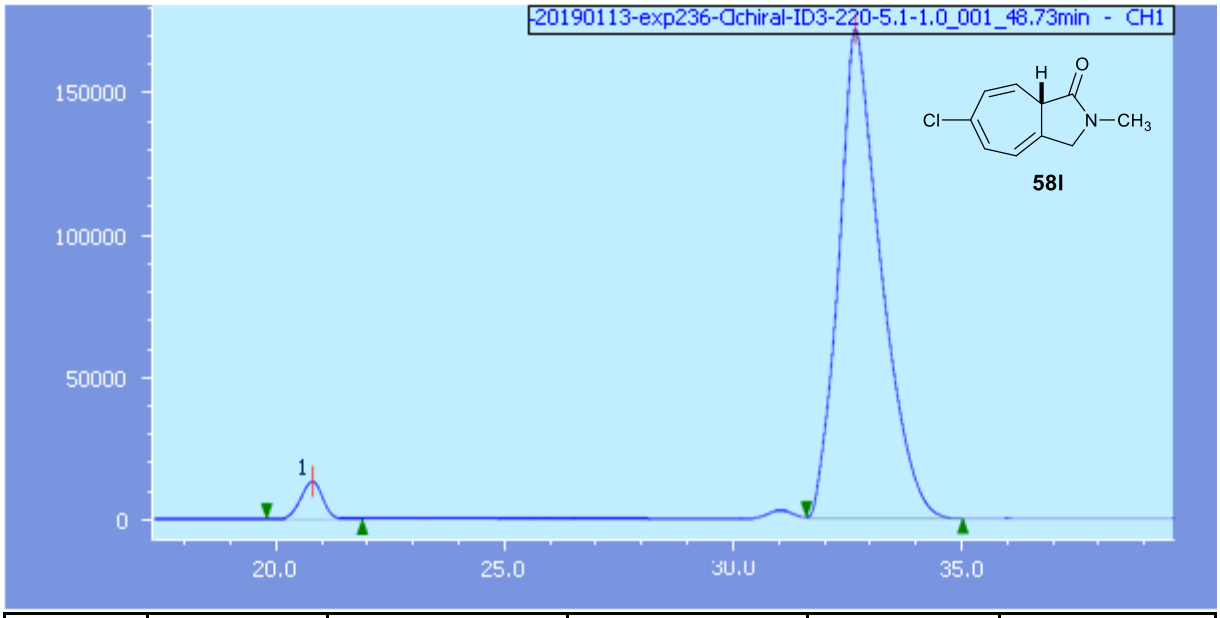

PEAK	RT [min]	AREA [µV-sec]	HEIGHT [µV]	AREA%	HEIGHT%
1	20.758	445946	13306	3.909	7.211
2	32.642	10963663	171225	96.091	92.789

Figure 157. HPLC data of chiral (*S*)-6-chloro-2-methyl-3,8a-dihydrocyclohepta[c]pyrrol-1(2H)-one.

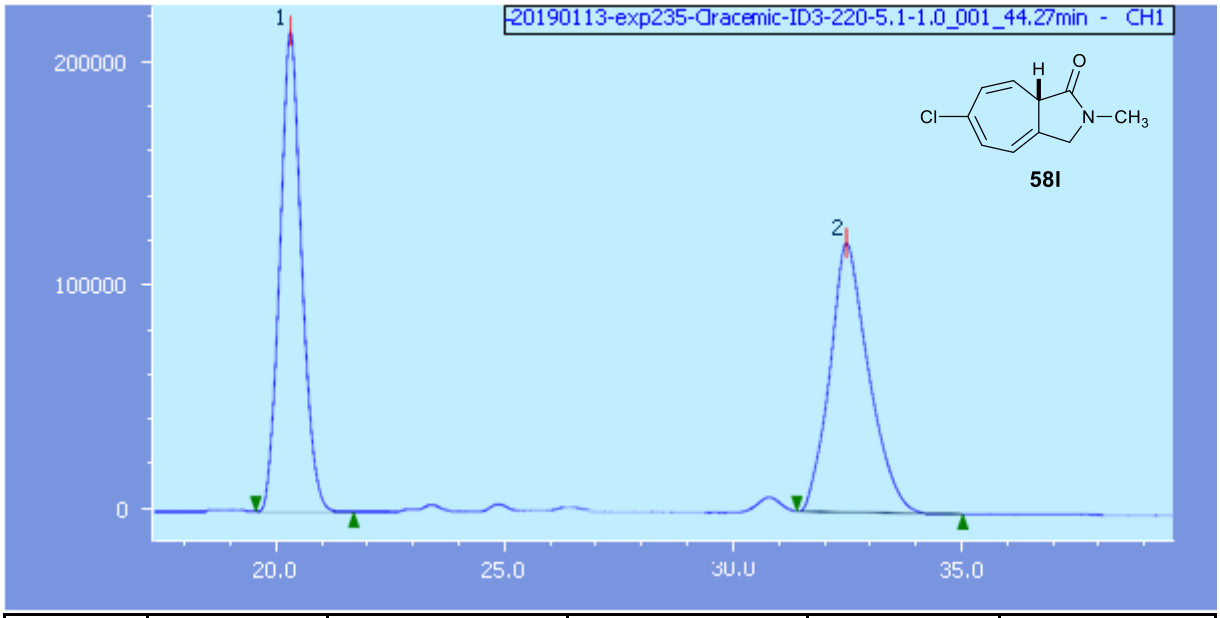

PEAK	RT [min]	AREA [µV-sec]	HEIGHT [µV]	AREA%	HEIGHT%
1	20.275	7136884	215242	50.024	64.095
2	32.442	7129926	120577	49.976	35.905

Figure 158. HPLC data of racemic 6-chloro-2-methyl-3,8a-dihydrocyclohepta[c]pyrrol-1(2H)-one.

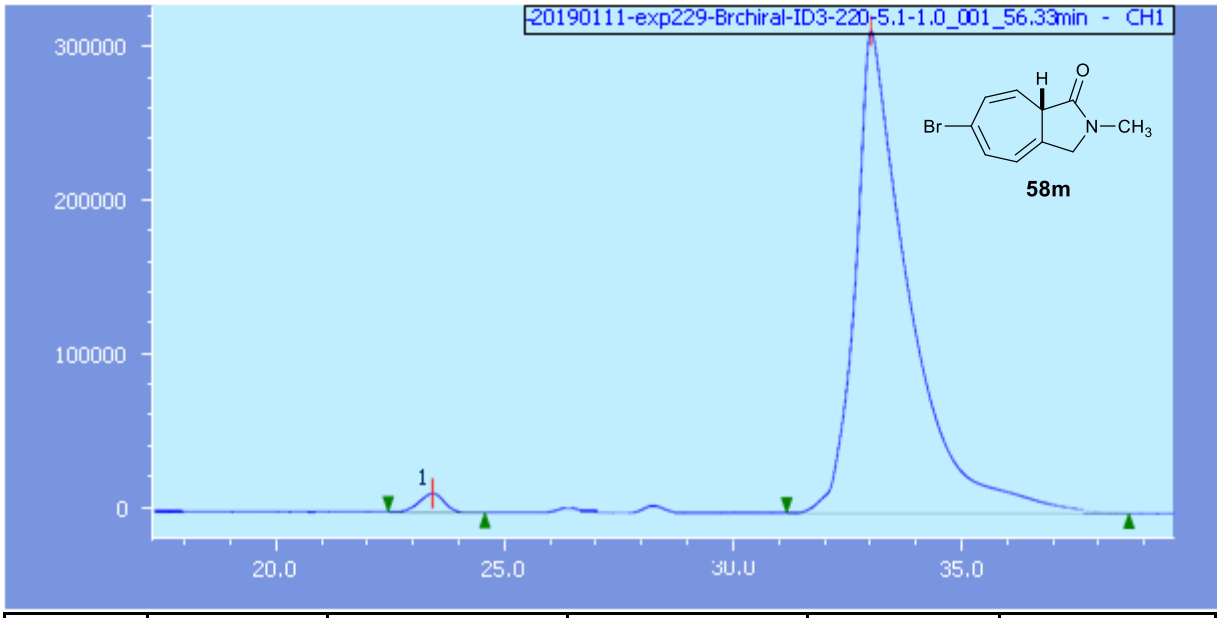

PEAK	RT [min]	AREA [µV-sec]	HEIGHT [µV]	AREA%	HEIGHT%
1	23.383	463948	12299	1.772	3.767
2	32.983	25721764	341184	98.228	96.233

Figure 159. HPLC data of chiral (*S*)-6-bromo-2-methyl-3,8a-dihydrocyclohepta[c]pyrrol-1(2H)-one.

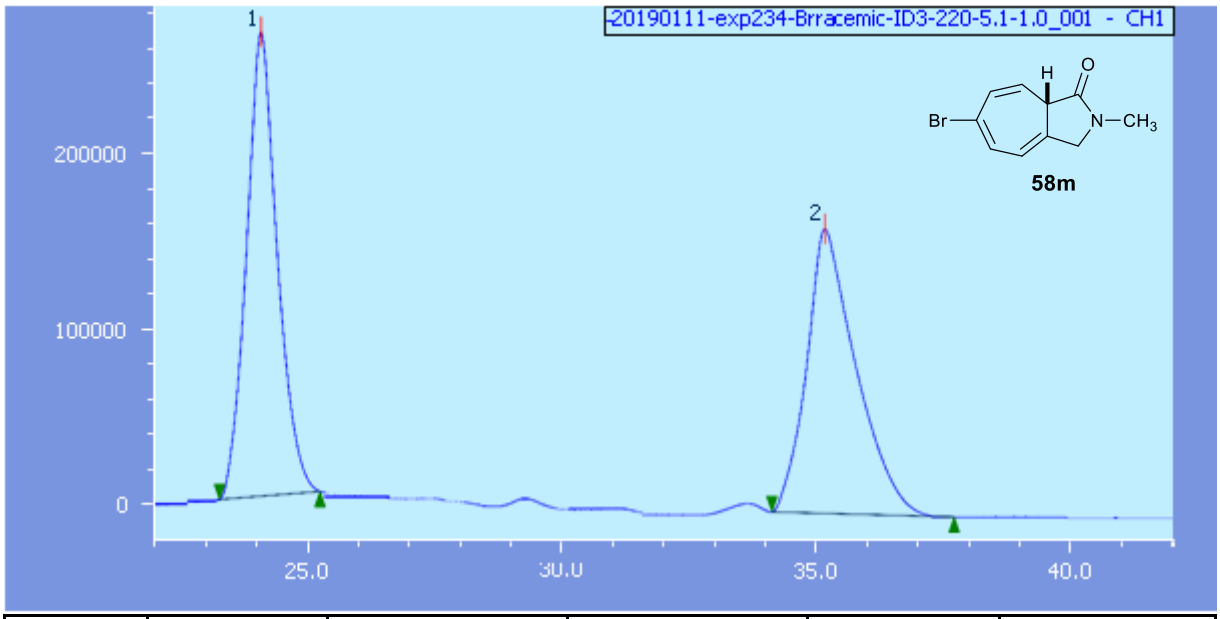

PEAK	RT [min]	AREA [µV-sec]	HEIGHT [µV]	AREA%	HEIGHT%
1	24.050	11156150	264719	50.414	61.992
2	35.133	10973026	162302	49.586	38.008

Figure 160. HPLC data of racemic 6-bromo-2-methyl-3,8a-dihydrocyclohepta[c]pyrrol-1(2H)-one.

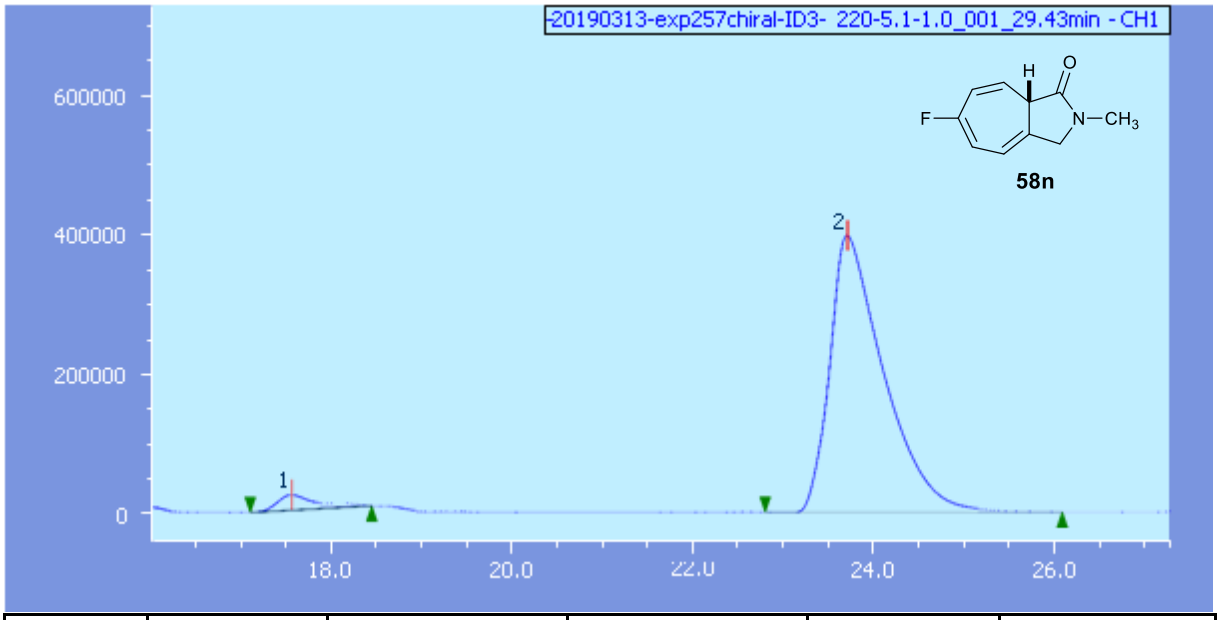

PEAK	RT [min]	AREA [µV-sec]	HEIGHT [µV]	AREA%	HEIGHT%
1	17.558	677713	21987	3.961	5.259
2	23.700	16432700	396131	96.039	94.741

Figure 161. HPLC data of chiral (*S*)-6-fluoro-2-methyl-3,8a-dihydrocyclohepta[c]pyrrol-1(2H)-one.

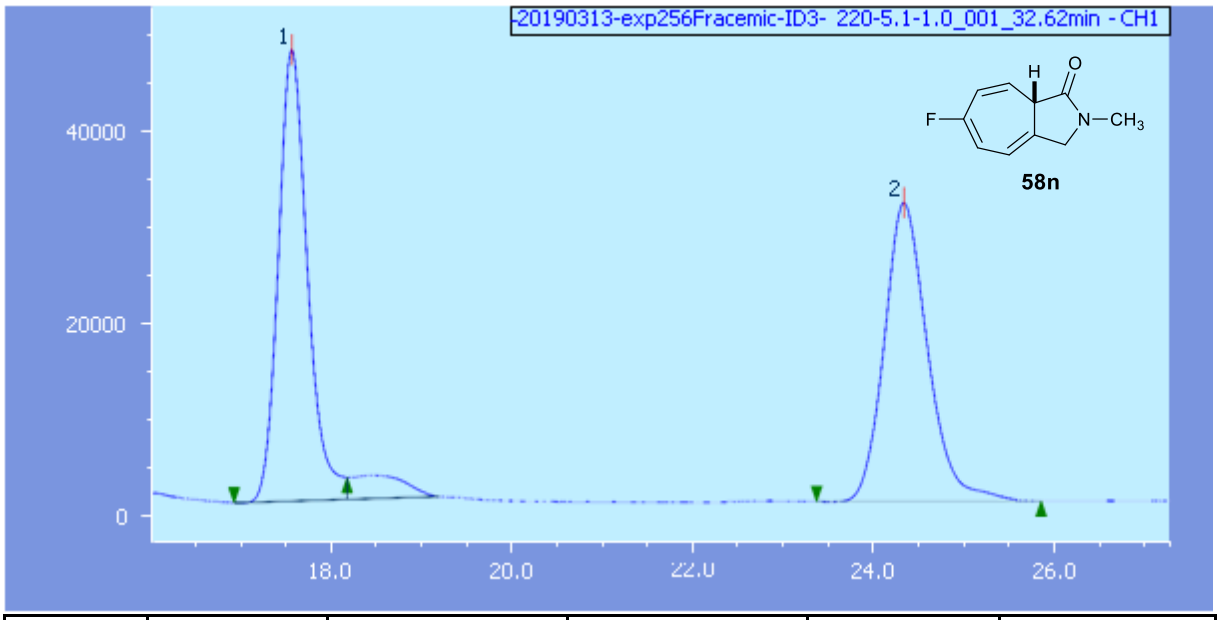

PEAK	RT [min]	AREA [µV-sec]	HEIGHT [µV]	AREA%	HEIGHT%
1	17.550	1055700	47015	50.449	60.178
2	24.317	1036894	31112	49.551	39.822

Figure 162. HPLC data of racemic 6-fluoro-2-methyl-3,8a-dihydrocyclohepta[c]pyrrol-1(2H)-one.

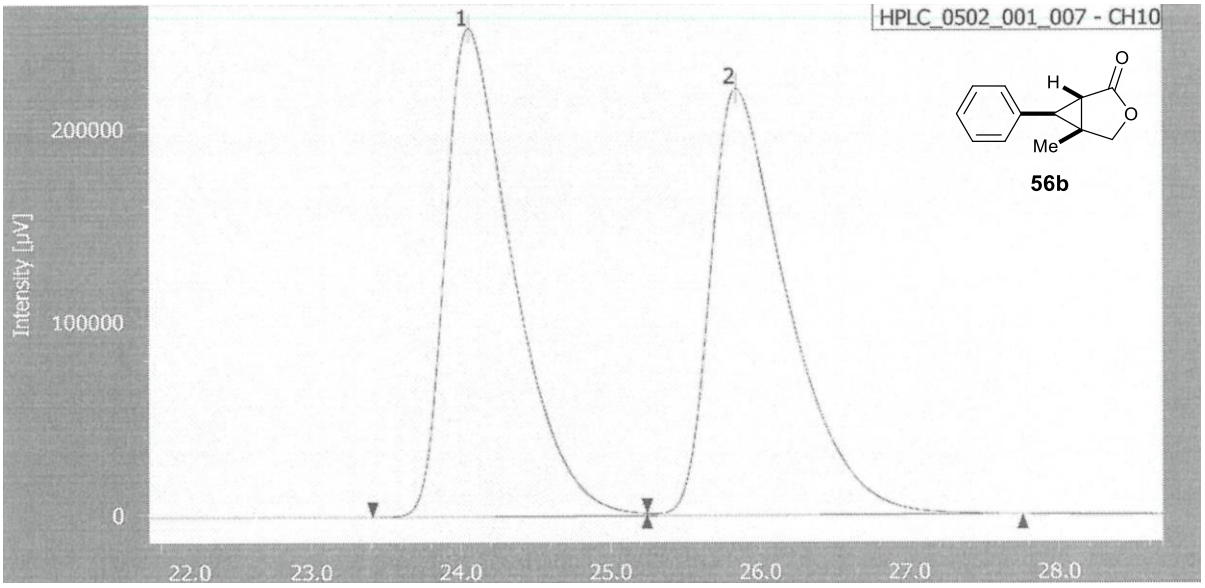

PEAK	RT [min]	AREA [µV-sec]	HEIGHT [µV]	AREA%	HEIGHT%
1	24.053	7933165	252439	49.962	53.327
2	25.840	7945341	220939	50.038	46.673

Figure 163. HPLC data of racemic 5-methyl-6-phenyl-3-oxabicyclo[3.1.0]hexan-2-one.

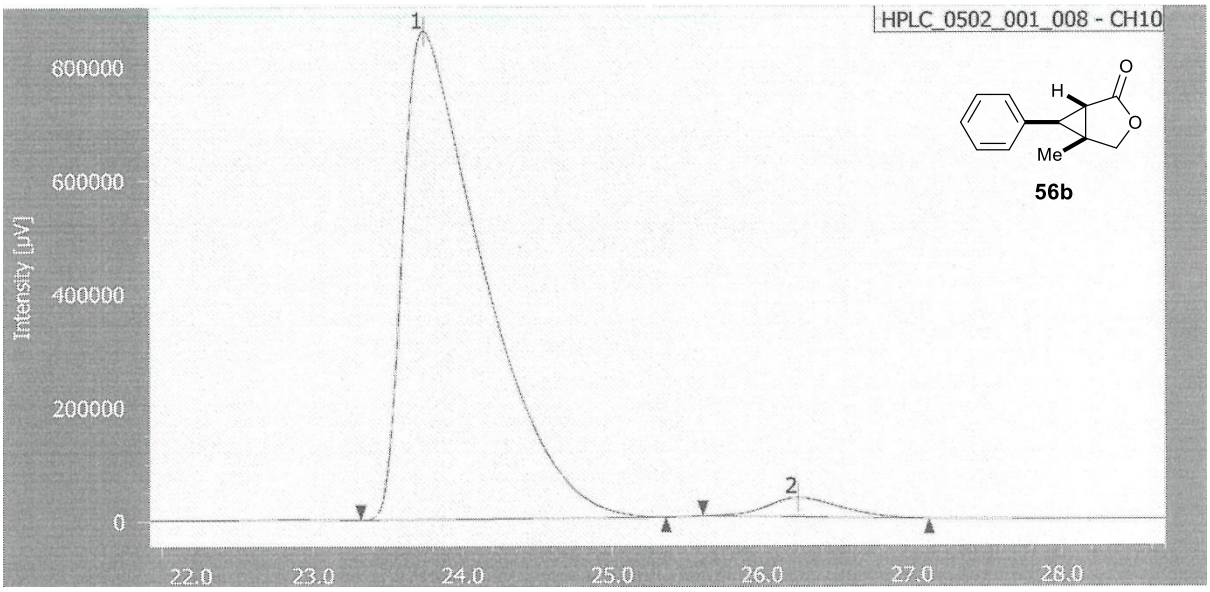

PEAK	RT [min]	AREA [µV-sec]	HEIGHT [µV]	AREA%	HEIGHT%
1	23.745	31944031	858180	96.547	96219
2	26.238	1142308	33720	3.453	3.781

Figure 164. HPLC data of chiral (1*S*,5*R*,6*R*)-5-methyl-6-phenyl-3-oxabicyclo[3.1.0]hexan-2-one.

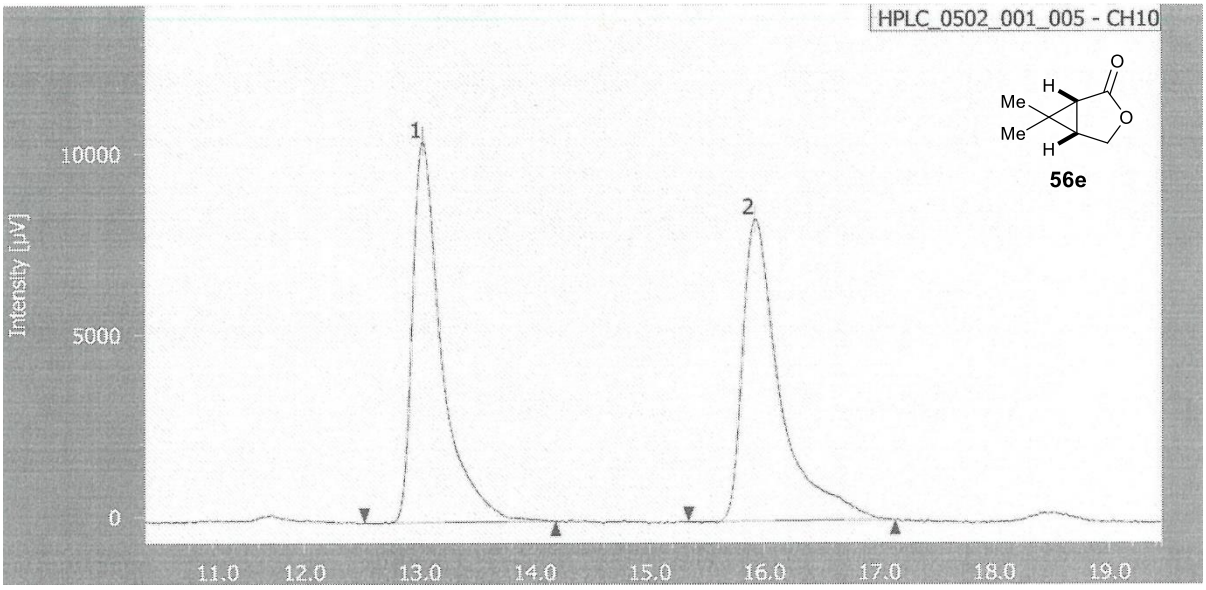

PEAK	RT [min]	AREA [µV-sec]	HEIGHT [µV]	AREA%	HEIGHT%
1	13.030	184827	10477	49.488	55.762
2	15.922	188650	8312	50.512	44.238

Figure 165. HPLC data of racemic 6,6-dimethyl-3-oxabicyclo[3.1.0]hexan-2-one.

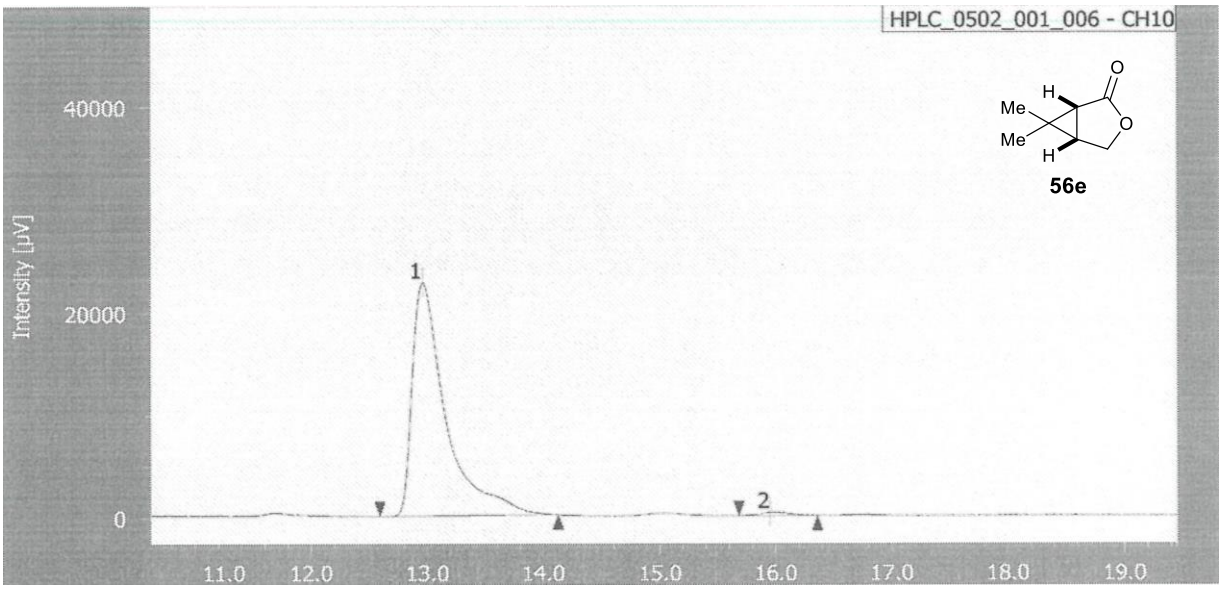

PEAK	RT [min]	AREA [µV-sec]	HEIGHT [µV]	AREA%	HEIGHT%
1	12.962	454706	22728	98.862	98.605
2	15.952	5235	321	1.138	1.395

Figure 166. HPLC data of chiral (1*R*,5*S*)-6,6-dimethyl-3-oxabicyclo[3.1.0]hexan-2-one.

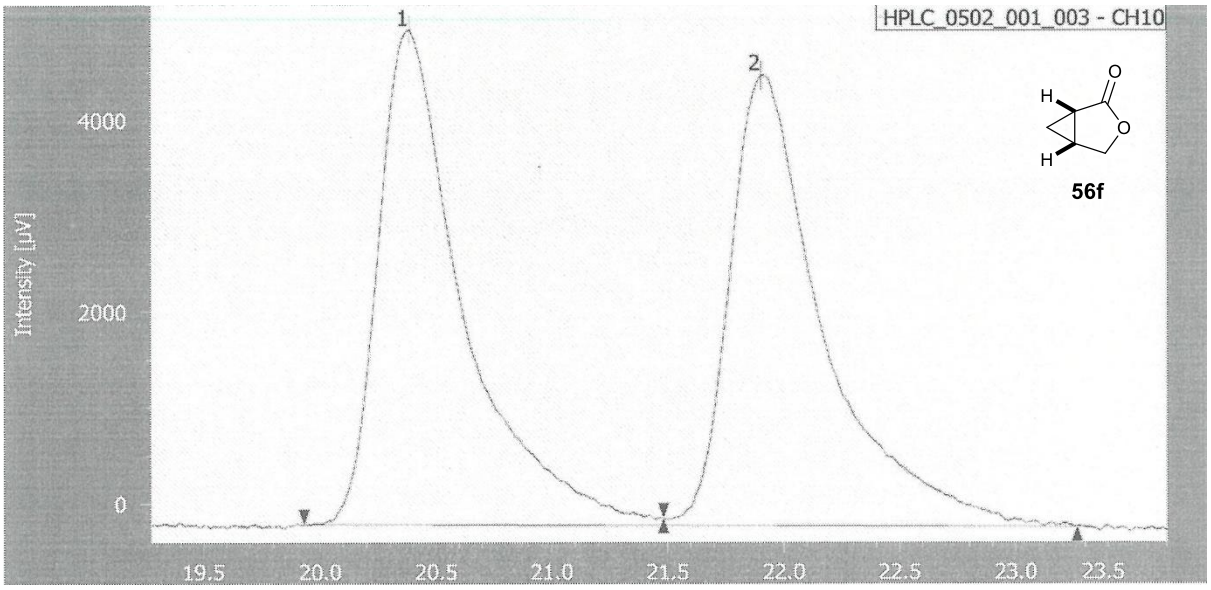

PEAK	RT [min]	AREA [µV-sec]	HEIGHT [µV]	AREA%	HEIGHT%
1	20.387	132241	5158	50140	52.327
2	21.903	131502	4699	49.860	47.673

Figure 167. HPLC data of racemic 3-oxabicyclo[3.1.0]hexan-2-one.

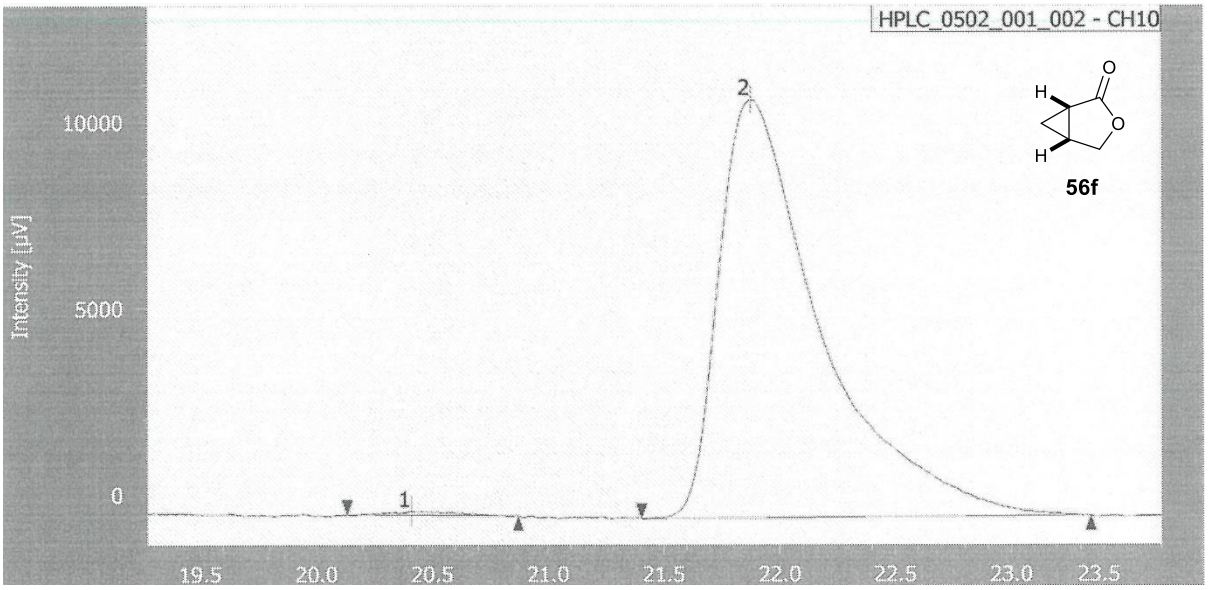

PEAK	RT [min]	AREA [µV-sec]	HEIGHT [µV]	AREA%	HEIGHT%
1	20.410	1906	112	0.553	0.988
2	21.875	342868	11210	99.447	99.012

Figure 168. HPLC data of chiral (1*S*,5*R*)-3-oxabicyclo[3.1.0]hexan-2-one.

REFERENCES

[1] Geuther, A.; Hermann, M. *Liebigs Ann. Chem.* **1855**, *95*, 211.

[2] Nef, J.U. *Liebigs Ann. Chem.*, **1897**, *298*, 202.

[3] Gomberg, M. *J. Am. Chem. Soc*. **1900**, *22*, 752.

[4] Pryor (Ed.), W.A. Organic Free Radicals, *American Chemical Society, Washington, D.C.*, **1977**.

[5] Staudinger, H.; Kupfer, O. *Berichte der Deutschen Chemischen Gesellschaft*, **1911** *44*, 2194.

[6] Staudinger, H.; Kupfer, O. *Berichte der Deutschen Chemischen Gesellschaft*, **1912**, *45*, 501.

[7] Kimse, W. *Angew*. *Chem*. *Int*. *Ed*. **1973**, *85*, 314.

[8] (a) Mulliken, R.S. *Rev. Mod. Phys.* **1932**, *4*, 1; (b) Hezberg, G. *Spectra of Diatomic Molecules*, (*D. van Nostrand Co., Princeton, NJ*), **1950**, 2nd ed., 369

[9] . (a) Hine, J. *J. Am. Chem. Soc.* **1950**, *72*, 2438; (b) Urry, W.H.; Eizner, J.R. *J. Am. Chem. Soc*. **1951**, *73*, 2977; (d) Hennion, G.F.; Maloney, D.E. *J. Am. Chem. Soc.* **1951**, *73*, 4735.

[10] Doering, W. von E.; Knox, L.H. *J. Am. Chem. Soc.* **1953**, *75*, 297.

[11] Doering, W. von E.; Hoffmann, A.K. *J. Am. Chem. Soc.* **1954**, 76, 6162.

[12] (a) Parham, W.E.; Reiff, H.E. *J. Am. Chem. Soc.* **1955**, *77*, 1177; (b) Parham, W.E.; Twelves, R.R. *J. Org. Chem.* **1957**, *22*, 730; (c) Skell, P.S.; Sandler, S.R. *J. Am. Chem. Soc.* **1958**, *80*, 2024.

[13] (a) Schoeller, W.W.; Eisner, D.; Grigoleit, S.; Rozhenko, A.B; Alijah, A. *J. Am. Chem. Soc.* **2000**, *122*, 10115; (b) Canac, Y.; Soleilhavoup, M; Conejero, S; Bertrand, G; *J. Organomet. Chem*. **2004**, *689*, 3857.

[14] (a) Harrison, J.F. *J. Am. Chem. Soc*. **1971**, *93*, 4112; (b) Harrison, J.F.; Liedtke, C.R.;. Liebman, J.F J. Am. Chem. Soc. **1979**, *101*, 7162; (c) Pauling, L. *J. Chem. Soc., Chem. Commun*. **1980**, *688*; (d) Irikura, K.K.; Goddard, W.A.; Beauchamp, J.L. *J. Am. Chem. Soc.* **1992**, *114*, 48.

[15] Bourissou, D.; Guerret, O.; Gabbaï, F.P.; Bertrand, G. *Chem. Rev*. **2000**, *100*, 39.

[16] Taylor, T.E.; Hall, M.B. *J. Am. Chem. Soc*. **1984**, *106*, 1576.

[17] Cardin, D.J; Cetinkaya, B.; Lappert, M.F. *Chem. Rev.* **1972**, *72*, 545.

[18] Lappert, M.F. *J. Organomet. Chem.* **1988**, *358*, 185.

[19] Frenking, G.; Solà, M.; Vyboishchikov, S.F. *J. Organomet. Chem.* **2005**, *690*, 6178.

[20] Vyboishchikov, S.F.; Frenking, G. *Chem. Eur. J.* **1988**, *4*, 1428.

[21] (a) Faust, R. Angew. *Chem., Int. Ed*. **2001**, *40*, 2251; (b) Salaun, J. *Top. Curr. Chem*. **2000**, *207*, 1; (c) Arlt, D.; Jautelat, M.; Lantzsch, R. *Angew. Chem., Int. Ed.* **1981**, *20*, 703.

[22] (a) Newman, M.S.; Kutner, A. *J. Am. Chem. Soc.* **1951**, *73*, 4199; (b) Newman, M.S; Weinberg, A.E; *J. Am. Chem. Soc.* **1956**, *78*, 4654; (c) Ye, T.; McKervey, M.A; *Chem. Rev.* **1994**, *94*, 1091.

[23] Regitz, V.M.; Maas, G. Academic Press: Orlando, **1986**, 596.

[24] Buchner, E.; Curtius, T. Ber. Dtsch. Chem. Ges. 1885, 18, 2377.

[25] (a) McNamara, O.A.; Maguire, A.R. *Tetrahedron* **2011**, *67*, 9; (b) Reisman, S. E.; Nani, R. R.; Levin, *Synthesis. Synlett* **2011**, 2011, 2437.

[26] Anciaux, A.J.; Demonceau, A.; Hubert, A.J.; Noels, A.F.; Petiniot, N.; Teyssie, P. *J. Chem. Soc., Chem. Commun.* **1980**, 765.

[27] (a) Vogel, E.; Wiedemann, W.; Roth, H. D.; Eimer, J.; Gunther, H. *Justus Liebigs Ann. Chem.* **1972**, *759*, 1; (b) Roth, W. R.; Klarner, F. G.; Siepert, G.; Lennartz, H. W. *Chem. Ber*. **1992**, *125*, 217.

[28] (a) Ciganek, E. *J. Am. Chem. Soc*. **1965**, *87*, 652; (b) Ciganek, E. *J. Am. Chem. Soc*. **1965**, *87*, 1149−1150; (c) Ciganek, E. *J. Am. Chem. Soc*. **1967**, *89*, 1454; (d) Reich, H. J.; Ciganek, E.; Roberts, J. D. *J. Am. Chem. Soc*. **1970**, *92*, 5166; (e) Ciganek, E. *J. Am. Chem. Soc.* **1971**, *93*, 2207.

[29] (a) Pommer, H. *Angew. Chem*. **1950**, *62*, 281. (b) Bartels-Keith, J.R.; Johnson, A.W.; Taylor, W.I. *J. Chem. Soc*. **1951**, 2352.

[30] (a) Kennedy, M.; McKervey, M.A.; Maguire, A. R.; Tuladhar, S.M.; Twohig, M.F. *J. Chem. Soc., Perkin Trans. 1* **1990**, 1047; (b) Sonaware, H.R.; Bellur, S.N.; Sudrick, S.G. *Ind. J. Chem., Sect. B* **1992**, *31*, 606.

[31] Costantino, A.; Linstrumelle, G.; Julia, S. *Bull. Soc. Chim. Fr*. **1970**, 907.

[32] McKervey, M.A.; Tuladhar, S.M.; Twohig, M.F. *J. Chem. Soc., Chem. Commun*. **1984**, 129.

[33] Cordi, A.A.; Lacoste, J.M.; Hennig, P. *J. Chem. Soc., Perkin Trans. 1* **1993**, 3.

[34] Manitto, P.; Monti, D.; Zanzola, S.; Speranza, G. *Chem. Commun*. **1999**, 543.

[35] Maguire, A.R.; O'Leary, P.; Harrington, F.; Lawrence, S.E.; Blake, A.J. *J. Org. Chem.* **2001**, *66*, 7166.

[36] Maguire, A. R.; Buckley, N. R.; O'Leary, P.; Ferguson, G. *Chem. Commun*. **1996**, 2595.

[37] Nani, R. R.; Reisman, S. E. *J. Am. Chem. Soc*. **2013**, *135*, 7304.

[38] (a) Nozaki, H.; Moriuti, S.; Takaya, H.; Noyori, R. *Tetrahedron Lett*. **1966**, 5239. (b) Nozaki, H.; Moriuti, S.; Yamabe, M.; Noyori, R. *Tetrahedron Lett.* **1966**, 59. (c) Moser, W. R. *J. Am. Chem. Soc*. **1969**, *91*, 1141. (d) Moser, W. R. *J. Am. Chem. Soc*. **1969**, *91*, 1135.

[39] Saba, A. *Synthesis-Stuttgart* **1984**, 268.

[40] (a) Rogers, D. H.; Morris, J. C.; Roden, F. S.; Frey, B.; King, G. R.; Russkamp, F. W.; Bell, R. A.; Mander, L. N. *Pure Appl. Chem*. **1996**, *68*, 515. (b) Morris, J. C.; Mander, L. N.; Hockless, D. C. R. *Synthesis-Stuttgart* **1998**, 455.

[41] O'Keeffe, S.; Harrington, F.; Maguire, A. R. Synlett **2007**, *2007*, 2367.

[42] (a) O'Neill, S.; O'Keeffe, S.; Harrington, F.; Maguire, A. R. *Synlett* **2009**, *2009*, 2312; (b) Slattery, C. N.; Clarke, L.-A.; O'Neill, S.; Ring, A.; Ford, A.; Maguire, A. R. *Synlett* **2012**, *23*, 765.

[43] Kennedy, M.; McKervey, M. A. *J. Chem. Soc., Perkin Trans. 1* **1991**, 2565.

[44] Foley, D. A.; O'Leary, P.; Buckley, N. R.; Lawrence, S. E.; *Tetrahedron* **2013**, *69*, 1778.

[45] (a) King, G. R.; Mander, L. N.; Monck, N. J. T.; Morris, J. C.; Zhang, H. *J. Am. Chem. Soc.* **1997**, *119*, 3828; (b) (316) Frey, B.; Wells, A. P.; Rogers, D. H.; Mander, L. N. *J. Am. Chem. Soc.* **1998**, *120*, 1914; (c) (317) Zhang, H.; Appels, D. C.; Hockless, D. C. R.; Mander, L. N. *Tetrahedron Lett*. **1998**, *39*, 6577.

[46] Jia, S.; Xing, D.; Zhang, D.; Hu, W. *Angew. Chem., Int. Ed*. **2014**, *53*, 13098.

[47] Zheng, C.; You, S.L. *RSC Adv*. **2014**, *4*, 6173.

[48] Tayama, E.; Yanaki, T.; Iwamoto, H.; Hasegawa, E. *Eur. J. Org. Chem*. **2010**, *2010*, 6719.

[49] Fructos, M. R.; Belderrain, T. R.; de Fremont, P.; Scott, N. M.;́ Nolan, S. P.; Díaz-Requejo, M. M.; Perez, P. *J. Angew. Chem., Int. Ed*. **2005**, *44*, 5284.

[50] Rivilla, I.; Gomez-Emeterio, B. P.; Fructos, M. R.; Díaz-Requejo, M. M.; Perez, P. *J. Organometallics* **2011**, *30*, 2855.

[51] Xie, J.; Pan, C.; Abdukader, A.; Zhu, C. Chem. Soc. Rev. **2014**, 43, 5245.

[52] Yu, Z.; Ma, B.; Chen, M.; Wu, H.-H.; Liu, L.; Zhang, J. *J. Am. Chem. Soc*. **2014**, *136*, 6904.

[53] Yu, X.; Yu, S.; Xiao, J.; Wan, B.; Li, X. *J. Org. Chem*. **2013**, *78*, 5444.

[54] Watanabe, N.; Ohtake, Y.; Hashimoto, S.-i.; Shiro, M.; Ikegami, S *Tetrahedron Lett.* **1995**, *36*, 1491.

[55] Doyle, M. P.; Shanklin, M. S.; Pho, H. Q.; Mahapatro, S. N. *J. Org. Chem*. **1988**, *53*, 1017.

[56] Wee, A. G. H.; Liu, B.; Zhang, L. *J. Org. Chem*. **1992**, *57*, 4404.

[57] Wang, H.-L.; Li, Z.; Wang, G.-W.; Yang, S.-D. *Chem. Commun*. **2011**, *47*, 11336.

[58] Chan, W.-W.; Kwong, T.-L.; Yu, W.-Y. *Org. Biomol. Chem*. **2012**, *10*, 3749.

[59] Mo, S.; Yang, Z.; Xu, J. *Eur. J. Org. Chem*. **2014**, *2014*, 3923.

[60] Hashimoto, T.; Yamamoto, K.; Maruoka, K. *Chem. Commun*. **2014**, *50*, 3220.

[61] Moody, C. J.; Doyle, K. J.; Elliott, M. C.; Mowlem, T. *J. Pure Appl. Chem.* **1994**, *66*, 2107.

[62] Yang, Z.; Xu, J. *Chem. Commun*. **2014**, *50*, 3616.

[63] Collomb, D.; Chantegrel, B.; Deshayes, C. *Tetrahedron* **1996**, *52*, 10455.

[64] Ma, B.; Chen, F.-L.; Xu, X.-Y.; Zhang, Y.-N.; Hu, L.H. *Adv. Synth. Catal*. **2014**, *356*, 416.

[65] Zhang, X.; Lei, M.; Zhang, Y.-N.; Hu, L.H. *Tetrahedron* **2014**, *70*, 3400.

[66] Etkin, N.; Babu, S. D.; Fooks, C. J.; Durst, T. *J. Org. Chem*. **1990**, *55*, 1093.

[67] (a) Salaun, J.; Baird, M.S. *Curr. Med. Chem*. **1995**, *2*, 511; (b) Gnad, F.; Reiser, O. *Chem. Rev*. **2003**, *103*, 1603; (c) Wessjohann, L.A.; Brandt, W.; Thiemann, T. *Chem. Rev*. **2003**, *103*, 1625; (d) Brackmann, F.; Meijere, A. *Chem. Rev*. **2007**, *107*, 4493.

[68] (a) Gagnon, A., Duplessis, M., and Fader, L. *Org.Prep. Proced. Int*. **2010**, *42*, 1; (b) Wang, H.; Zhou, X.; Mao, Y. *Heterocycles* **2014**, *89*, 1767; (c) Qian, D.; Zhang, J. *Chem. Soc. Rev*. **2015**, *44*, 677; 7 (d) Lebel, H.; Marcoux, J.F.; Molinaro, C.; Charette, A.B. *Chem. Rev*.**2003**, *103*, 977; (e) Pellissier, H. *Tetrahedron* **2008**, *64*, 7041; (f) Bartoli, G.; Bencivenni, G.; Dalpozzo, R. *Synthesis* **2014**, *46*, 979; (g) Arlt, D., Jautelat, M., and Lantzsch, R. *Angew. Chem. Int. Ed. Engl*. **1981**, *20*, 703

[69] (a) Simmons, H.E.; Smith, R.D. *J. Am. Chem. Soc*. **1958**, *80*, 5323; (b) Simmons, H.E.; Smith, R.D. *J. Am. Chem. Soc*. **1959**, *81*, 4256; (c) 13 Chan, J.H.H.; Rickborn, B. *J. Am. Chem. Soc*. **1968**, *90*, 6406; 14 (d) Boche, G.; Lohrenz, J.C.W. *Chem. Rev*. **2001**, *101*, 697; (e) Cornwall, R.G.; Wong, O.A.; Du, H.; Ramirez, T.A.; Shi, Y. *Org. Biomol. Chem*. **2012**, *10*, 5498.

[70] Nakamura, M.; Hirai, A.; Nakamura, E. *J. Am. Chem. Soc*. **2003**, *125*, 2341.

[71] Stiasny, H.C.; Hoffmann, R.W. *Chem. Eur. J*. **1995**, *1*, 619.

[72] Ramirez, A.; Truc, V.C.; Lawler, M.; Ye, Y.K.; Wang, J.; Wang, C.; Chen, S.; Laporte, T.; Liu, N.; Kolotuchin, S.; Jones, S.; Bordawekar, S.; Tummala, S.; Waltermire, R.E.; Kronenthal, D. *J. Org. Chem*. **2014**, *79*, 62333.

[73] Nozaki, H.; Moriuti, S.; Takaya, H.; Noyori, R. *Tetrahedron Lett*. **1966**, *7*, 5239.

[74] Dzik, W.I.; Xu, X.; Zhang, X.P.; Reek, J.N.H.; Bruin, B. *J. Am. Chem. Soc*. **2010**, *132*, 10891.

[75] (a) McManus, H.A.; Guiry, P.J. *Chem. Rev*. **2004**, *104*, 4151; (b) Desimoni, G.; Faita, G.; Jorgensen, K.A. *Chem. Rev*. **2006**, *106*, 3561.

[76] (a) Fraile, J.M.; Garcìa, J.I.; Martìnez-Merino, V.; Mayoral, J.A.; Salvatella, L. *J. Am. Chem. Soc.* **2001**, *123*, 7616; (b) 161 Mend, Q.; Li, M.; Tang, D.; Shen, W.; Zhang, J. *Theochem* **2004**, *711*, 193; (c) 162 Drudis-Solé, G.; Maseras, F.; Lledós, A.; Vallribera, A.; Moreno-Mañas, M. *Eur. J. Org. Chem*. **2008**, *2008*, 5614; (d) 163 Aguado-Ullate, S.; Urbano-Cuadrado, M.; Villalba, I.; Pires, E.; García, J.I.; Bo, C.; Carbó, J.J. *Chem. Eur. J*. **2012**, *18*, 14026.

[77] (a) Honma, M.; Takeda, H.; Takano, M.; Nakada, M. *Synlett* **2009**, 1695; (b) Chhor, R.B.; Nosse, B.; Sörgel, S.; Böhm, C.; Seitz, M.; Reiser, O. *Chem. Eur. J*. **2003**, *9*, 26070; (c) Nosse, B.; Chhor, R.B.; Jeong, W.B.; Böhm, C.; Reiser, O. *Org. Lett*. **2003**, *5*, 941; (d) Kalidindi, S.; Jeong, W.B.; Schall, A.; Bandichhor, R.; Nosse, B.; Reiser, O. *Angew. Chem. Int. Ed.* **2007**, *46*, 6361; (e) Jezek, E.; Schall, A.; Kreitmeier, P.; Reiser, O. *Synlett* **2005**, *6*, 915.

[78] Ozoduru, G.; Schubach, T.; Boysen, M.M.K. *Org. Lett*. **2012**, *14*, 4990.

[79] (a) Charette, A.B.; Wurz, R. *J. Mol. Catal. A: Chem*. **2003**, *196*, 83; (b) Charette, A.B.; Janes, M.K.; Lebel, H. *Tetrahedron: Asymmetry* **2003**, *14*, 867.

[80] Merlic, C.A; Zechman, A.L. *Synthesis* **2003**, 1137.

[81] Lindsay, V.N.G.; Fiset, D.; Gritsch, P.J.; Azzi, S.; Charette, A.B. *J. Am. Chem. Soc.* **2013**, *135*, 1463.

[82] Qin, C.; Boyarskikh, V.; Hansen, J.H.; Hardcastle, K.I.; Musaev, D.G.; Davies, H.M.L. *J. Am. Chem. Soc*. **2011**, *133*, 19198.

[83] Goto, T.; Takeda, K.; Anada, M.; Ando, K.; Hashimoto, S. *Tetrahedron Lett*. **2011**, *52*, 4200.

[84] Awata, A.; Arai, T. *Synlett* **2013**, *24*, 29

[85] Xue, Y.S.; Cai, Y.P.; Chen, Z.X. *RSC Adv*. **2015**, *5*, 57781.

[86] Lindsay, V.N.G.; Charette, A.B. *ACS Catal*. **2012**, *2*, 1221.

[87] Nishimura, T.; Maeda, Y.; Hayashi, T. *Angew. Chem. Int. Ed*. **2010**, *4*9, 7324.

[88] Nishiyama, H. *Top. Organomet. Chem*. **2004**, *11*, 81.

[89] (a) Garcia, J.I.; Jiménez-Osés, G.; Martinez-Merino, V.; Mayoral, J.A.; Pires, E.; Villalba, I. *Chem. Eur. J*. **2007**, *13*, 4064; (b) 333 Simpson, J.H.; Godfrey, J.; Fox, R.; Kotnis, A.; Kacsur, D.; Hamm, J.; Totelben, M.; Rosso, V.; Mueller, R.; Delaney, E.; Deshpande, R.P. *Tetrahedron: Asymmetry* **2003**, *14*, 3569.

[90] Marcin, L.R.; Denhart, D.J.; Mattson, R.J. *Org. Lett*. **2005**, *7*, 2651.

[91] Iwasa, S.; Tsushima, S.; Nishiyama, K.; Tsuchiya, Y.; Takazawa, F.; Nishiyama, H. *Tetrahedron: Asymmetry* **2003**, *14*, 855.

[92] Gao, M.Z.; Kong, D.; Clearfield, A.; Zingaro, R.A. *Tetrahedron Lett*. **2004**, *45*, 5649.

[93] Ito, J.I.; Ujiie, S.; Nishiyama, H. *Chem. Eur. J*. **2010**, *16*, 4986.

[94] (a) Stoop, R.M.; Bauer, C.; Setz, P.; Wörle, M.; Wong, T.Y.H.; Mezzetti, A. *Organometallics* **1999**, *18*, 5691; (b) Bachmann, S.; Furler, M.; Mezzetti, A. *Organometallics* **2001**, *20*, 2102; (c) Bachmann, S.; Mezzetti, A. (2001) *Helv. Chim. Acta.* **2001**, *84*, 3063; (d) Uchida, T., Irie, R.; Katsuki, T. *Synlett* **1999**, 1793; (e) Uchida, T.; Irie, R.; Katsuki, T. *Synlett* **1999**, 1163; (f) Uchida, T., Irie, R., and Katsuki, T. *Tetrahedron* **2000**, *56*, 3501; (g) Uchida, T. and Katsuki, T. *Synthesis* **2006**, 1715.

[95] Miller, J.A.; Jin, W.C.; Nguyen, S.T. *Angew. Chem. Int. Ed*. **2002**, *41*, 2953.

[96] Chanthamath, S.; Phomkeona, K.; Shibatomi, K.; Iwasa, S. *Chem. Commun.*, **2012**, *48*, 7750.

[97] Chanthamath, S.; Nguyen, D.T.; Shibatomi, K.; Iwasa, S. *Org. Lett.*, **2013**, *15*, 772.

[98] Abu-Elfotoh, A.M.; Nguyen, D.P.T.; Chanthamath, S.; Phomkeona, K.;Shibatomi, K.; Iwasa, S. *Adv. Synth. Catal.*, **2012**, *354*, 3435.

[99] Abu-Elfotoh, A.M.; Phomkeona, K.;Shibatomi, K.; Iwasa, S. *Angew. Chem. Int. Ed.*, **2010**, *49*, 8439.

[100] a) E. Rodriguez, G. H. N. Towers, J. C. Mitchell, *Phytochemistry*, **1976**, *15*, 1573; b) W. He, M. Cik, G. Appendino, L. Puyvelde, J. E. Leysen, N. Kimpe, *Mini-Rev. Med. Chem*., **2002**, *2*, 185; c) H. B. Wang, X. Y. Wang, L. P. Liu, G. W. Qin,T. G. Kang, *Chem. Rev*., **2015**, *115*, 2975.

[101] a) M. A. Battiste, P. M. Pelphrey, D. L. Wright, *Chem. Eur. J*., **2006**, *12*, 3438; b) H. Butenschon, H. *Angew. Chem., Int. Ed*., **2008**, *47*, 5287; c) X. Li, R. E. Kyne, T. V. Ovaska, *J. Org. Chem*., **2007**, *72*, 6624627

[102] a) H. Duddeck, M. Kennedy, M. A. Mckervey, F. M. Twohig, *J. Chem. Soc. Chem. Commun.*, **1988**, *24*, 1586; b) M. P. Doyle, D. G. Ene, D. C. Forbes, T. H. Pillow, *Chem. Commun.*, **1999**, *17*, 1691; c) A. Padwa, D. J. Austin, A. T. Price, M. A. Semones, M. P. Doyle, M. N. Protopopova, W. R. Winchester, A. Tran, *J. Am. Chem. Soc*., **1993**, *115*, 8669; d) A. A. Cordi, J. M. Lacoste, P. Hennig, *J. Chem. Soc. Perkin Trans. 1*, **1993**, 3; e) C. A. Merlic, A. L. Zechman, M. M. Miller, *J. Am. Chem. Soc*., **2001**, *123*, 11101; f) M. P. Doyle, W. Hu, D.

J. Timmons, *Org. Lett*., **2001**, *3*, 933; g) M. P. Doyle, I. M. Phillips, *Tetrahedron Lett*., **2001**, *42*, 3155; h) A. R. Maguire, P. O'Leary, F. Harrington, S. E. Lawrence, A. J. Blake, *J. Org. Chem*., **2001**, *66*, 7166; i) J. L. Kane, K. M. Shea, A. L. Crombie, R. L. Danheiser, *Org. Lett*., **2011**, *13*, 1081; j) O. A. McNamara, N. R. Buckley, P. O'Leary, F. Harrington, N. Kelly, S. O'Keeffe, A. Stack, S. O'Neill, S. E. Lawrence, C. N. Slattery, A. R. Maguire, *Tetrahedron*, **2014**, *70*, 6870; k) G. S. Fleming, A. B. Beeler, *Org. Lett*., **2017**, *19*, 5268.

[103] B. Frey, A. P. Wells, D. H. Rogers, L. N. Mander, *J. Am. Chem. Soc*. 1998, *120*, 1914.

[104] a) P. M. Doyle, M. S. Shanklin, S. M. Oon, H. Q. Pho, F. R. van der Heide, W. R. Veal, *J. Am. Chem. Soc*., **1988**, *53*, 3384; b) A. Padwa, G. E. Fryxell, L. Zhi, *J. Am. Chem. Soc*., **1990**, *112*, 3100; c) M. P. Doyle, R. J. Pieters, J. Taunton, H. Q. Pho, *J. Org. Chem*., **1991**, *56*, 820; d) P. M. Doyle, L. J. Westrum, W. N. E. Wolthuis, M. M. See, , W. P. Boone, V. Bagheri, M. M. Pearson, *J. Am. Chem. Soc*., **1993**, *115*, 958; e) T. Ye, M. A. McKervey, *Chem. Rev*., **1994**, *94*, 1091; f) P. M. Doyle, A. V. Kalinin, D. G. Ene,. *J.Am. Chem. Soc*., **1996**, *118*, 8837; g) J. P. Snyder, A. Padwa, T. Stengel, A. J. Arduengo, A. Jockisch, H. J. Kim, *J. Am. Chem. Soc*., **2001**, *123*, 11318; h) H. C. Yoon, J. M. Zaworoko, B. Moulton, W. K. Jung, *Org. Lett*., **2001**, *22*, 3539; i) W. H. Cheung, S. L. Zheng, G. C. Zhou, C. M. Che, *Org, Lett*., **2003**, *5*, 2535; j) Z. Chen, Z. Chen, Y. Jiang, W. Hu, *Synlett*, **2004**, *10*, 1763; k) K. W. Choi, W. Y. Yu,C. M. Che, *Org. Lett*., **2005**, *7*, 1081; l) L. D. Flanigan, H. C. Yoon, W. K. Jung, *Tetrahedron Lett*., **2005**, *46*, 143; m) M. Grohman, S. Buck, L. Schaffler, G. Mass, *Adv. Synth. Catal*., **2006**, *348*, 2203; n) M. Grohmann, S. Buck, L. Schäffler, G. Mass, *Tetrahedron*, **2007**, *63*, 12172; o) F. R.L. Gomes, F.A. Trindade, R. N. Candeias, M. P. Gois, A. M. C. Afonso, *Tetrahedron Lett*., **2008**, *49*, 7372; p) S. E. Reisman, R. R. Nani, S. Levin, *Synlett*. **2011**, *17*, 2437; q) P. A. McDowell, D. A. Foley, P. Oleary, A. Ford, A. R. Maguire, *J. Org. Chem*. **2012**, *77*, 2035; r) M. E. Zakrzewska, P. M. S. D. Cal, N. R. Candeias, R. B. Lukasik, C. A. M. Afonso, M. N. Ponte, P. M. P. Gois, *Green Chemistry Letters and Reviews*, **2012**, *5*, 211; s) X. Xu, Y. Deng, N. D. Yim, Y. P. Zavalij, P. M. Doyle, *Chem.Sci*., **2015**, *6*, 2196; t) Y. Deng, C. Jing, H. Arman, M. P. Doyle, *Organometallics*., **2016**, *35*, 3413; u) H. Li, X. Ma, M. Lei, *Dalton Trans*., **2016**, *00*, 1; v) Y. Deng, C. Jing, H. Arman, M. P. Doyle, *Organometallics*, **2016**, *35*, 3413.

[105] C. J. Moody, S. Miah, A. M. Z. Slawin, D. J. Mansfield, I. A. Richards, *J. Chem. Soc*., *Perkin Trans. 1*, **1998**, 4067; b) S. Mo, J. Xu, *ChemCatChem*, **2014**, *6*, 1679; c) S. Mo, X. Li,

J. Xu, *J. Org. Chem*., **2014**, *79*, 9186. d) J. Liu, J. Tu, Z. Yang, C. Pak, J. Xu, *Tetrahedron*, **2017**, *73*, 4616.

[106] X. Xu, Y. Dang, D. N. Yim, P. Y. Zavalij, M. P. Doyle, *Chem. Sci*., **2015**, *6*, 2196.

[107] a) A. M. Abu-Elfotoh, K. Phomkeona, K. Shibatomi, S. Iwasa, *Angew. Chem. Int. Ed*., **2010**, *49*, 8439; b) S. Chanthamath, K. Phomkeona, K. Shibatomi, S. Iwasa, Chem. Commun., **2012**, *48*, 7750; c) A. M. Abu-Elfotoh, T. P. D. Nguyen, S. Chanthamath, K. Phomkeona, K. Shibatomi, S. Iwasa, *Adv. Synth. Catal*., **2012**, *354*, 3435; d) S. Chanthamath, S. Thongjareun, K. Shibatomi, S. Iwasa, *Tetrahedron Lett*., **2012**, *52*, 4862; e) S. Chanthamath, T. D. Nguyen, K. Shibatomi, S. Iwasa, *Org. Lett*., **2013**, *16*, 772; f) S. Chanthamath, S. Takaki, K. Shibatomi, S. Iwasa, *Angew. Chem. Int. Ed*., **2013**, *125*, 5930; g) S. Chanthamath, S. Ozaki, K. Shibatomi, S. Iwasa, *Org. Lett*., **2014**, *16*, 3012; h) S. Chanthamath, W. H. Chua, S. Kimura, K. Shibatomi, S. Iwasa, *Org. Lett*., **2014**, *16*, 3408; i) Y. Nakagawa, S. Chanthamath, K. Shibatomi, S. Iwasa, *Org. Lett*., **2015**, *17*, 2792; j) S. Chanthamath, H. S. A. Mandour, T. M. T. Tong, K. Shibatomi, S. Iwasa, *Chem. Commun*., **2016**, *52*, 7814; k) S. Chanthamath, S. Iwasa, *Acc. Chem. Res*., **2016**, *49*, 2080; l) Y. Nakagawa, S. Chanthamath, I. Fujisawa, K. Shibatomi, S. Iwasa, *Chem. Commun*., **2017**, *53*, 3753; m) M. Kotozaki, S. Chanthamath, I. Fujisawa, K. Shibatomi, S. Iwasa, S, *Chem. Commun.*, **2017**, *53*, 12193; n) M. Kotozaki, S. Chanthamath, T. Fujii, K. Shibatomi, S. Iwasa, *Chem. Commun*., **2018**, *54*, 5110; o) Y. Nakagawa, Y. Imokawa, I. Fujisawa, N. Nakayama, H. Goto, S. Chanthamath, K. Shibatomi, S. Iwasa, *ACS Omega*, **2018**, *3*, 11286; p) M. Tone, Y. Nakagawa, S. Chanthamath, I. Fujisawa, N. Nakayama, H. Goto, K. Shibatomi, S. Iwasa, *RSC Advances*, **2018**, *8*, 39865; q) Y. Nakagawa, N. Nakayama, H. Goto, I. Fujisawa, S. Chanthamath, K. Shibatomi, S. Iwasa, *Chirality*, **2019**, *31*, 52; r) Y. Nakagawa, S. Chanthamath, Y. Liang, K. Shibatomi, S. Iwasa, *J. Org. Chem*., **2019**, *84*, 2607; s) H. S. A. Mandour, Y. Nakagawa, M. Tone, H. Inoue, N. Otog, I. Fujisawa, S. Chanthamath,S. Iwasa, *Beilstein J. Org. Chem*., **2019**, *15*, 357.

[108] a) Tokunaga, T.; Hume, W.E.; Nagamine, J.; Nagata, R. *Bioorg. Med. Chem. Lett*. **2005**, *15*, 1789; b) Tokunaga, T. ;Hume, W.E.; Umezome, T.; Okazaki, K.; Ueki, Y.; Kumagai, K.; Hourai, S.; Nagamine, J.; Seki, H.; Taiji, M.; Noguchi, H.; Nagata, R. *J. Med. Chem*. **2001**, *44*, 4641; c) Strigacova, J.; Hudecova, D.; Mikulasova, M.; Varecka, L.; Lasikova, A.; Vegh, D. *Folia Microbiologica*. **2001**, 46, 187.

[109] S.S. Rindhe, S.S.; B.K. Karale, B.K.; R.C. Gupta, R.C.; M.A. Rode, M.A. *Indian J. Pharm*

Sci. **2011**, *73*, 292.

[110] Davis, A.L.; Smith, D.R.; McCord, T.J. *J. Med. Chem*. **1973**, *16*, 1043.

[111] Estevao, M.S.; Carvalho, L.C.; Ferreira, L.M.; Fernandes, E.; Marques, M.M.B. *Tet. Lett*. **2011**, *52*, 101.

[112] a) Shintani, R.; Inoue, M.; Hayashi, T. *Angew. Chem. Int. Ed*. **2006**, *45*, 3353. b) Hills, I.D.; Fu, G.C. *Angew. Chem. Int. Ed*. **2003**, *42*, 3921.

[113] Dounay, A.B.; Hatanaka, K.; Kodanko, J.J.; Oestreich, M.; Overman, L.E.; Pfeifer, L.A.; Weiss, M.M. *J. Am. Chem. Soc*. **2003**, *125*, 6261.

[114] Hennessy, E.J.; Buchwald, S.L. *J. Am. Chem. Soc*. **2003**, *125*, 12084.

[115] Doyle, M.P.; McKervey, M.A.; Ye, T. John Wiley and Sons, New York, **1998**.

[116] Padwa, A.; Krumpe, K.E. *Tetrahedron*. **1992**, *48*, 5385.

[117] Doyle, M.P.; Forbes, D.C. *Chem. Rev*. **1998**, *98*, 911.

[118] A. Plalfz, Comprehensive Asymmetric Catalysis, vol. 2, Springer-Verlag, New York, **1999**.

[119] Davies, H.M.L.; Beckwith, R.E. *Chem. Rev*. **2003**, *103* 2861.

[120] a) Galliford, C.V.; Scheidt, K.A. *Angew. Chem. Int. Ed*. **2003**, *46*, 8748; b) Marti, C.; Carreira, E.M. *Eur. J. Org. Chem*. **2003**, *12*, 2209.

[121] Garg, P.; Jadhav, S.D.; Singh, A. *Asian J. Org. Chem*. **2017**, *6*, 1019.

[122] Doyle, M.P.; Shanklin, M.S.; Pho, H.; Mahapatro, S.N. *J. Org. Chem*. **1988**, *53*, 1017.

[123] Prandi, C.; Occhiato, E.G.; Tabasso, S.; Bonfante, P.; Novero, M.; Scarpi, D.; Bova, M.E.; Miletto, I. *Eur. J. Org. Chem*. **2011**, 3781.

[124] a) Che, C.M.; Huang, J.S.; Lee, F.W.; Li, Y.; Lai, T.S.; Kwong, H.L.; Teng, P.F.; Lee, W.S.; Lo, W.C.; Peng, S.M.; Zhou, Z.Y. *J. Am. Chem. Soc.*, **2001**, *123*, 4119. b) Tang, W.; Hu, X.; Zhang, X. *Tetrahedron Lett.*, **2002**, *43*, 3075. c) Bonaccrsi, C.; Bachmann, S.; Mezzetti, A. *Tetrahedron: Asymmetry,* **2003**, 845. d) Miller, J. A.; Hennessy, E. J.; Marshall, W. J.; Scialdone, M. A.; Nguyen, S. *J. Org. Chem.*, **2003**, *68*, 7884. e) Maas, G.; *Chem. Soc. Rev.*, **2004**, *33*, 183.

[125] Niimi, T.; Uchida, T.; Irie, R.; Kastuki, T. *Tetrahedron Lett.* **2000**, *40*, 3647.

[126] a) Nishiyama, H.; Sakaguchi, H.; Nakamura, T.; Horihata, M.; Kondo, M.; Itoh, K. *Organometallics*, **1989**, *8*, 846. b) Nishiyama, H.; Itoh, Y.; Mastumoto, H.; Park, S-B.; Itoh, K. *J. Am. Chem. Soc.*, **1994**, *116*, 2223. c) Nishiyama, H.; Itoh, Y.; Sugawara, Y.; Mastumoto, H.; Aoki, A.; Itoh, K. *Bull. Chem. Soc. Jpn.*, **1995**, *68*, 1247. d) Nishimaya, H.; Ito, J. *Chem.*

Commun., **2010**, *46*, 203.

[127] a) Jia, G.; Meek, W. D.; Gallucci, C. J. *Organometallics.*, **1990**, *9*, 2549. b) Coalter, N. J.; Streib, E. W.; Caulton, G. K. *Inorg. Chem.*, **2000**, *39*, 3749.